PHD

An investigation into the phosphorylation state of GLUT4

Richardson, Judith Diane

Award date:
2006

Awarding institution:
University of Bath

An Investigation into the Phosphorylation State of GLUT4

Judith Diane Richardson

A thesis submitted for the degree of Doctor of Philosophy

University of Bath

Department of Biology and Biochemistry

2006

JD Richardson.

ProQuest LLC
789 East Eisenhower Parkway
P.O. Box 1346
Ann Arbor, MI 48106-1346

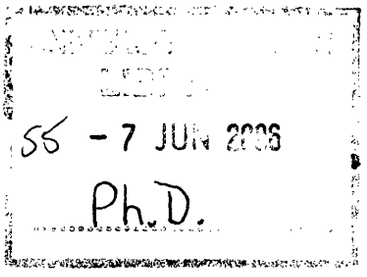
56 - 7 JUN 2006
Ph.D.

Abstract

Insulin stimulates the uptake of glucose in responsive tissues through the insulin-regulated glucose transporter (GLUT4). In the resting cell, GLUT4 is localised in an intracellular GLUT4 storage vesicle (GSV). In response to insulin stimulation, GLUT4 is rapidly mobilised from the GSV to the plasma membrane.

The work described in this thesis investigates the phosphorylation state of GLUT4. The FQQI motif at the N-terminus of GLUT4 has a potential downstream phosphorylation site at serine 10. The sequence surrounding serine 10 ($GS^{10}EDGE$) has a high sequence identity with a domain in GAD65α, which is phosphorylated by an unknown kinase. A phosphorylation site at serine 488 in GLUT4 has previously been identified.

To aid this study, work was undertaken to purify a phospho-specific antibody raised to a phosphorylated serine 10 peptide as well as raising an antibody to the C-terminus of GLUT4.

Experiments in which both adipocytes and cardiomyocytes were labelled with radioactive inorganic phosphate, and in which GLUT4 was subsequently cleaved with Endoproteinase Lys-C, have led to the identification of a phosphorylation site in the N-terminus of GLUT4 as well as confirming the presence of the C-terminal phosphorylation site. From comparison with a phosphorylation site prediction program, it is concluded that the putative phosphorylation site at serine 10 is likely to be a *bone fide* phosphorylation site at the N-terminus of GLUT4.

Site-directed mutagenesis was carried out to mutate serine 10 and serine 488 in GLUT4 to either alanine or aspartic acid residues which were designed to mimic the non-phosphorylated and phosphorylated state, respectively. The effect of the mutations on the rate of trafficking of GLUT4 to the plasma membrane was investigated. The only mutation to have an effect was the aspartic acid 10 mutation which resulted in a decreased level of GLUT4 at the plasma membrane in insulin-stimulated cells.

Acknowledgments

I would first like to thank Professor Geoff Holman for giving me the opportunity to study for my PhD in his laboratory and for all the supervision and advice he has given me over the last three years. My thanks must also go to Françoise Koumanov and Scott Lawrence whose knowledge, support and advice have been invaluable throughout my time in the lab and for which I will always be grateful.

I would also like to thank the present and past members of the Holman lab along with the other friends I have made in during my time in Bath for making Bath such a friendly and enjoyable place to work and live, namely Françoise Koumanov, Scott Lawrence, Jing Yang, Amelia Preedy, Bo Jin, Sunil Patel, David Ribé, Paul Whitley, Huai-Lo Lee, Joe Dukes III, Kate Ralphs, Carolyn Williamson, Emily Bennett, Ian Williams and Lucy Carruthers.

I would like to thank Françoise Koumanov for the work she has done on this phosphorylation project, including the confocal microscopy study in chapter 3 and the CNBr cleavage study in chapter 4. I would like to express my gratitude to Jing Yang and Scott Lawrence for the preparation of the cardiomyocytes in chapter 4 and to Scott Lawrence for the optimisation of the adipocyte transfection and antibody binding assay in chapter 5. Thanks must also go to Darren Harper who originally started this phosphorylation project and for the generation of the $pSer^{10}$ antibody serum raised in rabbit (chapter 3). I must also give a big thank you to the MRC for funding me throughout my PhD.

Last but not least, I must thank my Mum and my partner David Mitchell for all their love, patience and support (both emotional and financial) throughout my studies in Bath.

Abbreviations

Ab	Antibody
AEBSF	[4-(2-Aminoethyl)benzenesulfonylflouride, HCl]
AICAR	5-aminoimidazole-4-carboxyamide-1-β-D-ribofuranoside
AMP	Adenosine 5'-monophosphate
AMPK	AMP activated protein kinase
APS	Ammonium Persulphate
ATP	Adenosine 5'-triphosphate
BFA	Brefeldin A
BSA	Bovine Serum Albumin
CHO cells	Chinese Hamster Ovary cells
Ci	Curies
CKI	Casein kinase I
CKII	Casein kinase II
CNBr	Cyanogen Bromide
cpm	Counts per minute
C-term	C-terminal
Da	Daltons
ddH_2O	Double distilled water
DMEM	Dulbecco's modified Eagles medium
DMSO	Dimethyl Sulfoxide
DRB	5,6-Dichloro-1-β-D-ribofuranosylbenzimidazole
DTT	$_{DL}$-Dithiothreitol
ECL	Enhanced Chemiluminescence
EDTA	Diaminoethanetetra-acetic acid disodium salt
ELISA	Enzyme-Linked Immunosorbent Assay
Endo LysC	Endoproteinase Lys C
E. coli	*Escherichia coli*
FCS	Fetal Calf Serum
g	Gram

GCK	Golgi casein kinase
GLUT	Glucose Transporter
GLUT4	Glucose Transporter 4
GSV	GLUT4 Storage Vesicle
h	Hour
HA	Haemagglutinin
HDM	High density microsomes
HEPES	(N-[2-Hydroxyethyl]piperazine-N'-[2-ethenesulfonic acid])
HRP	Horseradish peroxidase
IRAP	Insulin-responsive aminopeptidase
IRGT	Insulin-regulatable glucose transport
IRS	Insulin receptor substrate
kb	Kilo base
kDa	Kilo daltons
KLH	Keyhole Limpet Hemocyanin
KRH	Krebs-Ringer-HEPEs
LB	Luria Broth
LDM	Low density microsomes
MBS	m-Maleimidobenzoyl-*N*-Hydroxysuccinimide ester
Min	Minutes
Mops	3-(N-Morpholino)propanesulfonic acid
Myo1c	Unconventional myosin 1C
NCS	Newborn Calf Serum
NSF	N-ethylmaleimide sensitive factor
N-term	N-terminal
O.D.	Optical density
PBS	Phosphate Buffered Saline
PBS-T	Phosphate buffered saline containing Tween-20
PCA	Perchloric acid
PCR	Polymerase Chain Reaction
PDK1	3'-phosphoinositide-dependent kinase-1

P_i	Inorganic phosphate
PI	Phosphatidylinositol
PI3K	Phosphatidylinositol 3-kinase
PH domain	Pleckstrin-homology domain
PKA	Protein Kinase A
PKB	Protein Kinase B
PKC	Protein Kinase C
PM	Plasma membrane
PNGase F	Peptide: N – Glycosidase F
pSer^{10}	GLUT4 phosphorylated at serine 10
PTPases	Protein tyrosine phosphatases
PTB domain	Phosphotyrosine binding domain
PVDF	Polyvinylidene fluoride
Rpm	Revolutions per minute
SDS	Sodium Dodecyl Sulphate
SDS-PAGE	Sodium Dodecyl Sulphate-Polyacrylamide Gel Electrophoresis
Sec	Seconds
SH2	Src homology 2
SH3	Src homology 3
siRNA	Small interfering RNA
SNAP	Soluble NSF attachment proteins
SNARE	SNAP receptors
TAE	Tris-acetate EDTA
TBB	4,5,6,7-Tetrabromobenzotriazole
TBS	Tris-buffered Saline
TBS-T	Tris-buffered Saline containing Tween-20
TEMED	N,N,N', N'-tetramethylethylenediamine
TES	Tris-EDTA Sucrose
TGN	Trans-Golgi Network
Thesit	Nonaethylene glycol monododecyl ether
TMB	Tetramethyl Benzidine

Tris	Tris(hydroxymethyl)methylamine
t-SNARE	SNARE proteins present on the plasma membrane
Tween-20	Polyoxyethylene sorbitan monolaureate
TX-100	Triton X-100
U	Units
UV	Ultra Violet
VAMP	Vesicle-associated membrane protein
v-SNARE	SNARE proteins present on the vesicle membrane

Contents

1 Introduction

1.1 Glucose Homeostasis

Glucose is the major source of fuel in eukaryotic cells; it is an important source of fuel for many tissues and an essential source for others. Glucose is catabolised via glycolysis, the citric acid cycle and oxidative phosphorylation to provide ATP, the cellular energy source. When the levels of blood glucose are high, glycogen, a polymer of glucose, is produced by glycogenesis. Glycogen is then stored until times of glucose shortage. Glucose homeostasis is therefore an important phenomenon, which maintains a constant source of glucose for the varying metabolic demands of the animal. Glucose circulates freely in the blood and is constantly being removed or replaced due to the metabolic demands of the surrounding tissues. Blood glucose levels remain relatively constant at 5 mM but post-prandial glucose levels can rise up to 7 mM (Reaven *et al.*, 1988). The constant level of glucose in the blood is achieved by the control of various aspects of glucose metabolism. Insulin and glucagon are two hormones that have antagonistic roles in glucose homeostasis. In response to elevated blood glucose levels, insulin is secreted by the β-cells from the islets of Langerhans found in the pancreas. Insulin stimulates glucose uptake and storage in insulin responsive tissues (muscle and adipose tissues) as well as inhibiting gluconeogenesis, particularly in the liver. Conversely, in situations where blood glucose is low, i.e. during periods of starvation, glucagon is released from the pancreas and promotes the breakdown of glycogen and thus the release of glucose into the blood by a process known as glycogenolysis.

Diabetes mellitus is a disease which is associated with a failure in glucose homeostasis. There are two forms of diabetes mellitus. Type 1 or insulin-dependent diabetes mellitus is due to a deficiency in insulin, which develops after the auto-immune destruction of the insulin-secreting cells in the pancreas. The only effective treatment is insulin injections. The other type of diabetes

mellitus is called Type 2 or non-insulin-dependent diabetes mellitus. Type 2 diabetes occurs as a result of insulin resistance, in which there is not a deficiency of insulin per se, but rather a failure of insulin to exert its effects. Having a strict diet is the most common way to control Type 2 diabetes, but drugs are available, e.g. metformin, which increase the sensitivity of the tissues to insulin. Type 2 diabetes was traditionally a disease that affected older people. However, insulin resistance is a prominent feature of obesity and, with the increasing problem of obesity in children following the prevalence of the TV and video gaming culture, Type 2 diabetes is becoming an increasing health problem in juveniles. Type 2 diabetes is one of the major risks to human health. It is currently estimated that there are 150 million people suffering from diabetes and this number is predicted to increase to 300 million in 2025 (Zimmet *et al.*, 2001). This has fuelled research into all aspects of glucose biology and the mechanism of Type 2 diabetes.

1.2 The Glucose Transporter Family

Following the post-prandial release of insulin, the blood glucose concentration returns to about 5 mM through the uptake of glucose into various tissues. Glucose is a hydrophilic molecule and thus cannot penetrate the plasma membrane by simple diffusion. Therefore, proteins must exist to transport glucose into the cell. There are two different types of transporter proteins that transport glucose and other sugars across the cell membrane, the Na^+-coupled carrier system (SGLT) and the facilitative glucose transporters (GLUT). Both types of transporters belong to families of the solute carrier gene series (SLC), SLC5 and SLC2 respectively.

Each member of the GLUT family of proteins forms a transporter across the cell membrane through which glucose can enter the cell. In 1985, the first glucose transporter to be cloned and sequenced was in erythrocyte cells

(Mueckler *et al.*, 1985). This transporter is now known as GLUT1. Over the last 20 years, thirteen more transporters have been identified which are at least 29% identical with GLUT1 (Scheepers *et al.*, 2004). The members of the GLUT family have varying tissue distributions, which suggest that each plays a distinct role in the regulation of whole body glucose homeostasis.

The GLUT family of proteins are predicted to have twelve transmembrane spanning helices with both the amino- and carboxyl-termini having a cytosolic localisation as well as a highly hydrophilic domain between helices 6 and 7 (Figure 1.1). Sequence comparisons of all the members of the GLUT family (Joost and Thorens, 2001) have further corroborated this structural model, which was first suggested by evidence from hydropathy plots (Mueckler *et al.*, 1985). This model was further confirmed after the 3D structure of the *Escherichia coli* (*E. coli*) glycerol-3-phosphate transporter (GlpT), a structurally-related protein to the glucose transporters, was solved (Lemieux *et al.*, 2003).

The 14 members of the extended GLUT family can be divided into three subclasses, classes I, II and III. Class I are the glucose transporters GLUT1 to 4 and 14, which differ in their subcellular localisation, affinity for glucose and their hormonal regulation. Class II are fructose-specific transporters (GLUT5) and related proteins (GLUT7, 9 and 11). Finally, class III transporters (GLUTs 6, 8, 10, 12 and HMIT1) are structurally atypical members of the GLUT family. They are composed of a shorter extracellular loop between helices 1 and 2, which results in a lack of glycosylation site in that region. However, a glycosylation site is present in the extracellular loop between helix 9 and 10 (Table 1.1) (Joost and Thorens, 2001, Scheepers et al., 2004). The term glucose transporter must also be used with care because the newer members of the GLUT family have different substrate specificities and may transport sugars or polyols other than glucose (e.g. GLUT5 transports fructose and HMIT1 transports myoinositol).

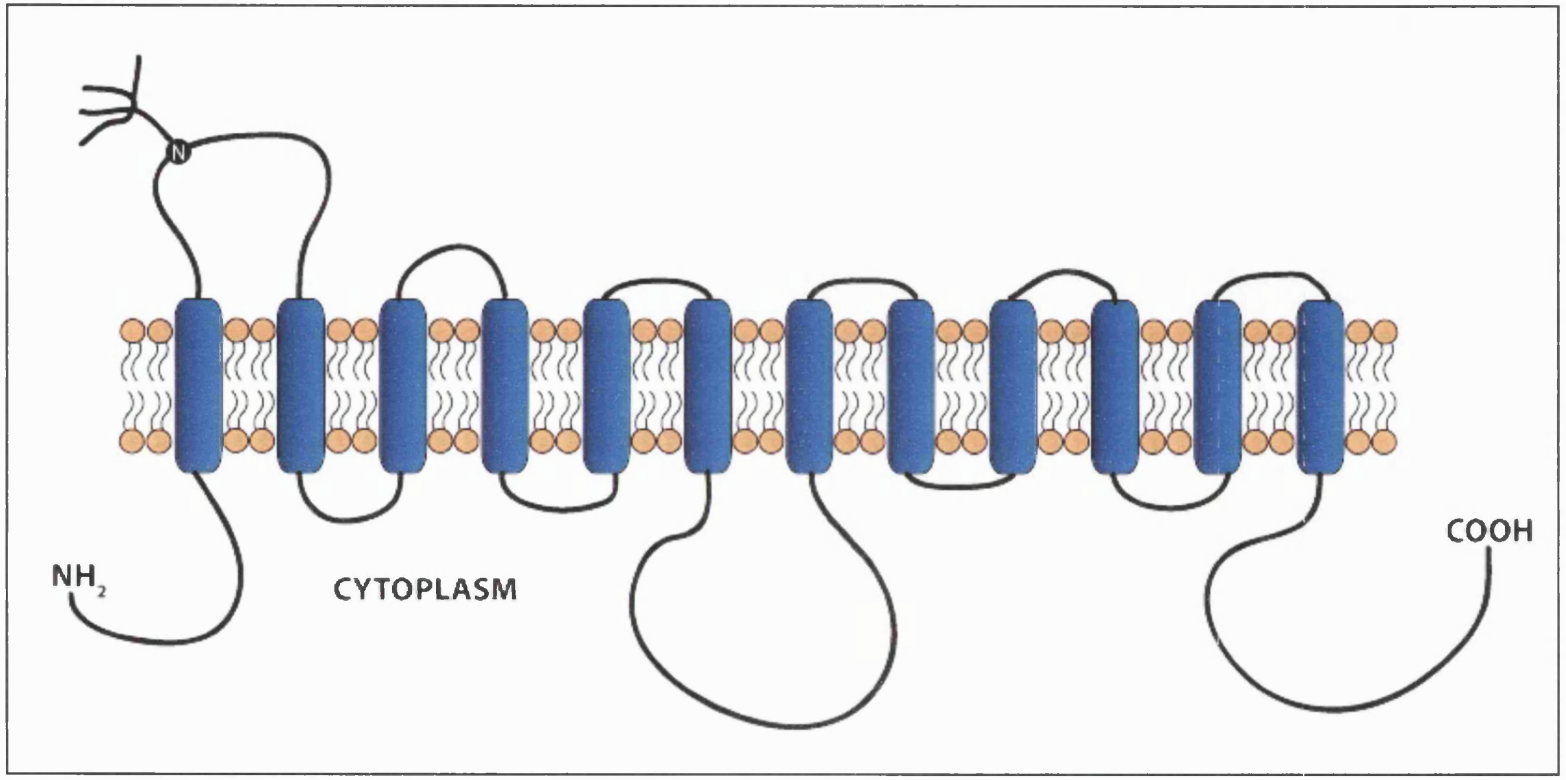

Figure 1.1 **Predicted structure of the class I family of GLUT proteins.** The GLUT family of proteins are predicted to have twelve transmembrane spanning helices with both the amino- and carboxyl-termini having a cytosolic localisation as well as a highly hydrophilic domain between helices 6 and 7. Adapted from (Joost and Thorens, 2001).

Human Gene Name + Locus	Protein	Alias	Predominant Substrates	Tissue Distribution	Sequence Accession ID	Splice Variants
SLC2A1 1p35-31.3	GLUT1		Glucose, Galactose, Mannose, Glucosamine	Erythrocytes, brain, blood brain barrier, blood-tissue barrier, adipocyte, muscle	NM_006516	
SLC2A2 3q26.2-27	GLUT2		Glucose, Galactose, Fructose, Mannose, Glucosamine	Liver, islet of Langerhans, intestine, kidney, brain	NM_000340	
SLC2A3 12p13.3	GLUT3		Glucose, Galactose, Mannose, Xylose	Brain (neurons), testis, low levels in placenta, liver and heart (humans)	NM_006931	
SLC2A4 17p13	GLUT4		Glucose, Glucosamine	Adipose tissue, skeletal and cardiac muscle	NM_001042	
SLC2A5 1p36.2	GLUT5		Fructose	Small intestine, kidney, testies	NM_003039	
SLC2A6 9q34	GLUT6	GLUT9	Glucose	Brain, spleen, leukocytes	NM_017585	
SLC2A7 1p36.2	GLUT7		Glucose, Fructose	Intestine (ileum), testis, prostate	NM_207420	
SLC2A8 9	GLUT8	GLUTX1	Glucose, Fructose, Galactose	Testis, brain, adrenal gland, liver, spleen, brown adipose tissue, lung	NM_014580	
SLC2A9 4p15.3-16	GLUT9	GLUTX	Glucose	Kidney, liver, small intestine, placenta, lung and leukocytes	NM_020041	
SLC2A10 20q12-13.1	GLUT10		Glucose, Galactose	Liver, pancreas, heart, lung, brain, skeletal muscle, placenta and kidney	NM_030777	
SLC2A11 22q11.2	GLUT11	GLUT10	Glucose, Fructose	Heart, muscle, pancreas, kidney, placenta	NM_030807	3
SLC2A12 6q23.2	GLUT12		Glucose, Galactose, Fructose	Heart, prostate, skeletal muscle, breast cancer	NM_145176	
SLC2A13 12q11.23	HMIT	GLUT13	*Myo*-inositol	Brain, astrocytes, neurons	NM_052885	
SLC2A14 12p13.3	GLUT14			Testis	NM_153449	4

Table 1.1 **Classification and tissue expression of the different GLUT isoforms.** (Joost and Thorens, 2001, Hediger et al., 2004).

1.2.1 The Insulin-Regulatable Glucose Transporter – GLUT4

Insulin increases the rate of glucose uptake into adipocytes by at least 20-fold. For many years, it was believed that insulin altered the intrinsic activity of the glucose transporters located in adipocyte cell membranes. However, in 1980 it was first demonstrated, by the use of cytochalasin B-binding, that in the basal state the glucose transporters were sequestered in intracellular membranes. Following stimulation with insulin, the glucose transporters then translocated to the plasma membrane where they could transport glucose into the cell (Cushman and Wardzala, 1980, Suzuki and Kono, 1980). In 1988, this transporter was identified as the insulin-regulatable glucose transport (IRGT), which is now more commonly known as GLUT4. The following year, five independent laboratories were successful in cloning GLUT4 from a variety of different tissues and cell lines (Birnbaum, 1989, Charron et al., 1989, Fukumoto et al., 1989, Kaestner et al., 1989, James et al., 1989b). The human and rat GLUT4 proteins consist of 509 amino acids (Birnbaum, 1989, Charron et al., 1989, James et al., 1989b), whereas, the mouse GLUT4 protein has 510 amino acids (Kaestner *et al.*, 1989). GLUT4 has 65% sequence homology to GLUT1. The major differences in identity are in the amino and carboxyl termini and the large cytoplasmic loop between helices 6 and 7. The sequence homology of this area is only 40%, compared to that of the putative membrane spanning regions which are reported to have 73% homology (Birnbaum, 1989).

GLUT1 is a ubiquitously expressed transporter and is also present in insulin responsive tissues, but only at low levels (Flier *et al.*, 1987). GLUT1 and GLUT4 must therefore both contribute to glucose uptake in adipocyte and muscle tissue. GLUT1 is present predominantly in the plasma membrane of both basal and insulin-stimulated cells and, following insulin stimulation, there is only a relatively small increase in the level of GLUT1 at the cell surface (~ 5-fold) (Holman *et al.*, 1990). However, GLUT4 contributes to about 90% of the

glucose transporters in the plasma membrane of insulin-stimulated adipocytes and the level of GLUT4 at the cell surface increases 15- to 20-fold above basal levels (Holman *et al.*, 1990). Thus it was concluded that the GLUT4 protein is the key glucose transporter involved in insulin-stimulated glucose uptake. The molecular mechanism by which insulin causes this redistribution of GLUT4 still has to be fully elucidated, and, while huge progress has occurred throughout the last 20 years, GLUT4 currently remains under intense investigation.

1.3 Insulin Signalling Pathways Involved in Glucose Uptake

An extensive signalling cascade is involved in insulin-stimulated glucose transport, the full extent of which has not, as yet, been identified. The translocation of GLUT4 to the plasma membrane following stimulation with insulin is complex and may require regulation in the various steps. Our understanding of the insulin signalling involved in glucose transport will be outlined below, the knowledge of which will help us to fully understand the mechanism of insulin-stimulated glucose transport (Figure 1.2). The signalling cascade described will focus on the signalling molecules involved in GLUT4 translocation to the plasma membrane. It is by no means a full description of all of the interacting molecules involved in signalling downstream from the insulin receptor. Insulin-stimulated glucose transport is mediated through a phosphatidylinositol 3-kinase-dependent pathway. A phosphatidylinositol 3-kinase-independent pathway has also been reported but has remained controversial in the GLUT4 field.

1.3.1 Phosphatidylinositol 3-Kinase-Dependent Pathway

1.3.1.1 The Insulin Receptor

The insulin receptor is a member of the receptor tyrosine kinase family. It is synthesised as a single polypeptide 'proreceptor' molecule and is cleaved in the trans-Golgi network (TGN) by furin, a serine protease, to give the mature receptor (Bravo *et al.*, 1994). The mature insulin receptor is a heterotetrameric structure comprising of two α- and two β-subunits ($\alpha_2\beta_2$). The two α-subunits are extracellular and are linked by disulfide bonds. The two β-subunits consist of transmembrane spanning and cytosolic domains. Each β-subunit can be phosphorylated following insulin binding to its receptor (Kasuga et al., 1982a, Kasuga et al., 1982b). The β-subunits have exogenous and endogenous tyrosine kinase activity and are each linked to one of the α-subunits through a disulfide bond. Insulin binds to the α-subunits of the insulin receptor, which causes a conformational change in the receptor. This triggers the transphosphorylation of one β-subunit by the other on specific tyrosine residues, which increases the catalytic activity of the kinase domain. There are also two other regions in the β-subunit, the juxtamembrane region and the C-terminal domain, which undergo autophosphorylation in response to insulin binding (Lee and Pilch, 1994, Watson et al., 2004b). Phosphorylation of the insulin receptor is important in substrate recognition for downstream proteins in the insulin-signalling cascade.

1.3.1.2 Insulin Receptor Substrates

The insulin receptor differs from other members of the receptor kinase family in that it does not interact directly with downstream effector molecules. Instead it binds and phosphorylates various scaffold proteins, which in turn bind to various effector molecules (Lee and Pilch, 1994). The major substrate of the insulin receptor, and the most widely studied, is the family of insulin receptor

substrate (IRS) proteins (Shepherd *et al.*, 1998). Six members of the IRS family have been identified. IRS-1 and IRS-2 (Sun et al., 1991, Sun et al., 1995) are ubiquitously expressed (muscle, liver, fat, and pancreatic islets). IRS-3 was cloned from rat adipocytes (Lavan *et al.*, 1997b). However, IRS-3 was not expressed in human adipocytes (Bjornholm *et al.*, 2002) and is therefore not involved in insulin signalling in humans. IRS-4 was first cloned in 1997 (Lavan *et al.*, 1997a) and is expressed in pituitary and thyroid glands but is undetectable in insulin-sensitive tissues (Uchida *et al.*, 2000). IRS-4 would therefore not have a role in insulin-stimulated GLUT4 uptake. IRS-5 is expressed in kidney and liver and IRS-6 is expressed in muscle (Cai *et al.*, 2003). Both proteins are substrates for the insulin receptor but further work is needed to determine if the classification as a member of the 'insulin receptor substrate' family is justified (Cai *et al.*, 2003). Three members of the IRS protein family may therefore be involved in glucose transport as they are expressed in the target, insulin-responsive tissue. However, IRS-3 is not expressed in humans so IRS-1 and IRS-2 are the most likely candidates to be involved in insulin-stimulated glucose transport. The effect each of these proteins has on insulin-stimulated glucose transport in muscle was investigated using small interfering RNA (siRNA). It was concluded that IRS-1 and IRS-2 have different roles in muscle cells. IRS-1 regulates GLUT4 translocation, glucose uptake, actin remodelling, and protein kinase B (PKB)α and PKBβ phosphorylation. IRS-2 regulates PKBβ activation but does not have a major effect on these other functions (Huang *et al.*, 2005). IRS-1 is, therefore, the major IRS protein to affect insulin-stimulated glucose transport.

The insulin receptor substrates are not classified according to their amino acid sequence but according to their similar structural features. There is an amino-terminal targeting domain that comprises a Pleckstrin-homology (PH) domain and / or a phosphotyrosine binding (PTB) domain. These domains mediate protein-lipid or protein-protein interactions. There is also a region in the C-terminus of the protein containing tyrosine residues, which, when

phosphorylated, act as a binding site for proteins which contain Src homology 2 (SH2) domains. There are also proline rich regions to bind Src homology 3 (SH3) / WW domain containing proteins, and serine / threonine rich regions, which are believed to regulate the overall function of the protein through protein-protein interactions (Shepherd et al., 1998, White, 1998).

The insulin receptor contains a NPEY motif in the juxtamembrane region and the PTB domain of the IRS binds through this (He et al., 1995, Wolf et al., 1995). The PH domain in the N-terminus of the IRS protein is also needed for insulin receptor association, through binding to phosphoinositides, and consequential phosphorylation by the insulin receptor (Voliovitch et al., 1995, Yenush et al., 1996). The majority of the phosphorylation sites in IRS proteins consist of YMXM or YXXM motifs (Shoelson *et al.*, 1992). After binding to the insulin receptor, multiple tyrosine residues are phosphorylated within the IRS-1 protein and promote the recruitment of a number of signalling molecules (Sun *et al.*, 1992).

1.3.1.2.1 Inhibition of Insulin Receptor Signalling

Protein tyrosine phosphatases (PTPases) attenuate the effect of insulin by rapidly dephosphorylating the insulin receptor. Many PTPases have been implicated in this but protein tyrosine phosphatase 1B (PTP-1B) is the most highly studied. PTP-1B knockout mice have been shown to have increased tyrosine phosphorylation of the insulin receptor and IRS proteins (Elchebly *et al.*, 1999).

Serine phosphorylation of the insulin receptor and IRS proteins is also a mechanism whereby the insulin signal can be controlled. There is a negative feedback system in which serine phosphorylation ultimately leads to a

decrease in insulin-stimulated tyrosine phosphorylation and is involved in insulin resistance pathways (Saltiel and Kahn, 2001).

1.3.1.3 Phosphatidylinositol 3-kinase

In 1993, it was first reported that phosphatidylinositol 3-kinase (PI3K) was involved in glucose transport because of the fact that low nano-molar concentrations of the PI3K inhibitor, wortmannin, inhibit insulin-stimulated glucose transport (Kanai *et al.*, 1993a). Furthermore, wortmannin inhibits the translocation of GLUT4 following insulin stimulation but has no effect on basal translocation of the transporter (Clarke *et al.*, 1994). The site of PI3K action in insulin-stimulated glucose transport has been narrowed down and has been shown to be involved in the exocytosis of GLUT4 from the intracellular storage compartment to the plasma membrane (Yang *et al.*, 1996).

There are three classes of PI3K – classes I, II and III. Each class is defined by its primary structure, regulation and *in vitro* lipid substrate specificity. Class I is further subdivided into two categories (I_A and I_B), differentiated by the adaptor subunit to which they bind. Class I_A PI3Ks bind to adaptor proteins containing SH2 domains. PI3Ks belonging to class I_B are stimulated by G-protein βγ subunits and do not interact with proteins containing SH2 domains (Vanhaesebroeck *et al.*, 1997).

Phosphatidylinositol 3-kinases are enzymes that catalyse the phosphorylation of phosphatidylinositol [PI], phosphatidylinositol-4-phosphate [PI(4)P] or phosphatidylinositol-4,5-bisphosphate [PI(4,5)P2] at the D-3 position of the inositol ring (Carpenter *et al.*, 1990) to produce phosphatidylinositol-3-phosphate [PI(3)P], phosphatidylinositol-3,4-bisphosphate [PI(3,4)P2] and phosphatidylinositol-3,4,5-trisphosphate [PI(3,4,5)P3] respectively. This broad substrate range has since been limited to PI3K from Class I but their preferred

substrate appears to be PI(4,5)P2. PI3K from Class II only phosphorylates PI and PI(4)P and PI3K from class III only uses PI as a substrate (Vanhaesebroeck *et al.*, 1997).

Class I_A is the major class of PI3Ks involved in insulin signalling (Shepherd, 2005). Each Class I_A PI3K is a dimer consisting of two subunits, a 110 kDa catalytic subunit (p110) and an 85 kDa adapter subunit (p85). The p85 subunit contains two SH2 domains and a SH3 domain. Three p110 isoforms have been identified (p110a, p110b and p110d) and seven adapter proteins have been identified. These arise as splice variants from three different genes: p85α and p85β express full-length proteins and the p55γ gene expresses a truncated protein. PI3K is activated when the phosphorylated YMXM motifs in the IRS protein occupy both SH2 domains in the p85 subunit (Backer *et al.*, 1992). Not only is PI3K activated, but binding to IRS targets the p110 catalytic subunit to its substrate in the plasma membrane – PI(4,5)P2. The production of a localised concentration of PI(3,4,5)P3 leads to the recruitment of downstream signalling molecules containing a pleckstrin homology (PH) domain.

1.3.1.4 Inhibition of PI3K Signalling

The action of PI3K is controlled through the action of lipid PI(3,4,5)P3 phosphatases. One enzyme is called 'Type II SH2-domain-containing inositol 5-phosphatase' (SHIP2) which removes the 5' phosphate from PI(3,4,5)P3 to form PI(3,4)P2 and can be regulated by tyrosine kinases through its SH2 domain. SHIP2 activity is found downstream of the insulin receptor (Guilherme *et al.*, 1996). SHIP2 regulates insulin-stimulated glucose transport as it has been shown that SHIP2 knockout mice have increased insulin sensitivity and increased recruitment of GLUT4 to the plasma membrane (Clement *et al.*, 2001).

The second enzyme involved is the 'phosphatase and tensin homologue' – PTEN. PTEN is a specific 3' phosphatase that results in the conversion of PI(3,4,5)P3 to PI(4,5)P2. Overexpression of PTEN prevents the formation of PI(3,4,5)P3 and results in the inhibition of GLUT4 translocation to the plasma membrane following insulin stimulation (Nakashima *et al.*, 2000).

1.3.1.5 Downstream Signalling from PI3K

1.3.1.5.1 3'-Phosphoinositide-Dependent Kinase-1

The pleckstrin homology (PH) domain is a specialised domain of about 100 amino acids which bind phospholipids. PI3K therefore generates lipids, through which signalling molecules bind, thus recruiting the proteins to the plasma membrane. 3'-phosphoinositide-dependent kinase-1 (PDK1) is a 63 kDa serine / threonine kinase ubiquitously expressed in human tissues. PDK1 consists of two domains, an N-terminal kinase domain and a C-terminal PH domain which binds PI(3,4,5)P3 and PI(3,4)P2 *in vitro*, with high affinity (Vanhaesebroeck and Alessi, 2000). PDK1 was first identified in 1997 as the kinase that phosphorylates protein kinase B (PKB) at threonine 308 (Alessi *et al.*, 1997). PKB had been shown to increase GLUT4 translocation (Kohn *et al.*, 1996) and is discussed further in section 1.3.1.5.2. PDK1 is a signalling molecule involved in insulin-stimulated GLUT4 translocation and the PH domain is essential in this process (Grillo *et al.*, 1999). Recently, a study using hearts from PDK1 knockout mice has provided genetic evidence that PDK1 plays a crucial role in promoting insulin-stimulated glucose uptake in cardiac muscle (Mora *et al.*, 2005). PDK1 therefore provides the link between PI3K and PKB in the insulin-stimulated glucose transport pathway. The subcellular distribution of PDK1 has not been definitively identified. In the basal cell, PDK1 is found in the cytosol and at the plasma membrane which is thought to be linked via the PH domain. There is also conflicting evidence as to whether PDK1 translocates to the plasma membrane following growth factor activation (Vanhaesebroeck and

Alessi, 2000). Activation of PDK1 ultimately leads to the phosphorylation and activation of further serine / threonine kinases namely PKB (isoforms α and β) (Section 1.3.1.5.2) and the atypical PKC isoforms ζ and λ (Section 1.3.1.5.4).

1.3.1.5.2 Protein Kinase B

Protein kinase B (PKB), so called due to its homology with protein kinase A and protein kinase C, is also known as Akt. PKB is a serine / threonine kinase and has a molecular weight of 57 kDa. Three main isoforms of PKB have been identified in mammalian cells: PKBα / Akt1, PKBβ / Akt2 and PKBγ / Akt3. PKB comprises an N-terminal PH domain, a catalytic domain and a C-terminal regulatory domain. PKB is phosphorylated at two sites – one residue is threonine 308 in the catalytic domain and the other is serine 473 in the regulatory domain. The inactive, unphosphorylated, form of PKB resides in the cytosol. The generation of PI(3,4,5)P3 by PI3K recruits PKB to the plasma membrane. The binding of PKB to the plasma membrane through its PH domain results in a conformational change in the kinase. This leads to the phosphorylation of Thr^{308} and Ser^{473}. PDK1 phosphorylates Thr^{308} in the catalytic domain (Brazil and Hemmings, 2001). The Ser^{473} kinase, known as 'PDK2' for many years, has been identified earlier this year as the mammalian target of rapamycin (mTOR) kinase complexed to the regulatory protein RICTOR (Sarbassov *et al.*, 2005). Since this initial study, the mTOR-RICTOR complex has also been shown to phosphorylate Ser^{473} in insulin-responsive tissues (Hresko and Mueckler, 2005). Therefore, mTOR-RICTOR is likely to be the Ser^{473} kinase involved in insulin-stimulated GLUT4 translocation to the plasma membrane. Following phosphorylation at both sites, the activated PKB then phosphorylates substrates at the plasma membrane, in the cytosol or in the nucleus containing a RXRXXS/T motif.

PKB is important in GLUT4 translocation. A constitutively active form of PKB increases the rate of glucose transport and the level of GLUT4 at the plasma

membrane (Kohn *et al.*, 1996), whereas a dominant-negative form of PKB prevents the insulin-dependent translocation of GLUT4 to the plasma membrane (Wang *et al.*, 1999). PKBβ is the most important PKB isoform involved in insulin-stimulated glucose uptake. Knockdown studies using small-interfering RNA (siRNA) have shown that reduction in the levels of PKBα alone slightly impairs insulin-stimulated glucose transport. However, a 70% reduction in the levels of PKBβ inhibits approximately half of the insulin responsiveness (Jiang *et al.*, 2003). Work using PKBα and PKBβ knockout mice also corroborates the significance for PKBβ in insulin-stimulated glucose uptake (Bae *et al.*, 2003). The role of PKBα cannot be excluded, however, as combined depletions of PKBα and PKBβ further attenuate the action of insulin on GLUT4 translocation (Jiang *et al.*, 2003). By fusing constitutively active and kinase-inactive mutants of PKB to the N-terminus of GLUT4 in intracellular vesicles, it was found that PKB activation at, or close to, the GLUT4 vesicle was necessary, but not sufficient, to induce GLUT4 vesicle translocation to the plasma membrane (Ducluzeau *et al.*, 2002). PKB must therefore phosphorylate substrates localised close to GLUT4 vesicles.

1.3.1.5.3 PKB Substrates

PKB phosphorylates proteins containing RXRXXS/T motifs. Two such proteins have been identified as being involved in insulin-stimulated glucose transport although many more PKB substrates have been identified. These two proteins are AS160 and 'phosphoinositide kinase for five position containing a fyve finger' (PIKfyve).

AS160 was first identified as a substrate for PKB in 2002 (Kane et al., 2002). The name derives from the fact that it is an Akt Substrate of 160 kDa. AS160 consists of two PTB domains, a Rab-GAP domain (GAP stands for GTPase-activating protein) and five PKB phosphorylation sites (Sano *et al.*, 2003). Rab proteins are small G-proteins involved in vesicle trafficking. In their GTP-bound

form, the Rab protein is involved in vesicle movement and fusion. The GAP for a Rab stimulates the intrinsic GTPase activity of the Rab to generate the inactive GDP-bound form of the Rab. The insulin-stimulated phosphorylation of AS160 and a functional GAP domain is required for GLUT4 translocation to the plasma membrane (Sano *et al.*, 2003), thus providing evidence that AS160 is important in insulin-stimulated glucose transport. AS160 is specific for Rabs 2A, 8A, 10 and 14 which are present on the GLUT4 vesicle (Larance et al., 2005, Miinea et al., 2005). AS160 is associated with GLUT4 vesicles in the basal state but not with insulin-stimulated GLUT4 vesicles (Larance *et al.*, 2005). A mechanism involving AS160 and GLUT4 translocation to the plasma membrane has been postulated, in which the insulin-stimulated translocation of GLUT4 requires a Rab in its active GTP form. In basal cells, the Rab involved in translocation is maintained in its inactive GDP form by the GAP domain of AS160. This GAP activity of AS160 is inhibited after AS160 is phosphorylated by insulin-activated PKB. This increases the level of the active GTP form of a Rab and thus GLUT4 vesicle translocation is triggered (Sano *et al.*, 2003). This theory has further been confirmed recently by the use of short-hairpin RNA (shRNA) to knockdown the AS160 protein. Results confirmed that the AS160 GAP activity was required for the basal retention of GLUT4 (Eguez *et al.*, 2005).

PIKfyve is the second protein identified as being downstream of PKB and involved in insulin-stimulated GLUT4 translocation. PIKfyve catalyses the synthesis of PI(5)P and PI(3,5)P2. PIKfyve consists of a PI(3)P-binding FYVE domain at the N-terminus, a DEP (dishevelled, Egl-10 and pleckstrin homology) domain of unknown function, a chaperonin-like region and a PI 5-kinase catalytic domain at the C-terminus. PIKfyve was first reported to have a role in insulin-stimulated glucose transport by the use of dominant-negative PIKfyve (Ikonomov *et al.*, 2002). PIKfyve is phosphorylated by PKB at serine 318 and this phosphorylation stimulated the PI(3)P 5-kinase activity of the enzyme. PIKfyve does co-localise with a highly motile subpopulation of GLUT4

vesicles. Furthermore, expression of a PIKfyve construct mutated at the PKB phosphorylation site enhances insulin-stimulated GLUT4 translocation (Berwick *et al.*, 2004). This gives evidence for the role of PIKfyve in GLUT4 trafficking. However, further experiments are needed to determine if PIKfyve is an important signalling molecule in this process.

1.3.1.5.4 Protein Kinase C

Protein kinase C (PKC) is a serine / threonine kinase. The PKC family of enzymes is subdivided into three categories (conventional, novel and atypical) depending on their activation requirements. The conventional (cPKC) isoforms (α, β_I, β_{II} and γ) require phosphatidylserine (PS), calcium and diacylglycerol (DAG) for activation. The novel (nPKC) isoforms (δ, ε, η, θ and μ) require PS and DAG, and the atypical aPKC isoforms (ζ, ι and λ) require PS but not calcium or DAG.

The general structure of a PKC molecule consists of a catalytic and a regulatory domain, composed of a number of conserved regions, interspersed with regions of lower homology, the variable domains. The aPKC isoforms, ζ, ι and λ, but not the conventional or novel isoforms, are required for insulin-stimulated glucose transport (Bandyopadhyay *et al.*, 1997). aPKC is composed of a regulatory N-terminus and a catalytic C-terminus. The N-terminus regulatory subunit includes a pseudosubstrate which binds to, and inhibits, its own kinase domain by preventing both autophosphorylation and phosphorylation by other signalling molecules. Binding of acidic phospholipids, PI(3,4,5)P3 and PS (although PKC lacks a PH domain), to the regulatory subunit of aPKC increases the catalytic activity of the protein in response to insulin, by three separate but interrelated pathways: (1) abolishing the pseudosubstrate-dependent autoinhibition, resulting in a conformational change in PKC and subsequent activation, (2) increasing the level of phosphorylation at threonine-410 by PDK-1, and (3) increasing the level of

autophosphorylation at threonine-560 (Standaert *et al.*, 2001). Thus there are both phosphorylation and PDK-1 dependent and independent pathways to activate aPKC.

Several studies have reported a role for aPKC in insulin-stimulated glucose transport and GLUT4 translocation. These are highlighted in a review by Farese (Farese, 2002). Insulin-stimulated glucose transport is inhibited by both general PKC inhibitors in all insulin-responsive tissues and by a cell permeable myristoylated PKC-ζ pseudosubstrate (Bandyopadhyay *et al.*, 1997).

Expression of constitutively active PKC-λ mimicked the effect of insulin-stimulated glucose transport and the expression of a kinase-dead form of PKC-λ completely blocked glucose uptake in insulin-stimulated but not in basal muscle cells. In agreement with the effect on insulin-stimulated glucose transport, constitutively active PKC-λ mimicked, and kinase-dead PKC-λ completely inhibited, insulin-stimulated GLUT4 translocation to the plasma membrane (Bandyopadhyay *et al.*, 2000).
Mouse embryonic stem cells have had both alleles that encode the major aPKC (PKC-λ) knocked out. The effect of insulin on glucose transport was severely compromised but can be fully rescued by the adenoviral-mediated expression of PKC-λ (Bandyopadhyay *et al.*, 2004). At present, it is not known how PKC mediates its effects to increase the level of GLUT4 at the plasma membrane. It is interesting to note that PKC is not involved in insulin-stimulated glucose transport in cardiomyocytes. Instead PKC activation induces insulin resistance by modifying the insulin sensitivity of the cardiomyocyte (Russ and Eckel, 1995).

1.3.2 Phosphatidylinositol 3-Kinase-Independent Pathway

PI3K is accepted as a critical component in the transmission of the insulin signal to mobilise GLUT4 to the plasma membrane. However it seems that PI3K alone is not sufficient to promote insulin-stimulated GLUT4 translocation and glucose uptake. Cell permeable derivatives of PI(3,4,5)P3 were unable to stimulate glucose transport in adipocytes. However, they did restore insulin-stimulated glucose transport in cells where PI3K was inhibited by wortmannin (Jiang *et al.*, 1998). Other evidence supporting this concept includes the fact that growth factors such as PDGF, IL4, or β1-integrin clustering, stimulate IRS-1 associated PI3K activity to a similar extent to that seen with insulin. However, only minor effects were observed with regard to changes in glucose uptake (Isakoff et al., 1995, Guilherme and Czech, 1998). It has therefore been postulated that a second insulin signalling pathway, distinct but perhaps acting in conjunction with the PI3K-dependent pathway, is necessary for insulin-stimulated GLUT4 translocation and glucose uptake in adipocytes. Several studies have identified this additional insulin-signalling pathway as the 'CAP/Cbl pathway'. However, the CAP/Cbl pathway stimulating GLUT4 translocation is only present in adipocytes, it is not functional in muscle (JeBailey *et al.*, 2004). The CAP/Cbl pathway has remained controversial in the GLUT4 field and recent evidence, presented below, has further questioned the relevance of this pathway.

1.3.2.1 The CAP/Cbl pathway

A subset of functional insulin receptors is present in specialised caveolae-enriched lipid raft microdomains in the plasma membrane (Gustavsson et al., 1999). The proto-oncogenes c-Cbl and Cbl-b are phosphorylated after activation of the insulin receptor and are recruited by adapter proteins to the caveolin-enriched lipid raft compartments (Baumann *et al.*, 2000). APS and

CAP are two adapter proteins involved in this recruitment. The CAP (c-Cbl-associated protein) adapter protein contains three SH3 domains in its C-terminus and a region of homology to the gut peptide sorbin in its N-terminus referred to as a SoHo domain. The proline-rich domains in Cbl bind to the SH3 domains in CAP and the CAP/Cbl complex forms. APS is a second adapter protein implicated in the CAP/Cbl pathway. APS contains a SH2 domain, through which it interacts with the insulin receptor. Following phosphorylation by insulin, APS binds to the SH2 domain of Cbl. This recruits the CAP/Cbl complex to the insulin receptor and Cbl is phosphorylated by the insulin receptor at three tyrosine residues (Liu *et al.*, 2002). The CAP/Cbl complex dissociates from the insulin receptor after Cbl is phosphorylated. The SoHo domain in the CAP protein binds to the lipid raft protein flotillin and so localises Cbl to the lipid raft domain in the cell membrane (Baumann et al., 2000, Kimura et al., 2001). Deletion of the SoHo domain disrupts this targeting and inhibits insulin-stimulated glucose uptake and GLUT4 translocation to the plasma membrane (Kimura *et al.*, 2001). The SH2 domain of another adapter protein, CrkII, binds to a phosphorylated tyrosine in Cbl. CrkII contains a SH3 domain, through which it is associated to a guanylnucleotide exchange factor (GEF) called C3G. C3G activates the Rho family protein TC10 by catalysing the exchange of GTP to GDP (Chiang *et al.*, 2001). Two isoforms of TC10 (TC10α and TC10β) are both activated by insulin and are both present in lipid raft domains in adipocyte cell membranes (Chiang *et al.*, 2002). TC10 is important in insulin-stimulated glucose transport as a dominant-interfering TC10 mutant inhibits insulin-stimulated glucose uptake (Chiang *et al.*, 2001). TC10 interacts with various effector molecules that may play a role in insulin-stimulated glucose transport. The CIP4/2 (Cdc42-interacting protein 4/2) protein has an intracellular localisation and, following insulin stimulation, it translocates to the plasma membrane. Insulin-stimulated GLUT4 translocation is inhibited following transfection of a mutant form of CIP4/2, suggesting a role for CIP4/2 in glucose uptake (Chang *et al.*, 2002). TC10 also interacts with a component from the exocyst complex, Exo70 (Inoue *et al.*, 2003). Exo70 translocates to

the plasma membrane after insulin-induced activation of TC10. The exocyst complex may have a role in GLUT4 vesicle fusion with the plasma membrane because mutant Exo70 does not affect the rate of trafficking of the GLUT4 vesicle but inhibits glucose uptake (Inoue *et al.*, 2003). Further work is needed to elucidate a mechanism whereby these signalling molecules stimulate the translocation of GLUT4 to the plasma membrane.

Two independent studies involving the use of small interfering RNA (siRNA) have given conflicting results as to the importance of the CAP/Cbl pathway in insulin-stimulated glucose uptake. The first study involved the siRNA depletion of APS or Cbl which resulted in the inhibition of insulin-stimulated glucose transport (Ahn *et al.*, 2004), implicating a role for the CAP/Cbl pathway in this mechanism. The second study used siRNA to deplete Cbl, CAP or CrkII. This depletion failed to diminish insulin-stimulated glucose transport or GLUT4 translocation (Mitra et al., 2004, Zhou et al., 2004). This study argues against the role of the CAP/Cbl pathway in insulin-stimulated glucose transport. It has not been resolved which of these studies is correct. However, following the knockdown of the proteins, the first study did not determine whether the levels of the GLUT4 protein were reduced due to the toxicity of the siRNAs used.

1.3.2.1.1 Intersection of the PI3K-Dependent and -Independent Pathways

Atypical PKC is phosphorylated by PDK1 in the PI3K-dependent pathway (Section 1.3.1.5.4). However, following the activation of TC10, aPKC has also been reported to be phosphorylated and recruited to lipid raft microdomains when it is in complex with Par3 and Par6 proteins (Kanzaki *et al.*, 2004). Thus, aPKC is also involved in the CAP/Cbl insulin-signalling pathway. Other downstream targets of TC10 may also prove to be sites of convergence in the two pathways.

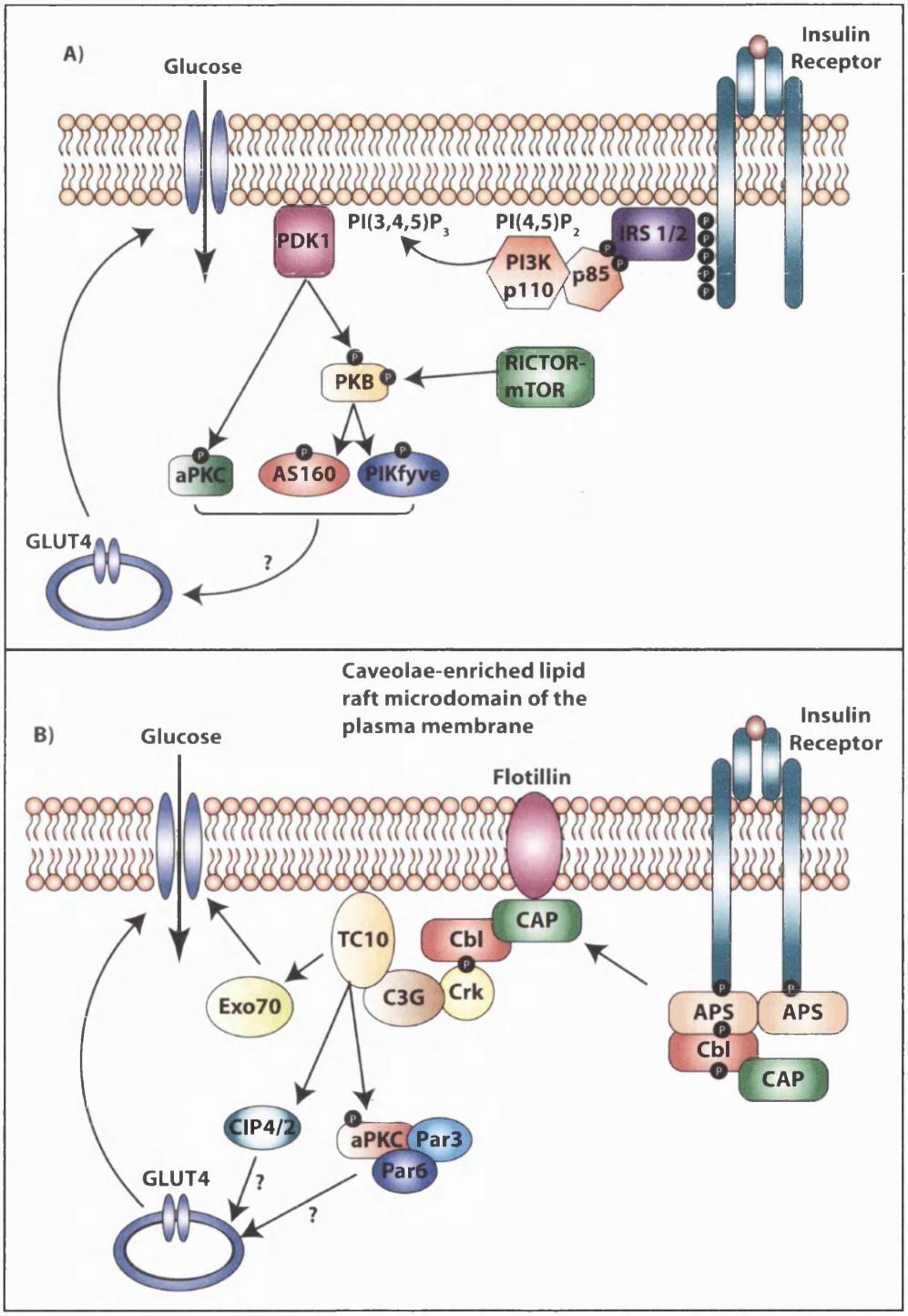

Figure 1.2 **Insulin signalling cascades which culminate in the translocation of GLUT4 to the plasma membrane.** Two insulin-dependent pathways are involved in GLUT4 translocation, a PI3K-dependent (A) and a PI3K-independent (B) pathway. See text for details. Adapted from (Saltiel and Kahn, 2001) and (Chang *et al.*, 2005).

1.4 Insulin-Independent Signalling Pathways Involved in Glucose Uptake

Contracting muscle increases glucose transport via stimulating the translocation of GLUT4 to the plasma membrane. The contraction-stimulated pathway occurs through an insulin-independent mechanism but the mediators of this signal are still unknown. AMP-activated protein kinase (AMPK) has been implicated as being involved in contraction-stimulated glucose transport. However, studies using transgenic mice expressing a dominant inhibitory form of AMPK suggest that other AMPK-independent pathways are also involved in contraction-mediated glucose uptake (Mu *et al.*, 2001).

It is difficult to assess the effect of contraction-stimulated GLUT4 translocation in basal cardiomyocytes because the heart is continually contracting. It has been proposed that in mice lacking the insulin receptor, glucose uptake in non-contracting cells is reduced. Therefore, in non-contracting cells the majority of GLUT4 is intracellular (Belke *et al.*, 2002). The mechanism for GLUT4 translocation in response to contraction in cardiomyocytes has been investigated in a few studies. The effect of insulin and contraction on glucose transport activation is not additive. This is more likely to be because the two pathways converge in cardiomyocytes rather than there being two separate pools of GLUT4 in the heart (Kolter et al., 1992, Till et al., 1997). Additional work has concluded that glucose transport in response to contraction, involves the activation of PI3K (i.e. a wortmannin-sensitive pathway) without the activation of the insulin receptor or IRS signalling molecules and also does not lead to the downstream activation of PKB (Till *et al.*, 2000). Like insulin stimulation, contraction stimulates the exocytosis of GLUT4 without any marked change in the rate of endocytosis (Yang and Holman, 2005). However, further work is needed before the mechanism of contraction-stimulated glucose transport in cardiomyocytes can be fully understood.

Skeletal muscle is composed of a heterogeneous population of fiber types. The contraction-stimulated signalling pathways that lead to GLUT4 translocation to the plasma membrane are variable between the different skeletal muscle fiber types. In slow twitch oxidative muscle fibers (e.g. soleus muscle), contraction stimulates glucose transport via a pathway that does not include the key signalling molecules involved in the insulin-stimulated pathway. The contraction-stimulated pathway does not involve PKB. PI3K is also not involved as contraction-stimulated glucose transport is not inhibited by wortmannin (a PI3K inhibitor). The effect of both insulin and contraction on glucose transport activity and the cell surface levels of GLUT4 were almost completely additive (Lund et al., 1995, Lund et al., 1998). In fast twitch glycolytic fibers (e.g. extensor digitorum longus muscle) the contraction-stimulated pathway does include the key signalling molecules involved in the insulin-stimulated glucose transport pathway. Contraction of fast twitch glycolytic fibers leads to the activation of PKB via a PI3K-sensitive pathway which is inhibited by wortmannin (Sakamoto et al., 2002, Sakamoto et al., 2003). Therefore, the signalling pathway initiated following contraction in cardiomyocytes (although very dependent on oxidative metabolism), may resemble the contraction-stimulated signalling pathway in fast twitch muscle more closely than in slow twitch skeletal muscle (Yang and Holman, 2005).

Hypoxia and ischemia are two important pathological conditions which also induce glucose uptake in muscle cells. Under hypoxic and ischemic conditions GLUT4 translocates to the sarcolemma and increases the glucose transport into the cell (Young et al., 1997, Montessuit et al., 1998, Fuller et al., 2001). This signalling pathway terminating in GLUT4 translocation is independent from the insulin-stimulated pathway but may have additive effects on GLUT4 translocation to the plasma membrane (Sun *et al.*, 1994). AMPK activity increases during ischemia. Therefore, Russell and colleagues investigated whether AMPK stimulates GLUT4 translocation through the use of 5-aminoimidazole-4-carboxyamide-1-β-D-ribofuranoside (AICAR), an activator of

AMPK. AICAR increases AMPK activation and GLUT4 translocation and use of a competitive inhibitor of AMPK decreases the level of glucose uptake. It has therefore been concluded that AMPK is important in GLUT4 translocation in hypoxic conditions (Russell, III *et al.*, 1999). The full mechanism by which AMPK activates GLUT4 translocation has not been fully elucidated but it is thought that an increase in the AMP/ATP ratio stimulates AMPK activity. The signalling pathways resulting in the translocation of GLUT4 to the plasma membrane in response to contraction and hypoxia must differ even though AMPK is implicated in both pathways. This is because the two pathways converge on the GLUT4 trafficking pathway at different steps. Contraction, like insulin stimulation, increases the rate of GLUT4 exocytosis with little effect on the rate of endocytosis. However, in contrast to insulin- and contraction-stimulated glucose transport, hypoxia and ischemia do not stimulate GLUT4 exocytosis. Instead, it leads to a reduction in GLUT4 endocytosis (Yang and Holman, 2005).

1.5 GLUT4 Trafficking

The following section will highlight the complexity of GLUT4 vesicle trafficking. However, as will be seen, a lot more investigation is needed before the full extent of GLUT4 trafficking will be fully understood. Figure 1.3 illustrates what has been identified thus far.

1.5.1 The Intracellular GLUT4 Compartment

GLUT4 constitutively cycles between intracellular compartments and the plasma membrane in both basal and insulin-stimulated adipocytes (Yang and Holman, 1993). Insulin increases the number of GLUT4 transporters on the plasma membrane without increasing the total number of transporters in the

cell. It does this by increasing the rate of exocytosis of GLUT4 to the plasma membrane and has little or no effect on the rate of endocytosis (Yang and Holman, 1993, Satoh et al., 1993). GLUT4 must therefore be sequestered inside the cell under basal conditions. Through the use of electron microscopy, GLUT4 has been found to have an intracellular localisation in basal conditions. GLUT4 is predominantly in the trans-Golgi network (TGN) and tubulo-vesicular structures throughout the cytoplasm (Slot et al., 1991, Malide et al., 2000). In unstimulated cells, a subset of GLUT4 transporters co-localise with endosomal markers (TGN-38, Mannose-6-phosphate, transferrin receptor) in the peri-nuclear region, probably late endosomes and the TGN. GLUT4 is also present in specialised compartments, which are associated with VAMP2. Following insulin stimulation, GLUT4 still co-localises with the endosomal markers but not with VAMP2. Therefore, the specialised GLUT4 vesicles associated with VAMP2 must be the predominant pool of GLUT4 that translocates to the plasma membrane in response to insulin (Malide *et al.*, 1997). Chemical ablation of endosomes using a transferrin/HRP construct has revealed that 60% of GLUT4 in basal adipocytes is not present in the endosomal system and that insulin-stimulated glucose transport is not affected by the ablation (Martin et al., 1996, Martin et al., 1998).

Insulin stimulates the fusion of GLUT4 vesicles with the plasma membrane. These vesicles are primarily VAMP2 positive vesicles but a small population of mannose-6-phosphate positive GLUT4 vesicles also fuses with the plasma membrane. The authors conclude that insulin causes the fusion of pre-existing VAMP2 positive GLUT4 vesicles and also increases the sorting of GLUT4 from the endosomal-TGN system (Ramm *et al.*, 2000). Other studies have shown that GLUT4 in the endosomal system as well as GLUT4 in the specialised compartments is translocated to the plasma membrane (through the specialised compartment) following insulin stimulation (Millar et al., 2000, Zeigerer et al., 2002).

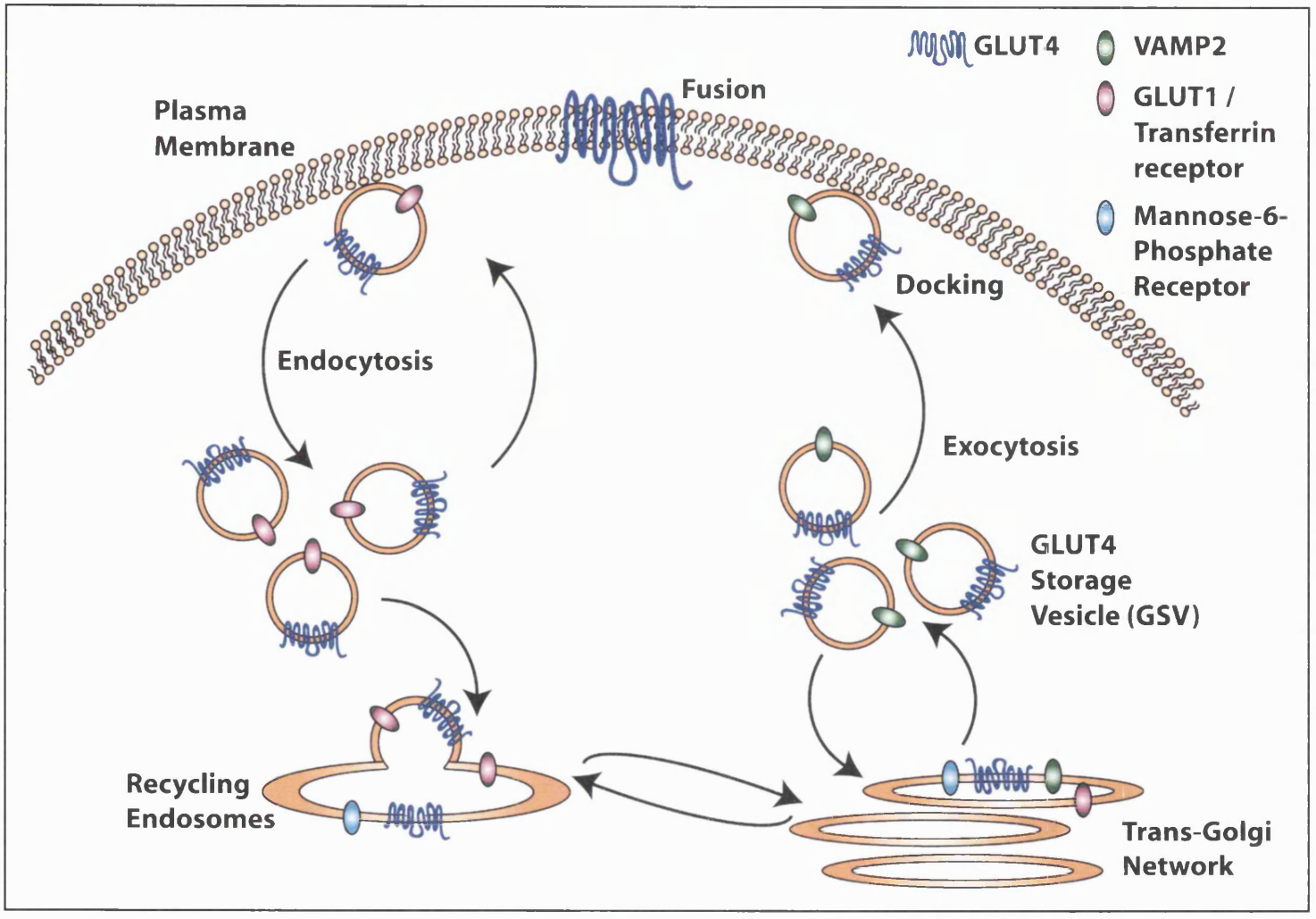

Figure 1.3 **The current understanding of GLUT4 vesicle trafficking.** See text for details.

The slow rate of basal GLUT4 exocytosis indicates that under basal conditions GLUT4 is specifically sequestered in intracellular compartments. These intracellular GLUT4 vesicles are highly specialised, insulin-sensitive compartments, distinct from the recycling endosomes and will be referred to as a 'GLUT4 storage vesicle' (GSV).

1.5.1.1 Proteins Identified in the GLUT4 Storage Vesicle

An insulin-responsive aminopeptidase (IRAP) has been identified as a major protein that co-localises with GLUT4 on GSVs. In response to insulin, IRAP traffics in a manner very similar to GLUT4. IRAP is not just present on GSVs but is present in all GLUT4-containing compartments (Keller et al., 1995, Ross et al., 1996). Interaction of the N-terminus of IRAP with a protein termed p115 in the peri-nuclear region of the cell has led to the theory that IRAP may have a role in the tethering of GLUT4 in an intracellular location (Hosaka *et al.*, 2005).

The v-SNARE vesicle-associated membrane protein 2 (VAMP2) is found on GSVs (where v-SNARE stands for a vesicular soluble N-ethylmaleimide-sensitive factor attachment protein receptor) but it is not found on other GLUT4-containing compartments. VAMP3 (cellubrevin) co-localises with GLUT4 in the endosomal compartments (Martin *et al.*, 1996). VAMP2 has been found to play a role in insulin-stimulated translocation of GLUT4 from GSVs (Olson et al., 1997, Martin et al., 1998).

A recent study has identified three Rab proteins that are present on GLUT4 vesicles. These proteins are Rab10, Rab11 and Rab14. In the basal state the downstream target of PKB, the Rab GTP-ase activating protein AS160 (Section 1.3.1.5.3), is associated with the GLUT4 vesicles. The Rab proteins on the GLUT4 vesicles could therefore be potential targets for AS160 (Larance *et al.*, 2005).

1.5.1.2 Adaptor Proteins

Adaptor proteins (AP) are a growing family of proteins that select cargo for inclusion into coated vesicles in the late secretory and endocytic pathways. The family is composed of four adaptor proteins (AP1-4) together with a family of monomeric adaptors called GGAs. Each member of the family of adaptor proteins has a distinct cellular distribution and they select specific cargo into distinct types of vesicles.

AP1, AP2, AP3 and AP4 have a heterotetrameric structure consisting of two large subunits, a medium sized μ subunit and a small σ subunit (AP1: γ, β1, μ1 and σ1, AP2: α, β2, μ2 and σ2, AP3: δ, β3, μ3 and σ3 and AP4: ε, β4, μ4 and σ4). AP1 and AP2 are found in clathrin-coated vesicles. AP1 is localised on the TGN and AP2 is localised on the plasma membrane. They attach the clathrin to the membrane, select the vesicle cargo and recruit accessory proteins that regulate vesicle formation. AP3 and AP4, like AP1, are localised on intracellular membranes. AP3 is predominantly found on endosomes and AP4 is found on the TGN. However, AP3 and AP4 differ from AP1 and AP2 because they are not found on clathrin coated-vesicles (Robinson, 2004).
The family of Golgi-localised, γ-ear-containing, ARF-binding (GGA) proteins have also been identified as adaptor proteins. GGA proteins are monomeric and take their name because the C-terminal domain contains an 'ear' domain similar to the γ subunit in AP1. The GGA proteins are found on the membrane of both the TGN and endosomes, similar to AP1. The extent of the co-localisation between AP1 and GGAs has not been fully determined. There is co-localisation but it is still under debate as to their relationship, whether they act in parallel or opposing trafficking pathways. The GGA proteins function with clathrin but they are not detected on clathrin-coated vesicles (Robinson, 2004).

The mechanism by which GLUT4 is sequestered from the endosomal system into the GSV may involve the interaction of GLUT4 with a range of adaptor

complexes. The first evidence to suggest this comes from observations using immunoelectron microscopy, which identified GLUT4 localised to intracellular vesicles containing the Golgi-derived γ-adaptin subunit of AP1 (Marsh *et al.*, 1998). In addition, GLUT4 vesicles have been shown to associate with significant levels of AP1 adaptor subunits γ, μ1 and δ1, which are localised in the TGN (Gillingham *et al.*, 1999). Further evidence for the interaction of GLUT4 with the AP1 complex, is the observation that the β1 subunit of AP1 binds a peptide based on the C-terminal sequence of GLUT4 which contains the di-leucine motif ($L^{489}L^{490}$) (Rapoport *et al.*, 1998). AP1 could be involved in the budding of vesicles containing GLUT4 to and from the TGN to the GSV. This could be particularly important in the basal retention of GLUT4 in its intracellular compartment in the proposed cycling models (Section 1.5.2). AP3 has also been found to associate with isolated GLUT4 vesicles and could also be involved in the intracellular sorting of GLUT4 into GSVs (Gillingham *et al.*, 1999).

Clathrin-mediated endocytosis from the plasma membrane involves the AP2 complex. AP2 facilitates the recruitment of proteins into clathrin coated pits for efficient endocytosis. AP2 interacts with proteins that contain a YXXΦ motif (Y is tyrosine or potentially phenylalanine, X is any amino acid and Φ is any hydrophobic amino acid). The FQQI motif in the N-terminus of GLUT4 is a possible interaction motif for AP2. Indeed, mutation of the FQQI domain has identified it as an important internalisation motif (Section 1.6.1). The GGAs are also important in GLUT4 intracellular sorting and will be explained in section 1.5.1.3.

1.5.1.3 Generation of GLUT4 Storage Vesicles

There are two possibilities for the mechanism whereby newly synthesised GLUT4 enters the GSV. The first is that the GLUT4 first traffics to the plasma membrane, where during sorting following endocytosis, GLUT4 is sorted into

the GSV. The second way is that GLUT4 is sorted directly from the TGN into the GSV. This issue has been resolved by the use of a dominant-interfering dynamin mutant, which inhibits endocytosis. The inhibition of endocytosis did not affect insulin-stimulated GLUT4 translocation (Watson *et al.*, 2004a). Newly synthesised GLUT4, therefore, directly traffics from the TGN to the GSV (the second scenario above). GGA proteins are involved in the sorting of the mannose-6-phosphate receptor at the TGN (Puertollano *et al.*, 2001). GLUT4 co-localises with a subset of mannose-6-phosphate receptors in the endosomal system and so the potential effect of the GGA adapter proteins on the sorting of GLUT4 into the GSV has been investigated. By using a dominant-interfering GGA mutant it was concluded that following GLUT4 biosynthesis, GLUT4 traffics and sorts into the GSV in a GGA-dependent process. This is either directly or indirectly through an endosomal intermediate. However, exit from the GSV is GGA independent (Watson *et al.*, 2004a). No direct interaction of GLUT4 and GGA proteins has been found so the authors concluded that the selection of GLUT4 by the GGA proteins must occur through interaction with another vesicular protein. In addition to newly synthesised GLUT4, the recycling pool of GLUT4, i.e. GLUT4 that had been translocated to the plasma membrane and had undergone endocytosis, localises to the GGA-containing compartments in the peri-nuclear region of the cell (in the TGN and in some endosomes) (Li and Kandror, 2005). From the use of immuno-adsorption and GST-pulldown assays, it was shown that GGA proteins interact with GLUT4 vesicles. As the newly synthesised and recycling pools of GLUT4 both undergo GGA-dependent entry into the GSV, the two pathways could converge in either the TGN or endosomal compartments (Li and Kandror, 2005). Further investigation is needed to determine the precise mechanism whereby GGA proteins control the entry of GLUT4 into GSVs. The role AP1 has in this process, either in a parallel or an opposing pathway, also needs to be investigated. Sortilin is a protein found in the TGN and on endosomes and has a GGA-binding motif in its cytoplasmic tail (Nielsen *et al.*, 2001). Sortilin is associated with GLUT4, probably in endosomal vesicles (Lin

et al., 1997, Morris et al., 1998). Further studies have shown that sortilin is necessary and sufficient for the formation of GSVs (Shi and Kandror, 2005). The authors predict that the induction of sortilin is the major event that leads to the formation of GSVs.

1.5.2 Models of GLUT4 Cycling

The mechanism of the storage and the cycling of GLUT4 to the plasma membrane in unstimulated cells and in response to insulin is still under debate. There are several mechanisms that can explain the basal retention of GLUT4. The retention of GLUT4 could occur in endosomes, perhaps involving an intracellular tethering factor. Alternatively, the retention of GLUT4 could occur in the GSVs. A combination of both of these mechanisms could also exist (Coster *et al.*, 2004). Over the years of research into GLUT4, different models have been proposed. The current theories are described below in more detail. Two different laboratories have put forward independent models of GLUT4 cycling in *bone fide* insulin target cells (3T3-L1 adipocytes). The two models differ in the basal trafficking of GLUT4 to the plasma membrane, the presence of a latent (non-translocating) pool of GLUT4 and the involvement of the TGN in the GSV. It is likely that the precise mechanism of the storage and cycling of GLUT4 is in fact a combination of the two models. McGraw and colleagues proposed one model and James and colleagues proposed the second. The models are illustrated diagrammatically in Figure 1.4 A and B respectively.

McGraw and colleagues have proposed that, in the basal state, GLUT4 is retained in the cell by a continual intracellular retrieval / retention mechanism but all GLUT4 can translocate to the plasma membrane in unstimulated cells (Karylowski *et al.*, 2004). GLUT4 rapidly recycles between the GSV and the endosomal compartments that contain the transferrin receptor. It was found that GLUT4-containing vesicles are five times as likely to fuse with endosomes

as they are to fuse with the plasma membrane and hence the intracellular retention of GLUT4. GLUT4 only localises with furin in transferrin receptor-containing endosomes. Furin is present in late endosomes and the TGN (Thomas, 2002) which implies that the TGN is not a major intracellular reservoir of GLUT4. Insulin can stimulate the translocation of GLUT4 to the plasma membrane from either the GSV or the endosomal pool (which traffics through the GSV) (Zeigerer *et al.*, 2002). Rab11 is a GTPase which is required for the trafficking of the transferrin receptor both between the endosomes and the TGN and between the endosomes and the plasma membrane (Ren et al., 1998, Wilcke et al., 2000). Rab11 is necessary for sorting GLUT4 from endosomes and into the GSV. The fact that failure to do this results in a decrease in the rate of translocation observed with insulin, gives further evidence that endosomal GLUT4 translocation is important in insulin-stimulated GLUT4 translocation (Zeigerer *et al.*, 2002) (Figure 1.4 A).

James and colleagues have provided a contrasting mechanism in which there are two interconnected trafficking loops. The first involves trafficking between the plasma membrane and endosomes and the second involves trafficking between endosomes and GSVs. It is proposed that the endosomal recycling pool of GLUT4 and the GSV do not co-operate and only GLUT4 in the endosomal pool transits to the plasma membrane in the basal state (Govers *et al.*, 2004). The James laboratory found that there are two insulin-regulatable pathways involved in insulin-stimulated GLUT4 translocation: (1) insulin increases the number of GLUT4 molecules in the recycling pathway in a dose-dependent manner, (2) insulin increases the rate of exocytosis from endosomes to the plasma membrane. Insulin induces the translocation of GLUT4 from the GSV to the endosomes before translocation to the plasma membrane (Coster *et al.*, 2004). Maximum doses of insulin do not result in all of the GLUT4 from the GSV being translocated to the plasma membrane. This 'latent pool' of GLUT4 could be 'older' GLUT4 i.e. synthesised earlier in the lifetime of the cell and 'newer' GLUT4 could preferentially translocate to the

plasma membrane in response to insulin (Govers *et al.*, 2004). The TGN has also been suggested to play a role in the site of storage for the insulin-responsive GLUT4 molecules i.e. the GSV. The role of the TGN as a GSV has largely been ignored in other models. It has been predicted that the TGN is part of the GSV because, following endocytosis, GLUT4 is translocated through endosomes to a subdomain of the TGN. This subdomain is enriched in the TGN target-soluble N-ethylmaleimide-sensitive factor attachment protein receptors (t-SNAREs) syntaxin 6 and 16. However, the TGN marker TGN38 is not present in this subdomain (Shewan *et al.*, 2003). Syntaxin 6 and 16 have both been implicated in the trafficking of cargo between the endosomes and TGN. However, further work is needed to determine if the TGN is part of the GSV (Figure 1.4 B).

1.5.3 GLUT4 Exocytosis

Insulin increases the rate of GLUT4 exocytosis (Yang and Holman, 1993, Satoh et al., 1993). As previously discussed, the insulin-signalling pathway is diverse and the full extent of how the insulin signal is transmitted to GLUT4 is not fully understood (Section 1.3). Insulin may exert its effects at a number of steps in the exocytotic pathway: (1) intracellular vesicle budding, (2) trafficking of GLUT4 to the plasma membrane, (3) vesicle docking at the plasma membrane, or, (4) vesicle fusion with the plasma membrane. The downstream target of insulin receptor stimulation, AS160 (Section 1.3.1.5.3), has shown a role for insulin in a step before the docking and fusion to the plasma membrane (Zeigerer *et al.*, 2004). Another downstream target of the insulin receptor, PIKfyve (Section 1.3.1.5.3), is believed to be involved in increasing the rate at which GLUT4 is sorted from the internalising endosomes through the TGN and into the GSV pool of GLUT4 (Welsh *et al.*, 2005).

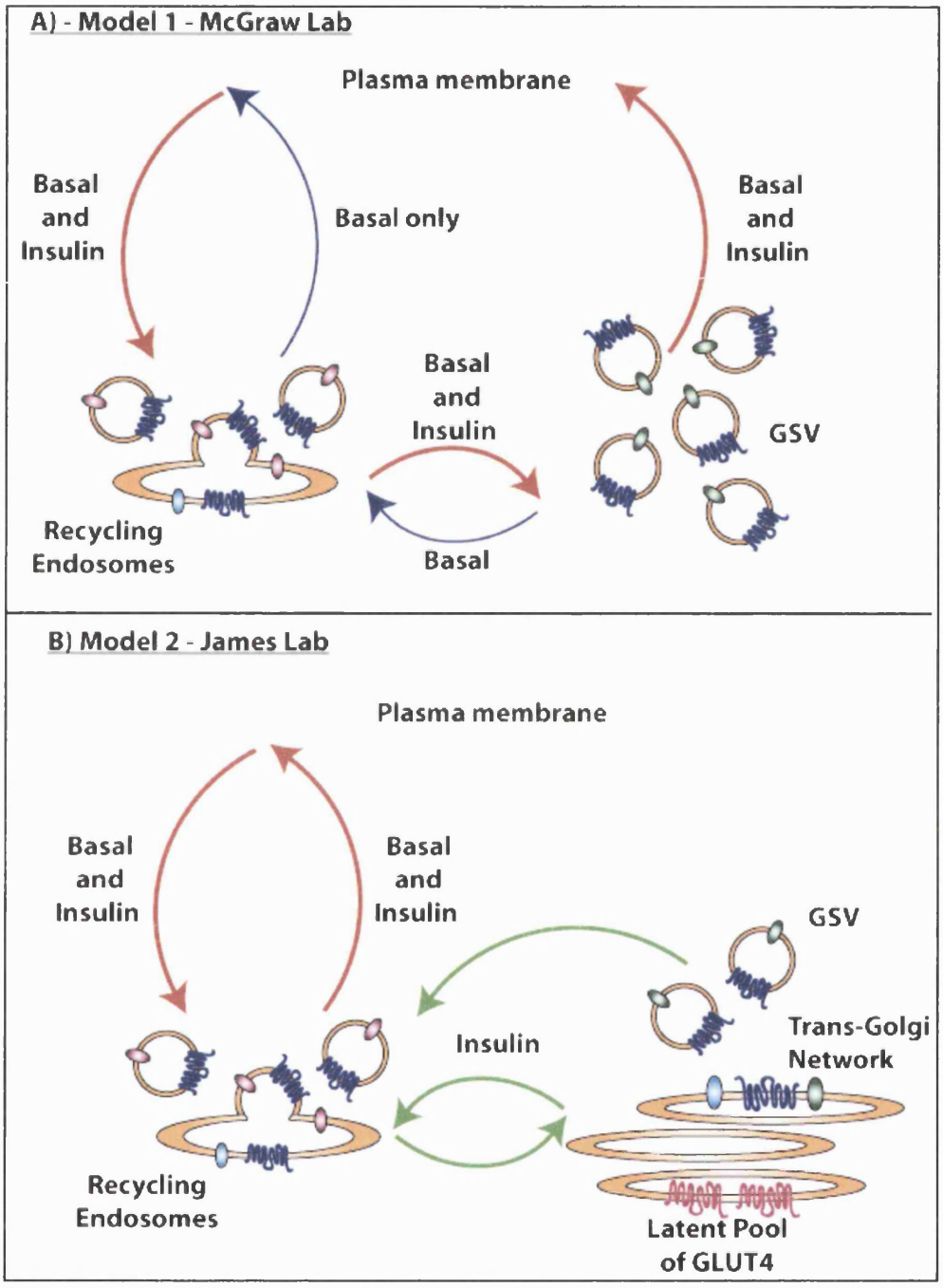

Figure 1.4 **Current models of GLUT4 storage and cycling.** The models differ in whether there is a latent pool of GLUT4 or if all transporters translocate to the plasma membrane, in the contribution of the TGN as an intracellular storage site for GLUT4, and in the route in which GLUT4 translocates to the plasma membrane. Blue arrows = basal translocation, green arrows = translocation in response to insulin and red arrows = translocation in basal and insulin stimulated conditions.

The mechanism by which GLUT4 translocates to the plasma membrane was discussed in section 1.5.2 and occurs either directly from the endosomal pool following trafficking from the GSV to the endosomal pool or from both the endosomal- and GSV-containing GLUT4 pools simultaneously. Studies in our laboratory have also concluded a role for insulin in stimulating GLUT4 vesicle fusion to the plasma membrane (section 1.5.4) (Koumanov *et al.*, 2005).

1.5.4 GLUT4 Fusion with the Plasma Membrane

Once GLUT4 has translocated to the plasma membrane, GLUT4 undergoes a docking and fusion step before it is fully inserted into the membrane and glucose can enter the cell. Fusion of GLUT4 vesicles with the plasma membrane requires specific proteins, which are present on both the GLUT4 vesicle and on the target plasma membrane. The cellular machinery involved in membrane fusion is conserved in all eukaryotes and includes the proteins N-ethylmaleimide sensitive factor (NSF), soluble NSF attachment proteins (SNAPs), SNAP receptors (SNAREs). There are two classes of SNARE protein, v-SNAREs are present on vesicles and t-SNAREs are present on 'target' plasma membranes.

In adipocytes, the vesicle-associated membrane protein 2 (VAMP2 or synaptobrevin 2) is the v-SNARE in the GSV and VAMP3 (cellubrevin) is the v-SNARE on GLUT4-containing endosomes (Cain et al., 1992, Timmers et al., 1996). There is another protein called pantophysin present on GLUT4 vesicles (Brooks *et al.*, 2000). It is believed that pantophysin binds to VAMP2 and thus limits the availability of this SNARE. The t-SNARE proteins involved in GLUT4 vesicle fusion in adipocyte plasma membranes are syntaxin4 (Timmers *et al.*, 1996) and SNAP23 (Rea *et al.*, 1998). Together syntaxin4, SNAP23 and VAMP2 can form an SDS-resistant complex *in vitro* supporting the fact that this complex forms in GSV fusion to the plasma membrane (Rea *et al.*, 1998). This

brings the GSV in close proximity to the plasma membrane. The core of the SNARE complex consists of a bundle of four helices, three from the t-SNARE and one from the v-SNARE (Poirier *et al.*, 1998). Syntaxin4 and VAMP2 each contribute one coil, and SNAP23 contributes two coils to the complex.

Syntaxin4-interacting proteins have been identified, which bind to syntaxin4 in the basal state and so are negative regulators of insulin-induced vesicle fusion. Munc18c prevents vesicle fusion with the plasma membrane by inhibiting the binding of syntaxin4 to VAMP2 (Tellam et al., 1997). Insulin relieves this inhibition by inducing the dissociation of Munc18c from syntaxin4 and by sequestering Munc18c to an alternative plasma membrane binding site (Thurmond *et al.*, 1998). The discovery of AS160 as a downstream target of the insulin receptor has led to the theory that phosphorylation of AS160 in response to insulin and the consequential disabling of its GAP activity leads to the activation of a Rab protein. The GTP-Rab could then directly or indirectly bind to munc18c, thus weakening the munc18c-syntaxin4 interaction. Syntaxin4 could then change its conformation, allowing GSVs to dock and fuse with the plasma membrane (James, 2005). In unstimulated cells, overexpression of Munc18c also enhances the level of GLUT4 in the plasma membrane. This may reflect a positive role for Munc18c in promoting SNARE assembly (Widberg *et al.*, 2003).

Synip, another syntaxin4-interacting protein, has been identified, which binds in the basal state but not in insulin-stimulated cells (Min *et al.*, 1999). Synip has been proposed to be a downstream target of PKBβ at serine 99. A Ser→Phe mutant prevents insulin-stimulated syntaxin4 dissociation, suggesting that phosphorylation at serine 99 is essential for the insulin-stimulated dissociation of synip from syntaxin4 (Yamada *et al.*, 2005). However, shortly after this report was published, another group showed that overexpression of a Ser→Ala mutant at residue 99 in synip, which lacks a phosphorylation site, has no effect on insulin-stimulated GLUT4 translocation. Therefore, this study concluded that phosphorylation of synip at serine 99 is not required for GLUT4 translocation

(Sano *et al.*, 2005). The major difference between the two studies was the amino acid the serine was mutated to. Alanine resembles the unphosphorylated form of serine and so this mutation is unlikely to have any major changes on protein structure. However, phenylalanine is a bulky hydrophobic molecule which might lead to a change in conformation of the protein. The study by Sano and colleagues is likely to be the more accurate due to their alanine mutation of serine 99. Thus phosphorylation of synip is unlikely to play a role in GLUT4 vesicle fusion (Sano *et al.*, 2005). Synip contains a PDZ domain in the N-terminus of the protein. Insulin could, therefore, regulate an interaction between the PDZ domain of synip and another regulatory protein (Min *et al.*, 1999).

Tomosyn is the final syntaxin4 interacting protein that has been identified and is present at the plasma membrane and in adipocyte cytosol. Tomosyn binds with high affinity to syntaxin4 and SNAP23 via a VAMP-2 like domain and overexpression of tomosyn inhibits the insulin-dependent translocation of GLUT4 to the plasma membrane (Widberg *et al.*, 2003). The exact function of insulin signalling intermediates in the tethering / docking step still needs further investigation to identify the actual site of insulin action. The fusion process is highly regulated. Insulin induces an 8-fold increase in the rate of fusion and insulin activation of the plasma membrane is the essential regulatory step. Fusion of the vesicle with the plasma membrane is SNARE-dependent and PKB recruitment to the insulin-activated plasma membrane is needed for fusion (Koumanov *et al.*, 2005). Use of the cell-free fusion assay developed in the study will be crucial for further investigation into the fusion of GLUT4 vesicles to the plasma membrane.

1.5.5 GLUT4 Endocytosis

Once GLUT4 has fused with the plasma membrane, it is rapidly internalised in both basal and insulin-stimulated cells (Yang and Holman, 1993, Satoh et al.,

1993). Insulin does result in a slight decrease in the rate of endocytosis, even though its main action is in the exocytotic arm of the trafficking pathway. The use of electron microscopy has identified a clustering of GLUT4 at the plasma membrane in clathrin-coated pits in both basal and insulin-stimulated cells (Slot et al., 1991, Robinson et al., 1992). This is further corroborated by the fact that decreasing the intracellular potassium concentration, which disassembles clathrin lattices and prevents their reassembly, results in an accumulation of GLUT4 at the cell surface, following the inhibition of endocytosis (Nishimura *et al.*, 1993). Clathrin-mediated endocytosis is the mode of internalisation for constitutively recycling proteins, e.g. GLUT1 and the transferrin receptor, thus GLUT4 is internalised by the same mechanism as constitutively recycling proteins. However, the means by which the clathrin coated pits bud from the plasma membrane is not fully understood. Dynamin is a 100 kDa GTPase and is an important protein involved in the formation of clathrin-coated vesicles (van der Bliek *et al.*, 1993). Hydrolysis of GTP by oligomeric rings of dynamin around the neck of the budding vesicle is required for vesicle scission (Takei and Haucke, 2001). Studies involving transfection of mutant dynamin have highlighted its importance in GLUT4 endocytosis, as a GTPase-negative dynamin mutant prevents GLUT4 endocytosis (Al Hasani et al., 1998, Kao et al., 1998). However, the molecular mechanism of GLUT4 endocytosis is not known.

1.5.6 Role of the Cytoskeleton in GLUT4 Trafficking

The cytoskeleton plays a role in many aspects of membrane trafficking, which includes the intracellular retention and trafficking of the GLUT4 protein. The first evidence that the cytoskeleton was involved in GLUT4 processes was through the use of immuno-electron microscopy. It was found that GLUT4 vesicles are associated with the intermediate filament protein vimentin and the microtubule protein α-tubulin.

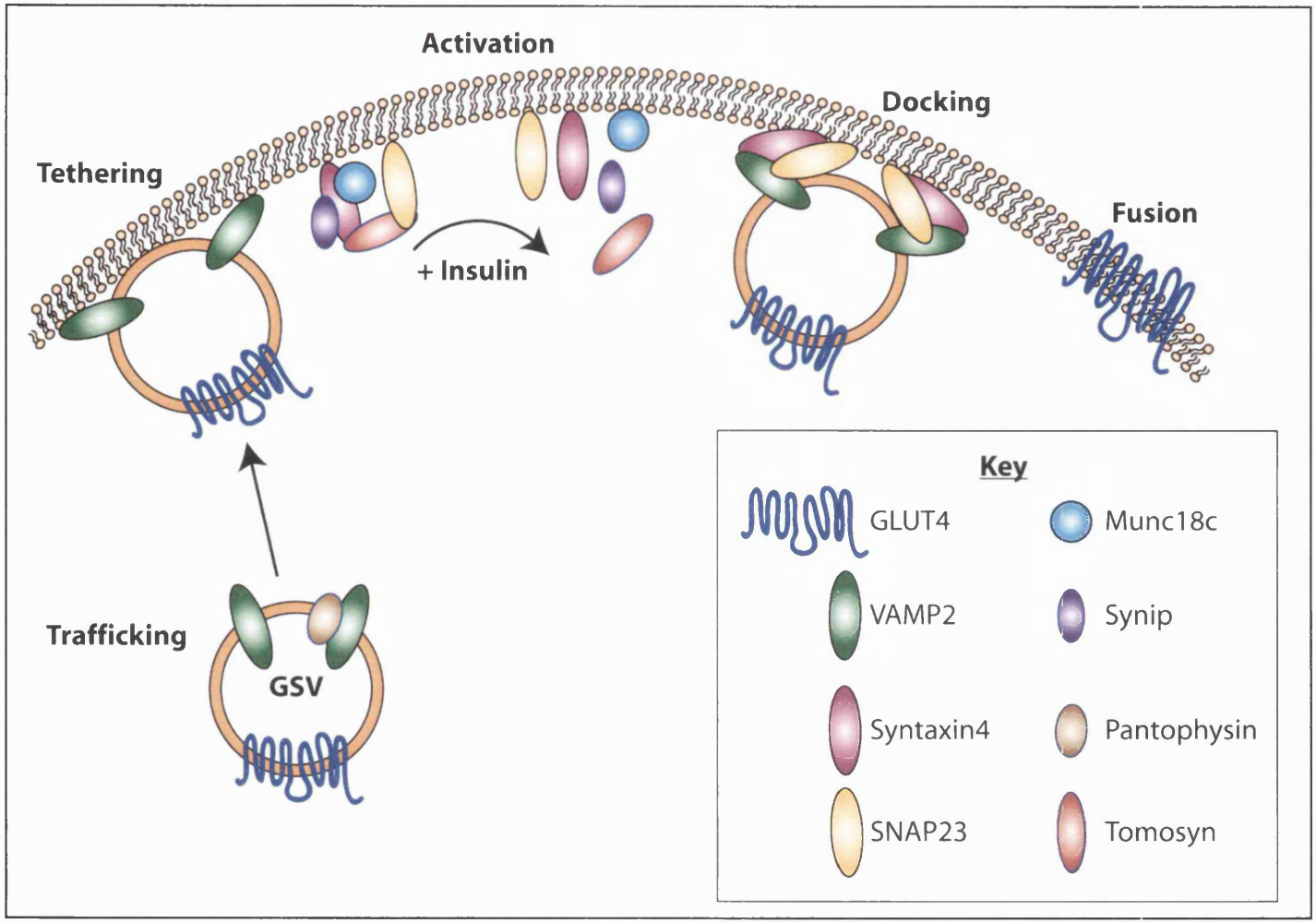

Figure 1.5 **Diagram illustrating the current understanding of GLUT4 fusion.** See text for details.

Following disruption of the intermediate filaments and microtubules in 3T3-L1 adipocytes, the localisation of GLUT4 changed from being peri-nuclear to the cell surface regions of the cell. The role of the microtubule-based motor, dynein, in GLUT4 trafficking was assessed. Inhibition of dynein inhibited insulin-stimulated GLUT4 translocation to the plasma membrane and so dynein was considered important for this process (Guilherme *et al.*, 2000). Furthermore, inhibition of microtubule and actin filament function decreased insulin-stimulated glucose transport by 70% and 50%, respectively. When both microtubule and actin filaments were impaired insulin-stimulated glucose transport was completely inhibited. This shows that both actin and microtubules are essential for insulin-stimulated GLUT4 translocation to the plasma membrane (Patki *et al.*, 2001). A few key studies will be illustrated below to show the importance and complexity of the involvement of the cytoskeleton in GLUT4 translocation.

Actin polymerisation plays an important role in insulin-dependent GLUT4 translocation. The use of latrunculin to inhibit G actin polymerisation results in a decrease in GLUT4 exocytosis but has no effect on the level of endocytosis (Omata *et al.*, 2000). Furthermore, the unconventional myosin 1C (Myo1c), the motor protein that drives movements along actin filaments, is present in GLUT4-containing vesicles purified from 3T3-L1 adipocytes. The use of a dominant-negative Myo1c has highlighted the requirement for Myo1c for the insulin-stimulated GLUT4 translocation from the intracellular compartment to the plasma membrane. Myo1c is not sensitive to wortmannin so Myo1c must function in a PI(3)K-independent insulin signalling pathway that controls the movement of intracellular GLUT4-containing vesicles to the plasma membrane. To fully confirm a role for Myo1c in insulin-stimulated GLUT4 translocation, siRNA was transfected into cells to prevent the endogenous expression of Myo1c. This inhibited insulin-stimulated glucose uptake (Bose *et al.*, 2002).

Microtubules also have an effect on insulin-stimulated GLUT4 trafficking. Dynein interacts with the small GTP-binding protein Rab5. Insulin inhibits Rab5-GTP loading and decreases binding of dynein to microtubules in a PI3-kinase-dependent manner. The authors concluded that insulin inhibits the inward movement of GLUT4 from the plasma membrane back to its intracellular compartment, thereby regulating endocytosis (Huang *et al.*, 2001). However, contrary to the work done by Huang *et al*, two independent laboratories have reported that microtubules do not have an effect on insulin-stimulated GLUT4 translocation but rather microtubules have an effect on the intracellular trafficking from endosomes to the GSV (Molero et al., 2001, Shigematsu et al., 2002). Microtubules, therefore, seem to play a role in the intracellular sorting of GLUT4 but the role in insulin-stimulated GLUT4 translocation is still not known.

A lot of work has been done to identify that the cytoskeleton is important in GLUT4 trafficking. However, the precise mechanism whereby the cytoskeleton controls GLUT4 function is not fully understood.

1.6 GLUT4 Sorting Motifs

GLUT4 has a highly controlled trafficking mechanism in both basal and insulin-stimulated cells and GLUT4 is found in many different cellular compartments throughout the trafficking pathway (Section 1.5). To maintain this unique feature of GLUT4 compared to the constitutively recycling homologue GLUT1, GLUT4 must contain specific targeting motifs. It has been the goal of many laboratories to define these domains. Figure 1.6 illustrates the location of these potential targeting domains in the GLUT4 protein. GLUT4 and GLUT1 share least homology in the stretches of amino acids at the amino- and carboxyl-termini, as well as the large cytoplasmic loop between helices 6 and 7. The

motifs involved in the targeting and sorting of GLUT4 are likely to be located in these regions.

1.6.1 The Amino-Terminal Targeting Motifs

The amino-terminus was first reported to be important in the intracellular retention of GLUT4 by Piper *et al.* Chimeras of GLUT1 and GLUT4 were generated and transiently expressed in CHO cells. When the full length GLUT1 or GLUT4 proteins were transfected into the CHO cells, GLUT1 had a predominantly cell surface localisation and GLUT4 had an intracellular localisation in the basal state. Substitution of the amino-terminal region of GLUT4, with that of GLUT1, abolished its intracellular localisation. Conversely, if the amino-terminal region of GLUT1 was substituted for that of GLUT4 the resulting protein was located in an intracellular compartment. A substitution of the carboxyl-terminus of GLUT4 and GLUT1 did not affect the subcellular localisation of the proteins (Piper *et al.*, 1992). The authors therefore concluded that the amino-terminus of GLUT4 is both necessary and sufficient for intracellular sequestration.

Further studies were carried out using deletion and alanine substitution mutants in the N-terminus of GLUT4 to identify the subcellular localisation of the mutants and narrow down the critical residues for the sequestration. The mutants in which the first eight amino acids were deleted in GLUT4 or where phenylalanine 5 was mutated to alanine resulted in an increase in the cell surface expression of the protein. This indicates that these residues are important for the intracellular sequestration (Piper *et al.*, 1993b). In addition, the Phe^5 to Ala mutant proteins were also excluded from their co-localisation with clathrin, suggesting that Phe^5 is involved in the endocytic process.

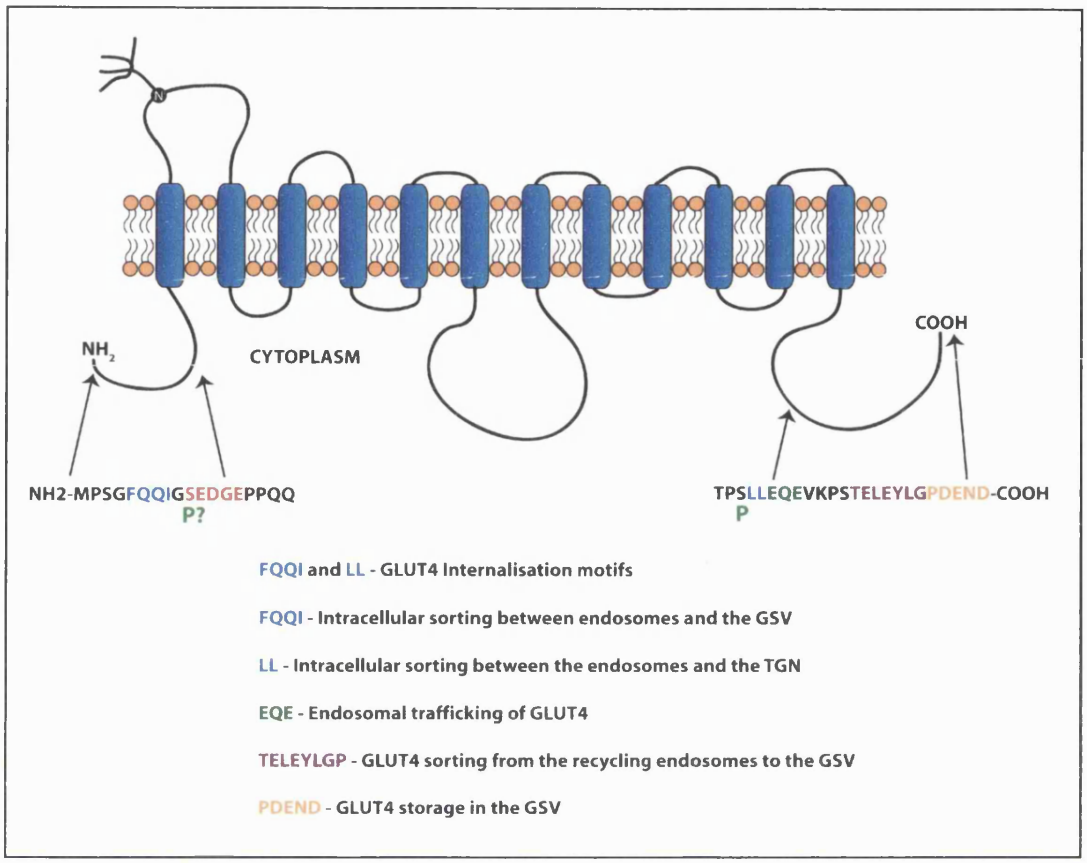

Figure 1.6 **Sorting Motifs within the cytoplasmic domains of GLUT4.** These motifs may be involved in the unique trafficking properties of GLUT4 through direct interaction with adaptor-binding proteins. The strength of this interaction may be facilitated by other surrounding motifs e.g. the phosphorylated residues (green P).

The FQQI domain fulfils the requirements for a functional clathrin-coated pit internalisation motif: an aromatic residue separated by two amino acids from a bulky hydrophobic residue. However, tyrosine-containing internalisation motifs, which have been identified in the cytoplasmic tails of the transferrin receptor, are more common than phenylalanine-based motifs (Collawn *et al.*, 1990). A year after the study by Piper and colleagues, the potential of the FQQI motif in facilitating the intracellular sequestration of GLUT4 was questioned, following kinetic studies using chimeras of GLUT4 and the transferrin receptor. The N-terminus of the transferrin receptor was substituted for that of GLUT4. The GLUT4:transferrin receptor chimera recycled back to the plasma membrane at the same rate as that observed for the wild type transferrin receptor. This suggests that the N-terminus of GLUT4 did not facilitate its intracellular sequestration (Garippa *et al.*, 1994). However, the FQQI motif was still implicated in internalisation as there was a 50% reduction in the internalisation rate of the chimeric protein. This finding was corroborated by a study by Araki *et al*, in which ATB-BMPA-tagged GLUT4 mutated at F^5Q^6 had a 40% reduction in the rate of internalisation compared to wild type GLUT4 (Araki *et al.*, 1996). Mutation of F^5 to a tyrosine residue in the GLUT4:transferrin receptor chimera, to form the classical consensus sequence, increased the rate of internalisation of the protein (Garippa *et al.*, 1994). These experiments suggest that the FQQI motif in the N-terminus of GLUT4 is important for internalisation, although its presence results in a reduced rate of endocytosis compared with the classical consensus sequence observed in other recycling proteins.

Further experiments involving mutagenesis of the FQQI motif have led to the conclusion that, in addition to its role in internalisation, the N-terminus of GLUT4 is also required for sorting between intracellular compartments. The F^5QQI motif at the N-terminus of GLUT4 was mutated to S^5QQI and transfected into 3T3-L1 adipocytes. The mutated GLUT4 was mis-targeted to the late endosomes / lysosomes, showing that F5 was essential for correct trafficking to the GSV (Palacios et al., 2001). In addition, GLUT4 was mutated

from F^5QQI to A^5QQI and transfected into 3T3-L1 adipocytes. Endosomal ablation illustrates that the mutated GLUT4 was only present in the endosomal-ablated compartment and not in the non-ablated GSV compartment. The mutated N-terminus of GLUT4 therefore results in the mis-trafficking of GLUT4, as the GLUT4 is not present in the GSV but only in the endosomes (Melvin *et al.*, 1999). These sorting motifs responsible for GLUT4 trafficking have all been studied in fully matured, continually cycling GLUT4. In one recent study, the trafficking motifs involved in the initial trafficking from the TGN to the GSV, following biosynthesis, was investigated (Khan *et al.*, 2004). GLUT4:GLUT1 chimeras were made and transfected into 3T3-L1 adipocytes. Substituting the carboxyl-terminal domain of GLUT4 with that of GLUT1 had no significant effect on the trafficking to the GSV. However, substitution of either the GLUT4 amino-terminal domain or the large cytoplasmic loop between transmembrane domains 6 and 7 resulted in the mis-targeting of GLUT4 to the plasma membrane. In agreement, only the substitution of the amino terminus plus the cytoplasmic loop of GLUT4 in the GLUT1 backbone resulted in the accurate trafficking of GLUT4 to the GSV. Following alanine-scanning mutagenesis, the essential residues for the efficient trafficking of GLUT4 from the TGN to the GSV were identified as F^5 and I^8 (and to a lesser extent $D^{12}G^{13}$) at the N-terminus and residues 227 – 271 in the large cytoplasmic loop. In conclusion, the N-terminus of GLUT4 is necessary for the efficient targeting of newly synthesised GLUT4 into the GSV (Khan *et al.*, 2004).

The FQQI motif in the N-terminus of GLUT4 is therefore important for the internalisation of GLUT4 from the plasma membrane as well as for the intracellular sorting process that separates GLUT4 away from the endosomal system into the peri-nuclear GSV compartment, for both recycling and newly synthesised GLUT4.

1.6.2 The Carboxyl-Terminal Targeting Motifs

At the same time as the N-terminus of GLUT4 was being reported as an important trafficking domain, the C-terminus of GLUT4 was also reported as the domain that was important for intracellular sequestration (Verhey et al., 1993, Marshall et al., 1993, Czech et al., 1993). The investigators created chimeras of GLUT4 and GLUT1, substituting the C-terminal regions of the protein. The chimeras were expressed in COS-7 cells (Czech *et al.*, 1993), *Xenopus* oocytes (Marshall *et al.*, 1993) or NIH 3T3 and PC12 cells (Verhey *et al.*, 1993). Each study showed that substitution of the GLUT4 C-terminal domain for that of GLUT1 resulted in the GLUT4 chimera displaying GLUT1 trafficking characteristics (localised at the cell surface). Conversely the substitution of the C-terminal domain of GLUT1 with that of GLUT4 led to the GLUT1 chimera being sequestered into an intracellular compartment. Verhey and colleagues did find a partial role for the first 183 amino acids of GLUT4 in the intracellular sequestration of the protein but concluded that the C-terminal region of GLUT4 was of primary significance. The region in the C-terminus of GLUT4 that was responsible for the intracellular sequestration has been narrowed down to the dileucine motif $L^{489}L^{490}$. Chimeras were made in which the C-terminus of GLUT4 was substituted onto the GLUT1 protein and the dileucine motif was mutated to an alanine-serine motif (Verhey and Birnbaum, 1994). Alternatively, the C-terminus of GLUT4 was substituted onto the transferrin receptor and the dileucine motif was mutated to a dialanine motif (Garippa *et al.*, 1996). Both mutants resulted in a decrease in the amount of GLUT4 in the GSV and a shift towards a cell surface localisation. The results from the chimera studies were supported by a study in which ATB-BMPA-tagged GLUT4 had the dileucine motif mutated to a dialanine motif. Transfection of this mutant protein resulted in a poor intracellular retention of GLUT4. The rate of endocytosis was not altered by the mutation but there was an increase in the rate of exocytosis (Araki *et al.*, 1996).

Like the FQQI motif, the dileucine motif appears to have an additional role in the sorting of intracellular GLUT4. The dileucine motif at the C-terminus of GLUT4 is also involved in sorting between the TGN and GSVs. The dileucine motif was mutated to a dialanine motif and expressed in 3T3-L1 adipocytes at endogenous levels i.e. the protein was not overexpressed. The subcellular location of the mutant was determined following ablation of the endosomal compartment. The mutant escaped ablation and so was not in the endosomal compartment. This mutant, therefore, does not prevent GLUT4 from reaching the non-ablated compartment and this implies a role for the dileucine motif in sorting from a separate intracellular compartment (Melvin *et al.*, 1999). Its role in the intracellular sorting of GLUT4 is further corroborated through the use of the mutated dialanine motif. It has been shown that the dileucine motif is involved in targeting from the TGN to the GSV (Martinez-Arca *et al.*, 2000). However, another study using chimeras of GLUT4 and GLUT1 have concluded that the dileucine motif, although important, is not sufficient for targeting GLUT4 to GSVs. Therefore, other residues within the C-terminal region must also have a role in the intracellular sorting of GLUT4 (Haney *et al.*, 1995).

Further studies have identified the other motifs in the C-terminus of GLUT4 that are important for efficient GLUT4 sorting (Cope et al., 2000, Shewan et al., 2000, Martinez-Arca et al., 2000). A chimera of GLUT4:GLUT3 was generated in which the last 12 amino acids of GLUT4 (residues 498 – 509) was substituted for the last 12 amino acids of GLUT3. The chimeric protein was then expressed in 3T3-L1 adipocytes. In unstimulated adipocytes, the chimeric protein had a cell surface expression instead of the typical intracellular compartment. This illustrates that it is not only the dileucine motif that is important in the intracellular sequestration but there is also a motif at the very C-terminus of GLUT4. The last 12 amino acids were mutated to alanine residues in groups of 4 residues (498-501 (TELE), 502-505 (YLGP) or 506-509 (DEND)). The mutants were again transfected into 3T3-L1 adipocytes and the subcellular localisation of the proteins was identified by subcellular

fractionation and endosome ablation. Residues T^{498}ELEYLGP^{505} were identified as being important in regulating the sorting of GLUT4 from recycling endosomes into the GSV post-endosomal compartment (Shewan *et al.*, 2000). Further work identified that, following internalisation, GLUT4 trafficked from the endosomes into a compartment of the TGN. Although the compartment did not contain the classical TGN marker TGN38, it co-localised with syntaxins 6 and 16 (which have been implicated in the trafficking of cargo between the endosomes and TGN). Mutation of the acidic targeting motif (E^{499}LEY) in the C-terminus of GLUT4 resulted in the retention of GLUT4 in an endosomal compartment. The authors therefore conclude that the acidic E^{499}LEY motif regulates the accumulation of GLUT4 in the syntaxins 6- and 16-positive TGN compartment (Shewan *et al.*, 2003).

An independent study also carried out a mutation at the very end of the GLUT4 protein. Amino acids P^{505}DEND^{509} were deleted from the C-terminus of GLUT4. This mutation prevented the storage of GLUT4 in the GSV and instead the protein had an endosomal location. In addition, tyrosine 502 was also shown to be important in GLUT4 retention in the GSV but this function was dependent on the presence of residues 505 – 509 (Martinez-Arca *et al.*, 2000).

Two further residues have also been shown to be important in the subcellular trafficking of GLUT4. The amino acids adjacent to the dileucine motif (E^{491}QE) were sequentially mutated to alanine. Mutation of glutamic acid residues 491 and 493 resulted in an increase in the levels of the mutated proteins at the cell surface, reduced insulin-stimulated translocation and increased susceptibility to endosomal ablation. The EQE may have a role in modulating the adjacent dileucine motif, or it may have an independent trafficking role (Cope *et al.*, 2000).

The regions downstream of the dileucine motif, therefore, play a critical role in GLUT4 trafficking. These motifs may all work together, in combination, or independently with the dileucine motif, to regulate distinct steps in the subcellular trafficking pathway of GLUT4.

1.6.3 Phosphorylation Motifs – Modulation of Intracellular Trafficking

A phosphorylation site has been identified in the C-terminus of GLUT4 at serine 488 (Lawrence, Jr. *et al.*, 1990a). The phosphorylated serine is the residue preceding the dileucine motif ($S^{488}L^{489}L^{490}$). An *in vitro* kinase assay identified the kinase responsible as being protein kinase A (PKA). Phosphorylation at serine 488 could therefore modulate the effect of the dileucine motif (Section 1.6.2) or it could have an independent function. The effect of phosphorylation at serine 488 has been investigated by several groups. The level of GLUT4 phosphorylation was calculated following the treatment of adipocytes with various agents. Investigations were also undertaken to determine whether the subcellular distribution of GLUT4 was affected by phosphorylation at serine 488.

It was reported that insulin does not have an effect on the relative level of phosphorylation in either intracellular or plasma membrane-localised GLUT4 (James *et al.*, 1989a). The authors therefore conclude that phosphorylation of GLUT4 is unlikely to promote the translocation of GLUT4 from an intracellular location to the plasma membrane.

Isoproterenol (a β-adrenergic agonist) inhibits insulin-stimulated glucose transport by 40% but increases the level of phosphorylation by twofold (James *et al.*, 1989a). However, isoproterenol does not lead to a decrease in the number of transporters at the plasma membrane but rather it affects the intrinsic activity of GLUT4 (Smith et al., 1984, Kuroda et al., 1987). It could therefore be concluded that the effect of the phosphorylation at serine 488 could be to alter the intrinsic activity of GLUT4 (James et al., 1989a). However, other studies have not observed a link between the phosphorylation and the intrinsic activity of the transporter (Joost et al., 1987, Nishimura et al., 1991).

Okadaic acid also leads to an increase in GLUT4 phosphorylation and, although okadaic acid stimulates basal glucose transport, it inhibits the level of insulin-stimulated glucose transport. The authors concluded that

phosphorylation of GLUT4 could promote internalisation of the transporter rather than stimulating translocation. This was due to the fact that insulin did not increase the level of GLUT4 phosphorylation and the fact that okadaic acid had an inhibitory effect on insulin-stimulated glucose transport (Lawrence, Jr. *et al.*, 1990b).

One group, while investigating the role of the dileucine motif on the subcellular trafficking of GLUT4, also mutated serine 488 (Garippa *et al.*, 1996). The mutation was carried out in a chimeric protein in which the C-terminus of the transferrin receptor had been substituted for the C-terminus of GLUT4. Serine 488 was mutated to either alanine or aspartic acid, to mimic an unphosphorylated form of serine or to mimic the negative charge of a phosphorylated serine respectively. The mutations resulted in a threefold reduction in the rate of internalisation of the chimeric protein. The mutations did not affect the GLUT4 recycling rate. These results suggest that serine 488, together with the dileucine motif, has a role as an internalisation motif. However, this study must be viewed with caution because the mutated chimeric proteins behaved the same when serine 488 was mutated to either an alanine or an aspartic acid residue (Garippa *et al.*, 1996). The effect of phosphorylation at serine 488 was also investigated in another study (Marsh *et al.*, 1998). Serine 488 was mutated to alanine and the effect of the phosphorylation on the intracellular trafficking of GLUT4 was examined. Phosphorylation of GLUT4 did not affect its subcellular localisation in either basal or insulin-stimulated adipocytes and so the authors concluded that phosphorylation does not play a major role in GLUT4 exocytosis. However, a difference was observed in the extent of the co-localisation between GLUT4 and the γ-adaptin subunit of the Golgi adaptor complex (AP1) (Section 1.5.1.2). The extent of co-localisation between GLUT4 and AP1 was significantly increased when serine 488 was mutated to alanine. Thus it was suggested that phosphorylation might modulate the intracellular sorting of GLUT4 at the TGN (Marsh *et al.*, 1998). The exact function of the phosphorylation of serine 488

still remains not fully understood. Section 4.1 will give a detailed account of the effect the phosphorylation of serine 488 has on GLUT4 trafficking.

The N-terminus of GLUT4 shares significant sequence identity with the N-terminal targeting domain of the α subunit of glutamic acid decarboxylase 65 (GAD65), in which eight out of eleven amino acids are identical to the N terminus of GLUT4 (Figure 1.7). There are two isoforms of GAD65 - α and β and, in 1997, it was shown that the α isoform but not β was phosphorylated on serine residues 4, 6, 10 and 13 by an unidentified membrane-associated kinase, which was thought to regulate the specific function of GAD65 in the synaptic vesicle membrane (Namchuk *et al.*, 1997). There is a potential casein kinase II (CKII) acidic cluster phosphorylation site within the area of homology between GLUT4 and GAD65α. The potential phosphorylation site on GLUT4 is S^{10}EDGE. Phosphorylation at serine 10 could modulate the interaction of proteins with the upstream FQQI motif or it could have an independent role by itself.

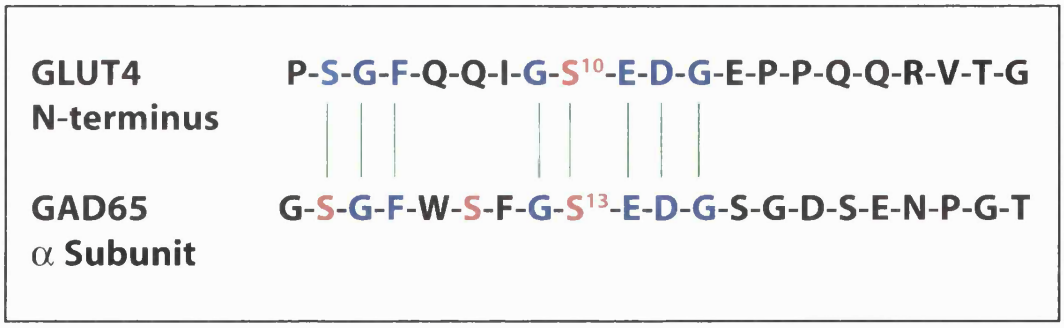

Figure 1.7 **Sequence identity between GAD65α and the N-terminus of GLUT4.** The sequences of GLUT4 and GAD65α were obtained from Entrez Protein (NCBI).

1.6.3.1 Casein Kinase Enzymes

Casein kinase (CK) enzymes are protein kinases and are defined by their ability to phosphorylate serine / threonine residues that are proximal to acidic amino acids instead of basic or prolyl residues. The name casein kinase comes from the ability to phosphorylate casein *in vitro.* There are three sub-families of casein kinase enzymes; casein kinase I (CKI), casein kinase II (CKII) and Golgi casein kinase (GCK). Each of the CK enzymes has a different phosphorylation consensus sequence. The consensus sequence for the CK enzymes are: CKI [pS/pT]-X_{2-3}-[S/T], CKII X-[S/T]-X-X-[D/E] and GCK is X-S-X-(E/pS) (pS stands for phospho-serine) (Pinna and Ruzzene, 1996). The predicted GLUT4 N-terminal phosphorylation site is S^{10}EDGE and so CKI is not a candidate for being the GLUT4 N-terminal kinase. Both CKII and GCK have phosphorylation consensus sequences similar for the GLUT4 N-terminal sequence but the sequence is not identical. The aspartic acid residue cannot be substituted for glutamic acid in the GCK consensus sequence (S-X-E- to S-X-D) (Lasa-Benito *et al.*, 1996). GCK is therefore unable to phosphorylate the N-terminus of GLUT4 but an unidentified kinase, related to GCK, may phosphorylate Ser^{10} in GLUT4. The consensus sequence for CKII has an acidic residue at n=3 but the N-terminus of GLUT4 contains a glycine residue at n=3. However, there are proteins that are phosphorylated by CKII that do not contain the CKII consensus sequence, e.g. the p53 tumour suppressor. The inverse is also true, the minimum consensus sequence does not guarantee CKII phosphorylation (Litchfield, 2003). Serine 10 in GLUT4 could therefore be phosphorylated by CKII through a novel CKII consensus sequence or by a kinase that is as yet unidentified but which is likely to be related to the casein kinase family of proteins.

1.7 Experimental Aims of the Work Described in this Thesis

The work described in this thesis has three main themes – the identification of any additional phosphorylation sites in GLUT4 (other than the previously identified serine 488) with a special focus on serine 10, the determination of the effect different stimuli have on the level of phosphorylation at each site and the effect the phosphorylation has on the trafficking of GLUT4 to the plasma membrane. Initially, work was undertaken to purify a highly phosphorylation-specific antibody raised to the phosphorylated form of serine 10 to aid the study.

Investigations were undertaken to determine the sites of GLUT4 phosphorylation in adipocytes and cardiomyocytes. The regions which contained the phosphorylation sites were identified following cleavage by Endoproteinase Lys C. Then comparison with the predicted GLUT4 phosphorylation sites, obtained from a web-based phosphorylation prediction program was made. Work was undertaken to determine what stimuli affected the level of phosphorylation and also the stoichiometry of phosphorylation.

Studies were also undertaken to investigate if the phosphorylation sites in GLUT4 had any role in translocation to the plasma membrane. To address this aim, site-directed mutagenesis was used to mutate the phosphorylation sites to either an alanine or an aspartic acid to mimic an unphosphorylated or phosphorylated residue respectively. The mutants were transfected into adipocytes and the level of GLUT4 at the plasma membrane was determined through the presence of an epitope tag in the first exofacial loop of GLUT4.

2 Materials and Methods

2.1 Materials

2.1.1 Laboratory Chemicals

All general laboratory chemicals were of analytical grade and purchased from either Sigma-Aldrich Chemical Company [S] or Fisher Scientific UK Ltd. [F], unless otherwise stated. Table 2.1 gives the address and website for each of the suppliers along with the abbreviation that will be used to denote each company.

Company	Address	Website	Abbreviation
Alexis Corporation	Nottingham, UK	www.alexis-biochemicals.com	[AC]
ATCC	Middlesex, UK	www.attc.org	[ATCC]
Amersham International	Little Chalfont, UK	www.amershambiosciences.com	[A]
Applied Biosystems	Warrington, Cheshire, UK	www.appliedbiosystems.com/index.cfm	[AB]
Atto Corporation	Tokyo, Japan	www.atto.co.jp/englishtop.html	[AT]
BD Biosciences	Oxford, UK	www.bdbiosciences.com	[BD]
BDH Laboratory Supplies	Poole, Dorset, UK	www.bdh.com	[BDH]
Beckman Coulter	High Wycombe, Bucks, UK	www.beckmancoulter.com	[BC]

Bibby Sterilin Ltd	Stone, Staffs, UK	www.bibby-sterilin.com	[BS]
Biogenesis Ltd	Poole, Dorset, UK	www.biogenesis.co.uk	[BG]
Bioline	London, UK	www.bioline.com	[BL]
Bio-rad	Hemei Hempstead, Herts, UK	www.bio-rad.com	[BR]
Calbiochem	Nottingham, UK	www.calbiochem.com	[CB]
Cambrex	Wokingham, Berks, UK	www.cambrex.com/bioproducts	[C]
Camlab	Cambridge, UK	www.camlab.co.uk	[CL]
Carl Zeiss, Ltd	Hertfordshire, UK	www.zeiss.co.uk	[CZ]
Covance Research Products, Inc	Berkeley, CA, USA	http://store.crpinc.com/default.aspx	[CV]
Diagnostics Scotland	Edinburgh, UK	www.diag-scot.co.uk	[D]
Eppendorf	Cambridge, UK	www.eppendorf.co.uk	[E]
Fisher Scientific UK Ltd.	Loughborough, UK	www.fisher.co.uk	[F]
Fujifilm (Raytek)	Sheffield, UK	www.raytek.co.uk	[FU]
Gelman Sciences	Ann Arbor, MI, USA	www.pall.com	[GE]
Greiner	Stonehouse, Glos, UK	www.gbo.com	[G]
Intergen Co.	Newark NJ, USA	www.intergenco.com	[IT]

Invitrogen	Paisley, UK	www.invitrogen.com	[I]
Lockertex	Clarcor UK, Warrington, Cheshire	www.clarcoruk.com/lockertex	[LK]
Merck	Nottingham, UK	www.merckbiosciences.co.uk	[M]
Millipore	Watford, UK	www.millipore.com	[ML]
MJ Research	Bio-Rad Labs, Waltham, MA, USA	www.mjr.com	[MJ]
Molecular Probes	The Netherlands	http://probes.invitrogen.com/	[MP]
MP Biomedicals	Cambridge, UK	www.mpbio.com	[MPB]
MWG Biotech	London, UK	www.mwg-biotech.com	[MWG]
Nalge Nunc International	Rochester, NY, USA	www.nuncbrand.com	[N]
National diagnostics, flowgen	Flowgen Bioscience Ltd, Nottingham, UK	www.nationaldiagnostics.com	[ND]
New England Biolabs	Hitchin, Herts, UK	www.neb.com	[NEB]
Oxoid Ltd	Basingstoke, Hampshire, UK	www.oxoid.com	[O]
Pierce	Northumberland, UK	www.piercenet.com	[P]
Rhone merieux	Harlow, Essex, UK	-	[RM]
Roche	Lewes, East Sussex, UK	www.roche-applied-science.com	[R]

Sarstedt	Leicester, UK	www.sarstedt.com	[SR]
Sigma-Aldrich	Poole, Dorset, UK	www.sigmaaldrich.com	[S]
Southern Biotech	Birmingham, Alabama, USA	www.southernbiotech.com	[SB]
Stratagene	La Jolla, Ca, USA	www.stratagene.com	[ST]
Tecan	Reading, UK	www.tecan.com	[TE]
Thomas scientific	Swedesboro, NJ, U.S.A.	www.thomassci.com	[T]
Upstate	Dundee, UK	www.upstate.com	[U]
UVP	Cambridge, UK	www.uvp.com	[UVP]
Vector Laboratories UK	Peterborough, UK	www.vectorlabs.com	[VL]
VWR	Lutterworth, Leics, UK	www.vwr.com	[V]
Worthington Biochemical Corporation	Freehold, NJ, USA	www.lornelabs.com	[W]

Table 2.1 **The address and website of each of the suppliers along with the abbreviation used to denote each company.**

2.1.2 Buffers

Dulbecco's Modified Eagles Medium – Newborn Calf Serum (DMEM-NCS): Dulbecco's Modified Eagles Medium [C], 100 IU/ml Penicillin, 100 µg/ml Streptomycin [S], 2 mM Glutamine [S] and 10% Newborn Calf Serum [I].

Dulbecco's Modified Eagles Medium – Fetal Calf Serum (DMEM-FCS): Dulbecco's Modified Eagle Medium [C], 100 IU/ml Penicillin, 100 µg/ml Streptomycin [S], 2 mM Glutamine [S] and 10% Fetal Calf Serum myoclone superplus [I].

Adipocyte Krebs-Ringer-HEPES (aKRH): 140 mM NaCl, 4.7 mM KCl, 2.5 mM $CaCl_2$, 1.25 mM $MgSO_4$, 2.5 mM NaH_2PO_4, 10 mM HEPES, (pH 7.4).

Low phosphate adipocyte Krebs-Ringer-HEPES (low P_i aKRH): 140 mM NaCl, 4.7 mM KCl, 2.5 mM $CaCl_2$, 1.25 mM $MgSO_4$, 0.2 mM NaH_2PO_4, 10 mM HEPES, (pH 7.4).

Cardiomyocyte Krebs-Ringer-HEPES (cKRH): 128 mM NaCl, 6 mM KCl, 1.4 mM $MgSO_4$, 0.2 mM NaH_2PO_4, 1 mM Na_2HPO_4, 10 mM HEPES, (pH 7.4) made up with double distilled water (ddH_2O) gassed with O_2 for at least 20 min.

Low phosphate cardiomyocyte Krebs-Ringer-HEPES (low P_i cKRH): 128 mM NaCl, 6 mM KCl, 1.4 mM $MgSO_4$, 0.2 mM NaH_2PO_4, 10 mM HEPES, (pH 7.4) made up with ddH_2O gassed with O_2 for at least 20 min.

Buffer A: cKRH buffer, 5.5 mM glucose, 2 mM ultrapure pyruvic acid [S].

Buffer B: Buffer A, 0.7% (w/v) BSA, 1.1 mg/ml collagenase [W], 2.65 mg/ml hyaluronidase Type 1-S [S], 15 mM 2,3-butanedione monoxime (BDM) [S].

Buffer C: Buffer A, 0.2 mg/ml DNAse I [R], 15 mM 2,3-butanedione monoxime (BDM), 200 µM $CaCl_2$, and 2% (w/v) BSA.

Buffer D: Buffer A, 1 mM $CaCl_2$ (physiological calcium concentration), and 2% (w/v) BSA.

Buffer E: Buffer A, 1 mM $CaCl_2$ and 0.5% (w/v) Fatty acid free Albumin, Fraction V, [R].

Low phosphate Buffer E (Low P_i Buffer E): Buffer E made from low P_i cKRH.

Phosphate Buffered Saline (PBS): 154 mM NaCl, 12.5 mM $Na_2HPO_4.12$ H_2O, (pH 7.2).

PBS-Tween 20 (PBS-T): PBS, 0.1% (v/v) Tween-20.

Tris Buffered Saline - Tween 20 (TBS-T): 10 mM Tris, (pH 7.4), 154 mM NaCl, 0.1% (v/v) Tween-20.

Tris-EDTA-Sucrose (TES): 10 mM Tris, (pH 7.2), 5 mM EDTA, 255 mM Sucrose.

TES Sucrose Cushion: 20 mM Tris, (pH 7.2), 1 mM EDTA, 1.12 M Sucrose.

Adipocyte Digestion Buffer: 3.5% (w/v) BSA in aKRH buffer supplemented with 5 mM glucose and 700 μg/ml Collagenase type 1 from *Clostridium histolyticum* [W].

Adipocyte Lysis Buffer: 2% (w/v) Nonaethylene glycol monododecyl ether (Thesit) ($C_{30}H_{62}O_{10}$) [S], PBS.

Cardiomyocyte Lysis Buffer: 1% (v/v) Triton X-100 (TX-100), 1% (w/v) Deoxycholic Acid, 0.2% (w/v) Sodium dodecyl sulphate (SDS), PBS.

Sample Buffer: Protein samples were solubilised in 2% (w/v) SDS, 62.5 mM Tris HCl (pH 6.8), 0.01% (w/v) bromophenol blue, 10% (v/v) glycerol. The reducing agent was 20 mM Dithiothreitol (DTT) unless otherwise stated.

Tris-Tricine Sample Buffer: 50 mM Tris HCl (pH 6.8), 0.5% (w/v) SDS, 0.01% (w/v) brilliant blue G, 12% (v/v) Glycerol. The reducing agent was 2% (v/v) β-mercapto-ethanol.

Resolving Gel Buffer: 1.5 M Tris HCl, 0.4% (w/v) SDS, (pH 8.8).

Stacking Gel Buffer: 0.5 M Tris HCl, 0.4% (w/v) SDS, (pH 6.1).

Electrophoresis Running Buffer: 25 mM Tris HCl, (pH 6.3), 0.1% (w/v) SDS, 0.2 M Glycine.

Gel Buffer: 3 M Tris, 0.3% (w/v) SDS, (pH 8.45).

Anode Buffer: 200 mM Tris, (pH 8.9).

Cathode Buffer: 100 mM Tris, 100 mM Tricine, 0.1% (w/v) SDS, (pH 8.5).

Transfer Buffer: 39 mM Glycine, 48 mM Tris, 0.0375% SDS (w/v), 20% methanol (v/v), (pH 8.8).

Ponceau S Stain: 0.1% (w/v) Ponceau S, 3% (w/v) trichloroacetic acid.

Stripping Buffer: 100 mM β-Mercaptoethanol, 2% SDS, 62.5 mM Tris HCl (pH 6.7).

Coupling Buffer: 50mM Tris, 5mM EDTA-Na, (pH 8.5).

ELISA Plate Coating Buffer: 15 mM Na_2CO_3, 35 mM $NaHCO_3$, 0.01% (v/v) Na Azide, (pH 9.6).

ELISA Plate Blocking Buffer: PBS, 0.1% (v/v) Tween-20, 1% (w/v) Casein, add casein and dissolve with mixing overnight at 4°C.

ELISA Sodium Acetate/Citrate Buffer: 1.66 M Sodium Acetate, 33 mM Citric acid, (pH6.0).

BCA Reagent B: 4% (w/v) $CuSO_4.5H_2O$.

Conjugation Buffer: 0.1 M Na_2HPO_4, 0.15 M NaCl, 1 mM EDTA, (pH 7.2).

Tris-acetate EDTA buffer (TAE): 40 mM Tris-acetate, 1 mM EDTA, (pH 8).

Luria Broth (LB): 1% (w/v) Bacto™ Tryptone [BD], 0.5% (w/v) Bacto™ Yeast Extract [BD], 0.5% NaCl, (pH 7.5) (autoclaved).

Agar Plates: 1% (w/v) Bacto™ Tryptone [BD], 0.5% (w/v) Bacto™ Yeast Extract [BD], 0.5% NaCl, 1.5% (w/v) Agar, (pH 7.5) (autoclaved).

Dulbecco's Modified Eagles Medium 1 (DMEM (1)): Dulbecco's modified Eagles medium [C], 0.2 µM Adenosine, 2 mM Glutamine.

Dulbecco's Modified Eagles Medium 2 (DMEM (2)): DMEM (1), 100 µg/ml Gentamicin.

Dulbecco's Modified Eagles Medium 3 (DMEM (3)): DMEM (2), 3.5% (w/v) BSA.

Confocal Permeabilisation Buffer: 1% (w/v) BSA, 3% (v/v) goat serum, 0.1% (w/v) saponin, PBS.

Confocal Wash Buffer: 1% (w/v) BSA, 0.1% (w/v) saponin, PBS.

2.1.3 Antibodies

The source and dilution of the primary and secondary antibodies used for Western blot analysis (Section 2.2.8.3), the antibody binding assay (Section 2.2.13) and confocal microscopy (Section 2.2.14) are shown in the tables below, Tables 2.2, 2.3, 2.4 and 2.5 respectively.

Antibody	Polyclonal/ Monoclonal Purified/Serum	Source	Dilution for Western Blotting
Rabbit anti-GLUT4 phosphorylated N-terminus	Polyclonal Purified	In House production	1:1000
Rabbit anti-GLUT4 C-terminus	Polyclonal Serum and Purified	In House production (Holman *et al.*, 1990)	1:20,000
Mouse anti-GLUT4 C-terminus	Monoclonal (clone 1F8) Purified	[BG]	1:1000
Sheep anti-GLUT4 Phosphorylated N-terminus	Polyclonal Serum and purified	In House production	1:1000
Sheep anti-GLUT4 C-terminus	Polyclonal Purified	In House production	1:1000
Mouse anti-Haemagglutinin (HA)	Monoclonal Purified	[CV]	1:1000

Table 2.2 **Source and dilution of primary antibodies used in Western blot analysis.** Antibodies were diluted in TBS-T, 1% (w/v) BSA, 0.02% (w/v) sodium azide.

Antibody	Source	Dilution for Western Blotting
Goat anti-rabbit IgG HRP conjugate	[S]	1:4000
Goat anti-mouse IgG HRP conjugate	[S]	1:1000
Goat anti-sheep IgG HRP conjugate	[S]	1:4000

Table 2.3 **Source and dilution of secondary antibodies used in Western blot analysis.** Antibodies were diluted in TBS-T containing 5% (w/v) Marvel.

Antibody	Polyclonal/Monoclonal Purified/Serum	Source	Dilution for Antibody binding assay
Mouse anti-HA	Monoclonal Purified	[CV]	1:1000
Goat anti-mouse IgG β-Galactosidase conjugate	-	[SB]	1:1000

Table 2.4 **Source and dilution of antibodies used in the antibody binding assay.** Antibodies were diluted in 5% (w/v) BSA / aKRH containing 2 mM KCN.

Antibody	Polyclonal/Monoclonal Purified/Serum	Source	Dilution for confocal microscopy
Rabbit anti-GLUT4 pSer^{10} from second bleed serum	Polyclonal Purified	In House production (chapter 3)	1:50
Rabbit anti-GLUT4 pSer^{10} from final bleed serum	Polyclonal Purified	In House production (chapter 3)	1:50
Mouse anti-GLUT4 C-terminus	Monoclonal (clone 1F8) Purified	[BG]	1:740 1 µg/ml
Rabbit anti-GLUT4 C-terminus	Polyclonal Purified	In House production	2 µg/ml
Sheep anti-GLUT4 pSer^{10}	Polyclonal Purified	In House production (chapter 3)	4 µg/ml
Sheep anti-GLUT4 C-terminus	Polyclonal Purified	In House production (chapter 3)	4 µg/ml
Alexa Fluor® 488 goat anti-rabbit IgG	-	[MP]	2 µg/ml
Alexa Fluor® 568 goat anti-mouse IgG	-	[MP]	2 µg/ml
Alexa Fluor® 633 goat anti-sheep IgG	-	[MP]	4 µg/ml
Alexa Fluor® 488 goat anti-sheep IgG	-	[MP]	4 µg/ml

Table 2.5 **Source and dilution of antibodies used in confocal microscopy.** Antibodies were diluted in confocal permeabilisation buffer (1% (w/v) BSA, 3% (v/v) goat serum and 0.1% (w/v) saponin in PBS).

2.1.4 Insulin

Monocomponent porcine insulin was kindly supplied by Dr. G. Daniellson (Novo Nordisk). 1 mg insulin was dissolved in 1 ml of 30 mM HCl and was subsequently diluted to 3 ml in PBS. 1 ml of this stock solution was then diluted to 50 ml in PBS with the resulting 1 μM solution aliquoted and stored at -20°C. Once thawed, aliquots were not re-frozen.

2.1.5 Bovine Serum Albumin (BSA)

BSA (Bovine Cohn Fraction V) [IT] was dissolved in double distilled water overnight at 4 °C. The BSA solution was filtered through Millipore type A (mixed cellulose esters) membrane filters (0.8 μm pore size) [ML] and the pH was adjusted to pH 7.6 with 10 M NaOH. The final BSA concentration was adjusted to 10% (w/v) with double distilled water. Aliquots were stored at -20°C.

2.1.6 Heparin

Heparin Grade 1A [S] isolated from porcine intestinal mucosa was reconstituted in 0.9% (w/v) NaCl (2000 Units/ml) and filter sterilised through a 0.2 μm filter [ML]. Aliquots were stored at 4 °C.

2.1.7 Protease and Phosphatase Inhibitors

Where it is not stated, the protease and phosphatase inhibitors, and the concentrations at which they were used are shown in Table 2.6.

Inhibitor	Inhibits	Working Concentration
Antipain	Ser and Cys Proteases	1 µg/ml (1.65 µM)
Aprotinin	Ser Proteases	1 µg/ml
Pepstatin A	Ser and Cys Proteases	1 µg/ml (1.46 µM)
Leupeptin	Acid Proteases	1 µg/ml (2.1 µM)
AEBSF	Ser protease	100 µM
Sodium Fluoride	Ser / Thr phosphatase	10 mM
Sodium Molybdate	Acid phosphatases	1 mM
Sodium Orthovanadate	ATPase, alkaline phosphatase tyrosine phosphatase	200 µM
Cypermethrin	PP2B	50 nM
Dephostatin	Protein Tyrosine Phosphatases	5 µM
Okadaic acid	PP2A, PP1, PP2B	100 nM
NIPP-1	PP1	10 pM

Table 2.6 **Protease and phosphatase inhibitors and the working concentration.**

2.2 Methods

2.2.1 Cell Culture of 3T3-L1 Fibroblasts

Cell culture and media preparations were carried out in sterile conditions. Mouse 3T3-L1 fibroblast cells were obtained from the American Type Culture Collection [ATCC] and stored in liquid nitrogen in cell freezing medium [S].

Fetal bovine serum (myoclone super plus) [I] and newborn calf serum [I] were heat treated before use. The serum was allowed to thaw slowly at 4 °C overnight and heat treated at 56 °C for 30 min. The serum was divided into 50 ml aliquots and stored at -20 °C until needed. 3T3-L1 cell culture was essentially carried out as described in Sadowski *et al* (Sadowski *et al.*, 1992). All buffers were warmed to 37 °C before use.

2.2.1.1 Seeding of 3T3-L1 Fibroblasts

3T3-L1 fibroblasts were removed from liquid nitrogen and rapidly thawed at 37 °C. The cells were transferred to a sterile universal tube containing 20 ml DMEM-NCS and centrifuged at 180 x g (1,000 rpm) for 3 min in an Eppendorf 5804 R centrifuge [E]. The medium was aspirated and the cells were resuspended in 2 ml DMEM-NCS. The cells were seeded into a 175 cm^2 flask containing 40 ml DMEM-NCS and incubated at 37 °C, in an atmosphere of 10% (v/v) CO_2. The media was changed on the following day to remove the dead cells. The media was then replaced every 2 days until the cells reached sub-confluency.

2.2.1.2 Harvesting of 3T3-L1 Fibroblasts

The cells were grown until they reached sub-confluency, usually about 7 days after seeding. The flask of sub-confluent cells was washed twice with 10 ml phosphate buffered saline (PBS) (Dulbecco A) [O]. 4 ml Trypsin [S] was added and the flask was incubated at 37 °C for 3 min. 20 ml DMEM-NCS was added to the flask and the suspension of cells were transferred into a sterile universal tube. The cells were centrifuged at 180 x g (1,000 rpm) for 3 min in an Eppendorf 5804 R centrifuge [E] to pellet the cells. The cells were resuspended in 20 ml of media and plated onto sterile coverslips in 35 mm petri dishes for immunocytochemistry. Cells were also plated into a 175 cm^2

flask and grown to sub-confluency to maintain the culture. The media was replaced every two days. The cells were passaged a total of twelve times before they were discarded.

2.2.1.3 Differentiation of 3T3-L1 Fibroblasts

The cells that had been plated onto petri dishes were grown until they had been confluent for 3 days (about 10 days after seeding) and then they were differentiated into adipocytes. The media was replaced with DMEM-FBS containing 0.25 μM dexamethasone [S], 0.5 mM isobutylmethylxanthine [S] and 0.2 μM insulin. After 2 days the media was replaced with DMEM-FCS containing 0.2μM insulin and then with DMEM-FCS every two days after that. The cells were fully differentiated after 9 days.

2.2.1.4 Treatment of 3T3-L1 adipocytes with Brefeldin A

Cells at different days of differentiation were washed with PBS and incubated in serum free media (DMEM only) for 2 h at 37 °C. The cells were then incubated with 10 μg/ml Brefeldin A [S] for 30 min at 37 °C.

2.2.2 Preparation of Insulin sensitive cells

2.2.2.1 Rat Adipocytes

2.2.2.1.1 Isolation of Rat Adipocytes

Adipose cells were isolated from the epididymal fat pads of male Wistar rats (180 – 220 g) fed *ad libitum*. The rats were stunned and their necks dislocated.

The whole epididymal fat pads were quickly removed and incubated briefly in 1% (w/v) BSA in adipocyte Krebs-Ringers-HEPES buffer (aKRH) at 37 °C. 200 nM adenosine was added to the aKRH buffer and the digestion buffer to prevent lipolysis. 4 fat pads were added per universal tube containing 5 ml digestion buffer. The fat pads were finely minced and incubated in a 37 °C shaking water bath for about 30 min until all the lumps had digested. The resulting cell suspension was filtered, through a nylon mesh with a 250 μm pore size [LK], into a 23 ml polystyrene flat-bottomed tube [SR]. The cells were washed with 1% (w/v) BSA / aKRH. The cells were allowed to float and the infranatant buffer was removed using a needle (2 mm dia. x 100 mm) attached to a 20 ml plastic syringe. 15 – 20 ml 1% (w/v) BSA / aKRH was added back to the cells and the wash step was repeated a further 3 times. The cell suspension was then adjusted to a 40% cytocrit. The cell density was estimated by taking a sample of cell suspension into a capillary tube and then sealing the end with plasticine. The tube was centrifuged briefly at 1,000 x g and the packed cell volume was calculated as the fraction of the length of packed cells to the total length of the cells and buffer in the tube.

2.2.2.1.2 Insulin Stimulation of Isolated Rat Adipocytes

The isolated adipocytes with a 40% cytocrit were stimulated with 20 nM insulin for 20 min at 37 °C.

2.2.2.1.3 Subcellular fractionation of Rat Adipocytes

The isolated adipocyte cells were washed with TES buffer containing protease and phosphatase inhibitors at 18 °C and the cells were left to float. The infranatant buffer was removed and 1 ml of TES was added to the cells. The cells were homogenised using 10 strokes of a 55 ml Potter-Elvehjem homogeniser [T] with a clearance of 0.15 mm at a rotation speed of

approximately 1,600 rpm. The homogenates were centrifuged at 1,000 x g at 4 °C for 1 min in a refrigerated Ole Dich centrifuge [CL]. This resulted in a pellet of red blood cells, an infranatant layer containing homogenised cells and a top layer of fat. The infranatant layer was removed using a needle (21 g x 1.5") and syringe. The following spins were carried out at 4 °C in a Beckman TL-100 benchtop ultracentrifuge with a TLA-100.3 fixed angle rotor (or a TLS-55 swing-out rotor, where stated otherwise). The following centrifugation scheme is illustrated in Figure 2.1. The infranatant layer was centrifuged at 17,500 x g (18,000 rpm) for 20 min to obtain a crude plasma membrane (PM) pellet containing both mitochondria and nuclei and a microsomal cytosolic fraction in the supernatant. The supernatant was centrifuged at 49,000 x g (30,000 rpm) for 9 min to pellet the high density microsomes (HDM), leaving the low density microsomes and cytosol in the supernatant. The pellet was resuspended in 2 ml TES and pelleted again at 49,000 x g (30,000 rpm) for 9 min. The high density microsomes were then resuspended in 50 µl TES. The low density microsomes (LDM) were pelleted by centrifugation at 541,000 x g (100,000 rpm) for 17 min with the remaining supernatant being the cytosol fraction. The low density microsome pellet was washed with 2 ml TES and again pelleted at 541,000 x g for 17 min. Finally the low density microsomes were resuspended in 100 µl TES. The pellet containing plasma membrane was resuspended in 1 ml TES by homogenisation with 5 strokes of a 2 ml homogeniser. The homogeniser was washed out with a further 1 ml TES which was added to the membranes and centrifuged at 17,500 x g (18,000 rpm) for 20 min. The pellet was resuspended in 300 µl TES and loaded onto a 600 µl TES sucrose cushion and centrifuged at 105,000 x g (35,000 rpm) for 20 min in the TLS-55 swing out rotor. The mitochondria and nuclei were found in the pellet. The plasma membrane was recovered from the cushion interface, resuspended in 2 ml TES and centrifuged at 74,000 x g (37,000 rpm) for 9 min. The plasma membrane pellet was washed with another 2 ml TES and re-pelleted at 74,000 x g for 9 min. The plasma membranes were then resuspended in 100 µl TES. All of the fractions were assayed for protein content and stored at –70 °C.

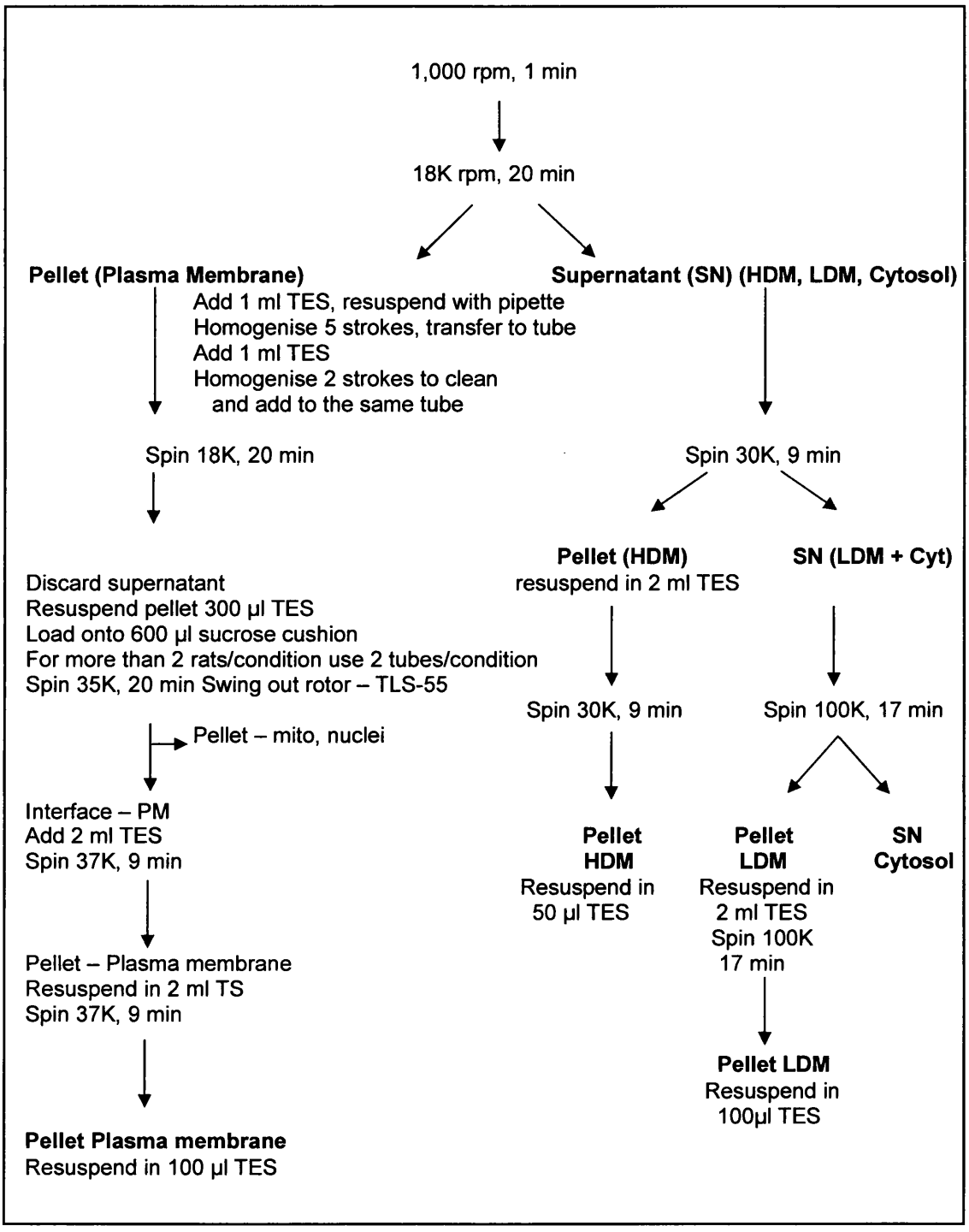

Figure 2.1 **The subcellular fractionation centrifugation method.**

2.2.2.1.4 Deglycosylation of Rat Adipocyte LDM Membranes

20 µg LDM membranes from basal adipocytes were denatured in glycoprotein denaturing buffer [NEB] for 10 min at 100 °C. G7 Buffer [NEB] and 1% (v/v) NP-40 [NEB] were added to the reaction. After the addition of 3 µl (1500 U) Peptide: N-Glycosidase F (PNGase F) [NEB] the reaction was incubated for 1 h at 37 °C. The reaction was terminated by the addition of sample buffer.

2.2.2.1.5 [$^{32}P_i$] Labelling and treatments of Rat Adipocytes

Isolated adipocytes were washed twice with 3% (w/v) BSA / low P_i aKRH. The cells were made back to a 40% cytocrit and incubated with radioactive ^{32}P orthophosphate [$^{32}P_i$] [A] at 0.3 mCi [$^{32}P_i$] / ml cells for 2 h, shaking gently at 37 °C. The buffer was removed and fresh buffer added back to a 40% cytocrit. The cells were then incubated with different treatments (Table 2.7). The cells were washed twice with low P_i aKRH containing no BSA, Ca^{2+} or Mg^{2+} but containing the treatments used. The cells were briefly centrifuged in the Allegra™ X-22 centrifuge [BC] at 1,000 rpm (193 x g) to pack the cells at the top of the tube. The infranatant was discarded and the cells were lysed in adipocyte lysis buffer containing protease and phosphatase inhibitors for 30 min at 4 °C. The insoluble material was pelleted at 16,000 x g at 4 °C in a Beckman GS-15R centrifuge [BC]. GLUT4 was then immunoprecipitated from the cell lysate.

Treatment	Incubation Time
20 nM Insulin	20 min after [$^{32}P_i$] incubation
1 µM Okadaic Acid [AC]	20 min after [$^{32}P_i$] incubation
50 µM 5,6-Dichloro-1-β-D-ribofuranosylbenzimidazole (DRB) [CB]	2 h during [$^{32}P_i$] incubation
25 µM 4,5,6,7-Tetrabromobenzotriazole (TBB) [CB]	2 h during [$^{32}P_i$] incubation
1 µM Isoproterenol [S] + 0.5 U/ml Adenosine deaminase [S]	10 min at end of insulin stimulation

Table 2.7 **The treatment and length of incubation carried out on [$^{32}P_i$] labelled adipocytes.**

2.2.2.2 Rat Cardiomyocytes

2.2.2.2.1 Isolation of Rat Cardiomyocytes

Calcium-resistant, rod-shaped cardiomyocytes from adult male Wistar rats (260-280 g fed *ad libitum*) were prepared using a method originally described (Fischer *et al.*, 1991) with some modifications. Briefly, animals were anaesthetised with 350 µl Sagatal™ (Pentobarbitone Sodium b.p., 60 mg/ml, [RM]) before administration of 500 units of heparin solution via the tail vein. After 5 min the neck was dislocated and the heart rapidly removed into semi-frozen Buffer A (0 – 4 °C). The heart was immediately mounted on to a cannula and perfused by the method of Langendorff, with Buffer A, at 37 °C, for 5 min

in order to remove blood and metabolites from the coronary vessels and atrial and ventricular chambers. The perfusion was then switched to Buffer B equilibrated with oxygen and was recirculated by means of a peristaltic pump. After approximately 30 min, 100 μM $CaCl_2$ was added to the recirculating buffer. The $CaCl_2$ concentration was raised to 200 μM after a further 2 – 3 min. The heart was perfused for a total of 40 min prior to its removal from the cannula. The heart tissue was dissociated in a buffer containing 10 ml Buffer B and 10 ml Buffer C pre-warmed to 37 °C and under an oxygen atmosphere. The calcium concentration was increased in 200 μM steps until the final concentration was 800 μM.

The digested suspension was filtered through 250 μm^2 nylon gauze [LK] and the cardiomyocytes were allowed to settle for 3 – 4 min to form a loose pellet. The supernatant was removed and the cells resuspended in 30 ml Buffer D. The cells were allowed to settle again for 3 – 4 min at room temperature and the supernatant was removed. The pellet was resuspended in 25 ml Buffer E and the cell suspension was incubated for 20 min at 37°C under an oxygen atmosphere to allow the cells to recover from the isolation procedure. Viability was assessed by counting the number of rod-shaped (viable) versus round-shaped (dead) cells under the light microscope.

2.2.2.2.2 Insulin Stimulation of Isolated Cardiomyocytes

The isolated cardiomyocyte cells were stimulated with 30 nM insulin for 30 min at 37 °C.

2.2.2.2.3 [$^{32}P_i$] Labelling and Treatments of Cardiomyocytes

Isolated cardiomyocytes were left to recover in a low P_i Buffer E for 20 min at 37°C. Cells were incubated with 0.3 mCi [$^{32}P_i$] / ml cells for 2.5 h shaking gently at 37°C under an oxygen atmosphere. During this incubation, the cells were treated where necessary with 5 µM oligomycin for 90 min and / or 30 nM insulin for 30 min. Following the [$^{32}P_i$] labelling, the cells were washed twice with low P_i cKRH containing no BSA, Ca^{2+} or Mg^{2+} but containing insulin or oligomycin depending on the treatments. After the second wash, the cells were centrifuged in the Allegra™ X-22 centrifuge [BC] at 700 rpm (94 x g) for 1 min. The supernatant was removed and the cells were lysed in cardiomyocyte lysis buffer containing protease and phosphatase inhibitors for 50 min at 4 °C, with rotation. The insoluble material was pelleted at 16,000 x g at 4 °C in a Beckman GS-15R centrifuge [BC]. GLUT4 was then immunoprecipitated from the cell lysate.

2.2.3 Perchloric Acid Precipitation

Adipocytes: 300 µl 40% (w/v) adipocytes were taken and added to 33 µl 25% (v/v) perchloric acid (PCA).

Cardiomyocytes: An aliquot of cardiomyocytes (1/5 of a heart) were taken and pulse spun to pellet the cells. The buffer was removed and 250 µl 2.5 % (v/v) PCA was added to the cells.

The cells (adipocytes or cardiomyocytes) and PCA were mixed vigorously and incubated on ice for 10 min. Following centrifugation at 10,000 x g for 10 min at 4 °C, the supernatant was neutralised with an equal volume of 4.2 M KOH, 1 M HEPES, and water (1:2:7) (pH 7.6) and incubated on ice for 10 min. The

precipitate was removed by brief centrifugation and the supernatant was frozen until needed.

2.2.4 ATP Determination Assay

The amount of ATP in the neutralised supernatant (Section 2.2.3) was determined using a bioluminescent ATP determination kit [MP] in which the level of ATP is determined using recombinant firefly luciferase and its substrate D-luciferin, according to the protocol provided by the manufacturer.

2.2.5 Protein Kinase A (PKA) Assay

Adipocytes: The PKA assay carried out was essentially that of Nishimura *et al.* The PKA assay reaction mixture contained 100 µM Kemptide [CB] or 100 µM Histone [S], 20 mM 3-(N-Morpholino)propanesulfonic acid (Mops) (pH 7.0), 16 mM magnesium acetate, 4 mM DTT and 20 µl neutralised supernatant (Section 2.2.3). The reaction was initiated by the addition of 2500 U PKA [NEB]. The 60 µl reactions were incubated for 1 h at 30 ^{o}C (Nishimura *et al.*, 1991). At the end of the incubation, the reactions were stopped. The tubes containing histone were placed on ice and the tubes containing kemptide were stopped with 20 µl stop solution consisting of 100 mM ATP (pH 7.0), 100 mM EDTA, 250 mM DTT and 5% (w/v) SDS.

The ^{32}P-labelled kemptide was purified using a tandem chromatographic column method from Egan *et al.* 1 ml of a washing solution consisting of 5 mM ATP (pH 6.8) was added to the stopped reaction and the reaction was added into a column containing CM-Sephadex cation exchange resin (C50). The ^{32}P-kemptide binds to the column and the ATP passes through in the eluate and is discarded. The CM-Sephadex column was washed with a further 1 ml of washing solution. The CM-Sephadex column was mounted on top of a column

containing Dowex 1X-8 anion exchange resin. The ^{32}P-kemptide was eluted from the CM-Sephadex column by the addition of 8 ml 30% (v/v) acetic acid. The ^{32}P-kemptide passed through the Dowex 1X-8 column, in which any residual [^{32}P-ATP] was trapped. The eluate was collected and counted in 1 ml fractions in the scintillation counter (Egan *et al.*, 1988).
The reactions containing histone were spotted onto P81 phosphocellulose squares [U] and allowed to dry. The squares were then washed four times in 75 mM phosphoric acid for 5 min each, followed by a few seconds in acetone. The squares were allowed to dry and then were added to scintillation fluid before being counted in the scintillation counter.

Cardiomyocytes: [γ-^{32}P] ATP [A] or 18 µl of the neutralised supernatant from the PCA precipitation was added to 40 µM Kemptide [CB] and PKA buffer [NEB]. The reaction was initiated by the addition of 2500 U PKA [NEB]. The 60 µl reactions were incubated for 1 h at 30 °C. At the end of the reaction the tubes were placed on ice. The reactions were then spotted in duplicate onto P81 phosphocellulose squares [U] and allowed to dry. The squares were then washed four times in 75 mM phosphoric acid for 5 min each, followed by a few seconds in acetone. The squares were allowed to dry and then were added to scintillation fluid before being counted in the scintillation counter.

2.2.6 Immunoprecipitation

2.2.6.1 Immunoprecipitation using Protein A

Immunoprecipitation was carried out using antibody linked to Protein A (immobilised on sepharose CL-4B) [S]. 5 mg Protein A Sepharose was swollen on ice in 1 ml PBS for 10 min and then washed with 1 ml PBS. All wash steps were followed by centrifugation at 6,000 rpm in a MSE microcentaur microfuge to pellet the beads. The beads were incubated overnight, at 4 °C, in 1 ml PBS

containing a 16-fold molar excess of antibody over the amount of GLUT4 to be immunoprecipitated. The unbound antibody was then removed by washing the pellet 4 times with PBS.

Whole cell fractions or low density microsomes (LDM), obtained after subcellular fractionation, were lysed in either adipocyte or cardiomyocyte lysis buffer containing protease and phosphatase inhibitors, for 20 min at 4 °C. The unsolubilised material was pelleted by centrifugation in a refrigerated Ole Dich centrifuge [CL] at 20,000 x g for 20 min.

The solubilised protein fractions were then incubated with the antibody-linked beads for 2 h at 4 °C with rotation. The supernatant was recovered after centrifugation at 6,000 rpm for 1 min and retained until the end of the experiment at –20 °C. The pellet was washed 3 times with lysis buffer, 3 times with a 10-fold dilution of lysis buffer and 3 times with PBS. The bound protein was then eluted from the pellets using sample buffer containing 100 mM Dithiothreitol (DTT) unless otherwise stated, for 20 min at room temperature, with occasional vortexing. The wash buffers and elution buffer contained the phosphatase inhibitors, sodium fluoride, sodium orthovanadate and sodium molybdate when phosphorylated samples were being analysed. Samples were then analysed by SDS-PAGE and Western blotting.

2.2.6.2 Seize® Primary Immunoprecipitation Kit

Immunoprecipitation using the Seize® Primary Immunoprecipitation Kit [P] was carried out according to the protocol provided by the manufacturer.

2.2.7 Protein Digestion Techniques

2.2.7.1 Endoproteinase Lys C Digestion

GLUT4, eluted from the immunoprecipitation, was incubated with 2 µg Endoproteinase Lys C (Endo LysC) [R] for 19 h at 37 °C.

2.2.7.2 Cyanogen Bromide Digestion

Following immunoprecipitation, GLUT4 was either excised from the gel (as for the adipocytes) or from polyvinylidene fluoride (PVDF) membrane following transfer of a SDS-PAGE gel (as for the 3T3-L1 adipocytes).

The gel containing the GLUT4 protein was macerated and the protein was precipitated using 67% (v/v) acetone including 4 µg BSA as a carrier protein, for 30 min at -20 °C. The pellet was resuspended in 3 mg/ml cyanogen bromide (CNBr) in 70% (v/v) formic acid and incubated for 15 h at room temperature.

The PVDF membrane was washed with methanol and ddH_2O and then incubated with 3 mg/ml CNBr in 70% (v/v) formic acid for 36 h at room temperature. Following the addition of a further 3 mg/ml CNBr (to give a final concentration of 6 mg/ml) for a further 15 h, the samples were vortexed and centrifuged and the supernatant was collected. The membrane was then washed with 70% (v/v) formic acid, followed by 0.1% (v/v) trifluoroacetic acid. The acid was evaporated on a speed vac and traces of acid were removed by washing the membrane with ddH_2O and evaporating again.

Tris-tricine sample buffer was added to each of the samples containing the cleaved GLUT4. The samples were resolved by tris-tricine SDS-PAGE.

2.2.8 Protein Biochemistry Techniques

2.2.8.1 Sodium Dodecyl Sulphate - Polyacrylamide Gel Electrophoresis (SDS-PAGE)

2.2.8.1.1 Tris-Glycine SDS-PAGE

Electrophoresis was carried out using the Laemmli discontinuous buffer system (Laemmli, 1970). Slab gels were prepared using either the mini-Protean II apparatus [BR] or the Atto Dual Mini Vertical PAGE cell system [AT]. All gels were made with a 1.5 mm thickness. Gels were prepared using acrylamide/bis-acrylamide (30% (w/v) acrylamide) [ND] and gel buffers. Polymerisation of the gels was initiated by the addition of 10% (w/v) ammonium persulphate (APS) [BR] and N,N,N,N'-tetramethylethylenediamine (TEMED) [BR]. The composition of the resolving and stacking gels is given in Table 2.8. Samples were solubilised by the addition of sample buffer and incubated for 20 – 30 min at room temperature with occasional vortexing. Samples were loaded onto the gels with high molecular weight (HMW) markers [S] and were run in electrophoresis buffer. The gels were run at 200 V for about 1 h until the dye front had run out of the gel. High molecular weight markers consist of myosin (205 kDa), β-galactosidase (116 kDa), phosphorylase b (97.4 kDa), bovine albumin (66 kDa), ovalbumin (45 kDa) and carbonic anhydrase (29 kDa).

Stock Solutions	Resolving Gel		Stacking Gel
	8%	10%	
Resolving gel buffer (ml)	25	25	-
Stacking gel buffer (ml)	-	-	5
Acrylamide stock (ml)	20	25	3.4
Double-distilled water (ml)	30	25	7.5
Ammonium persulphate (ml)	0.5	0.5	0.1
TEMED (μl)	40	40	20

Table 2.8 **Quantities of stock solutions required to make up the resolving gel (either 8 or 10 percent acrylamide) and the stacking gel for tris-glycine SDS-PAGE.**

2.2.8.1.2 Tris-Tricine SDS-PAGE

Electrophoresis was carried out using the method described in Schägger and von Jaglow (Schagger and von Jagow, 1987). This method gives better resolution for small peptides than the tris-glycine SDS-PAGE method. Slab gels were prepared using the Atto Dual Mini Vertical PAGE cell system [AT]. All gels were made to a thickness of 1.5 mm. Gels were prepared using 40 % (w/v) Acrylamide 29:1 [S] and gel buffer. Polymerisation of the gels was initiated by the addition of 10% (w/v) APS [BR] and TEMED [S]. The composition of the resolving, spacer and stacking gels are given in Table 2.9. The resolving gel was poured to 4 cm and the spacer gel to 1 cm. Samples were solubilised by the addition of Tris-Tricine sample buffer and heating for 2 min at 65 ^{o}C. Samples were loaded onto the gels with ultra-low range molecular weight (LMW) markers [S] and run with anode and cathode buffers in the corresponding chambers of the gel tank. The gels were run at 100 V for

about 3 h until the dye front had run out of the gel. Ultra-low range molecular weight markers consist of triose phosphate isomerase (26.6 kDa), myoglobin (17 kDa), α-lactalbumin (14.2 kDa), aprotinin (6.5 kDa), insulin chain B (3.496 kDa) and bradykinin (1.06 kDa).

Stock Solutions	16% Resolving Gel	10% Spacer Gel	5% Stacking Gel
Gel buffer (ml)	13.3	13.3	10
Acrylamide 29:1 (ml)	16	10	5
50% (v/v) Glycerol (ml)	7	-	-
Double-distilled water (ml)	3.7	16.7	25
Ammonium persulphate (ml)	200	200	320
TEMED (μl)	40	40	60

Table 2.9. **Quantities of stock solutions required to make up the resolving, spacer and stacking gels for tris-tricine SDS-PAGE.**

2.2.8.2 Electrophoretic Transfer of Proteins to Nitrocellulose Membranes

Following SDS-PAGE, proteins on the gel were transferred onto nitrocellulose membrane using the Multiphor II NovaBlot electrophoretic transfer apparatus [A]. The gel was incubated briefly in transfer buffer to remove the electrophoresis running buffer. The electrode paper and nitrocellulose were

also briefly immersed in transfer buffer. Nine pieces of NovaBlot electrode paper [A] cut to the size of the gel were placed on the anode, followed by a piece of nitrocellulose membrane with a 45 μM pore size [GE]. The resolving gel was then placed on top followed by another nine pieces of electrode paper and then the cathode. It was ensured that there were no bubbles trapped between any of the layers. The transfer was run at (area of the gel cm^2) x 0.8 mA for 1 h 50 min. Following transfer, the nitrocellulose membrane was washed briefly in ddH_2O, and stained with Ponceau S stain for a few minutes. Excess stain was washed off with ddH_2O and the protein bands were visualised. The nitrocellulose was left to air dry and the molecular weight markers were marked on the nitrocellulose.

2.2.8.3 Western Blotting

The nitrocellulose was washed in Tris-buffered Saline containing Tween-20 (TBS-T) to remove the Ponceau S stain. The nitrocellulose was then blocked in 5% (w/v) Marvel (dried skimmed milk powder) in TBS-T for 60 min (unless otherwise stated) to block non-specific protein sites. The membrane was washed 4 x 15 min in TBS-T followed by incubation with the primary antibody (Table 2.2) for 90 min. The nitrocellulose was washed 6 x 5 min with TBS-T followed by incubation with the secondary antibody (Table 2.3) for 45 min. Finally the nitrocellulose was washed again 6 x 5 min in TBS-T and developed using ECL or ECL Advance [A] following the manufacturers guidelines. Essentially solutions were mixed in a 1:1 ratio and the membrane incubated for 1 min for ECL and 5 min for ECL advance. The image was detected by use of a Hamamatsu camera attached to the EPI Chemi II darkroom [UVP].

2.2.8.4 Stripping a Western Blot

The nitrocellulose was added to the stripping buffer and incubated at 50 °C for 30 min with gentle agitation. The membrane was washed 2 x 10 min in TBS-T. Western blot analysis was then carried out as section 2.2.8.3.

2.2.8.5 BCA Protein Assay

The bicinchoninic acid (BCA) protein assay [P] was used to determine protein concentrations. A standard curve of BSA (1 mg/ml BSA in 0.1 M NaOH) was prepared. 10 µl of 0 – 10 µg BSA was added to a microtitre plate [BS] in duplicate. 10 µl of sample was also added to the plate, either undiluted or with a final concentration of 0.1 M NaOH. The BCA working solution was prepared by adding Reagent A [P] and Reagent B together in a ratio of 50:1. 200 µl of this was then added to each of the wells containing standard and sample. The plate was incubated at 37 °C for 30 min, allowed to cool and then read on a Spectra Rainbow Thermo microplate spectrophotometer [TE] at 565 nm.

2.2.8.6 Data Analysis

GraphPad PRISM version 4.0 was used for all graphical analysis. Labworks version 4 [UVP] was used for analysis of the Western blots. The intensity of the radioactive ^{32}P-containing bands was carried out using ImageGauge [FU].

2.2.9 Antibody Generation

2.2.9.1 Peptide Synthesis

Peptides were synthesised by Dr Graham Blcomberg at the University of Bristol (Figure 2.2). Peptides were synthesised with a cysteine at either the amino- or the carboxyl-terminus of the peptide. This was to facilitate conjugation of the peptide to other proteins or for its immobilisation onto a solid support to aid antibody purification. The peptides were over 95% pure and were lyophilised and stored at -20 °C until required.

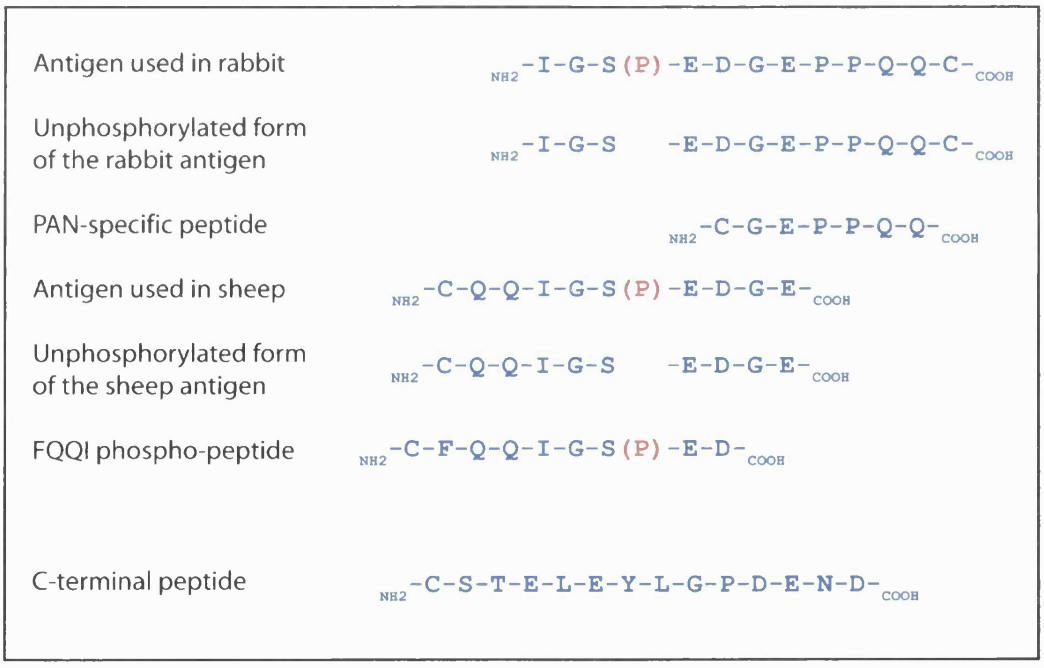

Figure 2.2 **Sequence of the peptides used in the antibody purification study.**

2.2.9.2 Quantification of the Free Sulphydryl Content in Peptides

The cysteine residue in the peptide needs to be in a reduced state for conjugation to carrier proteins. It is possible to determine the level of reduced cysteines by quantifying the free sulphydryl content within the peptide. 5,5'-Dithiobis (2-nitrobenzoic acid) or Ellman's reagent [P] will react with sulfhydryl groups to produce a chromaphore. Thus the amount of reduced peptide can be calculated by comparison to a standard curve of L-cysteine.

A 1 mg/ml stock of Ellman's reagent was made in PBS. 1 mg/ml stock solutions were also prepared of L-cysteine and peptide, both in PBS. 200 µl PBS was added to each well of a 96 well microtitre plates [N]. 10 µl of the peptide solution was added to two buffer containing wells. Serial dilutions of L-cysteine were prepared and 10 µl were added to buffer containing wells to give a standard curve of 0 – 10 µg L-cysteine. 20 µl of the 1 mg/ml Ellman's reagent was added to the each well containing the peptide or L-cysteine. The plate was incubated for 15 min at room temperature and the absorbance read at 412 nm in a Spectra Rainbow Thermo spectrophotometer [TE]. A negative control of buffer only was used as a background level. The level of reduced peptide was determined by comparing the O.D. of the peptides to that of the standard curve of cysteine.

2.2.9.3 Preparation of Peptide Conjugated to KLH

To effectively raise antibodies against small non-immunogenic molecules i.e. peptides, it is necessary to couple them to a carrier protein via a cross linker. The phosphorylated N-terminal peptide (antigen used in sheep) and the C-terminal peptide were coupled to the carrier protein, Imject® Mariculture Keyhole Limpet Hemocyanin (KLH) [P], using the crosslinker m-Maleimidobenzoyl-*N*-Hydroxysuccinimide ester (MBS) [P]. KLH was in a lyophilised form and was reconstituted with 2 ml ddH_2O to make a 10 mg/ml

solution containing PBS with proprietary stabiliser. MBS was dissolved in dimethyl sulfoxide (DMSO) to give a final concentration of 10 mg/ml. 1 mg MBS was added to 5 mg KLH (per antibody being produced) and mixed for 1 h at room temperature to allow amide bond formation.

The MBS-activated KLH was separated from free MBS via gel filtration on an 8 ml Sephadex G-25 column. The column was washed with 5 column volumes of conjugation buffer. The MBS-KLH sample was applied to the equilibrated column. 0.5 ml fractions were collected and the elution of the MBS-KLH was followed at 280 nm. Two peaks elute, with the first being the MBS activated KLH and the second unreacted MBS. The fractions containing MBS-KLH were pooled. 5 mg peptide was dissolved in 1.25 ml conjugation buffer and added to the pooled MBS-KLH fractions. This was incubated for 2 h at room temperature. The peptide-MBS-KLH conjugate was dialysed against 5 L PBS, overnight, at 4 °C to purify the conjugate and remove EDTA. The concentration of the conjugate was determined by BCA protein assay. 1 mg samples of the peptide-MBS-KLH conjugate were aliquoted and stored at -20 °C.

2.2.9.4 Injection Protocol

The immunisations were carried out by Diagnostics Scotland [D]. For each immunisation, 1 mg of the peptide-MBS-KLH conjugate was mixed with Freund's complete adjuvant (for the primary immunisation) or Freund's incomplete adjuvant (for subsequent booster immunisations) and injected subcutaneously into sheep. Injections were given every 28 days and test bleeds obtained 7 days after the booster injections. Three test bleeds were taken with further bleeds taken if needed. The sheep were not exsanguinated at the end of the procedure.

2.2.9.5 ELISA plate assay

A 50% (v/v) glycerol stock was made in ELISA plate coating buffer. 2 ml of this solution was added to 2 mg peptide. 100 µl of this was further diluted in 10 ml coating buffer resulting in a concentration of 10 µg/ml. The remaining peptide glycerol stocks were stored at –20 °C. C8 Maxisorp plates [N] were coated with 100 µl of the 10 µg/ml peptide solution per well, covered and incubated overnight at 4 °C. The plates were washed three times with PBS-T with rigorous expulsion of liquid out of the wells. The wells were filled with 200 µl ELISA plate blocking buffer and incubated, shaking, for 1 h at room temperature. The plate was washed twice with PBS-T. A 1:100 dilution of antibody was made in PBS-T. 200 µl of this was placed in the first well. 100 µl was withdrawn and placed into the second well containing 100 µl PBS-T. This serial dilution was performed 12 times across the plate. The plate was then covered and incubated with gentle shaking for 2 h at room temperature. The wells were washed three times with PBS-T. 100 µl anti-rabbit IgG HRP or anti-sheep IgG HRP (1:4000 dilution in PBS-T) was added to each well and incubated, shaking, for 2 h at room temperature. The plates were then washed three times with PBS-T and twice with PBS. ELISA sodium acetate/citrate buffer was diluted 1:20 in ddH_2O and the pH checked (pH 6.0). 49.5 ml of the solution was added to 0.5 ml Tetramethyl Benzidine (TMB) (10 mg/ml in DMSO) and 10 µl 30% (v/v) H_2O_2. 100 µl of this was added to each of the wells and incubated at room temperature until a blue colour has developed over the range of dilutions. The reaction was stopped by the addition of 50 µl 1.84 M H_2SO_4 per well. The plates were then read in a Spectra Rainbow Thermo microplate spectrophotometer [TE] with filter 1 measuring O.D. at 450 nm and filter 2 measuring O.D. at 700 nm (to eliminate background readings).

2.2.10 Antibody Affinity Purification

The antibody was purified against peptide coupled to SulfoLink® Coupling gel [P]. The gel binds peptides containing free sulfhydryl groups through iodoacetyl moieties attached to a 12 atom spacer arm, which reduces the steric hindrance and allows a more efficient binding. All buffers were degassed before use.

2.2.10.1 Generation of a Peptide Coupled Column

The SulfoLink® gel was brought to room temperature. 2 ml of gel was packed into a Talon 2 ml empty disposable column [BD]. The column was equilibrated with six column volumes coupling buffer. The bottom of the column was capped and 2 ml of 1 mg/ml peptide in coupling buffer was added. An aliquot of peptide was retained for protein analysis. The top of the column was capped and the column was incubated at room temperature for 15 min with rotation followed by 30 min without rotation. The column was drained and washed with 3 column volumes of coupling buffer. Both the flow through from the column and the wash were kept. A BCA protein assay was carried out to determine coupling efficiency. The bottom of the column was capped and 2 ml of 50 mM L-cysteine in coupling buffer was added to the column to block non-specific binding sites on the gel. The top cap was replaced and the column incubated at room temperature for 15 min with rotation followed by 30 min without rotation. The column was drained and washed with 16 column volumes 1 M NaCl and 16 column volumes 0.05% (w/v) sodium azide. The bottom cap was replaced and 2 ml 0.05% (w/v) sodium azide was added. The top cap was replaced and the column was stored in an upright position at 4 °C.

2.2.10.2 Affinity Purification of Serum

The column prepared in section 2.2.10.1 was brought to room temperature and drained. The column was equilibrated with 4 column volumes PBS. 3 ml serum was added to the column followed by 2 ml PBS. The caps were replaced and the column incubated at room temperature for 90 min with rotation. The column was drained and the flow through retained. The column was then washed with 2 column volumes 1 M NaCl to remove weakly associated proteins, followed by 6 column volumes PBS. The antibody was eluted from the column with 8 ml 100 mM Glycine (pH 2.75) with 1 ml fractions collected and neutralised by the addition of 50 µl 1 M Tris (pH 9.5). The column was washed with 8 column volumes PBS, followed by 16 column volumes 0.05% (w/v) sodium azide. The bottom cap was replaced and 2 ml 0.05% (w/v) sodium azide was added. The top cap was replaced and the column was stored in an upright position at 4 °C. The eluted fractions were analysed for protein content and the fractions containing high levels of protein were pooled together and dialysed overnight at 4 °C against 5 L PBS. The dialysed solution was concentrated using either PEG 20000 [BDH] which acts to remove water out of the solution or in a Centricon-plus 20 spin column [ML]. The protein content was measured using a modified BCA protein assay. An IgG protein standard curve was used, instead of BSA, to give the concentration of protein in mg/ml IgG. The affinity purified antibody solution was made up to a 40% glycerol stock and the protein concentration was adjusted accordingly. The antibody was stored at -20 °C until required.

2.2.11 Molecular Biology

2.2.11.1 Oligonucleotide Primers

DNA primers were made to order by MWG [MWG]. Primer sequences for site-directed mutagenesis and sequencing are given in Tables 2.10 and 2.11, respectively.

Primer	Sequence
Ala10 forward	C CAA CAG ATA GGC **GCC** GAA GAT GGG GAA CC
Ala10 reverse	GG TTC CCC ATC TTC **GGC** GCC TAT CTG TTG G
Asp10 forward	C CAA CAG ATA GGC **GAT** GAA GAT GGG GAA CC
Asp10 reverse	GG TTC CCC ATC TTC **ATC** GCC TAT CTG TTG G
Ala488 forward	CAC CGG ACA CCC **GCA** CTT TTA GAG CAG G
Ala488 reverse	C CTG CTC TAA AAG **TGC** GGG TGT CCG GTG
Asp488 forward	CAC CGG ACA CCC **GAT** CTT TTA GAG CAG G
Asp488 reverse	C CTG CTC TAA AAG **ATC** GGG TGT CCG GTG

Table 2.10 **Sequence of primers used for site directed mutagenesis.** The bases in bold represent the amino acid being mutated.

Primer	Sequence
N-terminal	CAGCCACGTCTCATTGTAGC
C-terminal	GGTTGTTGCGGAGGCTATGGGGCTCCAG

Table 2.11 **Sequence of primers used for DNA sequencing.**

2.2.11.2 Site-Directed Mutagenesis

Site-directed mutagenesis was carried out by polymerase chain reaction (PCR) using mutagenic primers to the amino acid being mutated. Complementary primers were used with a long annealing time so that the whole plasmid would be amplified. DNA was mutated by PCR with either 2.5 U PfuTurbo DNA polymerase [ST] or 2.5 U Platinum Pfx DNA polymerase [I] in 50 μl reactions using a MiniCycler [MJ]. A typical program is illustrated below (Table 2.12).

Segment	Cycles	Temperature	Time
1	1	95 °C	1 min
2	18	95 °C	50 sec
		64 °C	50 sec
		68 °C	18.75 min *
3	1	68 °C	17.5 min

Table 2.12 **An example of the cycling parameters used for the site-directed mutagenesis PCR.** * 2.5 min / kb of plasmid length.

2.2.11.3 *Dpn* I Digestion

10 U *Dpn* I was added to the PCR product and incubated at 37 °C for 1 h. The enzyme was then heat inactivated at 80 °C for 20 min.

2.2.11.4 DNA Analysis

PCR products were run on 1% (w/v) agarose Tris-acetate EDTA (TAE) gels at 160 V for 20 – 40 min. The bands was visualised by ethidium bromide staining under UV transillumination.

DNA sequencing was carried out using a PE Biosystems ABI 377 DNA Sequencer [AB] at the University of Bath sequencing facility.

2.2.11.5 Transformation

The *Dpn* 1 digested PCR product was transformed into XL1 Blue (*recA1 endA1 gyrA96 thi-1 hsdR17 supE44 relA1 lac [F' proAB lac1^{q}ZΔM15 Tn10 (Tet^{r})]*) competent *E.coli* cells [ST]. 2 µl PCR product was added to 50 µl chemically competent cells on ice and incubated for 30 min. The cells were heat shocked for 45 sec at 42 °C and then the cells were placed on ice for 2 min. 250 µl Luria Broth was added to the cells and incubated at 37 °C for 45 min. All of the cells were then plated on agar plates containing 50 µg/ml Ampicillin and incubated at 37 °C overnight.

2.2.11.6 Plasmid manipulations

Plasmid DNA was purified from cultures of the transformed XL1 Blue *E.coli* cells in 5 ml LB media using the Wizard Plus SV miniprep DNA purification system [P], according to the protocol provided by the manufacturer.

2.2.12 Electroporation of Rat Adipocytes

Rat adipocytes were prepared as in section 2.2.2.1.1 except that all buffers were sterile filtered through a 0.2 µm filter [ML] before use and all instruments were sterile. The cells were washed twice with 1% (w/v) BSA / aKRH and a further two times with DMEM (1). The cell suspension was adjusted to a 49% cytocrit. Four cuvettes were used per condition and 200 µl DMEM (1) containing 0.1 µg HA-GLUT4 DNA and 100 µg sheared herring sperm DNA was added to each cuvette. 200 µl of the 49% cell suspension was then added to the cuvette

and gently shaken to mix. Electroporation was carried out using the Biorad gene pulser [BR], with a capacitance extender attached. Each cuvette was electroporated once at 400 V, 500 µF. This gave a time constant in the region of 13 ms. The cells were washed with DMEM (2) and allowed to float at 37 °C. The infranatant was removed and the cells were resuspended with 4 ml DMEM (3). The cells were mixed by gentle inversion to disperse any clumps and transferred to 35 mm dishes and incubated for 5 h at 37 °C in 5% (v/v) CO_2.

2.2.13 Antibody Binding Assay

The electroporated cells were transferred into 4 ml tubes (50 mm x 13 mm polypropylene tube [N]) at 37 °C. The cells were washed 2 times with aKRH, filling to at least 2 ml and allowing the cells to float up each time. The tubes were filled to 1 ml and 20 µl of the cell suspension was removed for SDS-PAGE analysis to determine transfection levels. The cells were washed twice with 1% (w/v) BSA / aKRH, filling the tubes to 2 ml. 60 nM insulin was added to the cells and incubated at 37 °C for 20 min. Trafficking was stopped by the addition of 53 µl 80 mM KCN for 3 min at 37 °C. Unless otherwise stated, the buffers in the remainder of the assay contained 2 mM KCN. The cells were washed twice with 5% (w/v) BSA / aKRH. The primary antibody (Table 2.4) was added to the cells and incubated for 1 h, mixing every 15 min. The cells were again washed twice with 5% (w/v) BSA / aKRH followed the addition of the secondary antibody (Table 2.4) for 60 min, mixing every 15 min. The cells were washed once with 5% (w/v) BSA / aKRH and three times with aKRH containing no KCN. The cells were resuspended to 1 ml and aliquots were removed for protein assay. To assay the bound antibody, 90 µl KRH was added into wells of a black 96 well plate [G] and 10 µl of cell suspension was also added to each well. 100 µl 0.2 mM fluorescein digalactosidase (FDG) [MP] was quickly added to the wells and the plate was read in the FarCyte plate reader [A]. The plate reader was set to measure a Z position of 7808, a gain of

30, no lag time, 40 µs integration time and 30 readings / well. The plate was read for 100 cycles to determine where the rate of reaction was linear.

2.2.14 Confocal Microscopy

2.2.14.1 Cardiomyocytes

Basal and insulin-stimulated cardiomyocytes, prepared as in section 2.2.2.2.1, were washed three times in cKRH to remove any BSA. The cells were centrifuged at 1,000 x g to pellet the cells between washes. All of the incubations were carried out, with shaking, at room temperature. The cells were fixed in 4% (w/v) paraformaldehyde in PBS for 20 min. The cells were washed three times with PBS and permeabilised for 45 min with confocal permeabilisation buffer. The primary antibody (Table 2.5) was added to the cells and incubated for 1 h. The cells were then washed three times with confocal wash buffer and the secondary antibody (Table 2.5) was added for 1 h. Following three washes with the confocal wash buffer and three washes with PBS, an aliquot of the cells was mounted onto glass slides using Vectashield® [VL]. Images were obtained using a LSM 510 Zeiss confocal laser scanning microscope [CZ] with a 63x oil-immersion objective. The fluorophores were excited at 488 nm with an argon laser and at 568 nm or 633 nm with a helium-neon laser.

2.2.14.2 3T3-L1 Adipocytes

3T3-L1 adipocytes, plated on coverslips, were washed with 1 ml of PBS and incubated in serum free media (DMEM) for 2 h at different days after differentiation. The cells were quickly washed with ice cold PBS and fixed in cold methanol for 5 min at –20 °C. Following three washes with PBS, the cells

were blocked in confocal permeabilisation buffer for 45 min, with gentle shaking, at room temperature. The cells were washed four times in confocal wash buffer. The primary antibody (Table 2.5) was added to the cells. The mouse monoclonal anti-C-terminal GLUT4 antibody was incubated overnight at 4 °C and the anti-pSer^{10} antibody was incubated for 1 h at room temperature. The cells were washed four times with confocal wash buffer and the secondary antibody (Table 2.5) was incubated, shaking, for 1 h. After washing the cells four times with PBS, the coverslips were mounted onto glass slides using Vectashield® [VL]. Images were obtained using a LSM 510 Zeiss confocal laser scanning microscope [CZ] with a 63x oil-immersion objective. The fluorophores were excited at 488 nm with an argon laser and at 568 nm with a helium-neon laser.

3 Generation, Purification and Characterisation of Phospho-Specific Anti-GLUT4 Antibodies

3.1 Introduction and Experimental Aims

Antibodies have become an essential part of GLUT4 research and have helped enable the progress which has been seen in all aspects of GLUT4 research over the last 18 years. In 1980, subfractionation and cytochalasin B binding identified a subset of glucose transporters in rat adipocyte cells that were sensitive to insulin. Under basal conditions these transporters were sequestered in intracellular membranes. Following stimulation with insulin, the glucose transporters translocated to the plasma membrane where they could transport glucose into the cell (Cushman and Wardzala, 1980). In fact, it was from the use of a mouse monoclonal antibody (clone 1F8), in western blotting analysis, that James and colleagues confirmed that the insulin-responsive glucose transporter was solely expressed in insulin-responsive tissues (James *et al.*, 1988). This antibody is still frequently used today by many laboratories. Since the production of this monoclonal antibody, many other anti-GLUT4 antibodies have been raised and are frequently used to analyse many different areas of GLUT4 biology. For example, they are used to examine the cellular distribution and trafficking of GLUT4 as well as helping to identify other proteins that are present on GLUT4 containing vesicles (Holman et al., 1990, Cain et al., 1992).

Previous studies to identify potential phosphorylation sites within GLUT4 have used *in vitro* phosphorylation experiments, in which rat adipose tissue was incubated with [$^{32}P_i$] and, after proteolytic digestion of GLUT4, autoradiography was used to detect the sites of phosphorylation (Lawrence, Jr. *et al.*, 1990a). In the last decade, with the evolution of the immunology tools, it has become possible to raise antibodies which will specifically detect phosphorylated

residues within a protein. The use of phosphorylation-specific antibodies could play an important part in the study of the phosphorylation of GLUT4 by corroborating the results seen from the *in vitro* phosphorylation studies, as well as giving a safer alternative to the use of radioactivity.

A previous member of the laboratory, Darren Harper, had raised an antibody in rabbit, to a synthetic peptide corresponding to an area at the N-terminus of GLUT4 containing phosphorylated serine 10 ($pSer^{10}$) (Harper, 2002). However, raising a highly phospho-specific antibody is very difficult and purification of the antibody from the serum is essential. When an antigen is injected into the host, the host's immune response generates antibodies against this foreign body. When the antigen contains a phosphorylated residue, three different classes of antibody will be produced by the host: phospho-specific, non-phospho-specific and PAN-specific antibodies. The phospho-specific antibodies, in which the epitope encompasses the phosphorylated residue, are the desired population. However, antibodies will also be raised to exactly the same epitope as the phospho-specific antibodies, but they will not contain a phosphorylated residue because phosphatases in the host may dephosphorylate the antigen. This gives the second class of antibodies - non-phospho-specific antibodies. The final class of antibodies to be raised will have epitopes which do not contain the phosphorylated residue; these are referred to as PAN-specific antibodies (Figure 3.1).

The aim of the work described in this chapter was to try to purify and characterise a highly phospho-specific population of antibodies recognising the phosphorylated serine 10 residue in GLUT4. This chapter will describe the purification and characterisation of antibodies from the rabbit serum, which has previously been raised against $pSer^{10}$ in the N-terminus of GLUT4 by Darren Harper. The production, purification and characterisation of antibodies in sheep will also be discussed. Both antibodies were raised against $pSer^{10}$ but a different antigen sequence was used to raise the antibody in sheep compared to that used in rabbit. An antibody to the C-terminus of GLUT4 has previously

been raised in rabbit (Holman *et al.*, 1990) and the same antigen was used to raise an antibody in sheep. It was thought that a rabbit anti-C-terminal GLUT4 antibody could be used in conjunction with an anti-pSer^{10} antibody raised in sheep. Alternatively, the anti-pSer^{10} antibody raised in rabbit could be used with the anti-C-terminal antibody raised in sheep. This would be possible because there is no cross reactivity between the anti-sheep and the anti-rabbit secondary antibodies. This would provide an extensive range of antibodies available for use in investigating the phosphorylation status of GLUT4 and hopefully it would be possible to use the phospho-specific pSer^{10} antibodies to study the *in vivo* phosphorylation of GLUT4. Possibly the use of the antibody would enable the identification of any differences in localisation of the phosphorylated and non-phosphorylated forms of serine 10 in GLUT4. The antibody might also aid the characterisation of the function of this phosphorylation site.

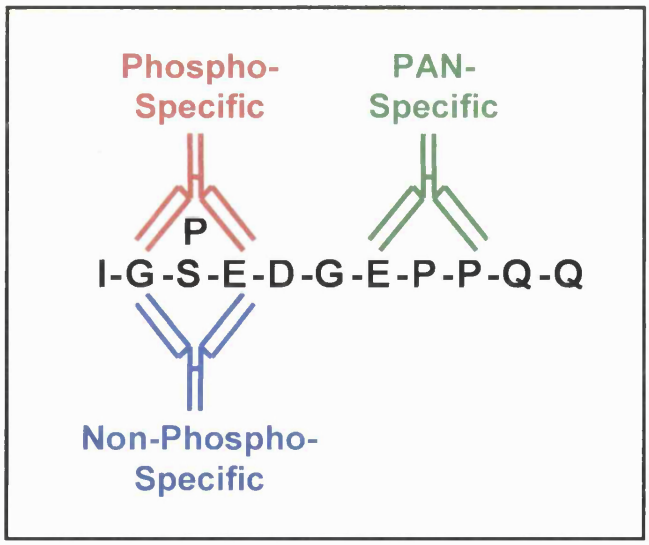

Figure 3.1 **Three classes of antibody are produced when an animal is injected with a phosphorylated antigen – phospho-specific, non-phospho-specific and PAN-specific antibodies.** The peptide illustrated is the antigen used to generate anti-pSer^{10} antibodies in rabbit.

3.2 Results

3.2.1 Purification of a Phospho-Specific Population of anti-GLUT4 Antibodies Raised to Serine 10 from Rabbit Serum

Previously, Darren Harper had found that the second bleed serum gave the best antibody titre for the phospho-specific antibody. He purified antibody from the second bleed serum using an immunoaffinity purification column in which SulfoLink® resin was coupled to the phosphorylated peptide (phospho peptide) used as the antigen (Figure 3.2) (Section 2.2.10). He showed that, by ELISA, there was a difference in specificity for the phosphorylated and non-phosphorylated forms of the peptide used as the antigen (Harper, 2002). However, the purified population of antibodies still recognised the non-phospho peptide, so further purification was needed to remove the contaminating population of non-phospho-specific antibodies.

Phospho peptide	$_{NH2}$-I-G-S(P)-E-D-G-E-P-P-Q-Q-C-$_{COOH}$
Non-phospho peptide	$_{NH2}$-I-G-S -E-D-G-E-P-P-Q-Q-C-$_{COOH}$
PAN-specific peptide	$_{NH2}$-C-G-E-P-P-Q-Q-$_{COOH}$
FQQI phospho-peptide	$_{NH2}$-C-F-Q-Q-I-G-S(P)-E-D-$_{COOH}$

Figure 3.2 **Sequences of the peptides used in the purification of anti-pSer[10] antibodies from rabbit serum.**

3.2.1.1 Analysis of the Different Rabbit Serum Bleeds

Darren Harper had purified an antibody population from the second bleed serum. However, the second bleed was a test bleed and so there was only a limited amount of serum. It was therefore necessary to investigate whether a different bleed of serum could be used for the antibody purification. For this, ELISA and Western blotting techniques were used (Section 2.2.9.5 and 2.2.8.3). The second and final bleed sera were screened against the phospho and non-phospho peptides by ELISA. There was not a large difference between the antibody titres of the second bleed and final bleed sera (Figure 3.3). Even though the second bleed serum did have a slightly higher antibody titre, the difference in specificity each serum had for the phospho and non-phospho peptides (the difference between the lines) was the same. This demonstrated that the two antibody populations were similar. Both sera recognised a protein of about 45 kDa (Figure 3.4). This was the same molecular weight as the protein recognised by the anti-C-terminal GLUT4 antibody and indicated that the sera recognised GLUT4. However, contrary to the ELISA data, the final bleed serum recognised the band at 45 kDa more strongly than the second bleed serum. This suggested that, by Western blot analysis, the final bleed serum was better than the second bleed serum. Purification was therefore carried out using the final bleed serum, as the two bleeds were comparable and there was also only a limited amount of second bleed serum remaining. Darren Harper had only analysed the serum by ELISA, which could be why he chose the second bleed serum for purification and not the final bleed serum.

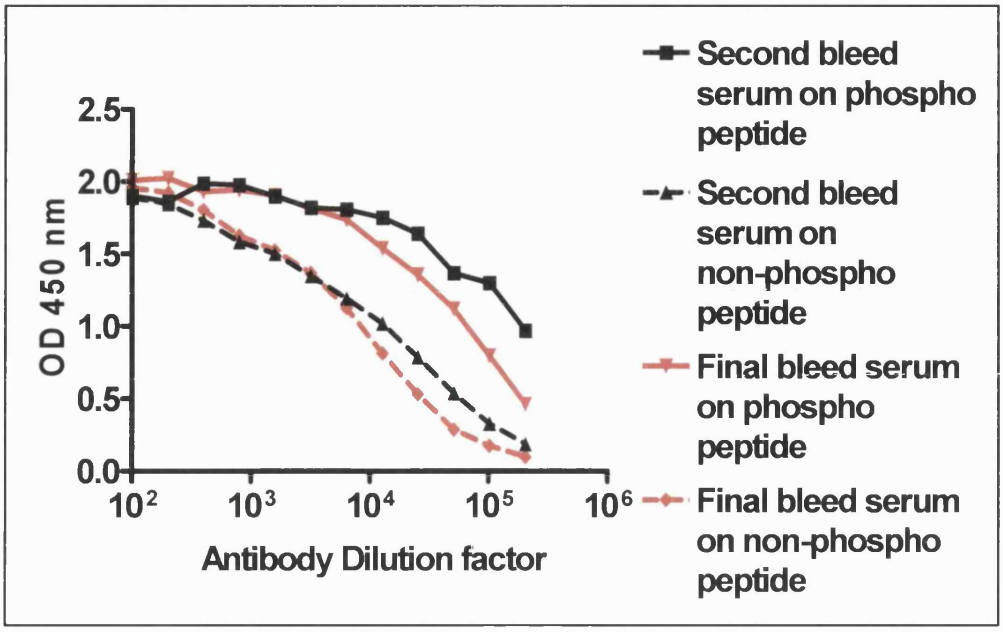

Figure 3.3 **ELISA analysis comparing the second bleed serum with the final bleed serum.** The second bleed serum (black line) and the final bleed serum (red line) were subjected to ELISA analysis against plates coated with the phospho (solid line) and non-phospho peptides (hashed lines). Titre values can be estimated by analysis of optical density readings at 450 nm over the logarithmic dilution range of the sera.

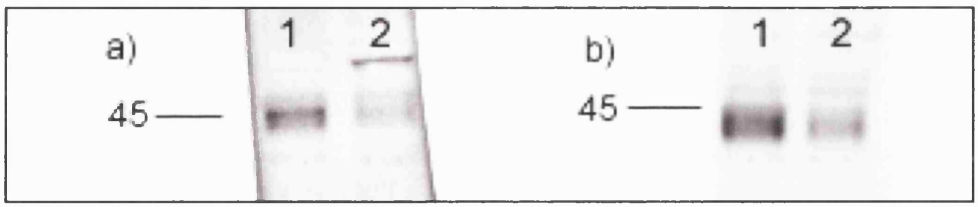

Figure 3.4 **Western blot analysis comparing the second bleed serum with the final bleed serum.** SDS-PAGE gels were loaded with 10 µg basal LDM (1) and insulin plasma membrane (2) adipocyte fractions and then transferred for Western blot analysis. The second bleed serum (a) and the final bleed serum (b) were both used at a 1:1000 dilution for detection.

3.2.1.2 Purification of Antibody from the Final Bleed Rabbit Serum

Antibodies from the final bleed serum were affinity purified against the phospho peptide used as the antigen. The resulting antibodies were analysed by ELISA, along with those purified from the second bleed by Darren Harper. ELISA analysis, testing the affinity of each antibody for the phospho and non-phospho peptide, confirmed that the antibody purified from the final bleed serum was similar to the antibody purified from the second bleed serum (Figure 3.5). However, the antibody purified from the final bleed serum had a higher antibody titre than the antibody purified from the second bleed serum, the inverse from that seen with the serum (Figure 3.3).

The fact that the purified antibody from the final bleed serum had a greater specificity for the phospho peptide than the non-phospho peptide was very encouraging. However, further purification of the serum was needed because the purified antibody recognised the non-phospho peptide. This indicated that a non-phospho-specific population of antibodies had been purified along with a phospho-specific population of antibodies.

3.2.1.3 Further Purification Strategies to Produce a Phospho-Specific Population of anti-pSer^{10} Antibodies

To make the antibody population more phospho-specific, cross purification was carried out. In this procedure the serum was first purified on a non-phospho peptide column to bind and remove all of the non-phospho-specific antibodies and the PAN-specific antibodies. The flow through from the non-phospho peptide column would contain the phospho-specific antibodies and other serum proteins. This flow through was then purified on a phospho peptide column. Here the phospho-specific antibodies should bind to the column and a phospho-specific population should be purified from the column. The serum proteins and other non-GLUT4 antibodies would therefore be removed. The

antibodies purified using both the non-phospho peptide and the phospho peptide columns were analysed by Western blot (Figure 3.6). The antibody which had bound to the non-phospho peptide column recognised bands similar to those seen previously with the anti-C-terminal GLUT4 antibody (Figure 3.6 b). Unfortunately, the antibody which was purified from the phospho peptide column did not recognise any bands above background level (Figure 3.6 a). As the phospho-specific antibodies cross reacted with the non-phosphorylated peptide, cross purification was not a method that could be used to purify anti-pSer^{10} antibodies.

As the cross purification method could not be used, a different purification strategy was tried using a slightly different phospho peptide (FQQI phospho peptide). This peptide had a smaller 'PAN' region so fewer non-phospho-specific antibodies should bind to the peptide. It was hoped that antibodies raised to the pSer^{10} residue would be purified on the FQQI phospho peptide as they had a number of overlapping residues which encompassed the epitope of the desired population of anti-pSer^{10} antibodies (Figure 3.7).

Unfortunately the FQQI phospho peptide did not lead to the purification of any antibody from the serum (result not shown). The actual peptide sequence and its fold must therefore be essential for the purification of the antibodies from the serum.

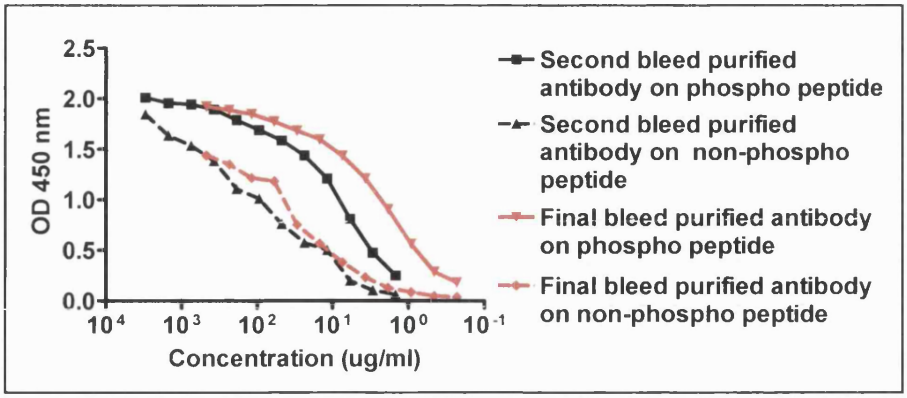

Figure 3.5 **ELISA analysis comparing affinity purified antibodies from the second bleed serum and the final bleed serum.** The affinity purified antibodies from the second bleed serum (black line) and the final bleed serum (red line) were subjected to ELISA analysis against plates coated with the phospho (solid line) and the non-phospho peptides (hashed line). Titre values were estimated by analysis of optical density readings at 450 nm over the logarithmic dilution range of the antibody.

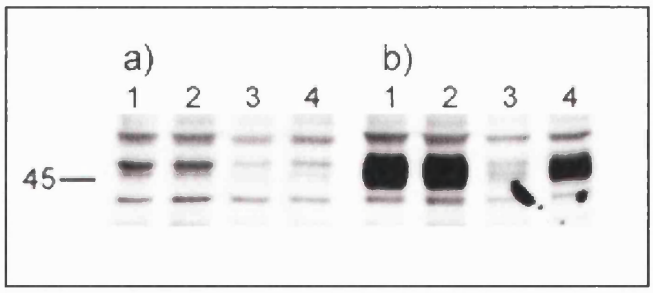

Figure 3.6 **Western Blot analysis comparing the antibodies purified after cross purification on the non-phospho peptide column followed by the phospho peptide column.** SDS-PAGE gels were loaded with 10 µg basal LDM (1), insulin LDM (2), basal plasma membrane (3) and insulin plasma membrane (4) adipocyte fractions. The gel was transferred for Western blot analysis. The final bleed serum was first purified on the non-phospho peptide column (b), this should remove the non-phospho and PAN-specific antibodies. The remaining serum was then purified on the phospho peptide column to obtain a phospho-specific population of anti-pSer[10] antibodies (a).

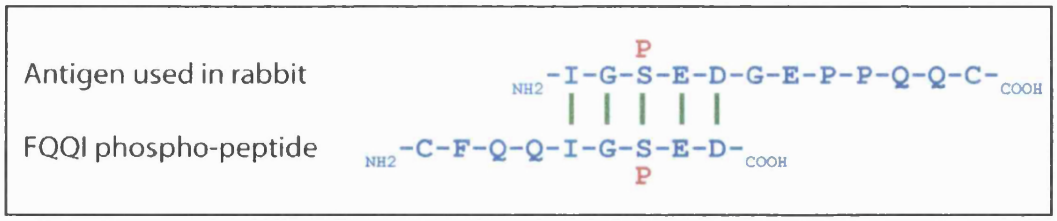

Figure 3.7 **Comparison of the sequence of peptides used in the antibody purification.** The FQQI phospho peptide had fewer 'PAN' residues so hopefully the peptide would purify a specific pSer[10] population of antibodies.

The final strategy that was attempted to purify a phospho-specific antibody population from the serum involved the use of another shorter peptide (PAN-specific peptide). This represented the area of the original antigen to which PAN-specific antibodies would have been raised (Figure 3.8).

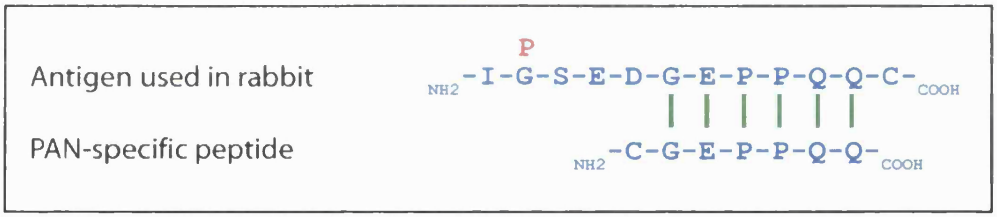

Figure 3.8 **Comparison of the sequence of peptides used in the antibody purification.** The PAN-specific peptide was used to remove the PAN-specific antibodies that had been purified along with the anti-pSer[10] antibodies on the phospho peptide column.

As it was not possible to use the non-phospho peptide in the cross purification technique, the PAN-specific peptide was used in the purification process after an initial purification on a phospho peptide column. Two antibody populations would have been co-purified from the phospho peptide column. Antibodies would have contained epitopes raised to the phosphorylated Ser[10] residue and to the PAN region of the peptide. These two antibody populations were

separated by affinity purification on a PAN-specific peptide column. The antibodies raised to the PAN region of the peptide bound to the PAN-specific peptide column and were eluted. The antibodies with epitopes encompassing $pSer^{10}$ did not bind to the column and were present in the flow through. The two antibody populations purified from the two columns were analysed by ELISA and Western blot (Figures 3.9 and 3.10, respectively). The newly purified phospho-specific antibody population (Figure 3.9, black line) was phospho-specific as the antibody had a higher specificity for the phospho peptide (Figure 3.9, solid line) than the non-phospho peptide (Figure 3.9, hashed line). This antibody population was also more phospho-specific than the antibody purified solely on the phospho peptide column because the difference between the phospho and non-phospho peptides was greater (Figure 3.9 compared to Figure 3.5). In purifying the PAN-specific antibody (Figure 3.9, blue line) away from the $pSer^{10}$ antibody, a large population of antibodies that recognised PAN-specific epitopes had been removed. The PAN-specific antibody had a high antibody titre for the non-phospho peptide (Figure 3.9, blue hashed line). However, the PAN-specific peptide did purify some antibodies that contained epitopes raised to the $pSer^{10}$ residue (Figure 3.9, blue solid line). The PAN-specific antibody (Figure 3.10 c) recognised a protein at the same molecular weight as the anti-C-terminal GLUT4 antibody (Figure 3.10 d) with the same expression pattern in basal and insulin-stimulated adipocytes. This was as expected, as the PAN-specific antibody primarily contained non-phospho-specific antibodies. A comparison of the phospho-specific antibody after purification on the PAN-specific peptide column (Figure 3.10 b) was carried out with the antibody which Darren Harper had purified from the second bleed serum on the phospho peptide column (Figure 3.10 a). Both antibodies recognised a weak protein band at 45 kDa (arrows on Figure 3.10 a and b). This was the same molecular weight as GLUT4 probed with the anti-C-terminal GLUT4 antibody. Both anti-$pSer^{10}$ antibodies presented similar bands but the bands identified by the antibody purified on the PAN-specific peptide column were less intense. Non-specific

bands were identified with both anti-pSer^{10} antibodies, just above 45 kDa, which made identification of the GLUT4 band difficult.

The data from the ELISA analysis looked promising in that the purification of a phospho-specific anti-pSer^{10} antibody from rabbit serum was possible. However, further work on the characterisation of the antibody and the optimisation of Western blots for the use of this antibody was needed before it could be used in meaningful experiments that quantified the level of phosphorylation at Ser^{10} in GLUT4.

3.2.1.4 Characterisation of a Phospho-Specific pSer^{10} Population of GLUT4 Antibodies that were Raised in Rabbit

Work was carried out over many months to characterise the anti-pSer^{10} antibody population purified from the phospho peptide and PAN-specific peptide columns and to characterise the best conditions for the use of the antibody.

The optimal conditions for Western blotting were sought in order to enhance the affinity of the anti-pSer^{10} antibody for GLUT4 (Figure 3.11). As non-specific bands were being detected around the 45 kDa area of interest, attempts were made to increase the resolution of the gel in this area. Both 8% and 10% (w/v) acrylamide resolving gels were run. 8% acrylamide gels gave a better resolution in the area around 45 kDa and so 8% gels were used for follow up studies.

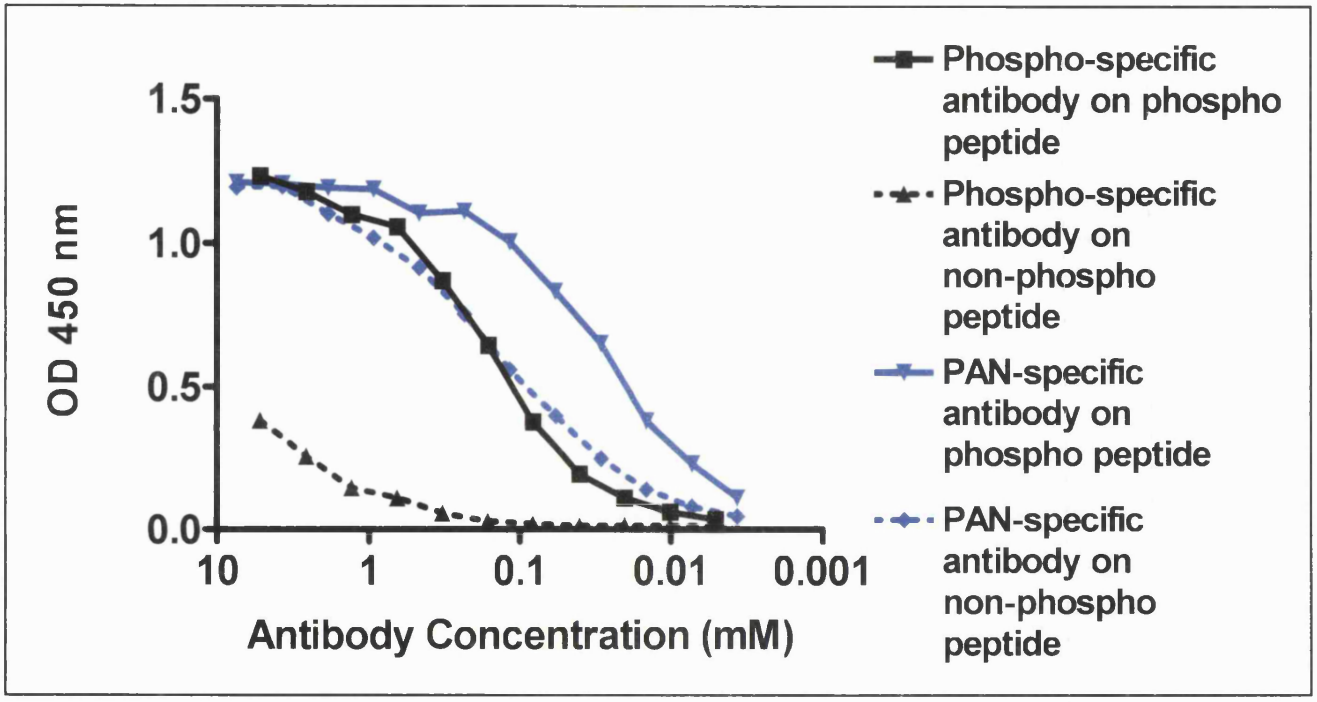

Figure 3.9 **ELISA analysis comparing the two antibody populations purified on a phospho peptide column followed by a PAN-specific peptide column.** Antibodies purified on a phospho peptide column were further purified on a PAN-specific peptide column. The antibodies that did bind to the PAN-specific peptide column (blue line) and the antibodies that did not bind to the PAN-specific peptide column (black line) were subjected to ELISA analysis against plates coated with the phospho (solid line) and non-phospho peptides (hashed line). Titre values can be estimated by analysis of optical density readings at 450 nm over the logarithmic dilution range of the antibody.

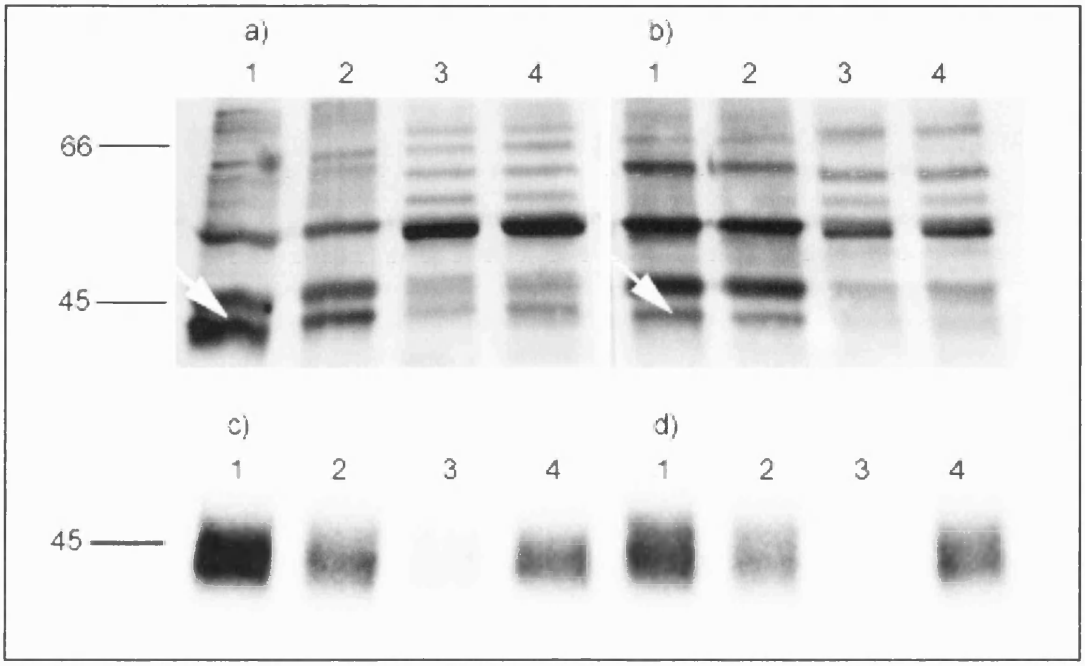

Figure 3.10 **Western blot analysis of the two antibody populations purified from the PAN-specific peptide column along with the anti-C-terminal GLUT4 antibody raised in rabbit and the antibody purified from the second bleed serum on the phospho peptide column.** SDS-PAGE gels were loaded with 10 µg basal LDM (1), insulin LDM (2), basal plasma membrane (3) and insulin plasma membrane (4) adipocyte fractions and then transferred for Western blot analysis. The anti-pSer[10] second bleed antibody (a), the antibody purified on the phospho peptide column but did not bind to the PAN-specific peptide column (b), the PAN-specific antibody (bound to both the phospho peptide and PAN-specific peptide (c) and the anti-C-terminal GLUT4 antibody purified from rabbit serum (d) were compared by Western blot analysis. The arrows point to the predicted GLUT4 band.

It was reported by Lawrence *et al* that incubation with milk (as a blocking agent) resulted in an almost complete dephosphorylation of the transporter (Lawrence, Jr. *et al.*, 1990b), so various blocking conditions (in TBS-T) were tested to try and optimise the blotting conditions (Figure 3.11). 5% (w/v) Marvel (Figure 3.11 a), 3% (w/v) TopBlock [S] (Fritsche *et al.*, 1999) (Figure 3.11 b), 5% (w/v) BSA (Figure 3.11 d) and 1% (w/v) casein (Figure 3.11 e) were tested. No major difference could be detected between the different blocking conditions in TBS-T. A band about 45 kDa was identified with all four different blocking solutions, which was likely to be GLUT4 (Figure 3.11 a – d arrows) based on a comparison with a Western blot using the anti-C-terminal GLUT4 antibody (Figure 3.11 c). The strong non-specific bands did not disappear after blocking with any of the tested conditions. Casein did decrease the number of non-specific bands but unfortunately the background from the Western blot was very dark and so was not suitable for use (Figure 3.11 e). The other three conditions did not decrease the number of non-specific bands.

The length of blocking, either 1 h at room temperature or overnight at 4 ^{o}C, was also tested to try to improve blocking conditions. One hour blocking gave better results than overnight. Therefore Marvel continued to be used for 1 h as the blocking agent.

The presence of Tween-20 in the wash buffer was investigated (Figure 3.11 f) as it had previously been reported that Tween-20 could be used as a blocking agent in the immunological detection of proteins transferred to nitrocellulose membranes (Batteiger *et al.*, 1982). However, denaturing agents such as detergents could reduce the binding capacity of antibodies to their antigen so, as the purified anti-pSer^{10} antibody had weak affinity for GLUT4, Tween-20 was omitted from the wash and antibody buffers. The omission of Tween-20 (Figure 3.11 f, lane 6) produced greater background staining on the Western blots and reduced the intensity of specific antibody bands. Therefore Tween-20 was included in the washing and blocking buffers (Figure 3.11 f, lane 5).

Different concentrations of secondary antibody were also tested (Figure 3.11 g). Even though lower concentrations of secondary antibody gave weaker non-specific bands (Figure 3.11 g, lanes 10, 11 and 12), the GLUT4 band was even weaker so the secondary antibody concentration remained at 1:4000. The non-specific bands on the Western blot were due to the secondary antibody as the bands were also present when no primary antibody incubation was carried out (Figure 3.11 g, lanes 7, 8 and 9).

Even though the GLUT4 band was still weak and the non-specific bands were still detected, the optimal Western blotting conditions to be used with the rabbit anti-pSer^{10} antibody were: 5% Marvel block for 1 h at room temperature, wash buffer TBS-Tween and secondary antibody anti-rabbit IgG HRP used at a dilution of 1:4000.

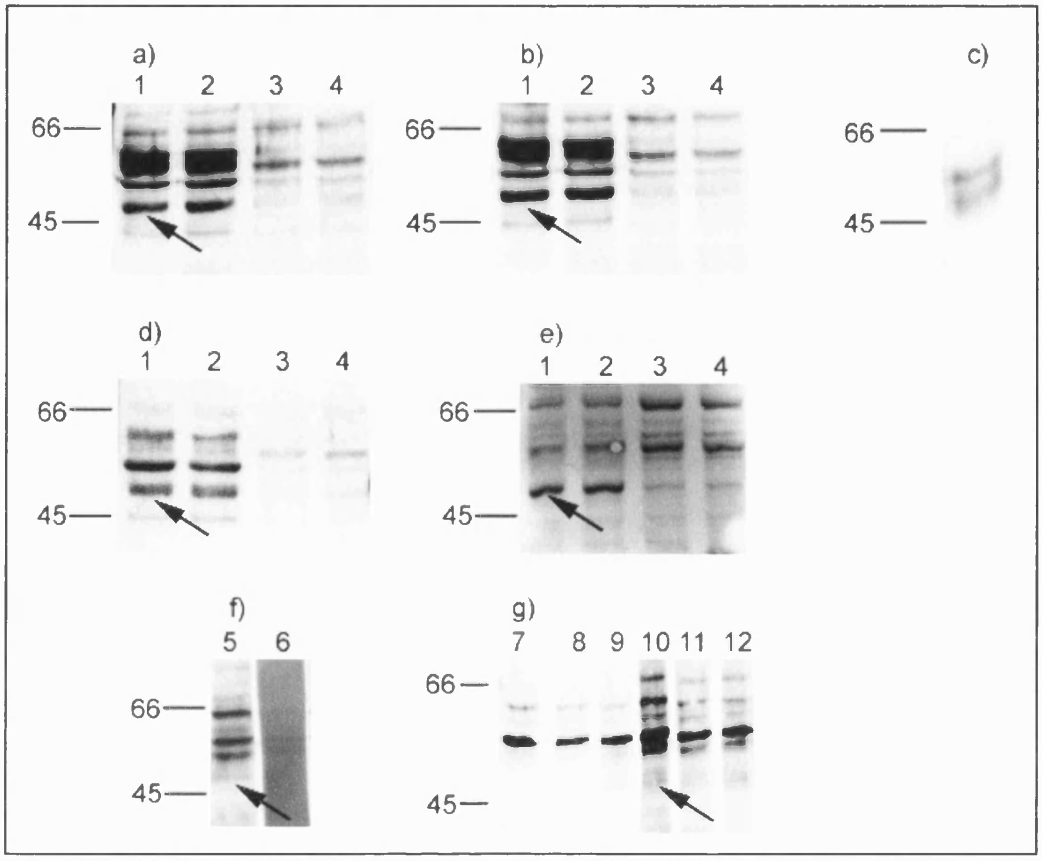

Figure 3.11 **Optimisation of Western blotting conditions.** SDS-PAGE gels were loaded with 10 µg basal LDM (1), insulin LDM (2), basal plasma membrane (3) and insulin plasma membrane (4) adipocyte fractions and then transferred for Western blot analysis, f) and g) are all basal LDM fractions. Different blocking conditions were tested, 5% (w/v) Marvel (a), 3% (w/v) TopBlock (b), 5% (w/v) BSA (d) and 1% (w/v) casein (e). The arrows indicate the predicted GLUT4 band after comparison with the anti-C-terminal GLUT4 antibody raised in rabbit (c). The requirement for the presence (lane 5) or absence (lane 6) of Tween-20 in the washing and blocking buffers was also tested (f). 1:4000 (lanes 7 and 10), 1:10000 (lanes 8 and 11) and 1:20000 (lanes 9 and 12) dilutions of secondary antibody in 5% Marvel TBS-T were tested (g). Lanes 7, 8 and 9 are secondary antibody incubation only and lanes 10, 11 and 12 have both primary and secondary antibody incubations.

As the apparent detection of GLUT4 on the gel was weak, it was imperative to further check that the antibody actually recognised GLUT4. Immunoprecipitation was used to ensure that the antibody recognised the full length GLUT4 protein. Immunoprecipitation (methods 2.2.6.1) was carried out using both the anti-pSer^{10} antibody and the mouse monoclonal anti-C-terminal GLUT4 antibody. GLUT4 was then identified, by Western blot analysis, using the mouse monoclonal anti-C-terminal GLUT4 antibody or the anti-pSer^{10} antibody, respectively. However, no bands were detected at about 45 kDa. This could be because the anti-pSer^{10} antibody and the mouse monoclonal anti-C-terminal GLUT4 antibody were both weak antibodies when compared to the rabbit anti-C-terminal GLUT4 antibody. The rabbit anti-C-terminal antibody could not be used in combination with the anti-pSer^{10} antibody because the IgG eluted following the immunoprecipitation would have been detected by Western blot analysis and would have masked the GLUT4 band (result not shown). An alternative immunoprecipitation method was carried out using the Seize® Primary Immunoprecipitation kit [P] in which the antibody was covalently bound onto an agarose gel via primary amino groups present on the antibody. The anti-pSer^{10} antibody was used to immunoprecipitate GLUT4 from basal LDM and the eluted protein was detected following Western blot analysis with the rabbit anti-C-terminal GLUT4 antibody. The anti-C-terminal GLUT4 antibody recognised a band at about 45 kDa. This suggested that the anti-pSer^{10} antibody immunoprecipitated GLUT4 from the LDM (Figure 3.12). Elution was carried out successively with eight 1 ml aliquots of elution buffer (lanes 1-8). The majority of GLUT4 was eluted in the first fraction but the protein was still detected in the eighth fraction. It was reported that the beads could be re-used but because it was not easy to elute all of the GLUT4 it was not viable to reuse the beads. However, this was a good result because it gave the first proof that the anti-pSer^{10} antibody recognised and bound to the native GLUT4 protein.

The remaining concern regarding the anti-pSer^{10} antibody was the identification of which band around 45 kDa on the Western blot was GLUT4, as there were also non-specific bands in the 45 kDa region. GLUT4 contains a single N-glycosylation site at asparagine 57 (Pessin and Bell, 1992) (Figure 1.1), therefore, it was considered that it would be possible to identify the GLUT4 band by deglycosylating the LDM membranes with Peptide:N-glycosidase F (PNGase F) (Section 2.2.2.1.4). This procedure should reduce the apparent molecular weight of GLUT4 on a Western blot. Basal LDM membranes were treated with PNGase F in the presence or absence of phosphatase inhibitors. A no-enzyme control was also carried out. The membrane was subjected to SDS-PAGE and following electrophoretic transfer to nitrocellulose, Western blot analysis using the anti-pSer^{10} antibody identified the GLUT4 band (Figure 3.13). The GLUT4 band and the non-specific band ran very close to one another (51 kDa and 47 kDa) on the nitrocellulose when the LDM was not deglycosylated (Figure 3.13 lane 4, arrows a and b). A no-enzyme control also gave the same result (Figure 3.13 lane 2). However, when the LDM had been deglycosylated, the GLUT4 band decreased in molecular weight and was clearly identified by the anti-pSer^{10} antibody as a band at 40 kDa (Figure 3.13 lane 1, arrow c). The GLUT4 band in lane 4 was therefore identified as the lower, 47 kDa, band (arrow b) because the non-specific upper band (51 kDa) (arrow a) did not move after deglycosylation. The deglycosylation conditions induced dephosphorylation as when the deglycosylation was carried out in the presence of phosphatase inhibitors, (sodium fluoride, sodium molybdate and sodium orthovanadate) the GLUT4 band detected was stronger (Figure 3.13 lane 3). This also gave strong evidence that the anti-pSer^{10} antibody was phospho-specific.

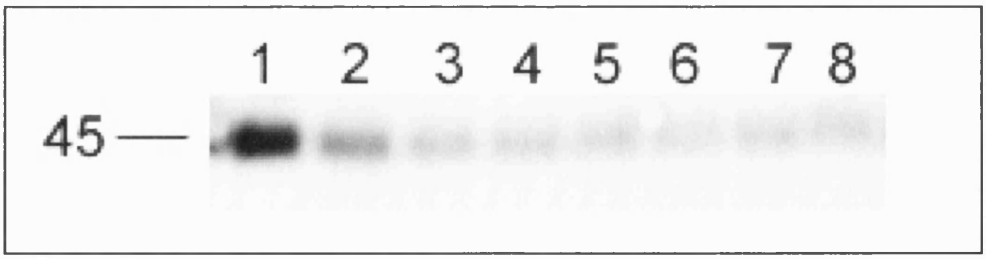

Figure 3.12 **GLUT4 was immunoprecipitated from LDM with the anti-pSer^{10} antibody and detected by Western blot analysis with the rabbit anti-C-terminal GLUT4 antibody.** Using the Seize Immunoprecipitation kit, in which IgG was retained in the immobilised gel matrix, the anti-pSer^{10} antibody was used to immunoprecipitate GLUT4 from 100 µg basal LDM. The precipitated GLUT4 was then detected on a Western blot by use of the rabbit anti-C-terminal GLUT4 antibody. The blot showed successive elutions from the beads using 1 ml elution buffer.

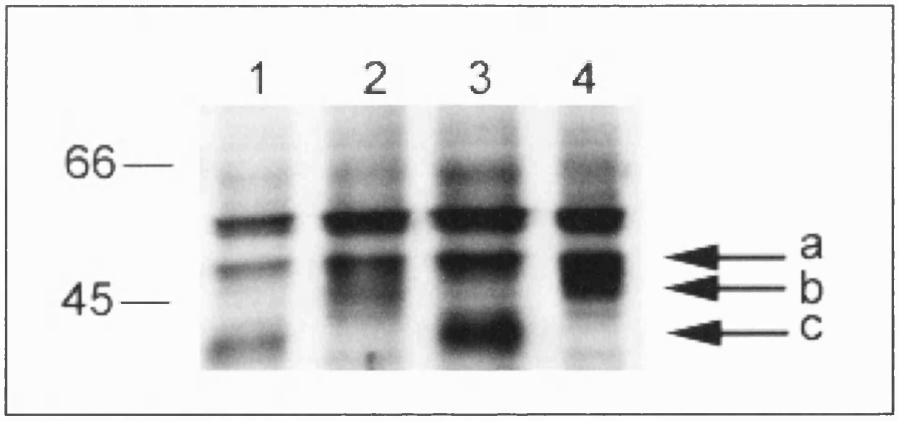

Figure 3.13 **Western blot analysis of deglycosylated LDM to identify the GLUT4 band detected by the anti-pSer^{10} antibody.** 20 µg basal LDM was deglycosylated with PNGase F. Western blot analysis with the anti-pSer^{10} antibody identified the GLUT4 band, following SDS-PAGE and electrophoretic transfer to nitrocellulose. Basal LDM was deglycosylated in the absence (lane 1) or presence (lane 3) of phosphatase inhibitors. A no enzyme control (lane 2) and untreated basal LDM (lane 4) were also run on the gel. Arrow a indicated the non-specific band, arrow b indicated glycosylated GLUT4 and arrow c indicated deglycosylated GLUT4.

3.2.1.5 Immunocytochemistry using Affinity Purified Anti-pSer^{10} GLUT4 Antibodies

The confocal microscopy studies which involved use of the rabbit anti-pSer^{10} antibodies were all carried out by Dr. Françoise Koumanov. The first study involved staining isolated basal and insulin-stimulated cardiomyocyte cells with anti-pSer^{10} antibodies. The staining observed with the anti-pSer^{10} antibody purified from the final bleed serum (on the phospho peptide and PAN-specific peptide columns) was compared to the staining observed with the anti-pSer^{10} antibody purified from the second bleed serum by Darren Harper (on the phospho peptide column) (Figure 3.14). In each case, cardiomyocyte cells were dual labelled with the anti-pSer^{10} antibody (Figure 3.14, green staining) and a mouse monoclonal anti-C-terminal GLUT4 antibody (Figure 3.14, red staining). This gave a comparison of the distribution of the GLUT4 that was phosphorylated at Ser^{10} compared to the distribution of the total GLUT4 protein and identified any co-localisation between the two (Figure 3.14, yellow staining). In the basal state, GLUT4 (regardless of phosphorylation state) was distributed beneath the plasma membrane, with the majority of GLUT4 sequestered in the peri-nuclear region of the cell. In the insulin-stimulated cardiomyocytes, there was a visible redistribution of GLUT4 to the plasma membrane. The anti-pSer^{10} antibody purified from the second bleed serum also stained an intracellular protein in basal cardiomyocytes which was concentrated in the peri-nuclear region of the cell. The staining partially co-localised with the anti-C-terminal GLUT4 antibody staining. This suggested that the anti-pSer^{10} antibody purified from the second bleed serum was recognising a subset of GLUT4 transporters. However, the protein recognised by the anti-pSer^{10} antibody purified from the second bleed serum did not translocate to the plasma membrane following insulin stimulation. The protein remained in a peri-nuclear localisation.The apparent distribution pattern of pSer^{10} GLUT4 observed when using the anti-pSer^{10} antibody purified from the final bleed serum was similar to that seen with the anti-pSer^{10} antibody purified from the

second bleed serum. The anti-pSer^{10} antibody from the final bleed serum also recognised a protein in the peri-nuclear region of the basal cardiomyocyte cell. Again, following insulin stimulation, the staining observed from use of the anti-pSer^{10} antibody purified from the final bleed serum remained concentrated in the peri-nuclear region of the cell. No staining occurred at the plasma membrane.

The anti-pSer^{10} antibodies, purified from the second bleed serum and the final bleed serum, were either recognising a peri-nuclear protein that was not GLUT4, or the antibodies were recognising a subset of GLUT4 in the peri-nuclear region of the cell. If the anti-pSer^{10} antibodies were recognising a subset of GLUT4, which was not stained by the anti-C-terminal GLUT4 antibody, then the GLUT4 phosphorylated at serine 10 might have been in a different conformation compared to unphosphorylated GLUT4. This could explain why, in insulin-stimulated cardiomyocytes, the anti-C-terminal GLUT4 antibody did not bind to the C-terminus of GLUT4 when it was phosphorylated at serine 10. Perhaps GLUT4 was folded in a different orientation during biosynthesis. Thus, if the anti-pSer^{10} antibody was phospho-specific, as suggested by ELISA, then GLUT4 could have been phosphorylated at Ser^{10} during biosynthesis and may have been dephosphorylated when it was correctly folded and able to transport glucose.

In the second confocal microscopy study, 3T3-L1 fibroblasts were differentiated into adipose like cells (Section 2.2.1). During differentiation, the cells started to synthesise lipogenic enzymes and became sensitive to the hormones involved in regulating fat metabolism (Mackall et al., 1976, Reed et al., 1977, Kuri-Harcuch and Green, 1977, Rubin et al., 1978). 3T3-L1 adipocytes were fixed at different days of differentiation – days 3, 5 and 12. The study started at day 3 because both GLUT4 mRNA and protein were first detected in the adipocytes on day 3 of differentiation and were not present in the fibroblast. The expression of GLUT4 mRNA increased from day 3 to day 6, when it then stabilised (Garcia de Herreros and Birnbaum, 1989).

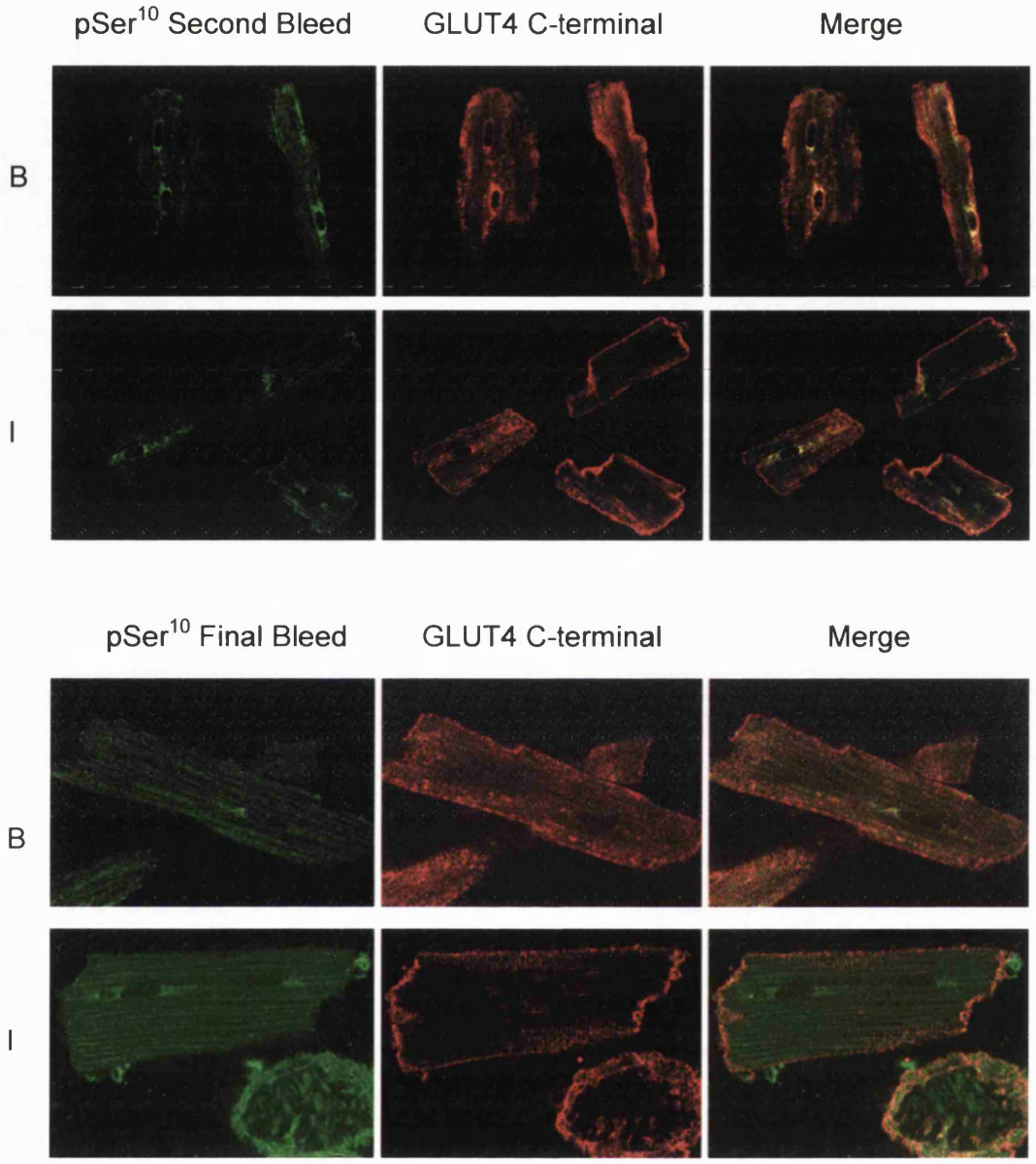

Figure 3.14 **Confocal microscopy comparing the purified anti-pSer^{10} antibodies from the second and final bleed serums (green) with an anti-C-terminal GLUT4 antibody (red).** Confocal microscopy was carried out on basal (B) and insulin (I) stimulated cardiomyocytes. Any co-localisation was shown in yellow. The images were kindly supplied by Dr. Françoise Koumanov.

Confocal microscopy was carried out on the 3T3-L1 adipocytes at days 3, 5 and 12 of differentiation using the monoclonal anti-C-terminal GLUT4 antibody (Figure 3.15, red staining) and the anti-pSer^{10} antibody purified from the final bleed serum (Figure 3.15, green staining). The anti-pSer^{10} antibody purified from the final bleed serum will be referred to just as the anti-pSer^{10} antibody in the remainder of this section.

On day 3 of differentiation, GLUT4 was identified in a few discreet vesicular structures throughout the cytoplasm, from the use of the anti-C-terminal GLUT4 antibody. These vesicular structures were not identified by the anti-pSer^{10} antibody but instead, a protein in the peri-nuclear region of the cell, located asymmetrically on one side of the nucleus, was stained. By day 5, GLUT4, in addition to being in discreet vesicular structures, was also concentrated in the peri-nuclear region of the cell. This peri-nuclear staining partially co-localised with the staining of the anti-pSer^{10} antibody. The anti-pSer^{10} antibody staining was only present in the peri-nuclear region of the cell. On day 12, when the cells were fully differentiated, GLUT4 was located in the peri-nuclear region, as well as throughout the cytoplasm. The anti-pSer^{10} antibody, again, only stained a protein in the peri-nuclear region of the cell, but it was less intense than either day 3 or day 5. The anti-pSer^{10} antibody could have stained a small pool of GLUT4 transporters. In which case, GLUT4 phosphorylated at serine 10 co-localised with a subset of GLUT4 transporters, which were stained by the anti-C-terminal GLUT4 antibody, in the peri-nuclear region of the cell. This subset of GLUT4 could have been GLUT4 in the biosynthetic pathway, as mentioned previously. Therefore, if the antibody was phospho-specific, GLUT4 could have been phosphorylated at serine 10 during biosynthesis.

Brefeldin A (BFA) is a fungal metabolite that is often used to study intracellular membrane trafficking. It causes the disassembly of the Golgi apparatus, prevents vesicles budding from the Golgi to the trans-Golgi and also causes the retrograde transport of Golgi proteins back to the endoplasmic reticulum

(Fujiwara et al., 1988, Orci et al., 1991). Treating 3T3-L1 adipocytes with BFA will help to identify the localisation of GLUT4, whether the stained protein is in the Golgi or whether it is post-Golgi. 3T3-L1 adipocytes were treated with BFA before the cells were fixed at different days of differentiation – days 3, 5 and 12.

The discreet vesicular structures containing GLUT4, at day 3 of differentiation, did not disappear after treatment with BFA. The same was true of the vesicular GLUT4 structures on day 5 of differentiation. At day 5 and day 12, there was a sharp concentration of the peri-nuclear GLUT4 staining after BFA treatment. This perhaps resulted from the trans-Golgi collapsing back to the cis-Golgi. Thus, the GLUT4 stained by the monoclonal anti-C-terminal GLUT4 antibody at day 3 of differentiation was derived from a post-Golgi, BFA insensitive pool of GLUT4, and at day 5 the GLUT4 stained were from both BFA sensitive and insensitive pools of GLUT4.

At day 3 of differentiation, with no BFA treatment, the anti-pSer^{10} antibody recognised a protein in the peri-nuclear region of the cell. Following treatment with BFA, the peri-nuclear staining disappeared. The protein stained with the anti-pSer^{10} antibody was therefore BFA sensitive and was present in the Golgi apparatus. This was also true at both day 5 and day 12 of differentiation. Even when GLUT4 was fully differentiated, the protein stained by the anti-pSer^{10} antibody was BFA sensitive. This was representative of three separate experiments.

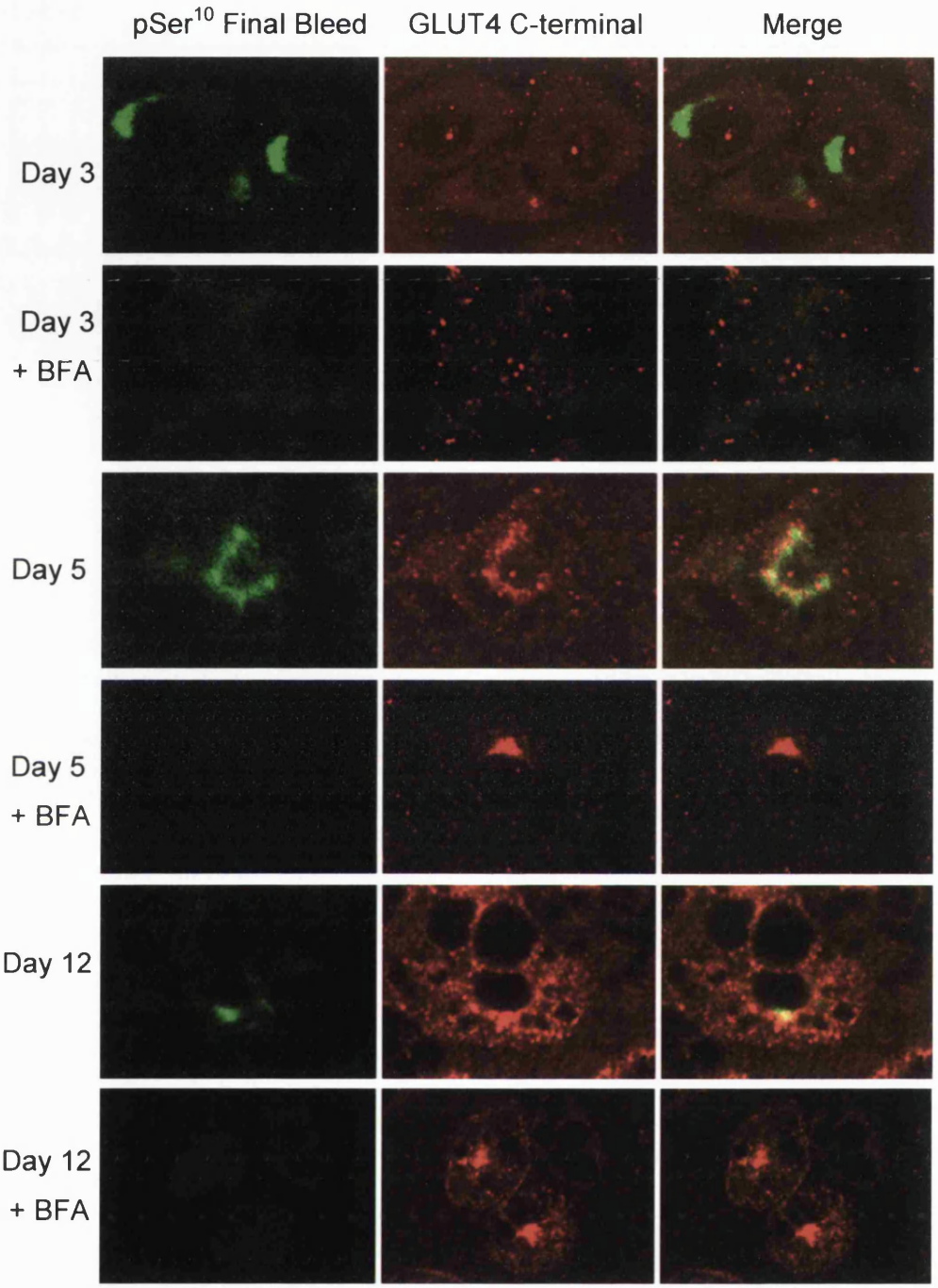

Figure 3.15 **Confocal microscopy comparing the anti-pSer^{10} antibody (green) purified from the final bleed serum with the anti-C-terminal GLUT4 antibody (red) at different days of differentiation of 3T3-L1 adipocytes, with and without Brefeldin A treatment (+ BFA).** Any co-localisation was shown in yellow. The images were kindly supplied by Dr. Françoise Koumanov and were representative of three separate experiments.

3.2.2 Generation of Antibodies Against pSer^{10} and the C-terminus of GLUT4 in Sheep

A phospho-specific population of anti-pSer^{10} antibodies, that recognised the native GLUT4 protein, had been purified from rabbit serum. However, there was a problem in using the antibody to detect any differences in localisation of the phosphorylated and non-phosphorylated forms of serine 10 in GLUT4. The problem was the presence of non-specific bands on Western blots that were recognised by the secondary antibody. Another antibody was raised to pSer^{10}, but this time in sheep, to try to combat the problems encountered with use of the antibody raised in rabbit. The antigen design was different to the one used in rabbit as the phosphorylated serine 10 was in the middle of the peptide rather than at the end. This choice was made so hopefully more of the antibody epitopes would encompass the phosphorylated serine, with fewer antibodies being raised to the PAN-specific region (Figure 3.16 A). Sheep was the host of choice for raising the antibodies because the previous antibodies raised in the laboratory (anti-C-terminal, anti-N-terminal and anti-pSer^{10} antibodies) were raised in rabbit. It is useful to have antibodies raised in different species so that the antibodies can be used in combination, for example in confocal microscopy in which different secondary antibodies have to be used. An antibody was also raised in sheep to the C-terminus of GLUT4, using the same antigen as the anti-C-terminal GLUT4 antibody raised in rabbit (Figure 3.16 B). It was considered that having an antibody raised to the C-terminus of GLUT4 in sheep would be a useful tool when working with the anti-N-terminal and anti-pSer^{10} antibodies raised in rabbit. Two sheep were immunised with the phospho peptide and one sheep was injected with the C-terminal peptide (Section 2.2.9 gives a full explanation of the antibody generation procedure). Initially, three bleeds were taken per sheep and ELISA analysis was undertaken to ensure that a specific immune reaction had occurred to the injected immunogen.

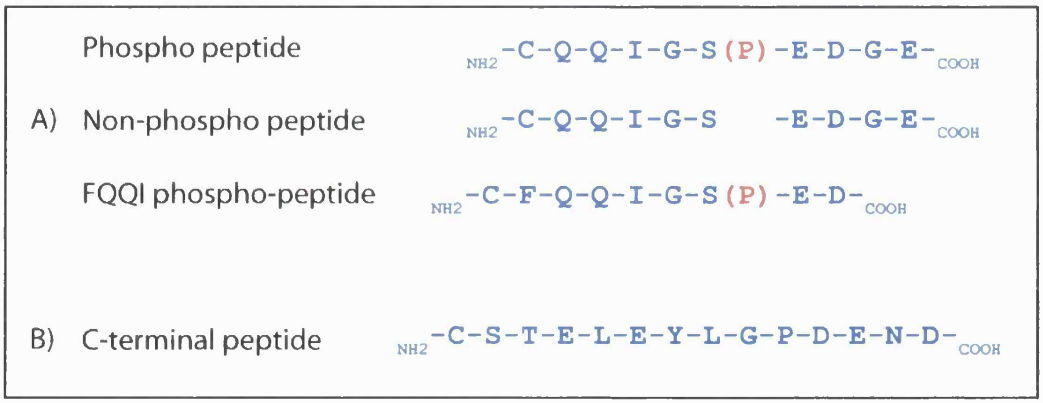

Figure 3.16 **Sequences of the peptides used for the generation and purification of (A) anti-pSer[10] antibodies and (B) anti-C-terminal GLUT4 antibodies.**

3.2.2.1 Analysis of Antibodies Generated Against the C-terminal GLUT4 Peptide in the Different Bleeds of Sheep Serum

ELISA and Western blot analysis was carried out to compare the difference between the different serum bleeds and to ensure that the GLUT4 serum recognised the native protein. ELISA analysis was carried out to test the affinity of the three test bleeds and the pre-immune bleed for the C-terminal peptide (Figure 3.17). An immune response had been elicited to the C-terminal peptide because antibodies which were not present in the pre-immune bleed were produced after immunisation. There was not a big difference in affinity for any of the serum bleeds with the C-terminal peptide.

To confirm that the anti-C-terminal GLUT4 antibody raised in sheep was recognising the GLUT4 protein, Western blot analysis of rat adipocyte sub-cellular fractions was carried out (Figure 3.18). This study compared the serum (Figure 3.18 a) to that of the purified anti-C-terminal GLUT4 antibody raised in rabbit (Figure 3.18 c). The sheep serum reacted with a protein about 45 kDa, which was the same molecular weight as the GLUT4 protein identified with the anti-C-terminal GLUT4 antibody raised in rabbit. The expression of GLUT4 in

each fraction of basal and insulin-stimulated adipocytes was recognised to the same extent by the serum and the anti-C-terminal GLUT4 antibody raised in rabbit. The level of GLUT4 in the LDM decreased after the cell was stimulated with insulin and a corresponding increase in the level of cell surface GLUT4 was detected.

3.2.2.2 Immunoaffinity Purification and Characterisation of an anti-C-terminal GLUT4 antibody Raised in Sheep

The ELISA analysis of the different serum bleeds (Figure 3.17) showed that there was not a great difference between any of the bleeds. Therefore the first bleed serum was affinity purified on a C-terminal peptide linked column. The affinity purified antibody was then tested by Western blot analysis on different fractions of rat adipocytes and compared to the anti-C-terminal GLUT4 antibody raised in rabbit. The affinity purified anti-C-terminal GLUT4 antibody raised in sheep (Figure 3.18 b) gave a very clean blot. Only one protein was identified at 45 kDa. This was the same molecular weight as the protein identified by the anti-C-terminal GLUT4 antibody raised in rabbit (Figure 3.18 c). The characteristic GLUT4 pattern was identified by Western blot analysis of basal and insulin-stimulated adipocyte cell fractions. In the basal state, GLUT4 was sequestered in an intracellular compartment as more GLUT4 was present in the LDM than in the PM. Insulin stimulation resulted in a translocation of GLUT4 from the intracellular compartment to the plasma membrane which is reflected by an increase in the plasma membrane levels of GLUT4. However, the affinity purified anti-C-terminal GLUT4 antibody raised in sheep gave a weaker signal than the affinity purified anti-C-terminal GLUT4 antibody raised in rabbit. The sheep antibody was used at a concentration of 1.4 µg/ml whereas the rabbit antibody was only used at a concentration of 0.06 µg/ml.

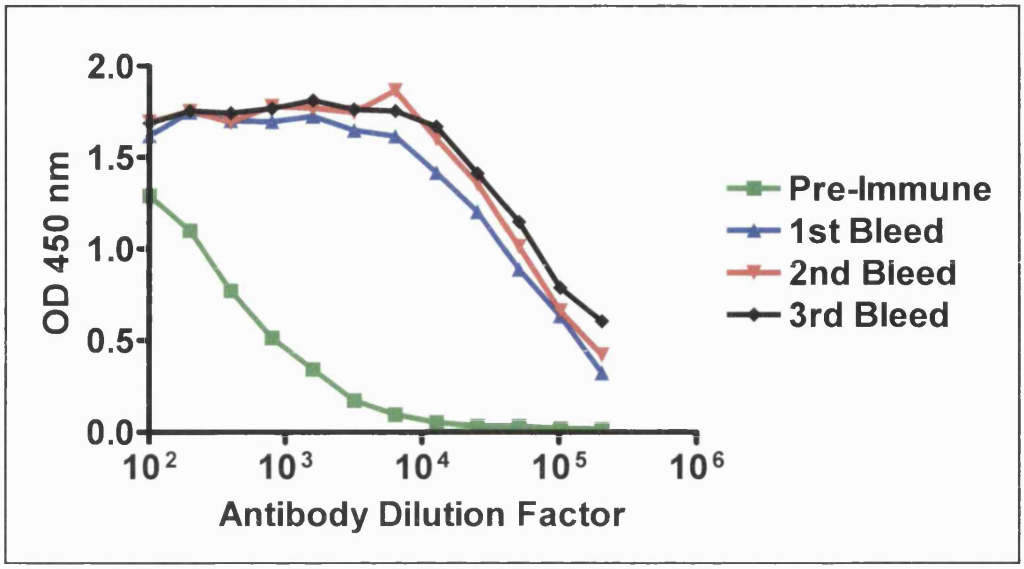

Figure 3.17 **ELISA analysis comparing the different serum bleeds after injection with the C-terminal peptide.** All of the serum bleeds from the sheep injected with the C-terminal peptide were subjected to ELISA analysis against plates coated with the C-terminal peptide. The pre-immune serum was used as a negative control to show that the sheep possessed no intrinsic immune response to the peptide antigen before immunisation. Titre values can be estimated by analysis of optical density readings at 450 nm over the logarithmic dilution range of the sera.

Immunoprecipitation was also carried out to ensure that the antibody did recognise the GLUT4 protein, even though the anti-C-terminal GLUT4 antibody raised in sheep appeared to recognise GLUT4 after Western blot analysis. GLUT4 was immunoprecipitated from LDM with the anti-C-terminal GLUT4 antibody raised in rabbit and was detected by subsequent Western blot analysis using the anti-C-terminal GLUT4 antibody raised in sheep. The anti-C-terminal GLUT4 antibody raised in sheep did recognise the native GLUT4 protein at 45 kDa, which corresponds to the molecular weight of GLUT4 (Figure 3.18 d).

The affinity purified anti-C-terminal GLUT4 antibody raised in sheep was also tested by confocal microscopy on cardiomyocyte cells, but unfortunately no staining was detected (results not shown). Secondary antibodies labelled with different fluorophores (Alexa Fluor 633 and Alexa Fluor 488) were used in combination with the anti-C-terminal GLUT4 antibody raised in sheep to ensure that the secondary antibody was working. However, no staining was seen with either secondary antibody. This suggested that the anti-C-terminal GLUT4 antibody affinity purified from the first bleed serum was not suitable for confocal microscopy. Analysis of the other two bleeds of the sheep C-terminal serum needs to be carried out to determine whether the antibodies purified from these bleeds are suitable for confocal microscopy.

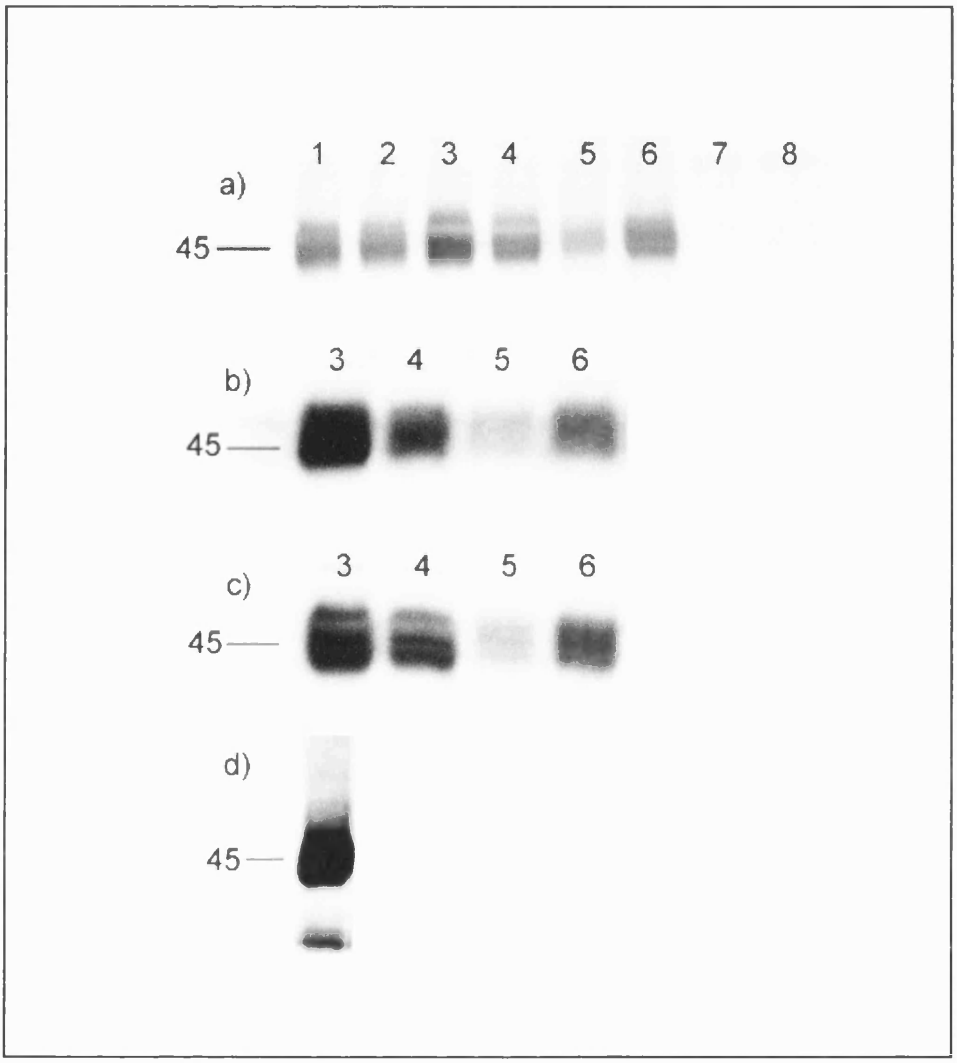

Figure 3.18 **Western blot analysis testing the serum and the affinity purified anti-C-terminal GLUT4 antibody raised in sheep.** SDS-PAGE gels were loaded with 10 µg basal HDM (1), basal HDM (2), basal LDM (3), insulin LDM (4), basal plasma membrane (5), insulin plasma membrane (6), basal cytosol (7) and insulin cytosol (8) adipocyte fractions and then transferred to nitrocellulose for Western blot analysis. The first bleed C-terminal serum (a) and the affinity purified anti-C-terminal GLUT4 antibody raised in sheep (b) were compared to the affinity purified anti-C-terminal GLUT4 antibody raised in rabbit (c). GLUT4 was immunoprecipitated with the anti-C-terminal GLUT4 antibody raised in rabbit, run on an SDS-PAGE gel, transferred to nitrocellulose and probed with the anti-C-terminal GLUT4 antibody raised in sheep (d).

3.2.2.3 Analysis of Antibodies Generated Against the pSer^{10} GLUT4 Peptide in the Different Bleeds of Sheep Serum

The different serum bleeds from sheep injected with the phospho peptide (Sheep A and Sheep B) were analysed by ELISA and Western blot to check if an immune response had been elicited and if the serum contained phospho-specific antibodies. ELISA analysis compared the affinity of the three serum bleeds from both Sheep A and Sheep B, along with the pre-immune bleeds, to the phospho peptide. Antibodies had been raised to the phospho peptide in both Sheep A and Sheep B. The antibody population was not present in the pre-immune serum (Figure 3.19). Sheep B was used for the subsequent antibody purifications because Sheep B had a slightly higher antibody titre even though there was not a big difference between Sheep A (Figure 3.19 hashed line) and Sheep B (Figure 3.19 solid line). The affinity of the serum bleeds for the phospho and non-phospho peptides was also tested by ELISA analysis (Figure 3.20). However, no difference was detected in the specificity of the antibody for the phospho (Figure 3.20 solid line) or non-phospho peptides (Figure 3.20 hashed line).

Two further boost bleeds were taken from Sheep B after injections were given with a slightly different peptide (Figure 3.21). The decision to carry out the boost bleeds came as a result of the fact that there was no difference in the specificity of the serum for the phospho and non-phospho peptides. It was hoped that the additional bleeds would boost the antibody population that had an epitope containing pSer^{10} and not boost antibodies with epitopes containing PAN residues.

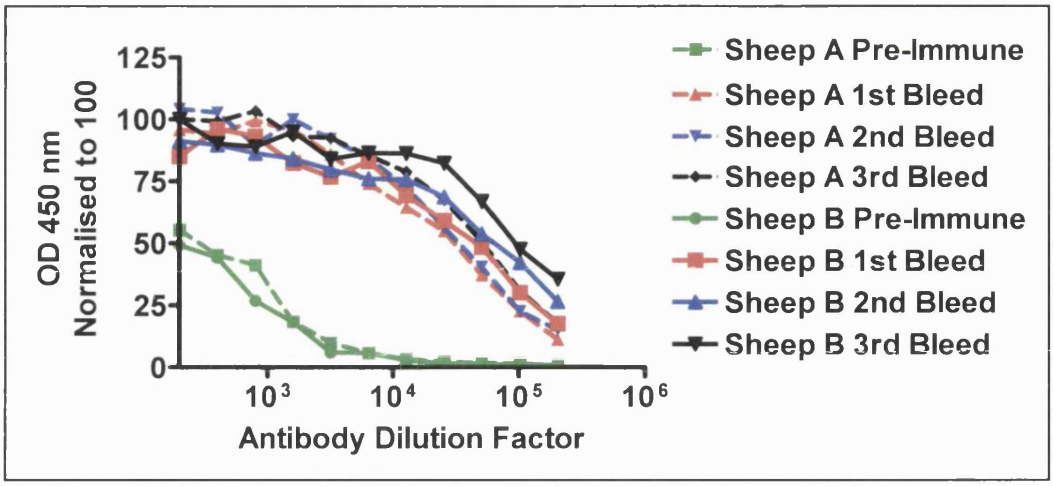

Figure 3.19 **ELISA analysis comparing the different serum bleeds from Sheep A and Sheep B.** All of the serum bleeds along with the pre-immune bleeds from Sheep A (hashed line) and Sheep B (solid line) were subjected to ELISA analysis against plates coated with the phospho peptide. Titre values can be estimated by analysis of optical density readings at 450 nm over the logarithmic dilution range of the sera. The optical density readings were normalised to the 1:200 dilution of the 3rd bleed serum, which was set to 100, to compare Sheep A and Sheep B.

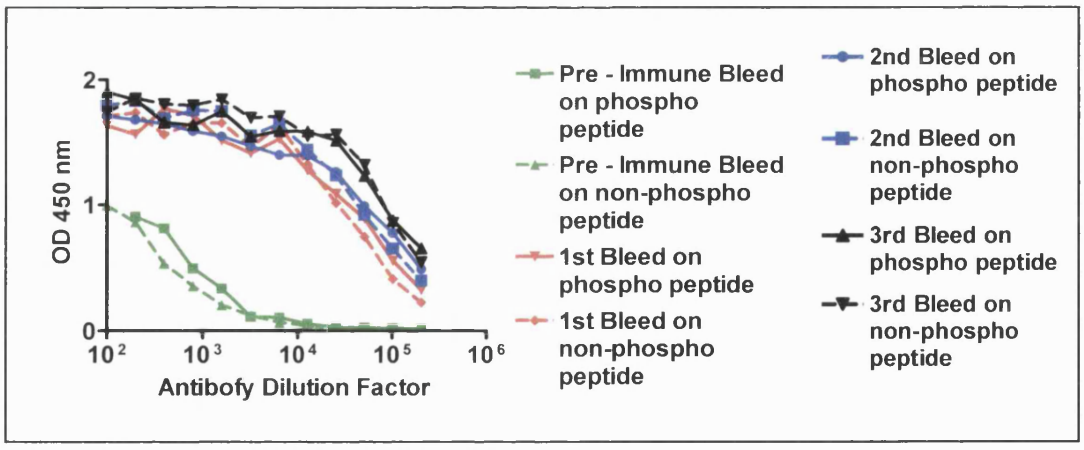

Figure 3.20 **ELISA analysis comparing the different serum bleeds after injection with the phospho peptide - antigen 1.** The serum from Sheep B was subjected to ELISA against plates coated with the phospho peptide (solid line) and non-phospho peptide (hashed line). Titre values can be estimated by analysis of optical density readings at 450 nm over the logarithmic dilution range of the sera.

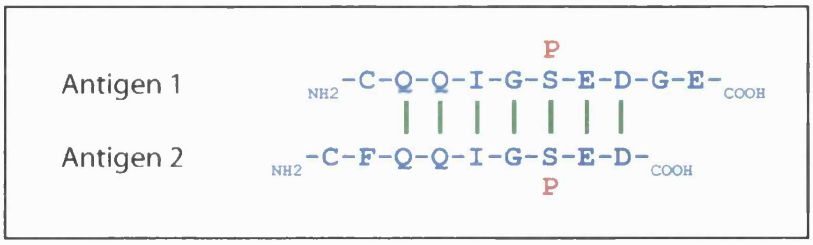

Figure 3.21 **Comparison of the sequences of the two antigens used to produce anti-pSer[10] antibodies in sheep.**

The fourth and fifth bleed serums were again tested by ELISA analysis (Figure 3.22). The serum was tested against antigen 1 and antigen 2 as well as the unphosphorylated form of antigen 1. The antibody recognised antigen 1 more strongly than the peptide used in the boost injection – antigen 2. This would be because the immune response was made by the initial immunisation (antigen 1), and antigen 2 would just boost a population of the already existing antibodies. The fact that the serum recognised both phospho peptides more strongly than the non-phospho peptide was a very encouraging start that led to further purification.

3.2.2.4 Immunoaffinity Purification of an Anti-pSer[10] GLUT4 Antibody from Sheep Serum

Different strategies were tried in the purification of a phospho-specific population of antibodies and these will be detailed below. The purification of the antibody did not involve use of the same strategy as that used for the anti-pSer[10] antibody raised in rabbit.

Immunoaffinity purification of antibody from the fifth bleed serum was carried out using antigen 1 bound to the SulfoLink® column. The purified antibody was again tested by ELISA and Western blotting techniques. The ELISA analysis gave a similar result to that obtained with the fifth bleed serum (result not

shown). The antibody had a greater specificity for antigen 1 than antigen 2, with the unphosphorylated form of antigen 1 recognised the least. Non-phospho-specific antibodies were still present as an antibody population still bound to the non-phospho peptide in an antibody concentration dependent manner. Western blot analysis of the antibody affinity purified from the fifth bleed serum (Figure 3.23) gave a similar result to the anti-C-terminal GLUT4 antibody. The level of GLUT4 in the LDM decreased after insulin stimulation and increased in the plasma membrane. Further purification of the antibody was needed due to the presence of a non-phospho-specific antibody population.

Cross purification was carried out on the third bleed serum from Sheep B to determine whether the non-phospho-specific antibodies could be removed. The cross purification method was previously described in section 3.2.1.2. Cross purification was carried out using the phospho peptide (antigen 1) and non-phospho peptide linked columns. Cross purification did not purify a good population of phospho-specific antibodies (result not shown).

Cross purification, in which a fixed amount of non-phospho peptide was bound to a solid support, appeared to have poor utility for purification of a phospho-specific population of antibodies. Therefore a different method of purifying the antibody was needed. The cross purification procedure required the use of a large molar excess of non-phospho peptide over specific antibody. Therefore, it was tested whether a lower concentration of free non-phospho peptide could be used to block the non-phospho-specific antibody in the serum, without affecting the subsequent purification of the phospho-specific antibody population (Berwick *et al.*, 2004).

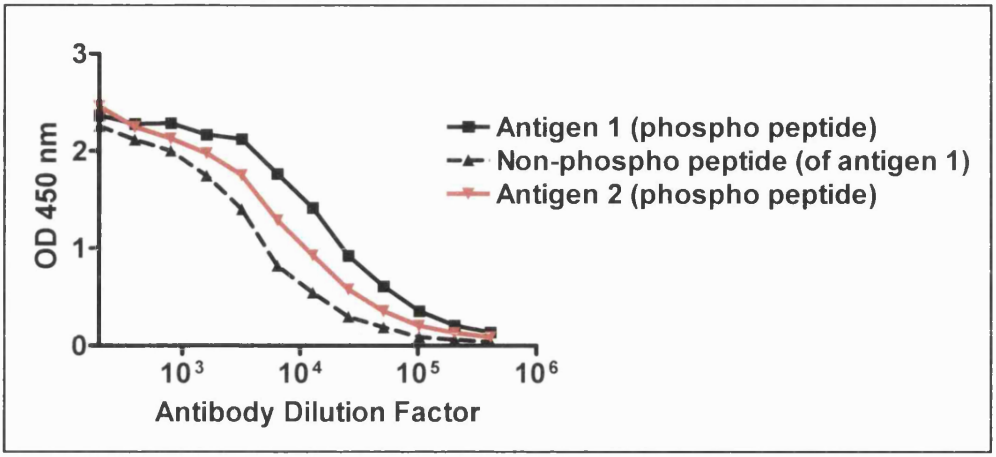

Figure 3.22 **ELISA analysis comparing the specificity of the fifth bleed serum for antigen 1 (black solid line), antigen 2 (red solid line) and the non-phosphorylated form of antigen 1 (black hashed line).** Titre values can be estimated by analysis of optical density readings at 450 nm over the logarithmic dilution range of the sera.

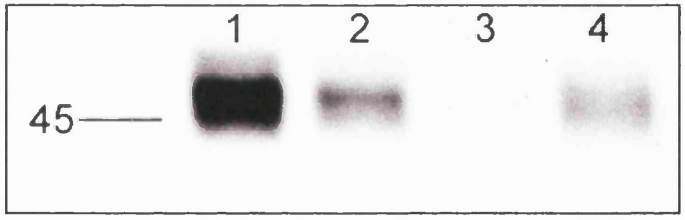

Figure 3.23 **Western blot analysis of the antibody affinity purified on antigen 1 from the fifth bleed serum.** SDS-PAGE gels were loaded with 10 µg basal LDM (1), insulin LDM (2), basal plasma membrane (3) and insulin plasma membrane (4) adipocyte fractions and then transferred to nitrocellulose for Western blot analysis with the fifth bleed serum.

The serum was incubated overnight, rotating at 4 °C, with a one, two, or tenfold molar excess of non-phospho peptide over specific antibody (it was estimated that there was 4 mg of specific IgG per ml of sheep serum [MPB]). As a control, an incubation was set up without peptide. The specificity of the pre-blocked serum for the phospho and non-phospho peptides was tested by ELISA analysis (Figure 3.24). In all of the conditions tested (Figure 3.24 A, B, C and D), the serum had greater specificity for the phospho peptide than the non-phospho peptide. The serum that had been pre-incubated with a one, two or tenfold molar excess of non-phospho peptide (Figure 3.24 A, B and C respectively), had an increased specificity for the phospho peptide than the serum alone (Figure 3.24 D) (the difference between the phospho and non-phospho peptide lines was greater for the pre-blocked serum than the serum alone). However, no differentiation could be made between the different concentrations of non-phospho peptide used in the pre-incubation of the serum (Figure 3.24 A, B and C). A population of non-phospho-specific antibodies was still present in the serum, even after the serum had been pre-blocked with the non-phospho peptide, because a signal was detected after ELISA analysis on the non-phospho peptide. The serum needs to be pre-blocked with more than a tenfold molar excess of non-phospho peptide to remove the entire non-phospho-specific population of antibodies.

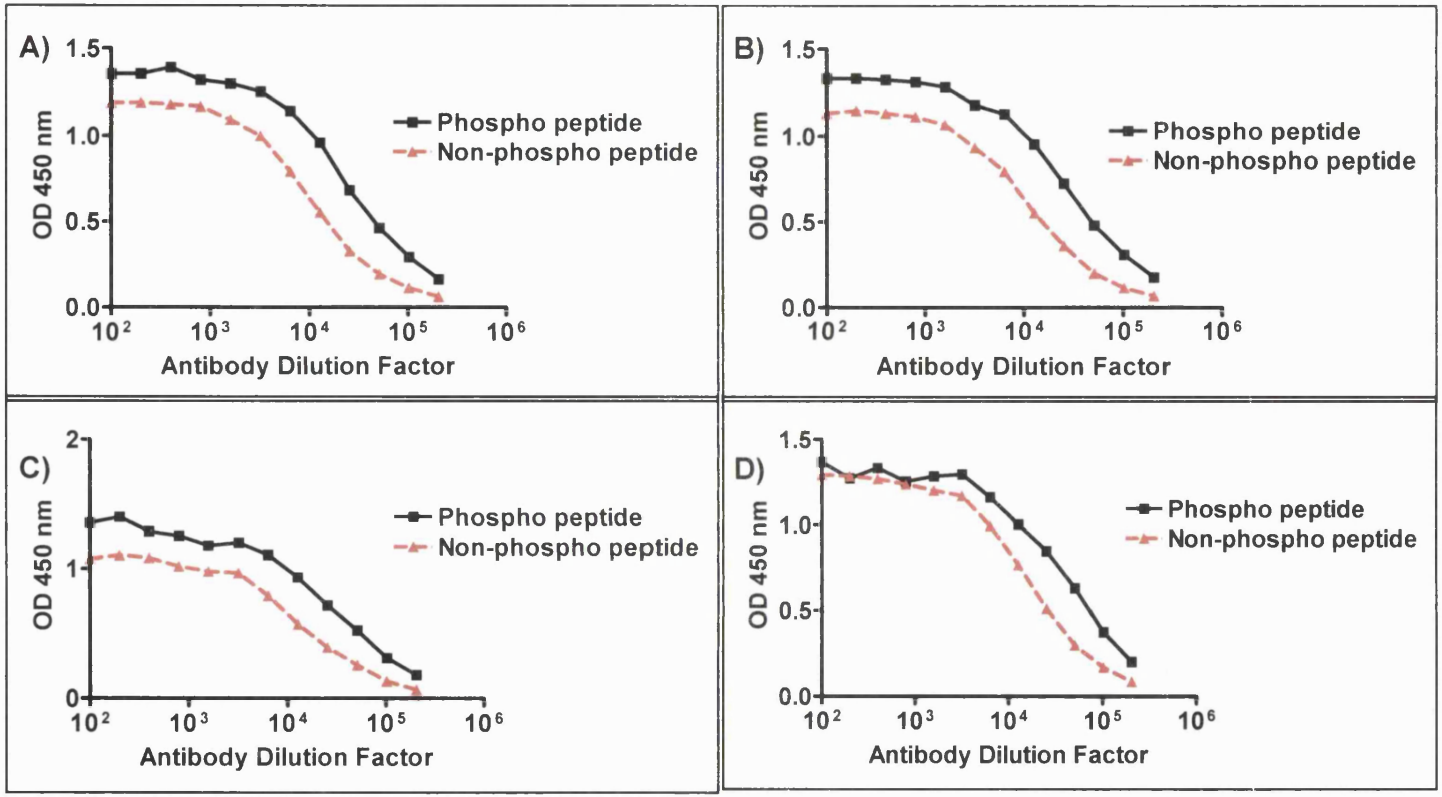

Figure 3.24 **ELISA analysis comparing the serum that had been pre-blocked with a one, two or tenfold molar excess of non-phospho peptide with the serum that had not been pre-blocked.** The serum from the fifth bleed of Sheep B was pre-blocked with a one (A), two (B) and tenfold (C) molar excess of non-phospho peptide before the serum was subjected to ELISA analysis on a phospho peptide (black line) and non-phospho peptide (red line) coated plate. As a control, an incubation was also set up with no non-phospho peptide (D). Titre values can be estimated by analysis of optical density readings at 450 nm over the logarithmic dilution range of the sera.

It was necessary to find the optimal ELISA conditions to ensure that the maximum signal had been achieved between the antibody and the phospho and non-phospho peptides.

The ELISA conditions tested involved changes in the peptide coating buffer and the blocking conditions. The peptides were bound to the plate in either the carbonate / bicarbonate buffer (as described in methods Section 2.2.9.5) or in TBS (Coghlan *et al.*, 1994). When TBS was used to coat the plate, no difference in signal was detected between the phospho or non-phospho peptide. This experiment showed that TBS was not a suitable medium for binding these peptides and that the original coating buffer, the carbonate / bicarbonate buffer, was better. The different blocking buffers tested were 1% (w/v) casein (as described in methods Section 2.2.9.5) and 1% (w/v) BSA. No difference between the two blocking conditions was detected (results not shown). So for further ELISA plate assays the coating buffer used was the carbonate / bicarbonate buffer and the blocking buffer used was 1% (w/v) BSA.

A competition ELISA was carried out to test whether the antibody could discriminate between the phospho and non-phospho peptides (Coghlan et al., 1994, Coba et al., 2003). The fifth bleed serum from Sheep B was pre-bound, overnight, with different concentrations of different peptides; phospho peptide (antigen 1), non-phospho peptide and a non-specific peptide (the C-terminal peptide). An ELISA was carried out on a 96 well plate coated with the phospho peptide. The results were plotted as the percentage of antibody bound to the plate, with 100% being the level of no peptide pre-incubation (Figure 3.25).

The serum contained a population of phospho-specific antibodies. Two pieces of evidence led to this conclusion; (1) the amount of antibody that bound to the plate, after the serum was pre-bound to the phospho peptide, decreased in a peptide concentration dependent manner (Figure 3.25 blue line). (2) When the serum was incubated with the same concentration of the non-phospho peptide compared to the phospho peptide, more antibody bound to the phospho peptide coated plate when the serum was pre-blocked with the non-phospho

peptide (this population of phospho-specific antibodies did not bind to the non-phospho peptide) (Figure 3.25 red line). The decrease in signal, with increasing concentrations of blocking peptide, was due to the specificity of the antibody towards the specific sequence of the peptides. There was no loss in the amount of antibody binding to the plate when the serum was incubated with a non-specific peptide (Figure 3.25 black line).

From the ELISA analysis, it was possible to find the optimal concentration of peptide necessary to block the non-phospho-specific antibody population that was present in the serum. Previously, a tenfold molar excess of peptide over antibody was used and this corresponded to a peptide concentration of 2×10^{-6} M (Figure 3.25). For maximal removal of the non-phospho-specific antibody, without removing any phospho-specific antibody, a blocking peptide concentration of about 1×10^{-5} M was needed (this was the maximum difference between the phospho and non-phospho peptide lines). This was calculated as a fiftyfold molar excess of peptide.

The serum was incubated with a fiftyfold molar excess of non-phospho peptide. ELISA analysis assessed the affinity of the pre-blocked serum for the phospho and non-phospho peptides coated on a 96 well plate. A comparison was made with the affinity of the unblocked serum for each peptide (Figure 3.26). The affinity of the pre-blocked serum (Figure 3.26 black line) for the non-phospho peptide (Figure 3.26 hashed line) had decreased in comparison with the unblocked serum (Figure 3.26 red hashed line). A population of non-phospho-specific antibodies had therefore been removed from the serum following pre-incubation with the non-phospho peptide. A small population of antibodies that had bound to the phospho peptide was also removed in the pre-incubation step. Nevertheless, a phospho-specific population of antibodies was present in the pre-blocked serum.

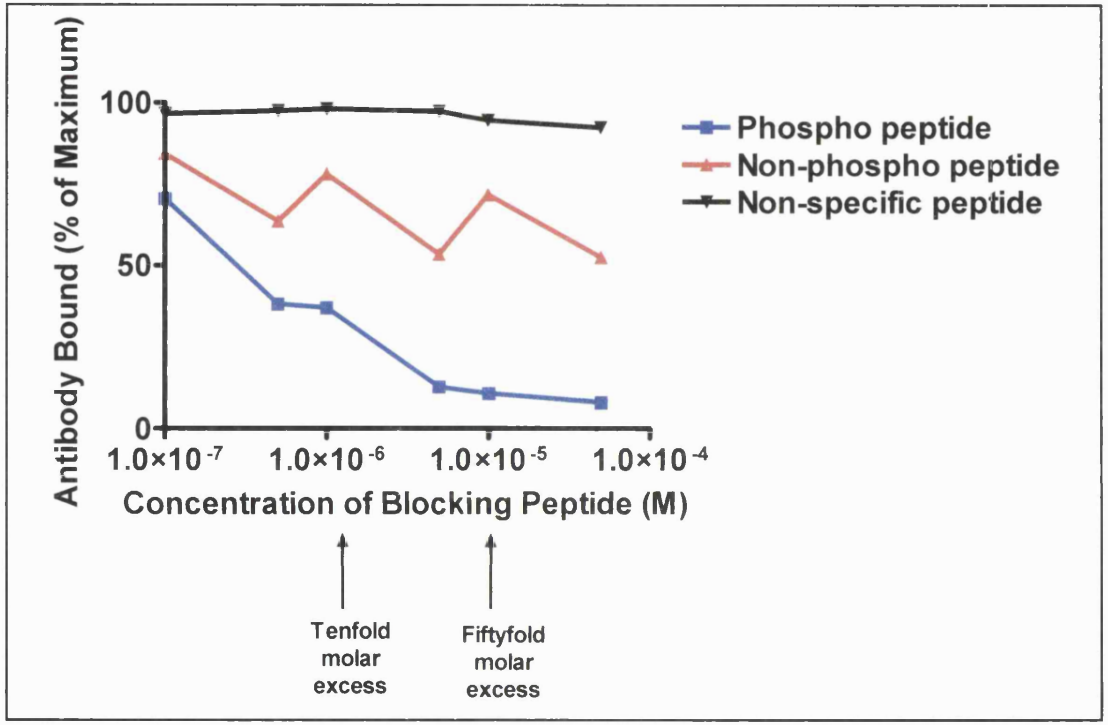

Figure 3.25 Analysis of a competition ELISA in which the serum was pre-incubated with the phospho (blue line), non-phospho (red line) and non-specific (black line) peptides before the ELISA was carried out on a phospho peptide coated plate. The results were displayed as optical density readings at 450 nm versus the $\log_{10}$ of the concentration of blocking peptide used for the ELISA analysis.

The pre-blocked antibody population was analysed by using a competition ELISA on a phospho peptide coated 96 well plate (Figure 3.27). Before the ELISA, the pre-blocked serum was incubated with the three peptides (the phospho, the non-phospho and the non-specific peptides) at the concentrations previously used. The competition ELISA provided further evidence that the pre-blocked serum contained a population of phospho-specific antibodies. The affinity of the phospho-specific antibody population to the plate was not affected by incubation with low concentrations of the non-phospho peptide (Figure 3.27 red line). The level of antibody that bound to the plate was similar to that observed with the non-specific peptide. Thus, the non-phospho peptide was acting like a non-specific peptide at low concentrations and did not affect the amount of phospho-specific antibody that bound to the plate. It was only higher concentrations of non-phospho peptide that prevented the antibody binding to the plate. The pre-blocked serum incubated with the phospho peptide, bound to the plate in a concentration dependent manner i.e. the level of phospho-specific antibody binding to the plate decreased as the concentration of blocking peptide increased (Figure 3.27 blue line). Pre-incubation of the serum with the phospho peptide at concentrations of 5×10^{-6} M or greater caused the peptide to bind to the entire population of phospho-specific antibody. This was evident because the level of antibody binding to the plate started to plateau at a peptide concentration of 5×10^{-6} M. Any antibody binding at higher concentrations of peptide was a background level of binding. The effect of incubating the phospho and non-phospho peptides with the pre-blocked serum was specific because the level of antibody binding to the plate was not affected by incubating the serum with a non-specific peptide (Figure 3.27 black line).

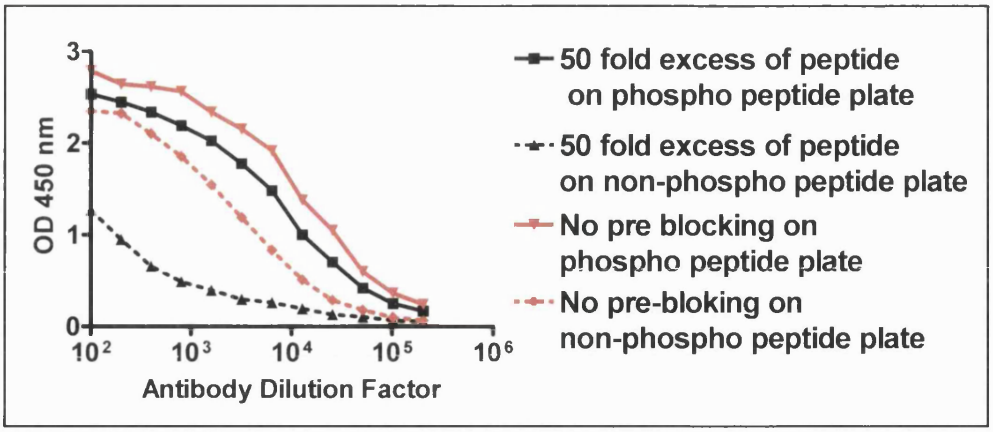

Figure 3.26 **ELISA analysis comparing pre-blocking the serum with a fiftyfold molar excess of non-phospho peptide (black line) with no pre-blocking (red line).** The ELISA was carried out on a phospho peptide (solid line) and a non-phospho peptide coated plate (hashed line). Titre values can be estimated by analysis of optical density readings at 450 nm over the logarithmic dilution range of the sera.

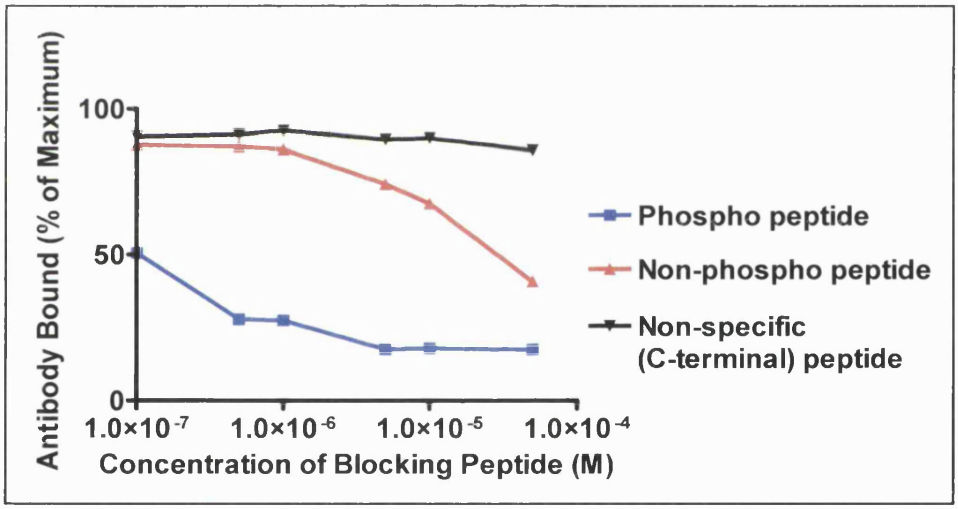

Figure 3.27 **Analysis of a competition ELISA in which serum pre-blocked with a fiftyfold molar excess of non-phospho peptide, was incubated with different amounts of phospho (blue line), non-phospho (red line) and non-specific peptides (black line) before an ELISA was carried out on a phospho peptide coated plate.** The results were displayed as optical density readings at 450 nm versus the $\log_{10}$ the concentration of blocking peptide used for the ELISA analysis.

Pre-blocking the serum with a fiftyfold molar excess of non-phospho peptide produced a population of phospho-specific antibodies. Affinity purification of the pre-blocked serum was carried out on a phospho peptide column to remove any contaminating serum proteins. This affinity-purified antibody was analysed by ELISA (Figure 3.38) and Western blot (Figure 3.29). ELISA analysis compared the antibody that did bind to the phospho peptide column to the antibody that did not bind to the column. A highly phospho-specific antibody population had been purified from the pre-blocked serum (Figure 3.29 A). The antibody had a strong affinity for the phospho peptide (Figure 3.29 A, black line) and had very little affinity for the non-phospho peptide (Figure 3.29 A, red line). A population of phospho-specific antibodies was detected in the flow through from the phospho peptide column (Figure 3.29 B). This population was not purified from the serum (Figure 3.29 B black line). Non-phospho-specific antibodies had been separated from the purified phospho-specific antibody population (Figure 3.29 B red line). Even though there was a phospho-specific antibody population present in the flow through, the purified antibody contained a highly specific population of phospho antibodies raised to serine 10.

The ability of the purified antibody to detect the phosphorylated GLUT4 protein was tested using Western blot analysis (Figure 3.29 c). A comparison was made with the affinity-purified antibody from the fifth bleed serum, which had not been pre-blocked with the non-phospho peptide (Figure 3.29 b). Quantification of the intensity of the bands identified by both antibodies was carried out (Figure 3.29 d). Western blot analysis was also carried out using the anti-C-terminal GLUT4 antibody, raised in rabbit, to quantify the total GLUT4 independent of the phosphorylation state (Figure 3.29 a). Both of the phospho-specific antibodies were used at the same concentration (2 µg/ml). All three antibodies recognised a protein at 45 kDa (Figure 3.29 arrows). Stimulating adipocytes with insulin led to a decrease in the level of intracellular GLUT4 and a corresponding increase in the level of cell surface GLUT4.

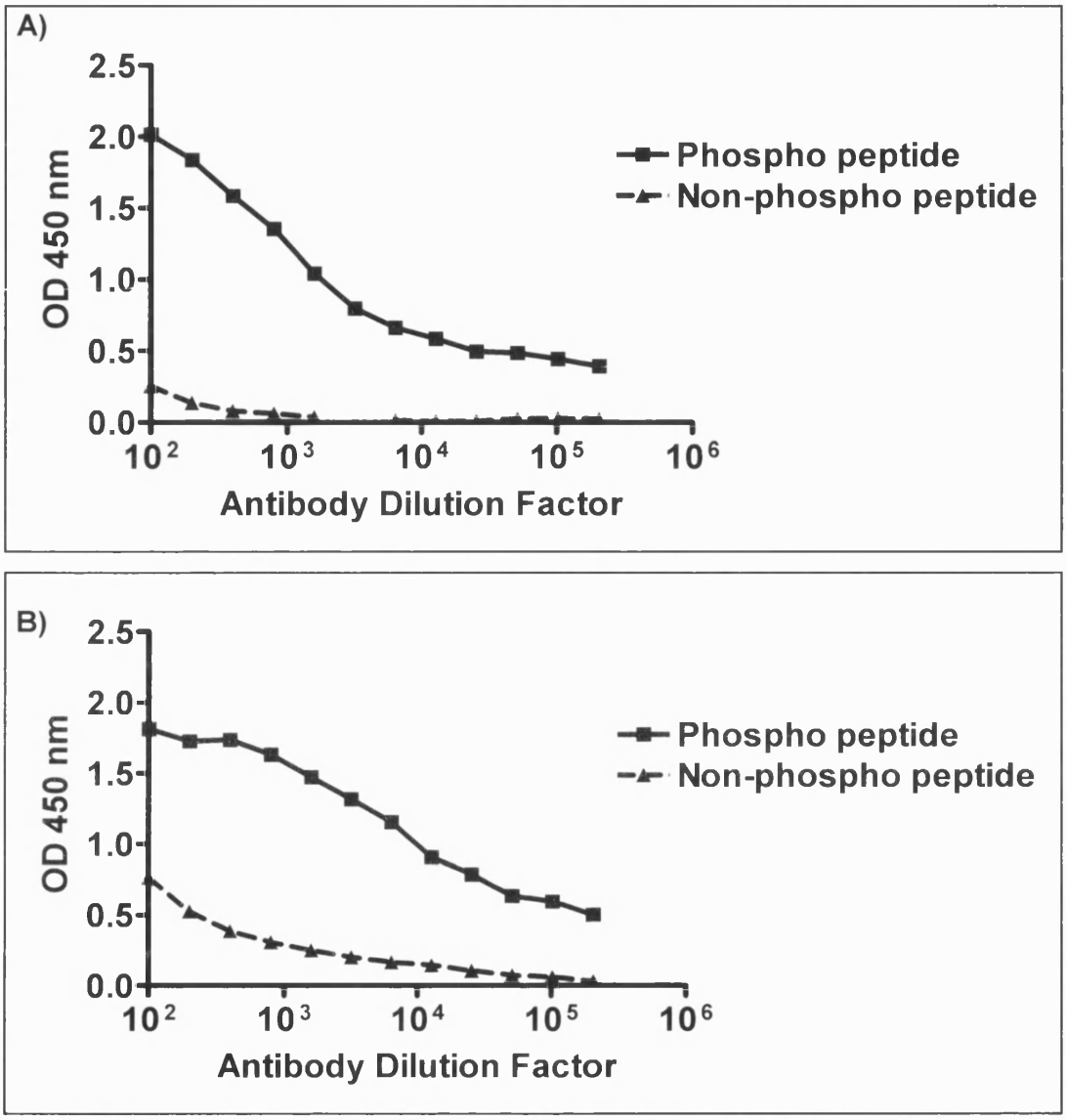

Figure 3.28 **ELISA analysis of the antibodies purified from the phospho peptide column after the serum had been pre-blocked with a fiftyfold molar excess of non-phospho peptide.** The phospho-specific antibody population purified from the phospho peptide column (A) and the population that did not bind to the phospho peptide column (B) were subjected to ELISA analysis against plates coated with the phospho (black line) and non-phospho peptides (red line). Titre values can be estimated by analysis of optical density readings at 450 nm over the logarithmic dilution range of the antibody.

However, the quantification of the level of GLUT4 in each cellular fraction did differ. Insulin caused a decrease in the level of phosphorylation at Ser^{10} in GLUT4 in the LDM fraction (Figure 3.29 b and c). This decrease was larger than that observed for the total GLUT4 protein (a), i.e. the decrease could have been due to dephosphorylation and not just due to the translocation of the transporter out of the LDM compartment. Only a fraction of total GLUT4 was phosphorylated at Ser^{10} at the plasma membrane in the basal state (the intensity of the signal at the plasma membrane was less than the signal from the C-terminal antibody). A very weak signal was detected by the Western blot with the pre-blocked serum even though the same concentrations of anti-$pSer^{10}$ antibodies were used. This could have been because the population of GLUT4 phosphorylated at Ser^{10} was very small in adipocytes and so the signal intensity detected on the Western blot from the affinity purified pre-blocked serum was weak. Even though the anti-$pSer^{10}$ antibody purified from unblocked serum was used at the same concentration as the pre-blocked serum, the antibody population still contained epitopes to unphosphorylated GLUT4. The presence of the unphosphorylated epitopes would result in an increased signal from binding to unphosphorylated GLUT4. The quantification of the Western blot with the pre-blocked serum may not be accurate due to the weakness of signal. The antibody needs to be tested further using a higher concentration of adipocyte sub-fractions run on an SDS-PAGE gel and a higher primary antibody concentration used in the Western blot. If the phosphorylation of GLUT4 was limited to a small subset of transporters, then running more protein on the gel would result in a stronger signal.

The antibody was also tested by confocal microscopy on basal and insulin-stimulated cardiomyocytes. Unfortunately, neither of the affinity purified anti-$pSer^{10}$ antibodies raised in sheep (either pre-blocked or not pre-blocked) stained the cardiomyocytes. This may be due to problems with the secondary antibody or the antibody may not be suitable for confocal microscopy (Section 3.2.2.2).

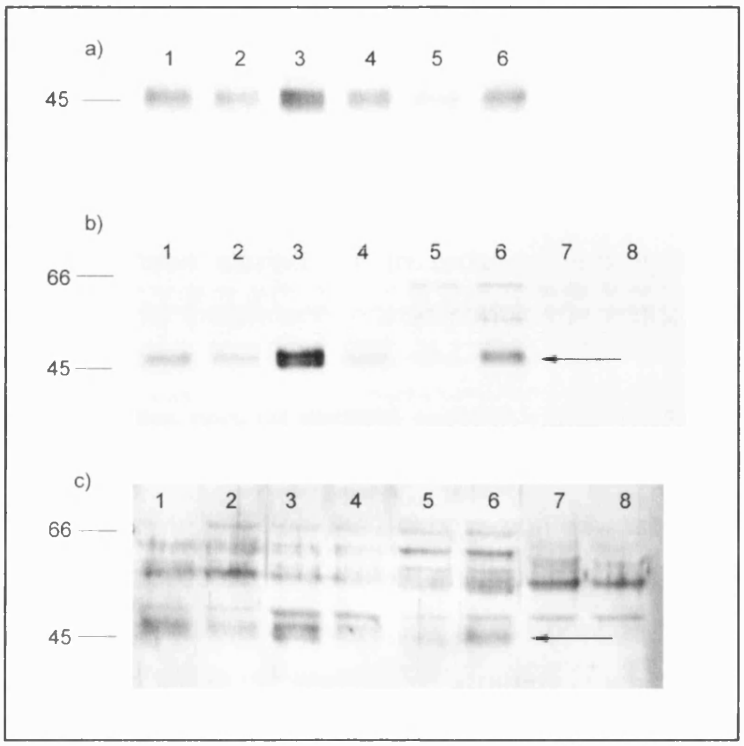

d)	LDM		PM	
	B	I	B	I
A	100.0	69.2	42.8	79.3
B	100.00	24.56	7.22	22.79
C	100.00	40.21	22.94	56.33

Figure 3.29 **Western blot analysis comparing total GLUT4 (a), the anti-pSer[10] antibody purified on the phospho peptide column (b) and the anti-pSer[10] antibody pre-blocked with a fiftyfold molar excess of non-phospho peptide before purification on the phospho peptide column (c).** SDS-PAGE gels were loaded with 10 µg basal HDM (1), insulin HDM (2), basal LDM (3), insulin LDM (4), basal plasma membrane (5), insulin plasma membrane (6), basal cytosol (7) and insulin cytosol (8) adipocyte fractions and then transferred to nitrocellulose for Western blot analysis. The arrows indicated the GLUT4 band. Quantification of the Western blot showed the amount of GLUT4 in the relevant fractions compared to basal LDM set to 100% (d) (PM = plasma membrane, B = basal, I = insulin).

3.3 Discussion

A polyclonal anti-pSer^{10} antibody has been raised in two different species of animal (rabbit and sheep). The antibody in rabbit had been raised by a previous member of the laboratory. The two antibodies have been purified and characterisation has been carried out in order to investigate whether the antibodies are specific for the phosphorylated serine 10 residue.

Due to the design of the original antigen used in rabbit (IGSPEDGEPPQQ), there is a large proportion of peptide sequence to which 'PAN-specific' antibodies will be raised. In addition, the acidic region downstream of serine 10 and the two proline residues in the peptide (which will cause a kink in this area of the peptide), may cause this 'PAN' region of the peptide to become highly immunogenic. This fact led to the purification strategy in which a PAN-specific peptide (GEPPQQ) was used to remove the PAN-specific antibodies from the serum. A population of phospho-specific antibodies has been purified from the final bleed serum (Figure 3.9). This phospho-specific antibody did bind to the native GLUT4 protein because it was able to immunoprecipitate GLUT4 from LDM (Figure 3.12). However, the antibody is, at present, unsuitable for use on Western blot. The GLUT4 band is difficult to identify due to the presence of non-specific bands in the 45 kDa area on the nitrocellulose (Figure 3.10). The pSer^{10} GLUT4 band is weak and not detected at 45 kDa when ECL [A] was used to develop the Western blot. ECL Advance [A] (a highly sensitive chemiluminescent detection agent) is required for a signal to be detected on the Western blot. However, the ECL advance will not only increase the intensity of the GLUT4 band, it will also increase the intensity of the stronger, non-GLUT4 bands that are detected on the nitrocellulose. There are two possible explanations for the weak GLUT4 signal. The phosphorylation of GLUT4 at serine 10 may only occur in a small subset of transporters, or the antibody is a poor antibody and so it does not recognise the phosphorylated GLUT4 population with a high intensity. The non-specific bands that are

detected on the Western blot are due to the secondary antibody (Figure 3.11 g). Before the anti-pSer^{10} antibody can be used for Western blot analysis, different rabbit IgG secondary antibodies need to be tested. The secondary antibody used had only been adsorbed against human protein. A secondary antibody adsorbed against rat proteins would hopefully detect fewer non-specific bands on the Western blot.

In confocal microscopy studies, the anti-pSer^{10} antibody purified from rabbit serum recognises a protein in cardiomyocytes and 3T3-L1 adipocytes. The anti-pSer^{10} antibody recognises a peri-nuclear protein in both basal and insulin-stimulated cardiomyocytes. The staining does not co-localise with the anti-C-terminal GLUT4 antibody staining in insulin-stimulated cardiomyocytes and only partially co-localises in basal cardiomyocytes. The anti-pSer^{10} antibody may be either binding to a peri-nuclear protein that is not GLUT4 or the antibody is recognising a subset of GLUT4 that is concentrated in the peri-nuclear region of the cell. If the anti-pSer^{10} antibody is recognising phosphorylated GLUT4, then the GLUT4 phosphorylated at serine 10 is in a different conformation to unphosphorylated GLUT4 and so the anti-C-terminal GLUT4 antibody could not bind to the C-terminus. This may occur during biosynthesis. The anti-pSer^{10} antibody also recognises a protein in the peri-nuclear region of 3T3-L1 adipocytes which is Brefeldin A (BFA) sensitive at day 3, 5 and 12 of differentiation. The expression of GLUT4 in differentiating 3T3-L1 adipocytes has previously been reported (Garcia de Herreros and Birnbaum, 1989). On day 3 after differentiation, GLUT4 was mainly peri-nuclear and was located asymmetrically on one side of the nucleus. The GLUT4 protein was also observed in vesicles throughout the cytoplasm. The same distribution of GLUT4 was also seen on day 5. In the present study, the anti-C-terminal GLUT4 antibody did not stain a peri-nuclear protein at day 3 of differentiation. This difference could occur because the GLUT4 antibodies used in the present study and by Garcia de Herreos and Birnbaum may be raised to a different peptide sequence. Perhaps the C-terminus of GLUT4 is in an

orientation that is not accessible to the anti-C-terminal GLUT4 antibody at day 3 of differentiation and so the anti-C-terminal GLUT4 antibody cannot bind to the C-terminus of GLUT4. However, if the anti-pSer^{10} antibody is binding GLUT4, the N-terminus is in an accessible orientation for the anti-pSer^{10} antibody. This difference in protein fold may occur during biosynthesis and the anti-C-terminal GLUT4 antibody may only recognise the GLUT4 protein at a later stage of synthesis than the anti-pSer^{10} antibody. The anti-C-terminal GLUT4 antibody could recognise a small proportion of GLUT4 vesicles that had left the biosynthetic pathway at day 3. By day 5, more of the native protein has gone through the synthetic pathway and would now be in an orientation so that the anti-C-terminal GLUT4 antibody could detect the GLUT4 protein. Phosphorylation of GLUT4 at serine 10 may therefore occur during biosynthesis so that no staining is seen at serine 10 once the protein has left the biosynthetic pathway. This is further corroborated because by day 12, the intensity and number of pSer^{10} positive cells is less than at day 3 or 5. At day 12, the cells are fully differentiated so there is less GLUT4 in the biosynthetic pathway. It has previously been reported that there are both BFA sensitive and insensitive pools of GLUT4 and that the insulin sensitive pool of GLUT4 is BFA insensitive (Bao *et al.*, 1995). Both BFA sensitive and insensitive pools of GLUT4 are stained by the anti-C-terminal GLUT4 antibody. However, only a protein in the BFA sensitive pool is stained by the anti-pSer^{10} antibody. There is no definitive proof that the anti-pSer^{10} antibody is recognising the GLUT4 protein in the confocal images and it could be recognising a different peri-nuclear localised protein. If the anti-pSer^{10} antibody did detect GLUT4 in the biosynthetic pathway, then the GLUT4 would be present in the Golgi and it would be BFA sensitive. The protein stained with the anti-pSer^{10} antibody needs to be identified before the antibody can be used to investigate the localisation of GLUT4 phosphorylated at serine 10. The cells could also be treated with kinase inhibitors and the effect of the inhibitors on the level of phosphorylation could be investigated. The protein stained with the anti-pSer^{10} antibody could perhaps be identified by RNA interference (RNAi). RNAi is a

mechanism whereby double stranded RNA specifically suppresses the expression of the targeted gene. If the peri-nuclear staining in the cell is GLUT4, then suppressing the GLUT4 gene would abolish any staining observed from the anti-pSer^{10} antibody.

An anti-C-terminal GLUT4 antibody has successfully been raised in sheep. This could be used in experiments involving Western blot and immunoprecipitation techniques, with the anti-pSer^{10} antibody raised in rabbit, to aid the study of GLUT4 phosphorylation. However, the antibody would not be suitable for use in confocal microscopy studies without future work.

The anti-pSer^{10} antibody raised in sheep has been successfully purified on a phospho peptide column. However, the serum has to be pre-blocked with a fiftyfold molar excess of non-phospho peptide over specific antibody before a phospho-specific antibody population could be purified. This strategy has been successful because the non-phospho-specific antibody bound to the peptide and so did not bind to the phospho peptide column in the purification technique. However, not all of the phospho-specific antibody has been purified from the serum. Nevertheless, a highly phospho-specific population of antibodies has been purified from the sheep serum (Figure 3.28). Further characterisation of the antibody purified from sheep serum is also needed to ensure that the antibody recognises the native GLUT4 protein. This can be done by testing the ability of the antibody to immunoprecipitate GLUT4 or to recognise GLUT4 that has been immunoprecipitated using the anti-C-terminal GLUT4 antibody raised in rabbit.

Both of the anti-pSer^{10} antibodies raised are phospho-specific as analysed by ELISA. The antibodies also bind to a 45 kDa band identified by Western blot analysis but the band is weak. This is likely to be because the population of GLUT4 phosphorylated at Ser^{10} is very small. However, due to the weak band, at present the antibodies are not suitable for use in Western blot analysis.

Further characterisation is needed using a large amount of protein in the SDS-PAGE and using a higher primary antibody concentration to detect the bands on Western blot. Due to the high level of non-specific bands detected on the Western blot by the anti-pSer^{10} antibody raised in rabbit, the anti-pSer^{10} antibody purified from the pre-blocked sheep serum is likely to be the most useful antibody to use in future. However, if future studies are going to involve confocal microscopy, the anti-pSer^{10} antibody purified from rabbit serum would be the antibody of choice, if the antibody does detect the GLUT4 protein. The anti-pSer^{10} antibody raised in sheep is not suitable for confocal microscopy.

As both pSer^{10} antibodies give a good signal in ELISA analysis, an ELISA plate assay could be developed to investigate the phosphorylation state of GLUT4. Many photoaffinity labelling reagents have been used for studying glucose transporters (Holman et al., 1990, Yang and Holman, 1993, Araki et al., 1996). The GLUT4 protein can be photolabelled because the photolabel has a glucose moiety, which will covalently bind to the GLUT4 protein after UV irradiation. There is a biotin moiety on the other end of the photolabel. The GLUT4 can then be separated and bound to a streptavidin coated 96 well plate. An assay can then be carried out in which the anti-pSer^{10} antibody detects differences in the phosphorylation state of GLUT4 under different conditions.

The antibody could also be used to carry out an *in vitro* kinase assay on a peptide corresponding to the N-terminus of GLUT4. The serine 10 kinase could then be identified using fluorescence resonance energy transfer (FRET). FRET occurs when the fluorescence spectra of two fluorescent tags overlap. Specifically, the emission spectrum of the donor molecule overlaps the excitation spectrum of the acceptor. The donor and acceptor molecules must be in close proximity, typically 10 - 100 Å. Cy3 and Cy5 [A] are two such molecules with overlapping spectra. A peptide corresponding to the N-terminus of GLUT4 can be labelled with Cy3 [A] and the anti-pSer^{10} antibody can be

labelled with Cy5 [A]. If the Cy3 and Cy5 molecules are in close proximity, i.e. when the antibody binds to the phosphorylated peptide, an enhanced fluorescent signal will be detected. A kinase could therefore be identified if it had phosphorylated the N-terminal peptide. A whole cell lysate or different cellular fractions could be used to identify in which fractions the kinase is located. The use of recombinant protein kinases and known kinase inhibitors in this assay system could also be used to identify the GLUT4 N-terminal kinase.

3.4 Conclusion

Two different anti-pSer^{10} antibodies have been raised and will be useful in investigating the phosphorylation state of GLUT4 at serine 10 in combination with the anti-C-terminal GLUT4 antibodies that have been raised in rabbit and sheep. However, further characterisation of both antibodies is needed before they can be used in further experiments. The anti-pSer^{10} antibody raised in sheep was used to identify the GLUT4 N-terminal peptide in the phosphorylation experiments discussed in chapter 4.

4 An Investigation into the Phosphorylation State at the N- and C- termini of GLUT4

4.1 Introduction

The many years of investigating insulin signalling have led to the conclusion that phosphorylation is a key event in the insulin-signalling cascade which ultimately leads to the translocation of GLUT4 to the plasma membrane (Section 1.3). The phosphorylation level of many adipose cell proteins increases due to the effect of insulin (Belsham et al., 1980, Avruch et al., 1982). The first studies investigating GLUT1 phosphorylation concluded that there was no phosphorylation in response to insulin or isoproterenol in either primary adipocytes or 3T3-L1 adipocytes (Gibbs et al., 1986, Joost et al., 1987). However, GLUT4 contains several potential phosphorylation sites (James *et al.*, 1989a). GLUT4 has a 65% identity to GLUT1 and the transmembrane regions are the most highly conserved between the two proteins. Phosphorylation of GLUT4 is, therefore, likely to occur in the regions that are not conserved between the two proteins, these are at the N- and C-termini as well as the large intracellular loop between helices 6 and 7 (Figure 4.1).

Previous studies investigating the phosphorylation status of GLUT4 involved '*in vitro*' phosphorylation experiments in which rat adipocyte preparations were pre-incubated with a source of [$^{32}P_i$]. The results of these experiments concluded that GLUT4 was phosphorylated in rat adipocytes (Joost et al., 1987, James et al., 1989a, Lawrence, Jr. et al., 1990a, Schurmann et al., 1992). It was reported that there was a basal labelling of at least 0.2 mole of phosphate per mole of GLUT4. The relative level of phosphorylation did not change after insulin stimulation at either the LDM or plasma membrane (James *et al.*, 1989a). However, the authors did point out that a small subset of transporters could be phosphorylated at the plasma membrane in response to

insulin but could not be detected due to the low number of transporters at the plasma membrane in unstimulated cells. In addition, phosphorylation of GLUT4 was observed in response to isoproterenol after the cells had been stimulated by insulin. Isoproterenol stimulated a twofold increase in the level of GLUT4 phosphorylation compared to the basal level of GLUT4 phosphorylation (James *et al.*, 1989a).

In addition to insulin-stimulated glucose transport, glucose transport is also stimulated by lipolytic agents, i.e. agents that modulate adenyl cyclase and lipolysis (Taylor et al., 1976, Kashiwagi et al., 1983). However, lipolytic agents (e.g. isoproterenol) inhibit insulin-stimulated glucose transport in the absence of antilipolytic agents (e.g. adenosine) in both muscle and adipose tissue (Kashiwagi et al., 1983, Smith et al., 1984, James et al., 1986, Kuroda et al., 1987). Insulin-stimulated glucose transport was inhibited 40% by the presence of isoproterenol (James *et al.*, 1989a). In addition, the inhibition was not mediated by a change in the localisation of the transporter but was a result of a change in the intrinsic activity of the transporter (Smith et al., 1984, Kuroda et al., 1987).

Adenyl cyclase catalyses the conversion of ATP to cAMP, so lipolytic agents mediate cAMP synthesis as well as stimulating glucose transport. It was shown that the cAMP derivatives 8-bromo-cAMP and dibutyryl-cAMP produced the same increased level of phosphorylation of GLUT4 as seen with isoproterenol (James *et al.*, 1989a). Protein kinase A (PKA) modulates many of the actions of intracellular cAMP and it was therefore considered that GLUT4 could be a substrate for PKA. In fact, PKA did phosphorylate GLUT4 vesicles *in vitro* (James et al., 1989a, Lawrence, Jr. et al., 1990a, Nishimura et al., 1991, Schurmann et al., 1992).

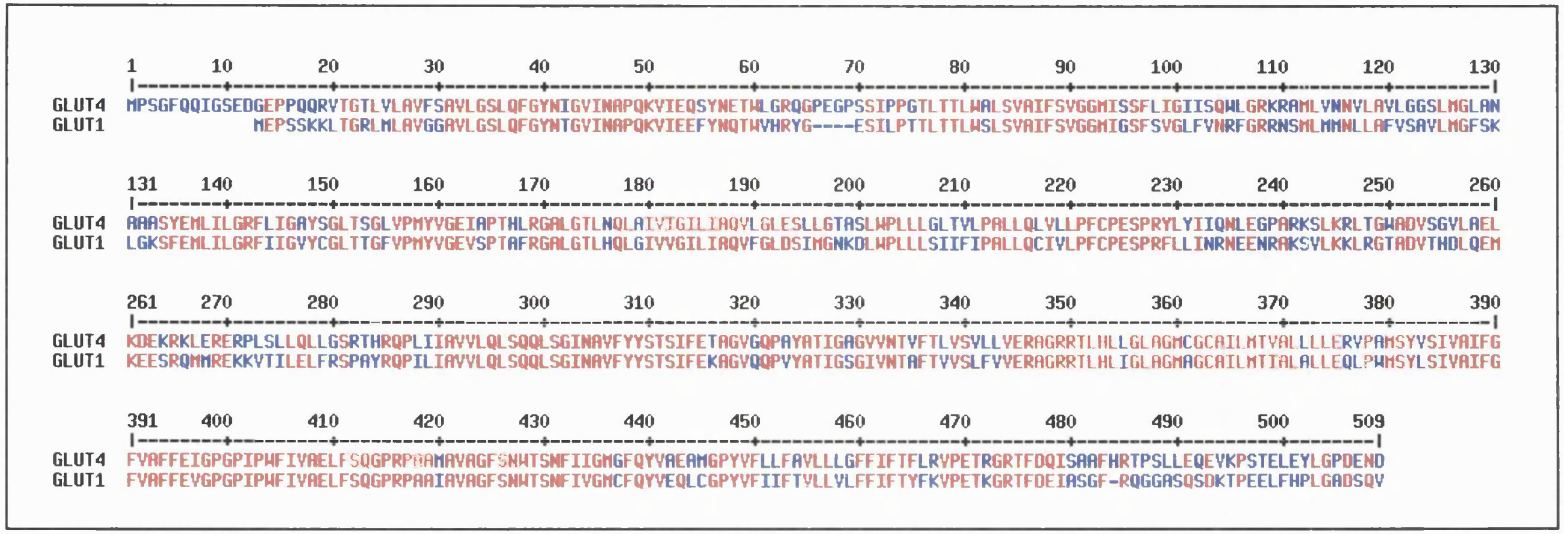

Figure 4.1 **Alignment of the GLUT4 and GLUT1 transporter proteins.** There is a 65% sequence identity between the two glucose transporters – GLUT1 and GLUT4. The N- and C- termini along with the large intracellular loop between helices 6 and 7 have the least homology. The residues in red are identical in GLUT4 and GLUT1, whereas the residues in blue differ between the two proteins. – indicates where there are additional amino acids in the other protein. The alignment was carried out using Multalin (Corpet, 1988).

It has been suggested that the inhibition of insulin-stimulated glucose transport, by isoproterenol, was mediated by the phosphorylation of GLUT4 (James *et al.*, 1989a). However, alternative studies have given a different interpretation. It was reported that there was not a link between the isoproterenol stimulation of PKA and inhibition of insulin-stimulated glucose transport. This suggested that changes in GLUT4 phosphorylation, by PKA, were not responsible for the inhibition of insulin-stimulated glucose transport (Kuroda *et al.*, 1987). Isoproterenol also inhibited the insulin-stimulated transport of glucose through the GLUT1 transporter (Joost *et al.*, 1987). However, the fact that GLUT1 was not phosphorylated by insulin, adenosine or isoproterenol, suggested that there was not a direct link between the inhibition of insulin-stimulated glucose transport and the isoproterenol stimulation of PKA.

Nishimura *et al* attempted to address whether the inhibition of glucose transport, by isoproterenol, was mediated by the phosphorylation of GLUT4. The study confirmed that GLUT4 was phosphorylated and isoproterenol stimulated a 40% increase in the level of phosphorylation in intracellular membranes. This increased level of phosphorylation occurred both in the absence and presence of adenosine receptor activation. In contrast, the inhibition of glucose transport, by isoproterenol, only occurred without adenosine receptor activation (Nishimura *et al.*, 1991). This suggested that the phosphorylation of GLUT4, in response to isoproterenol, did not mediate the inhibition of insulin-stimulated glucose transport. The phosphorylation must have an, as yet, unidentified role. This was further corroborated in a study by Schürmann *et al.* They showed that phosphorylation of GLUT4, by PKA, produced a much smaller population of phosphorylated GLUT4 at the plasma membrane compared to intracellular membranes. The phosphorylation did not affect the rate of glucose transport (Schurmann *et al.*, 1992). A final study using chimeras of GLUT4 and GLUT1 attempted to identify the region of GLUT4 that was involved in the inhibition of insulin-stimulated glucose transport as seen by the cAMP derivative dibutyryl cAMP. It found that the

inhibitory effect was modulated by the binding of the nucleotide to the C-terminus of GLUT4 and was distinct from the site of phosphorylation (Piper *et al.*, 1993a).

It has also been reported that high cytosolic calcium levels stimulate GLUT4 phosphorylation and that increased GLUT4 phosphorylation decreases the transporters intrinsic activity. This results in a decrease in insulin-stimulated glucose transport. The authors conclude that high cytosolic calcium levels induce insulin resistance by interfering with the dephosphorylation of GLUT4 (Reusch et al., 1991, Reusch et al., 1993, Begum et al., 1993). However, further study is required to establish if the observed decreases in glucose transport activity are the direct result of increased GLUT4 phosphorylation or are mediated by another mechanism involving elevated cytosolic calcium levels.

When adipocytes are incubated with the phosphatase inhibitor, okadaic acid, there is a threefold increase in the level of GLUT4 phosphorylation at the plasma membrane (Lawrence, Jr. *et al.*, 1990b). Okadaic acid is a tumour promoter that was originally isolated from the sea sponge, *Halichondria okadaii* (Tachibana K *et al.*, 2005), and inhibits Type I and Type IIa protein phosphatases (Bialojan and Takai, 1988, Cohen et al., 1990). These two enzymes are responsible for most of the protein phosphatase activity in the fat cells (Haystead *et al.*, 1989). Okadaic acid stimulates 2-deoxyglucose uptake in rat adipocytes (Haystead *et al.*, 1989) and results in a fourfold increase in the level of GLUT4 at the plasma membrane. Although okadaic acid stimulates GLUT4 translocation, it partially inhibits insulin-stimulated GLUT4 transport. Okadaic acid alone or in combination with insulin increases the level of phosphorylation of GLUT4 threefold at the plasma membrane relative to the intracellular pool of transporters (Lawrence, Jr. *et al.*, 1990b). It is unlikely that the phosphorylation alone would induce translocation as insulin does not increase the phosphorylation of the protein. The inhibitory effect of okadaic

acid on insulin-stimulated translocation is consistent with the hypothesis that the phosphorylation of GLUT4 promotes internalisation.

A single phosphorylation site has been identified in GLUT4 (Lawrence, Jr. *et al.*, 1990a). Cyanogen bromide (CNBr) was used to cleave GLUT4 at methionine residues from [$^{32}P_i$] labelled adipocytes. Autoradiography of the peptides, separated by SDS-PAGE, identified a single phosphorylated band from either the N- or the C-terminus of GLUT4. The band was identified as being from the C-terminus after use of an antibody raised to the C-terminus of GLUT4 to detect the band. An antibody to the N-terminus of GLUT4 was not available at the time of the study. Tryptic digestion identified the phosphorylated residue as serine 488. It is interesting to note that this site is not present in GLUT1 (Lawrence, Jr. *et al.*, 1990a). Phosphorylation at the amino-terminus was not reported and has not been investigated since.

The lack of investigation into the potential phosphorylation of the amino-terminus of GLUT4 is surprising as the N-terminal region of GLUT4, downstream of the FQQI motif, bears a close sequence identity to a known multiple phosphorylation site within the GAD65α subunit (Section 1.6.3). This site contains an acidic cluster region that is similar to regions found in CD-MPR and furin. Casein Kinase II (CKII) is known to phosphorylate these proteins. It is predicted that GLUT4 is phosphorylated by a kinase that is closely related to the one that phosphorylates GAD65α. The phosphorylation of this region may be involved in modulating GLUT4 cellular routing, sorting from the cell surface, or possibly removal of GLUT4 from the recycling endosomal pool into the TGN and/or the specialised intracellular insulin-responsive compartment.

Experiments involving GLUT4 phosphorylation have mainly been carried out in adipocytes, with one brief report of phosphorylation occurring in GLUT4 isolated from skeletal muscle (James *et al.*, 1989a). There have been no reports investigating phosphorylation in cardiomyocytes. However,

cardiomyocytes and skeletal muscle are interesting targets as they have an additional mechanism that regulates GLUT4 translocation. In addition to insulin-stimulated GLUT4 translocation that occurs in adipocytes, GLUT4 translocation occurs in muscle cells during ischemia and hypoxia by a pathway that is not inhibited by wortmannin (Sun et al., 1994, Egert et al., 1997). This mechanism is believed to involve AMP-activated protein kinase (AMPK) (Russell, III *et al.*, 1999) (Section 1.4).

The aim of the work described in this chapter was to investigate the phosphorylation state of GLUT4 in adipocytes and cardiomyocytes, to identify any previously unidentified phosphorylation sites especially at serine 10 and to confirm that serine 488 was phosphorylated. It was planned that the change in phosphorylation in response to different agents would also be investigated as well as the relative level of phosphorylation at each terminus. The stoichiometry of phosphorylation would then be calculated in both adipocytes and cardiomyocytes. In addition, the identity of the kinase(s) responsible for phosphorylation would be investigated from kinase inhibitor studies.

4.2 Results

4.2.1 Prediction of the Phosphorylation Sites in GLUT4

Phosphorylation prediction programs have become available since the advent of bioinformatics. The NetPhos 2.0 server predicts serine, threonine and tyrosine phosphorylation sites in eukaryotic proteins (Blom *et al.*, 1999). NetPhos 2.0 was used to predict the phosphorylation sites in GLUT4 (Table 4.1). Numerous phosphorylation sites were predicted in GLUT4. The potential phosphorylation sites would most likely be localised in the cytoplasmic regions

of the transporter (highlighted in blue) since they would be accessible to cytoplasmic protein kinases. However, it could not be ruled out that phosphorylation could occur in extracellular regions of GLUT4 as these regions are intra-luminal in the recycling vesicles. Kinases inside these vesicles could then phosphorylate GLUT4 (highlighted in red). The potential phosphorylation sites included the two residues of interest, serine 488, which was the residue identified by Lawrence *et al* (Lawrence, Jr. et al., 1990a), and serine 10, which was the predicted second phosphorylation site.

4.2.2 Prediction of Possible GLUT4 Kinase(s)

In addition to predicting phosphorylation sites, it is also possible to predict the kinase responsible for phosphorylation. The NetPhosK 1.0 Server was used to predict the kinase (Table 4.2) (Blom *et al.*, 2004). Currently, NetPhosK covers the following kinases: PKA, PKC, PKG, CKII, Cdc2, CaM-II, ATM, DNA PK, Cdk5, p38 MAPK, GSK3, CKI, PKB, RSK, INSR, EGFR and Src. The kinases identified were those above the threshold value of 0.5 (values were in the range of 0.1 – 1.0). The predicted kinase(s) responsible for phosphorylation at serine 10 and serine 488 were CKII and PKA, respectively. GLUT4 had previously been shown to be a substrate for PKA (Lawrence, Jr. *et al.*, 1990a) and CKII was predicted as a candidate for the serine 10 kinase due to the acidic cluster at the N-terminus of GLUT4.

A)

Serine Phosphorylation Predictions			
Site	Sequence	Score	Region
3	--MPSGFQQ	0.003	C
10	QQIGSEDGE	0.263	C
30	LAVFSAVLG	0.005	TM
35	AVLGSLQFG	0.011	TM
55	VIEQSYNAT	0.042	E
71	GGPDSIPQG	0.253	E
84	LWALSVAIF	0.016	TM
89	VAIFSVGGM	0.092	TM
95	GGMISSFLI	0.002	TM
96	GMISSFLIG	0.002	TM
103	IGIISQWLG	0.003	C
134	NAAASYEIL	0.874	E
149	IGAYSGLTS	0.008	TM
153	SGLTSGLVP	0.020	TM
194	LGLESMLGT	0.041	E
226	FCPESPRYL	0.724	C
243	PARKSLKRL	0.997	C
254	WADVSDALA	0.015	C
274	ERPLSLLQL	0.948	C
281	QLLGSRTHR	0.006	C
297	VLQLSQQLS	0.009	TM
301	SQQLSGINA	0.600	TM
310	VFYYSTSIF	0.054	E
312	YYSTSIFEL	0.285	E
340	FTLVSVLLV	0.003	TM
379	ERVPSMSYV	0.342	E
381	VPSMSYVSI	0.932	E
384	MSYVSIVAI	0.488	E
412	AELFSQGPR	0.026	C
426	VAGFSNWTC	0.002	TM
480	FDQISATFR	0.204	C
488	RRTPSLLEQ	0.993	C
497	EVKPSTELE	0.775	C

B)

Threonine Phosphorylation Predictions			
Size	Sequence	Score	Region
21	QQRVTGTLV	0.075	C
23	RVTGTLVLA	0.515	C
59	SYNATWLGR	0.014	E
76	IPQGTLTTL	0.134	E
78	QGTLTTLWA	0.190	E
79	GTLTTLWAL	0.134	E
152	YSGLTSGLV	0.450	TM
166	EIAPTHLRG	0.033	C
174	GALGTLNQL	0.073	TM
198	SMLGTATLW	0.021	E
200	LGTATLWPL	0.211	E
209	LLAITVLPA	0.029	TM
248	LKRLTGWAD	0.300	C
283	LGSRTHRQP	0.433	C
311	FYYSTSIFE	0.030	E
326	PAYATIGAG	0.181	TM
334	GVVNTVFTL	0.093	TM
337	NTVFTLVSV	0.471	TM
351	AGRRTLHLL	0.370	C
368	AILMTVALL	0.013	TM
429	FSNWTCNFI	0.003	TM
464	FFIFTFLRV	0.036	TM
471	RVPETRGRT	0.489	C
475	TRGRTFDQI	0.089	C
482	QISATFRRT	0.367	C
486	TFRRTPSLL	0.760	C
498	VKPSTELEY	0.241	C

C)

Tyrosine Phosphorylation Predictions			
Size	Sequence	Score	Region
40	LQFGYNIGV	0.015	TM
56	**IEQSYNATW**	**0.221**	**E**
135	**AAASYEILI**	**0.156**	**E**
148	LIGAYSGLT	0.010	TM
159	LVPMYVGEI	0.016	TM
229	**ESPRYLYII**	**0.709**	**C**
231	**PRYLYIIRN**	**0.109**	**C**
308	NAVFYYSTS	0.072	TM
309	**AVFYYSTSI**	**0.022**	**E**
324	EQPAYATIG	0.974	TM
382	**PSMSYVSIV**	**0.579**	**E**
440	**MGFQYVADA**	**0.309**	**E**
448	AMGPYVFLL	0.778	TM
502	**TELEYLGPD**	**0.814**	**C**

Table 4.1 **Potential GLUT4 phosphorylation sites predicted using a phosphorylation prediction program.** Phosphorylation sites have been predicted using the NetPhos 2.0 Server (Blom *et al.*, 1999). Phosphorylation sites at serine (A), threonine (B) and tyrosine (C) residues are given. The predicted phosphorylation sites are shown, along with the sequence surrounding the residue. The output scores (value in the range [0.000-1.000]) are tabulated. The higher the number, the more confidence there is that phosphorylation occurs at the said site. The position of the residues in GLUT4 are also given; C = cytoplasmic (blue), TM = transmembrane, E = extracellular (red).

Site	Kinase (Score)
S-3	PKA (0.51)
S-10	CKII (0.60)
T-21	PKA (0.63)
S-35	PKA (0.52)
S-55	PKC (0.51)
T-59	PKC (0.58)
T-79	PKC(0.51)
S-84	PKC (0.51)
S-89	CKI (0.56)
S-96	cdc2 (0.54)
S-103	DNAPK (0.61), ATM (0.56)
T-152	PKC (0.59)
T-166	cdc2 (0.57)
T-209	cdc2 (0.57)
S-226	p38MAPK (0.52), GSK3 (0.52), Cdk5 (0.64)
Y-229	EGFR (0.51)
S-243	PKC (0.85), PKA (0.81)
S-254	CKII (0.62)
S-274	RSK (0.54), PKB (0.50), PKA (0.84)
S-281	PKC (0.51), cdc2 (0.56)
T-283	PKC
S-297	DNAPK (0.60), ATM (0.57)
S-312	CKII (0.52)
T-351	PKA (0.80)
T-368	PKA (0.60)
S-379	PKA (0.54)
S-381	cdc2 (0.51)
S-412	DNAPK (0.50)
T-464	CKI (0.50), PKC (0.71)
S-480	cdc2 (0.51)
T-482	PKC (0.92)
T-486	p38MAPK (0.52)
S-488	RSK (0.53), PKA (0.81)
S-497	CKII (0.52), PKA (0.63)
T-498	CKII (0.55)

Table 4.2 **Potential kinases involved in phosphorylating GLUT4 at the predicted phosphorylation sites.** Kinases have been predicted using the NetPhosK Server 1.0 (Blom *et al.*, 2004). The predicted kinases are given alongside the site of phosphorylation and the score (above the threshold score of 0.5). The higher the score the more confidence there is in the kinase phosphorylating the said site.

4.2.3 Phosphorylation of Full Length GLUT4 in Adipocytes and Cardiomyocytes

Adipocyte and cardiomyocyte cells were labelled with radioactive inorganic phosphate [$^{32}P_i$]. Following the labelling, GLUT4 was immunoprecipitated from the cell lysate. The GLUT4 was run on a SDS-PAGE gel and transferred to nitrocellulose. The ^{32}P signal on the nitrocellulose was detected on a PhosphoImager [FU], after exposure on an imaging plate [FU]. In adipocytes, the ^{32}P was recovered as a single species of 45 kDa (Figure 4.2 a). Western blot analysis identified the GLUT4 band by use of the anti-C-terminal GLUT4 antibody raised in sheep (described in chapter 3). The band corresponding to GLUT4 was also detected at 45 kDa in adipocytes (Figure 4.2 b). Thus, GLUT4 was phosphorylated in adipocytes. The same was true with the cardiomyocytes. The ^{32}P was recovered as a single species of 43 kDa (Figure 4.2 c). The band corresponding to GLUT4 was also detected at 43 kDa in cardiomyocytes (figs 4.2 d). This was the first evidence that GLUT4 was phosphorylated in cardiomyocytes.

4.2.4 Identification of Phosphorylation Sites in GLUT4

4.2.4.1 Cleavage using Cyanogen Bromide

Cyanogen bromide (CNBr) cleaves proteins on the C-terminal side of methionine residues and it is often used to map proteins immobilised onto membranes (Luo *et al.*, 1991). In the GLUT4 protein there are 12 methionine residues, including the initiation methionine. On cleavage with CNBr, 13 peptides would be generated (Table 4.3). The predicted size of the N- and C-terminal peptides, which include serine 10 and serine 488, would be 9.5 kDa and 7.4 kDa, respectively.

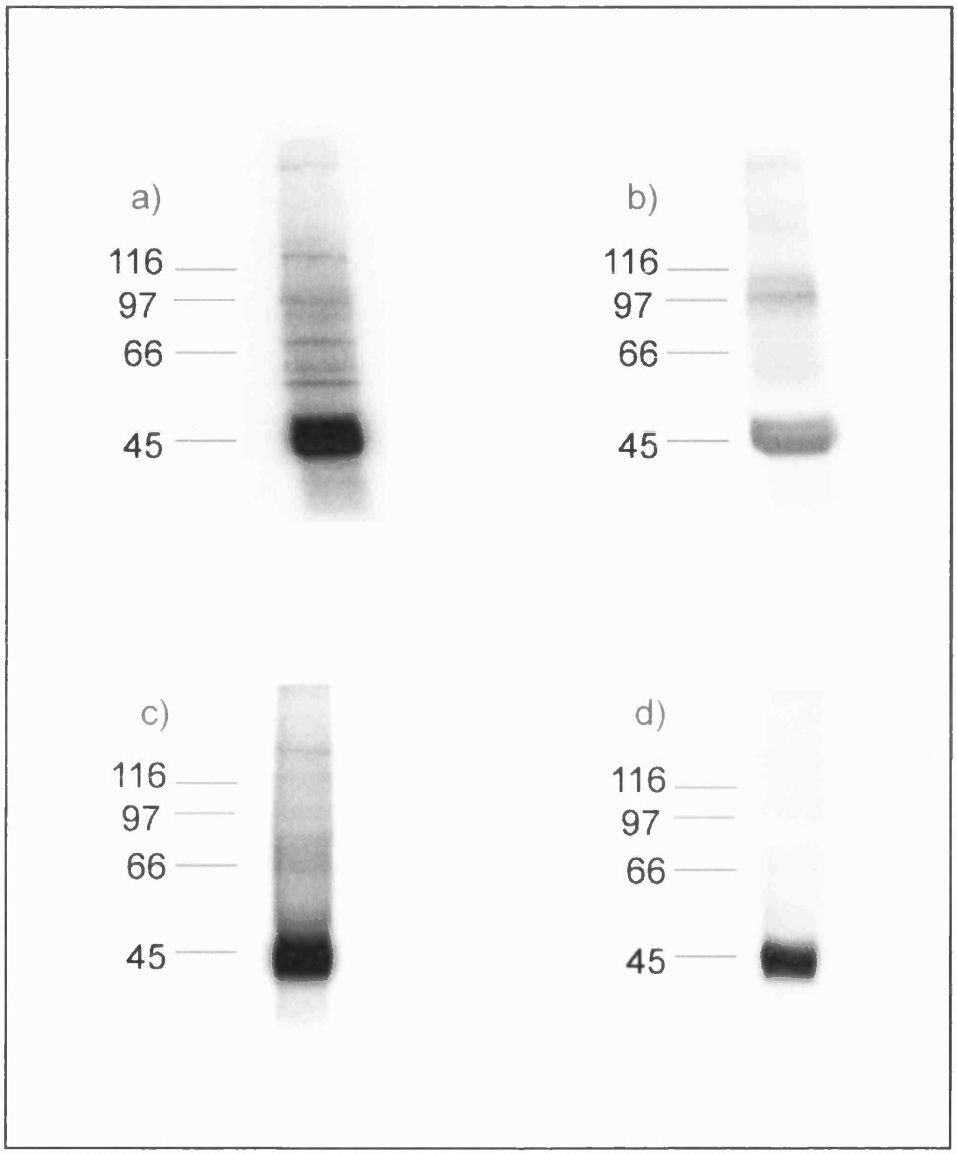

Figure 4.2 **Full length GLUT4 was phosphorylated in both adipocyte and cardiomyocyte cells.** Adipocyte (a and b) and cardiomyocyte (c and d) cells were labelled with [$^{32}P_i$]. GLUT4 was immunoprecipitated from the cell lysate. After SDS-PAGE, autoradiography detected any ^{32}P incorporated into GLUT4 (a and c). The anti-C-terminal GLUT4 antibody, raised in sheep, was used to detect the GLUT4 protein by Western blot analysis (b and d).

Residue Number	Molecular Weight	Peptide Sequence
1	131	m
2 – 93	9523	psgfqqigsedgeppqqrvtgtlvlavfsavlgslqfgynigvinap qkvieqsynatwlgrqgpggpdsipqgtlttlwalsvaifsvggm
94 – 112	2128	lssfligiisqwlgrkram
113 – 126	1308	lannvlavlggalm
127 - 158	3191	glanaaasyeililgrfligaysgltsglvpm
159 - 195	3782	yvgeiapthlrgalgtlnqlaivigilvaqvlglesm
196 – 360	18125	lgtatlwpllaitvlpallqllllpfcpesprylyiirnlegparkslkrltg wadvsdalaelkdekrklererplslllqllgsrthrqpliiavvlqlsq qlsginavfyystsifelagveqpayatigagvvntvftlvsvllvera grrtlhllglagm
361 – 367	662	cgcailm
368 – 380	1394	tvalllllervpsm
381 – 420	4280	avagfsnwtcnfivgm
421 – 436	1669	gfqyvadam
437 – 445	953	syvsivaifgfvaffeigpgpipwfivaelfsqgprpaam
446 – 509	7396	gpyvfllfavlllgffiftflrvpetrgrtfdqisatfrrtpslleqevkpstel eylgpdend

Table 4.3 **The predicted sequence and size of the peptides generated after GLUT4 had been cleaved with Cyanogen Bromide.** Cleavage was predicted using the PeptideCutter tool on the ExPASy server (Gasteiger *et al.*, 2003). The residues in red are found in the intracellular regions of GLUT4. The residues in blue are transmembrane residues and the green residues are found in the extracellular regions of GLUT4.

4.2.4.1.1 CNBr Cleavage of GLUT4 in Primary Adipocytes

Dr Françoise Koumanov carried out the preliminary experiments in which adipocytes were labelled with [$^{32}P_i$] and the GLUT4 phosphorylation sites were mapped by cleaving GLUT4 with CNBr. The experiment used the method essentially carried out by Lawrence and colleagues (Lawrence, Jr. *et al.*, 1990a). The cells were labelled with [$^{32}P_i$]. GLUT4 was immunoprecipitated from the cell lysate and subjected to tris-glycine SDS-PAGE. The GLUT4 was excised from the gel and was cleaved with CNBr. The cleaved fragments were resolved on a tris-tricine SDS-PAGE gel and transferred to nitrocellulose. Autoradiography detected the bands that contained radioactivity. The peptides that contained serine 10 and serine 488 were detected by Western blot analysis. The rabbit anti-pSer^{10} antibody purified from the second bleed serum (chapter 3) was used to detect the N-terminal peptide. The Western blot was then stripped and reprobed. The C-terminal peptide was detected by use of the monoclonal anti-C-terminal GLUT4 antibody.

The majority of radiolabelled GLUT4 derived peptides were resolved in one major radioactive fragment at 10 kDa (Figure 4.3 b). However, there were also five weaker bands that contained ^{32}P (arrows on Figure 4.3 b). When comparing the molecular weight of the ^{32}P bands on the ^{32}P scan with the predicted weights of the cleaved peptides (Table 4.3), the peptide closest in weight to 10 kDa is the 9.5 kDa N-terminal peptide (residues 2 – 93). In comparison, the C-terminal peptide (residues 446 – 509) is predicted to be 7.4 kDa. Both of these peptides contain a predicted phosphorylation site, serine 10 or serine 488. Contrary to the molecular weight of the peptide, Western blot analysis with the anti-C-terminal antibody identified the strongly phosphorylated band at 10 kDa to be the peptide at the C-terminus of GLUT4 (Figure 4.3 a). Thus, the peptide that included the serine 488 residue was phosphorylated. Western blot analysis with the anti-pSer^{10} antibody identified many bands, although, none of the bands were of high intensity in the region of interest (Figure 4.3 c). Strong bands were identified at the top of the

nitrocellulose at 30 and 34 kDa. The bands at 30 and 34 kDa could contain the N-terminus of GLUT4 or the bands could contain IgG which was identified by the secondary antibody. The presence of IgG could not be ruled out because a secondary antibody control was not carried out. This would have identified any non-specific IgG bands. However, using Table 4.3 to take into account missed cleavage sites, no peptides would have been produced at either 30 or 34 kDa that would have included the N-terminal peptide. A peptide with six missed cleavage sites would have a molecular weight of 20 kDa and a peptide with seven missed cleavage sites would have a molecular weight of 38 kDa. Thus the bands at 30 kDa or 34 kDa could not have been due to any missed cleavage sites in GLUT4. It seems likely that the strong band was due to IgG as the antibodies used in the immunoprecipitation and in the N-terminal peptide Western blot analysis were raised in the same species (rabbit). The sheep antibodies were not available for use at this point. Therefore any IgG that had been eluted after the immunoprecipitation and had been carried though the procedure would have been detected strongly by the anti-rabbit secondary antibody in the Western blot analysis. This gave a good example of the need to raise an antibody to the N-terminus of GLUT4 in sheep. The bands were not identified in the C-terminal peptide blot because an anti-mouse secondary antibody was used, which did not detect the rabbit IgG. The anti-pSer^{10} antibody recognised weak bands at 5, 7, 10, 17 and 25 kDa in the area of interest. Bands at 10, 17 and 25 kDa were also detected on the ^{32}P scan. However, the bands on the Western blot were weak. This was because the anti-pSer^{10} antibody was very weak (chapter 3), and so it was difficult to identify which band corresponded to the N-terminal peptide of GLUT4. The band at 10 kDa, which was the predicted weight of the N-terminal peptide, was resolved at the same molecular weight as the C-terminal peptide. This would suggest that the N-terminal and the C-terminal peptides may be running at the same molecular weight, in which case the N-terminal peptide could also be phosphorylated. However, the anti-pSer^{10} antibody could be cross reacting with the C-terminal peptide which would provide an explanation as to why the

peptides were running at the same molecular weight. Further investigation was therefore needed to investigate whether the bands identified by the anti-pSer[10] antibody were real and were those of the N-terminal peptide.

4.2.4.1.2 CNBr Cleavage of GLUT4 in 3T3-L1 Adipocytes on Day 5 of Differentiation

Dr Françoise Koumanov carried out [$^{32}P_i$] labelling and CNBr cleavage of GLUT4 in 3T3-L1 adipocytes on day 5 of differentiation. Day 5 of differentiation was chosen because a confocal microscopy study with the anti-pSer[10] antibody had identified an intracellular protein at day 5 and this suggested that the phosphorylation of GLUT4 could be involved in the GLUT4 synthetic pathway (Section 3.2.1.5). The cells were labelled with [$^{32}P_i$]. GLUT4 was then immunoprecipitated from the cell lysate. The GLUT4 was transferred to PVDF membrane after the GLUT4 had been subjected to SDS-PAGE. The PVDF membrane was cut to excise the region around GLUT4. CNBr was used to cleave the GLUT4 on the PVDF membrane. The cleaved GLUT4 was subjected to tris-tricine SDS-PAGE and transferred to nitrocellulose. Autoradiography of the nitrocellulose detected the radioactive bands. Western blot analysis, carried out with the anti-pSer[10] antibody, purified from the final bleed serum from rabbit (on the phospho and PAN specific peptides) (chapter 3), and the mouse monoclonal anti-C-terminal GLUT4 antibody, identified the N- and C-terminal peptides, respectively. The blot was stripped between the probing with the two antibodies.

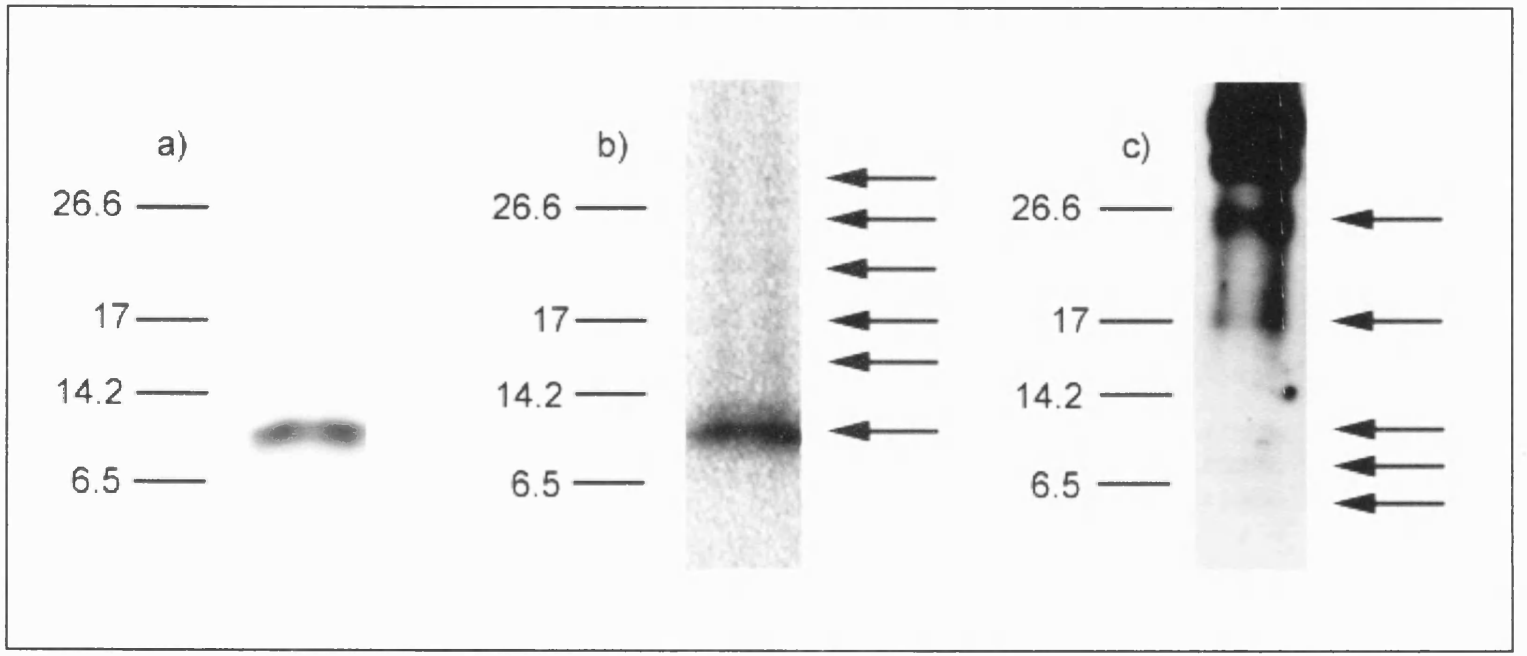

Figure 4.3 **Identification of the phosphorylation sites in GLUT4 from rat adipocytes.** Primary adipocyte cells were labelled with [$^{32}P_i$]. GLUT4 was immunoprecipitated from the cell lysate and subjected to SDS-PAGE. The GLUT4 was sliced from the gel and cleaved with CNBr. The CNBr fragments were subjected to tris-tricine SDS-PAGE and transferred to nitrocellulose. Autoradiography was carried out on the nitrocellulose (b). The fragments that contained the C-terminal and N-terminal peptides were detected by Western blot analysis, (a) and (c) respectively. Arrows indicate the bands identified in (b) and (c). Images were kindly supplied by Dr Françoise Koumanov.

Cleaving the GLUT4 isolated from 3T3-L1 adipocytes at day 5 of differentiation, resulted in two bands being identified that contained ^{32}P, one at 7 kDa and the other at 4 kDa (Figure 4.4 b). Following Western blot analysis, the C-terminal peptide was identified at 9 kDa (Figure 4.4 a). The N-terminal antibody identified two bands, one band had a molecular weight of 7 kDa and the second, stronger, band had a molecular weight of 5 kDa (Figure 4.4 c). The 7 kDa band was the same molecular weight as the upper band on the ^{32}P scan suggesting that the upper band on the ^{32}P scan contained the GLUT4 N-terminal peptide. However, neither the stronger N-terminal band nor the C-terminal band corresponded to the lower, ^{32}P-containing 4 kDa band. The fact that the lower N-terminal peptide fragment did not contain ^{32}P was a concern. This could suggest that one of the bands from the Western blot analysis was not the N-terminal peptide. The fact that the upper, 7 kDa fragment, is closest in molecular weight to the predicted weight of 9 kDa would suggest that the upper band is the N-terminal band and that this band is phosphorylated. Another concern was that the molecular weight of the GLUT4 C-terminal peptide, as identified by Western blot analysis, did not correspond to a ^{32}P-containing band, even though phosphorylation had previously been identified in the C-terminal peptide (Lawrence, Jr. *et al.*, 1990a).

In an attempt to further resolve the N- and C-terminal phosphorylation sites, alternative cleavage strategies were then investigated which were aimed at giving a clearer distinction between the two fragments.

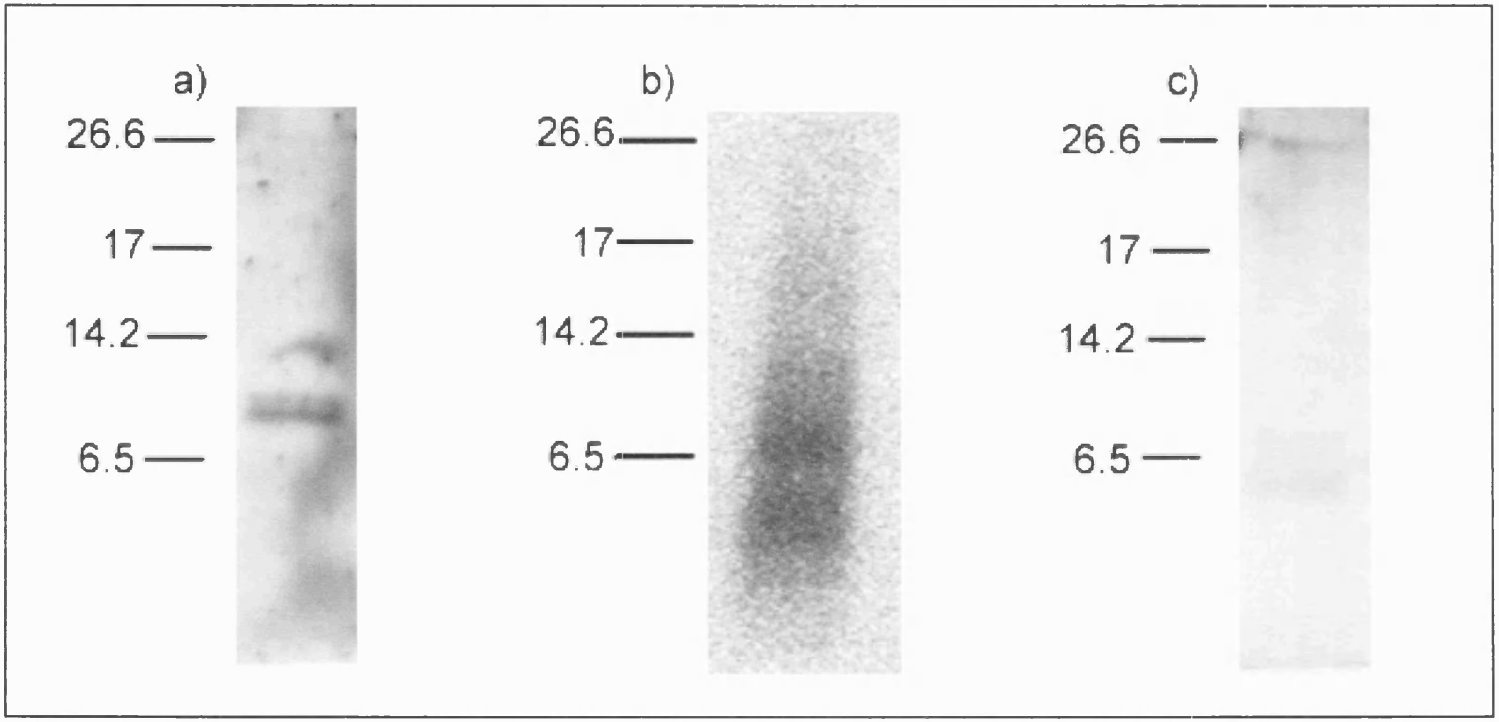

Figure 4.4 **Identification of the phosphorylation sites in GLUT4 from 3T3-L1 adipocytes.** 3T3-L1 adipocyte cells at day 5 of differentiation were labelled with [$^{32}P_i$]. GLUT4 was immunoprecipitated from the cell lysate and subjected to SDS-PAGE. The gel was transferred to PVDF membrane. The membrane was cut around the GLUT4 region and cleaved with CNBr. The CNBr fragments were subjected to tris-tricine SDS-PAGE and transferred to nitrocellulose. Autoradiography was carried out on the nitrocellulose (b). The fragments that contained the C-terminal and N-terminal peptides were detected by Western blot analysis, (a) and (c) respectively. Images were kindly supplied by Dr Françoise Koumanov.

4.2.4.2 Cleavage using Endoproteinase Lys C

Endoproteinase Lys C (Endo LysC) is an enzyme that cleaves at the C-terminal side of lysine residues. GLUT4 has 8 lysine residues so on cleavage 9 peptides will be generated (Table 4.4). The predicted size of the N- and C-terminal peptides, which would include serine 10 and serine 488, would be 5.2 kDa and 25.1 kDa, respectively. In theory this would give a good alternative to the use of CNBr as the predicted bands should be more easily resolved. The use of Endo LysC, as an alternative to CNBr, was tested to ensure that the N- and C- terminal peptides could be detected. GLUT4 was immunoprecipitated from an adipocyte cell lysate using the anti-C-terminal GLUT4 antibody raised in rabbit. Following elution with 25 mM Tris-Cl, 1 mM EDTA, 0.5% (w/v) SDS, pH 8.5, the sample was split into two. One of these samples was digested with Endo LysC. The other sample was a control in which no enzyme was used. No protease inhibitors were added in the reaction because the Endo LysC enzyme would be inhibited. The control was essential as it ensured that the cleavage was due to the specific action of the enzyme and not due to proteolysis during the reaction incubation. After the incubation, the samples were again split into two. The samples were subjected to SDS-PAGE, either on a tris-tricine gel for the digested samples or a tris-glycine gel for the undigested samples. The gels were transferred to nitrocellulose. Western blot analysis with the mouse monoclonal anti-C-terminal GLUT4 antibody and the sheep anti-pSer^{10} antibody identified the C- and N- terminal peptides of interest (Figure 4.5). Full length GLUT4 was identified by both the anti-pSer^{10} (Figure 4.5 a) and the anti-C-terminal GLUT4 antibodies (Figure 4.5 b) in both of the control, uncleaved, samples. After digestion with Endo LysC, the C-terminal peptide was identified as being at 23 kDa (Figure 4.5 d) and the N-terminal peptide was identified at 5 kDa (Figure 4.5 c). This gave a good correlation to the predicted molecular weights of 25.1 and 5.2 kDa, respectively. The 17 kDa band was identified as IgG due to the interaction of the band with non-immune IgG (result not shown).

Residue Number	Molecular Weight	Peptide Sequence
1 – 50	5246	mpsgfqqigsedgeppqqrvtgtlvlavfsavlgslqfgynigvinapqk
51 – 109	6274	vieqsynatwlgrqgpggpdsipqgtlttlwalsvaifsvggmissfligiis qwlgrk
110 – 242	13996	ramlannvlavlggalmglanaaasyeililgrfligaysgltsglvpmyvg eiapthlrgalgtlnqlaivigilvaqvlglesmlgtatlwpllaitvlpallqllllp fcpesprylyiirnlegpark
243 - 245	347	slk
246 – 261	1745	rltgwadvsdalaelk
262 – 264	391	dek
265 - 266	303	rk
267- 495	25132	lererplslllqllgsrthrqpliiavvlqlsqqlsginavfyystsifelagveqp ayatigagvvntvftlvsvllveragrrtlhllglagmcgcailmtvallllervp smsyvsivaifgfvaffeigpgpipwfivaelfsqgprpaamavagfsnw tcnfivgmgfqyvadamgpyvfllfavlllgffiftflrvpetrgrtfdqisatfrrt pslleqevk
496 - 509	1579	psteleylgpdend

Table 4.4 **Table showing the sequence and predicted size of the peptides produced after GLUT4 had been cleaved with Endo-LysC.** Cleavage was predicted using the PeptideCutter tool on the ExPASy server (Gasteiger *et al.*, 2003). The residues in red are found in the intracellular regions of GLUT4. The residues in blue are transmembrane residues and the green residues are found in the extracellular regions of GLUT4.

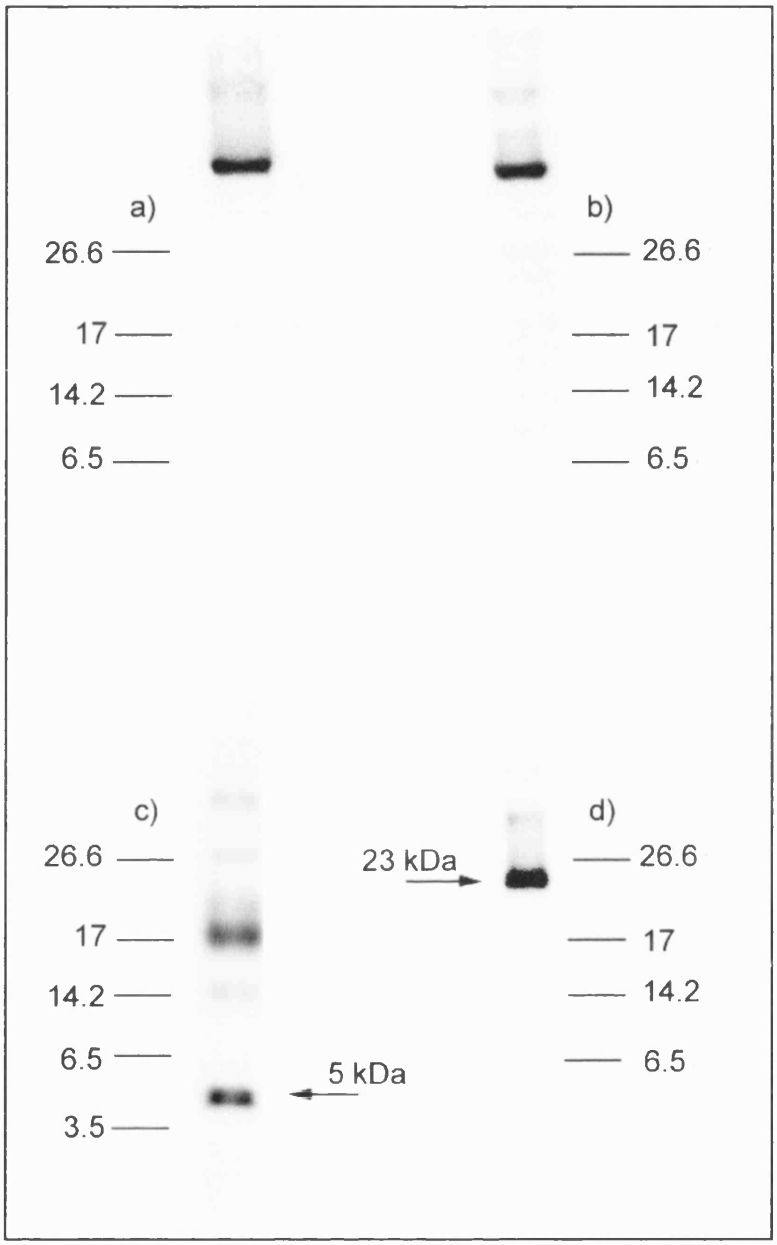

Figure 4.5 **Endo LysC digestion test.** GLUT4 was immunoprecipitated from an adipocyte cell lysate. The elution buffer used was 25 mM Tris-Cl, 1 mM EDTA, 0.5% (w/v) SDS, pH 8.5. GLUT4 was digested with Endo LysC. A control of no enzyme was also carried out. The peptides were resolved by SDS-PAGE. Following electrophoretic transfer to nitrocellulose, Western blot analysis identified the N- (a and c) and C-terminal fragments (b and d) in both uncleaved (a and b) and cleaved (c and d) samples.

4.2.4.2.1 Identification of the Phosphorylation Sites in Adipocytes and Cardiomyocytes

As the N- and C- terminal peptides were well resolved following Endo LysC cleavage, the sites of phosphorylation were investigated in GLUT4 isolated from adipocyte and cardiomyocyte cells.

Adipocyte and cardiomyocyte cells were labelled with [$^{32}P_i$] and lysed in their respective lysis buffers. GLUT4 was cleaved with Endo LysC, as above, and run on tris-tricine SDS-PAGE gels and transferred to nitrocellulose. The nitrocellulose was exposed on a phospho screen for 2 – 4 days before monitoring the radioactivity on the PhosphoImager. Western blot analysis involving the use of the sheep anti-pSer^{10} antibody and the mouse monoclonal anti-C-terminal antibody led to the detection of the N- and C-terminal peptides, respectively. The blots were not stripped between the probing with the two antibodies. This prevented any loss of signal due to the stripping process. Stripping was not necessary because the peptides were well resolved on the gel. Prior to the Western blot analysis using the primary antibodies, a control experiment was carried out in which the secondary antibodies, both anti-sheep and anti-mouse, were independently incubated with the nitrocellulose. The control experiment would identify any bands that were due to a non-specific interaction with non-immune IgG that would also be identified following the Western blot analysis with the anti-GLUT4 antibodies.

Autoradiography detected two phosphorylated peptides in GLUT4 isolated from adipocytes, at 23.6 kDa and 5.0 kDa (Figure 4.6 b). The peptides could be identified by comparison with the predicted molecular weight of the cleaved peptides (Table 4.4). The 23.6 kDa peptide would be the C-terminal peptide (residues 267 – 495) as it is the peptide with a molecular weight nearest to 25 kDa. By comparison with Table 4.4, two peptides could account for the lower ^{32}P-containing band. Peptide 1 – 50 and peptide 51 – 109 would theoretically be 5.2 and 6.3 kDa respectively. The molecular weight of lower ^{32}P-containing

band in adipocytes corresponded exactly to the predicted molecular weight for peptide 1 – 50. The identities of the peptides were further confirmed by Western blot analysis. The C-terminal peptide was identified as a 23.6 kDa band in adipocytes (Figure 4.6 a). The upper ^{32}P-containing band therefore corresponded to peptide 267 – 495 from GLUT4. The peptide identified by the anti-pSer^{10} antibody was detected at 5.0 kDa in adipocytes (Figure 4.6 c). The molecular weight of the lower ^{32}P-containing band corresponded to the molecular weight of the N-terminal peptide 1 – 50. Phosphorylation had been identified in two GLUT4 peptides; peptide 1 – 50 and peptide 267 – 495. The anti-pSer^{10} and anti-C-terminal antibodies had a specific interaction with the ^{32}P-containing bands as no interaction was observed between the 23.6 and 5 kDa bands and non-immune IgG (result not shown).

Two peptides containing ^{32}P were identified, by autoradiography, from GLUT4 isolated from cardiomyocytes. The two peptides had molecular weights of 28.0 kDa and 6.2 kDa (Figure 4.7 b). As in adipocytes, comparison with the predicted molecular weight of the peptides (Table 4.4) led to the identification of the 28 kDa band as being the 267 – 495 C-terminal peptide. Western blot analysis with the anti-C-terminal GLUT4 antibody detected the C-terminal peptide at 26.6 kDa. Thus providing further evidence that the phosphorylated peptide was the 267-495 C-terminal peptide (Figure 4.7 a). After comparison of the predicted peptide molecular weights, the 6.2 kDa band on the ^{32}P scan seemed to correspond more closely to peptide 51 – 109 (6.3 kDa) than peptide 1 – 50 (5.2 kDa). However, following comparison with the Western blot analysis, the N-terminal peptide was identified at 5.8 kDa (Figure 4.7 c). The lower band on the ^{32}P scan was therefore identified as peptide 1 – 50. Both of the peptides identified from the ^{32}P scan ran at slightly higher molecular weights than either the predicted molecular weights of the peptides or the weights of the peptides identified on the ^{32}P scan from GLUT4 isolated from adipocytes. This could have been due to the experimental differences in the running of the markers between experiments. The discrepancy between the

molecular weight of the peptides could also have occurred because the markers had to be manually labelled onto the image from the ^{32}P scan. A small error in the labelling of the markers would have resulted in a large difference in the calculated molecular weight of the peptides.

4.2.4.2.2 Missed Phosphorylation Sites

A comparison was carried out, in cardiomyocytes cells, to investigate whether the sum of the phosphorylation that was found in the two GLUT4 peptides following Endo LysC cleavage equalled the total phosphorylation that was detected in the uncleaved GLUT4 protein.

The intensity of the ^{32}P-containing bands on the ^{32}P scan was calculated in photostimulated luminescence (PSL) units. The intensity was calculated using the ImageGauge software [FU]. The intensity of the ^{32}P band from the uncleaved GLUT4 sample was calculated, along with the sum of the intensities of the ^{32}P-containing bands obtained following the Endo LysC cleavage of GLUT4. A background value was subtracted from each band. The background luminescence was taken as the average background above and below each phosphorylated band. The amount of GLUT4 (pmole) in each lane was also calculated. For a direct comparison between cleaved and uncleaved GLUT4, the intensity (PSL) / pmole of GLUT4 was calculated. Uncleaved GLUT4 had a value of 7576 intensity (PSL) / pmole and the sum of the cleaved GLUT4 bands had a value of 7445 intensity (PSL) / pmole (Table 4.5). Thus the intensity of the phosphorylated, uncleaved GLUT4 protein was the same as the sum of the intensity of the phosphorylated N- and C-terminal peptides. This experiment was only carried out once but it suggested that all of the phosphorylation sites in GLUT4 were localised in the N-terminal peptide (residues 1 – 50) and the C-terminal peptide (residues 267-495).

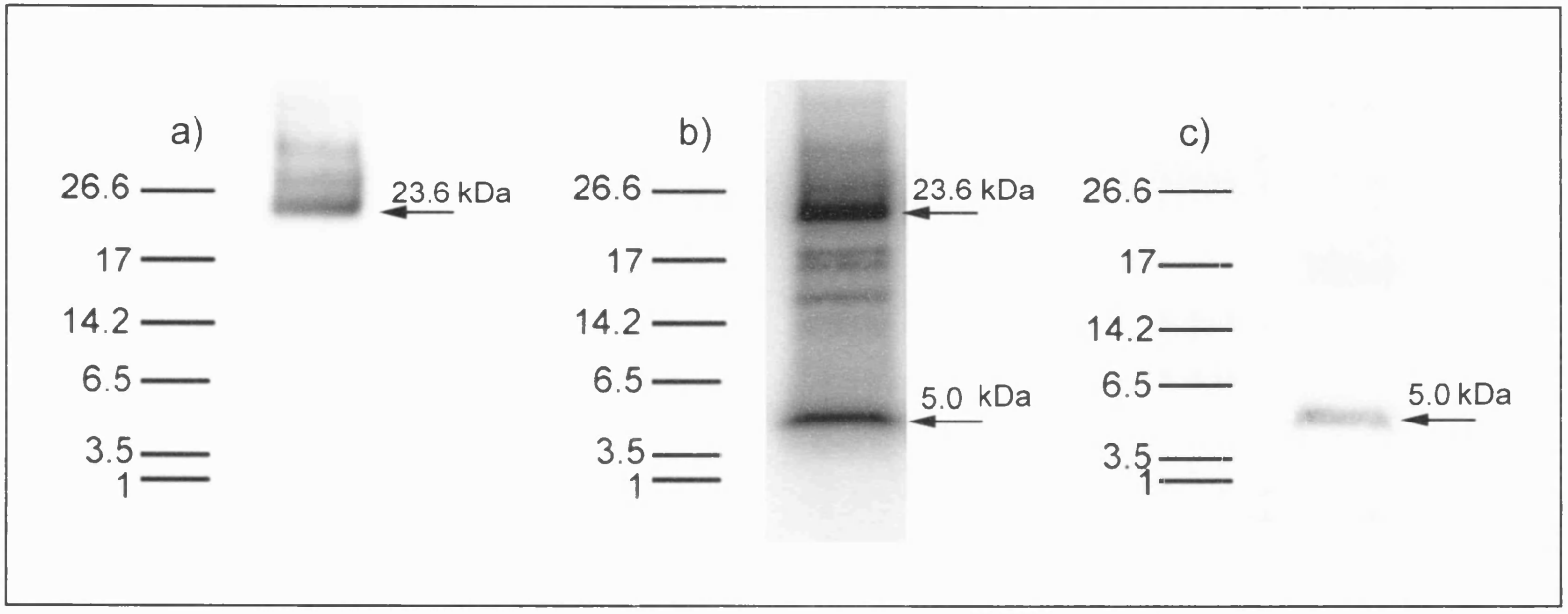

Figure 4.6 **The N- and C-terminal peptides are phosphorylated in primary adipocytes.** Primary adipocyte cells were labelled with [$^{32}P_i$]. GLUT4 was immunoprecipitated from the cell lysate and cleaved with Endo LysC. The fragments were subjected to tris-tricine SDS-PAGE and transferred to nitrocellulose. Autoradiography was carried out on the nitrocellulose (b). The fragments that contained the C-terminal and N-terminal peptides were detected by Western blot analysis, (a) and (c) respectively.

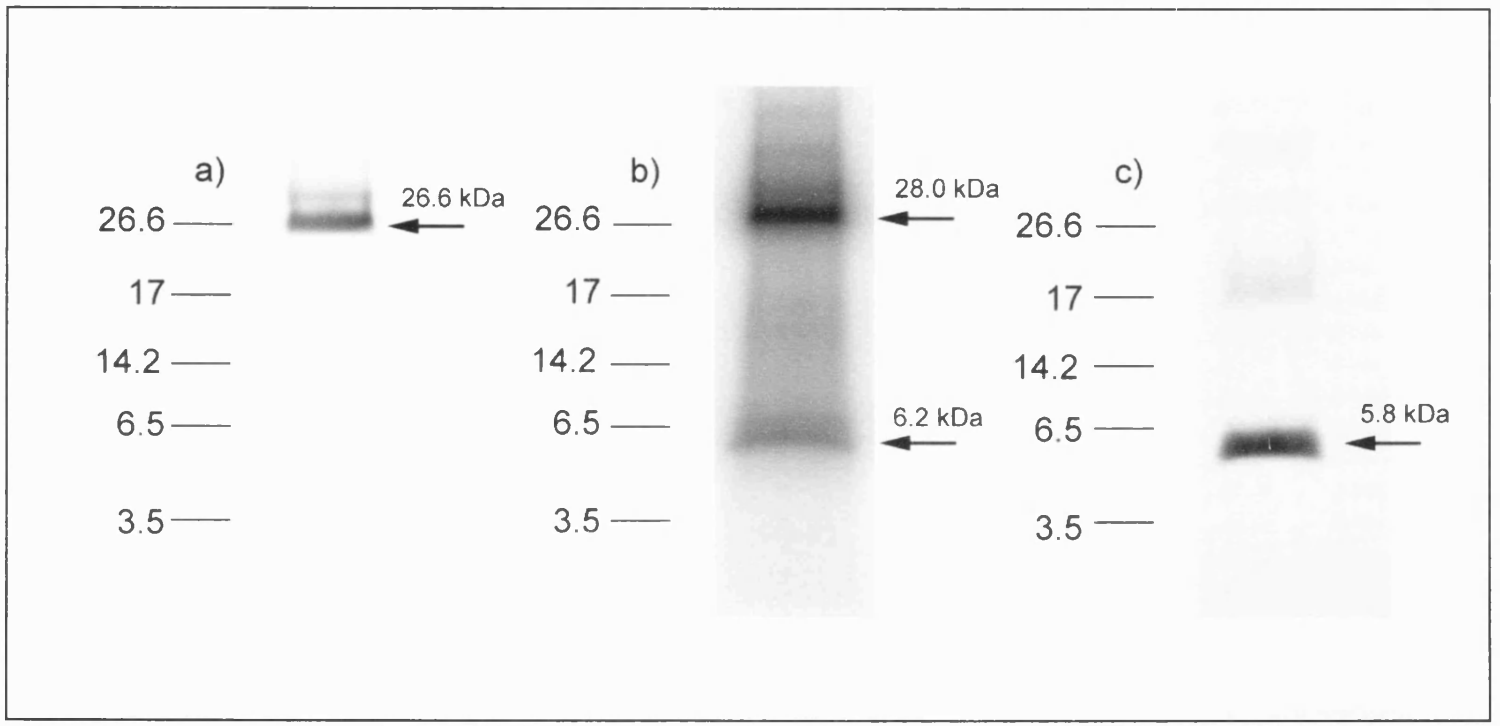

Figure 4.7 **The N- and C-terminal peptides are phosphorylated in cardiomyocytes.** Cardiomyocyte cells were labelled with [$^{32}P_i$]. GLUT4 was immunoprecipitated from the cell lysate and cleaved with Endo LysC. The fragments were subjected to tris-tricine SDS-PAGE and transferred to nitrocellulose. Autoradiography was carried out on the nitrocellulose (b). The fragments that contained the C-terminal and N-terminal peptides were detected by Western blot analysis, (a) and (c) respectively.

	Intensity (PSL) / Lane	GLUT4 (pmole)	PSL / pmole of GLUT4
Cleaved	36841.5	4.9	7444.5
Uncleaved	30697.2	4.1	7575.9

Table 4.5 **Identification of any missed phosphorylation sites.** The intensity (photostimulated luminescence (PSL)) of the phosphorylated band obtained from the uncleaved GLUT4 sample was compared to the sum of the intensities of the phosphorylated bands obtained from the cleaved GLUT4 sample. A background level of luminescence was subtracted from each band. To compare samples, the total GLUT4 was calculated per lane and the results were expressed as intensity (PSL) / GLUT4 (pmole).

4.2.4.2.3 The Effect of Insulin and Okadaic Acid on the Phosphorylation State of GLUT4 in Adipocytes

The effect both insulin and okadaic acid had on the phosphorylation state of GLUT4 was investigated. The method used was as described previously, except that the adipocytes were stimulated with either insulin or okadaic acid for 20 min (Table 2.7). The levels of phosphorylation under these two conditions were compared to the level of phosphorylation in the basal state (in which the cells had had no additional treatment).

Insulin increased the level of phosphorylation by 1.5-fold at the N-terminus and by 1.2-fold at the C-terminus of GLUT4. This increase was significant at both the N-terminus ($p = 0.0109$) and the C-terminus ($p = 0.0118$). Insulin, therefore, had a greater effect on the level of phosphorylation at the N-terminus of GLUT4 compared to the C-terminus (Figure 4.8 A). This was calculated from an average of 4 individual experiments.

Okadaic acid also increased the level of phosphorylation by 1.6-fold at the N-terminus and by 2.1-fold at the C-terminus of GLUT4 (Figure 4.8 B). The increase was greater than that seen by insulin. In contrast to insulin, okadaic acid had a greater effect on the level of phosphorylation at the C-terminus of GLUT4. An increase in phosphorylation would be expected as okadaic acid is a phosphatase inhibitor that inhibits PPI and PPIIa (Bialojan and Takai, 1988, Cohen et al., 1990). The action of PPI and PPIIa accounts for most of the phosphatase action in adipocytes and so inhibition of the phosphatase would result in an increase in phosphorylation. The result was only representative of one experiment, so the investigation of the effect of okadaic acid needs to be repeated to confirm the results.

4.2.4.2.4 Relative Levels of Phosphorylation at the N- and C- terminus of GLUT4 in Adipocytes

To compare the relative level of phosphorylation at each terminus, the percentage phosphorylation was calculated. This was compared to the total GLUT4 phosphorylation per condition, which was set to 100%. This form of analysis would give some indication as to the relative importance of each phosphorylation site in basal, insulin- and okadaic acid-stimulated adipocytes.

In the basal state, 56.0% of GLUT4 phosphorylation occurred at the C-terminus, with 44.0% of the phosphorylation at the N-terminus. This ratio changed following insulin stimulation to 49% of the total phosphorylation being at the C- terminus and 51% at the N-terminus (Figure 4.9 A). There was not a significant difference in the relative level of phosphorylation, at either terminus, following insulin stimulation, compared to the relative level of phosphorylation in the basal state. This was the mean of 4 independent experiments.

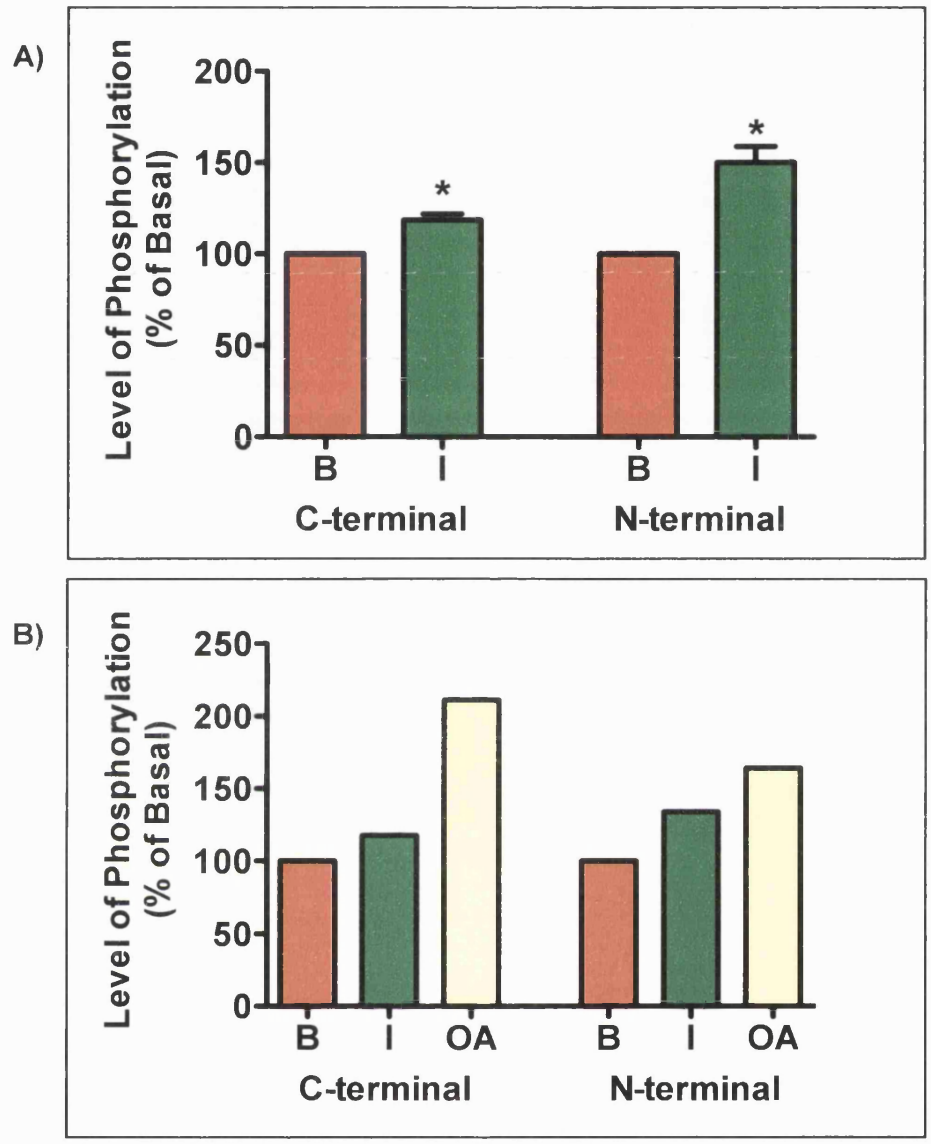

Figure 4.8 **Insulin and okadaic acid increased the level of phosphorylation at the N- and C-termini of GLUT4.** Adipocytes were labelled with [$^{32}P_i$] and treated for 20 min with insulin or for 20 min with okadaic acid. GLUT4 was immunoprecipitated and cleaved with Endo LysC. The level of phosphorylation was calculated as a percentage of basal phosphorylation. The data in A are the combined mean ± S.E.M from 4 independent experiments. *, $p<0.05$ (paired t-test; compared with the basal state). The data in B are from one experiment.

Treatment with okadaic acid resulted in 52.7% of the total phosphorylation occurring at the C-terminus of GLUT4 and 47.3% occurring at the N-terminus (Figure 4.9 B). This was the result from one individual experiment and needs to be repeated to obtain an averaged result. Okadaic acid did not significantly change the relative level of phosphorylation at either the N- or the C- terminus of GLUT4, compared to the relative level of phosphorylation in the basal state.

4.2.4.2.5 The Role of Casein Kinase II Inhibitors on the Phosphorylation State of GLUT4 Isolated From Adipocytes

The effect which two different casein kinase II inhibitors had on the level of GLUT4 phosphorylation was investigated. It was hoped that this would help to identify the kinase that was responsible for phosphorylating GLUT4 at serine 10 because CKII was predicted to be the kinase responsible for phosphorylating serine 10 (Table 4.2). Two different casein kinase II (CKII) inhibitors, 5,6-Dichloro-1-β-D-ribofuranosylbenzimidazole (DRB) and 4,5,6,7-Tetrabromobenzotriazole (TBB), were investigated. TBB is a specific CKII inhibitor while DRB inhibits CKII and to a lesser extent, inhibits CKI. CKII was the predicted kinase to phosphorylate serine 10, but Golgi casein kinase (G-CK) also has a consensus sequence similar to the serine 10 site (Pinna and Ruzzene, 1996) (Section 1.6.3.1). DRB was tested as it is not a specific CKII inhibitor and therefore may inhibit G-CK as well as CKII and CKI. Adipocyte cells were treated with the CKII inhibitors for 2 h during the [$^{32}P_i$] labelling (Table 2.7). Both inhibitors were tested on basal and insulin-stimulated adipocytes. TBB was also tested on adipocytes treated with insulin and isoproterenol.

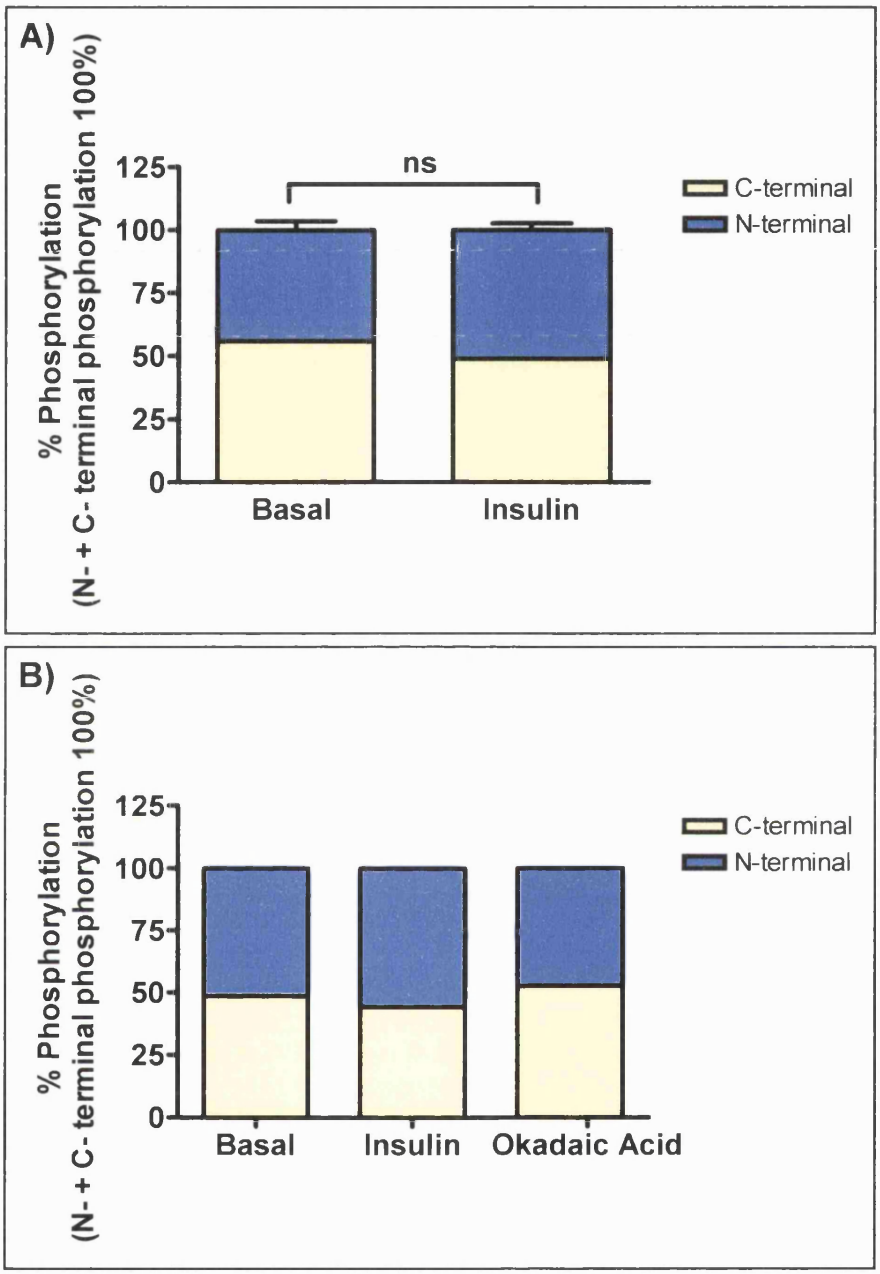

Figure 4.9 **Relative level of phosphorylation at the N- and C-terminus of GLUT4 in basal (A), insulin (A) and okadaic acid (B) stimulated adipocytes.** Total GLUT4 per lane was set to 100% and the percentage of this that was phosphorylated at each terminus was calculated. The data in A are the combined mean ± S.E.M. from 4 independent experiments. ns, $p>0.05$ (paired t-test; compared with the basal state). The data in B are from one experiment.

DRB did not have an effect on the level of phosphorylation at the C-terminus of GLUT4 in either basal or insulin-stimulated cells (Figure 4.10). This was expected because there was not a casein kinase phosphorylation site in the C-terminal peptide. There was also no difference in the level of phosphorylation at the N-terminus of GLUT4 in basal adipocytes. However, following DRB treatment, there was a slight decrease in the level of phosphorylation at the N-terminus of GLUT4 in insulin-stimulated adipocytes. The data is only from one experiment and so caution must be taken in this analysis. Therefore, if DRB did have an effect on the level of GLUT4 phosphorylation, even if it was small, it occurred at the N-terminus of GLUT4, which does contain a potential CKII phosphorylation site.

The effect TBB had on the level of phosphorylation at the N- and C- termini of GLUT4 was tested on basal, insulin and insulin + isoproterenol stimulated cells. The data from basal and insulin-stimulated cells were taken from two experiments and the data from insulin + isoproterenol stimulated cells was only representative of one experiment. The results from the two basal and insulin-stimulated adipocyte experiments were variable and so for this reason the individual data, as well as the mean value, were represented in Figure 4.11.

As reported in the previous experiments (Figure 4.8 A), insulin increased the level of phosphorylation, above the basal level of phosphorylation, at both the N- and C-termini of GLUT4. On average, TBB had no effect on the level of phosphorylation of GLUT4 at the C-terminus in basal adipocytes. However, when basal adipocytes were treated with TBB there was a decrease in the level of phosphorylation at the N-terminus of GLUT4. This would be expected as the predicted CKII site is at the N-terminus of GLUT4.

The effect TBB had on insulin-stimulated adipocytes was variable. At the C-terminus of GLUT4, TBB treatment resulted in an increase in the level of phosphorylation in experiment 1, but a decrease in the level of phosphorylation

in experiment 2, in GLUT4 isolated from insulin-stimulated adipocytes. Whereas, at the N-terminus of GLUT4, there was a small increase in the level of phosphorylation in experiment 1, but there was a large decrease in the level of phosphorylation in experiment 2, in GLUT4 isolated from insulin-stimulated adipocytes. It is therefore impossible to conclude whether TBB had an effect on the phosphorylation state of GLUT4.

GLUT4 isolated from isoproterenol treated insulin-stimulated adipocytes had a lower level of phosphorylation than GLUT4 isolated from insulin-stimulated adipocytes. The level of phosphorylation at the C-terminus was the same as the level of phosphorylation in basal adipocytes. Whereas, at the N-terminus of GLUT4, phosphorylation increased 10% in comparison to basal adipocytes (Figure 4.11 I and I + ISO). This did not agree with previous reports in which insulin and isoproterenol treatment led to a twofold increase in the level of phosphorylation of GLUT4 which was isolated from total membrane (James *et al.*, 1989a). TBB decreased the level of phosphorylation in insulin and isoproterenol stimulated adipocytes at the N-terminus of GLUT4. There was no effect on the level of phosphorylation at the C-terminus (Figure 4.11). This suggests that TBB had an effect at the N- but not the C-terminus of GLUT4. However, due to the variability, the experiments need to be repeated before a conclusion can be reached as to whether TBB has any effect on the phosphorylation state of GLUT4.

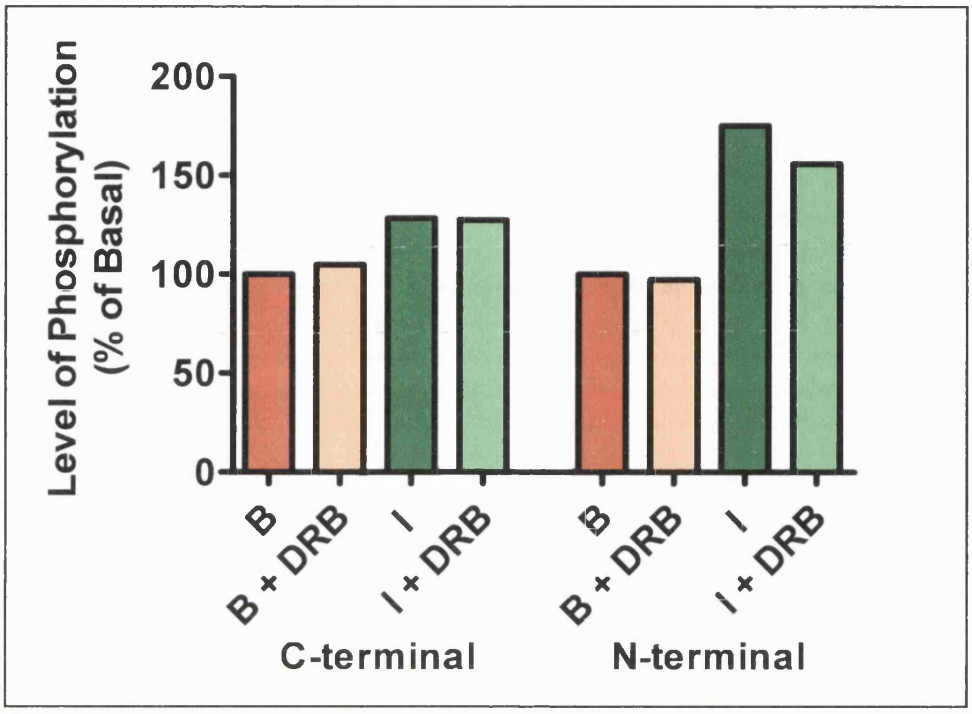

Figure 4.10 **The effect of DRB, a casein kinase II inhibitor, on the phosphorylation state of the N- and C-termini of GLUT4.** Adipocytes were labelled with [$^{32}P_i$] and treated for 20 min with insulin and/or for 2 h with DRB. GLUT4 was immunoprecipitated and cleaved with Endo LysC. The level of phosphorylation was calculated as a percentage of basal phosphorylation. The data are from one experiment.

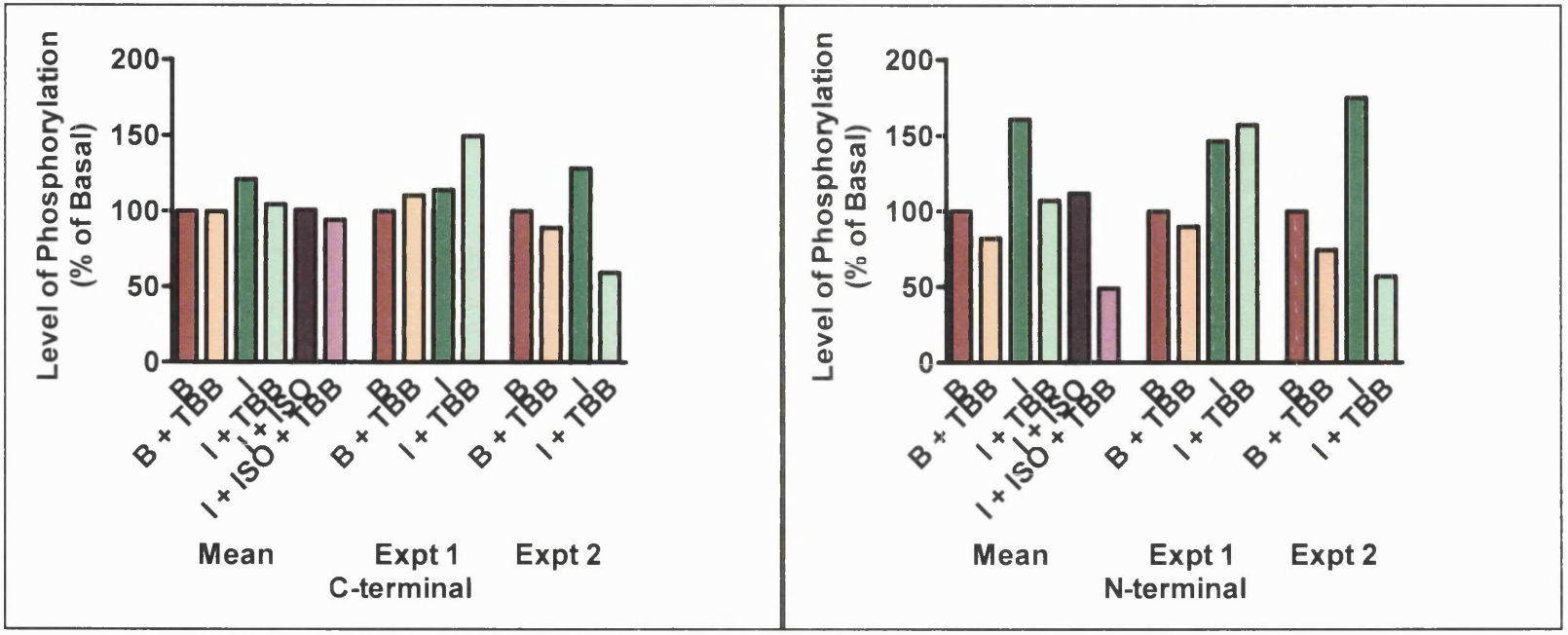

Figure 4.11 **The effect of TBB, a casein kinase II inhibitor, on the phosphorylation state of GLUT4 at the N- and C-termini.** Adipocytes were labelled with [$^{32}P_i$] and treated for 20 min with insulin, 10 min with isoproterenol and adenosine deaminase or for 2 h with TBB. GLUT4 was immunoprecipitated and cleaved with Endo LysC. The level of phosphorylation was calculated as a percentage of basal phosphorylation. Basal, Insulin ± TBB conditions were tested twice and insulin + isoproterenol ± TBB was carried out once. The mean of the experiments and the data from each of the individual experiments were plotted.

4.2.4.2.6 Level of Phosphorylation of GLUT4 in Adipocytes

To understand the relative importance of the phosphorylation at each site, it was imperative to calculate the stoichiometry of the GLUT4 phosphorylation. This gave a value for the number of moles of phosphate per mole of GLUT4. The level of phosphorylation was calculated for the whole (uncleaved) protein isolated from basal adipocytes. The level of phosphorylation at each site (serine 10 and serine 488) could then be calculated from the ratio of phosphorylation at each site (Section 4.2.4.2.4).

Rat adipocytes were labelled with [$^{32}P_i$] and an aliquot of cells was retained. GLUT4 was immunoprecipitated from the cell lysate of the remaining cells and split into two samples. The samples were run on a tris-glycine SDS-PAGE gel and transferred to nitrocellulose. The nitrocellulose containing one of the GLUT4 samples was cut into 2 mm pieces and counted in a scintillation counter. Western blot analysis was carried out on the second sample, with the anti-C-terminal GLUT4 antibody raised in sheep, to determine which of the 2 mm nitrocellulose pieces contained GLUT4. A small aliquot of the sample eluted from the immunoprecipitation was also run on a tris-glycine SDS-PAGE gel with known amounts of GLUT4 to act as a standard curve. The gel was transferred to nitrocellulose and Western blot analysis was carried out with the anti-C-terminal GLUT4 antibody raised in sheep to determine the amount of GLUT4 that was counted in the scintillation counter. It was then possible to calculate the cpm / pmole GLUT4.

In addition, the specific activity of ATP (cpm / mole γ phosphate) was calculated. Perchloric acid precipitation was used to precipitate the protein from the aliquot of cells retained before cell lysis (Section 2.2.3). The concentration of ATP in the resulting supernatant was determined using a luciferase bioluminescence assay (Section 2.2.4). A PKA assay was also carried out to determine the cpm per γ phosphate of ATP. The γ phosphate

was transferred to kemptide (a substrate of PKA) in the presence of PKA. The phosphorylated kemptide was separated from the ATP and counted in a scintillation counter (Section 2.2.5).
The stoichiometry of GLUT4 phosphorylation (mole phosphate / mole GLUT4) was then calculated from the cpm / pmole GLUT4 and the cpm / mole γ phosphate.

The experiment was carried out twice but unfortunately the results are neither reproducible nor sensible. The two individual results obtained were 31.34 and 22.57 mole phosphate / mole GLUT4 (Table 4.6). These values were too high. A figure of 0.1 – 0.2 mole phosphate / mole GLUT4 had been reported previously in basal adipocytes (James et al., 1989a, Nishimura et al., 1991). The method used in the study described here was similar to that by Nishimura and colleagues. They reported that the specific activity of ATP was ~500 cpm / pmole. The calculated specific activity of 1.91 or 3.06 cpm / pmole γ phosphate was lower in this study than the previously reported 500 cpm / pmole γ phosphate (Nishimura et al., 1991). If the reported specific activity of 500 cpm / pmole γ phosphate was used with the GLUT4 cpm / pmole obtained in the present study, then the stoichiometry of GLUT4 phosphorylation works out to be ~0.1 mole phosphate / mole GLUT4. As this is in agreement with the previous reports it would suggest that the error in the present study lies in the specific activity determination. This could have occurred in the PCA precipitation, ATP determination, the PKA assay or the kemptide purification strategy.

To find out if an error had occurred during the ATP determination assay, the value obtained from the assay was used calculate the concentration of ATP that would be present in the cell. This experimentally calculated value was then compared to the published values for the cellular concentration of ATP.

Experiment	1	2
ATP (cpm)	115.5	284.5
ATP (pmole) (in 10 µl SN)	60.59	93.15
ATP (cpm / pmole γ phosphate **)**	1.91	3.06
GLUT4 (cpm)	709.15	4037.73
GLUT4 (pmole)	11.85	58.46641
GLUT4 (cpm / pmole)	59.86	69.06
Phosphorylation Stoichiometry (mole phosphate / mole GLUT4)	**31.34**	**22.57**

Table 4.6 **Quantification of the level of phosphorylation in basal adipocytes.** The level of phosphorylation was calculated from the GLUT4 cpm / pmole and the ATP cpm / pmole γ phosphate. The data are from two independent experiments.

From the ATP determination assay, and using the protein assay calculated following cell lysis, the concentration of ATP in the cell was calculated as 3.8 and 12.5 nmole ATP / mg cell protein for the two experiments, respectively. The concentration of ATP in adipocytes had been reported as 8.3 nmole / mg cell protein (Pryor *et al.*, 2000). The experimental level of ATP was similar to the published level of ATP in the cell. Thus, the ATP determination assay appeared to be accurate in determining the level of ATP. The PKA assay was therefore likely to be the section of the specific activity measurement in which the error had occurred. The fat from the adipocytes may not have been totally removed during the PCA precipitation and so traces of fat could have affected the PKA assay.

If the value of 0.1 mole phosphate / mole GLUT4 was correct, then this would lead to a value of 0.05 mole of phosphate at the N-terminus, and 0.05 mole of phosphate at the C-terminus, per mole of GLUT4. However, further work is needed to determine where the problem actually lies in the experimental procedure and, after this has been rectified, then the stoichiometry of GLUT4 phosphorylation in adipocytes can be calculated further.

4.2.4.2.7 Effect of Insulin and Oligomycin on the Phosphorylation State of GLUT4 Isolated From Cardiomyocytes

The effect of insulin and / or oligomycin on the phosphorylation state of GLUT4 was tested in rat cardiomyocytes. In cardiomyocytes, there are two different mechanisms for glucose transport. The first is insulin-stimulated glucose transport and the second occurs during ischemia and hypoxia, which is believed to involve AMP-activated protein kinase (AMPK) (Section 1.4). AMPK is activated by an increase in the ratio of intracellular AMP:ATP (Hardie *et al.*, 1998). An increase in intracellular AMP, at the expense of ATP, can be achieved physiologically by an increase in workload, e.g. contraction, and pharmacologically by mitochondrial inhibitors. Oligomycin is a potent inhibitor of mitochondrial F_1F_0-ATPase and it elevates the AMP:ATP 2.5-fold in cardiomyocytes (Luiken *et al.*, 2003). In this way, oligomycin mimics hypoxic conditions. Thus, by testing insulin and oligomycin, the level of GLUT4 phosphorylation will be investigated in both pathways.

Cardiomyocytes were labelled with [$^{32}P_i$]. The cells were stimulated with either insulin for 30 min and / or oligomycin for 90 min (Section 2.2.2.2.3). GLUT4 was immunoprecipitated from the cell lysate and cleaved with Endo LysC, as previously. The levels of phosphorylation under these two conditions were compared to phosphorylation in the basal state, in which the cells had had no additional treatment. Both insulin and oligomycin decreased the level of phosphorylation at both the N- and the C-termini of GLUT4 (Figure 4.12). There was a greater decrease at the N-terminus compared to the C-terminus. There was an extremely significant ($p = 0.0004$) decrease in the level of phosphorylation at the N-terminus of GLUT4 isolated from insulin-stimulated cells, compared to the level from basal cardiomyocytes. This result was consistent throughout six experiments. The effect of insulin on the phosphorylation state of GLUT4 was the inverse of that in adipocytes, where there was a significant increase in the level of GLUT4 phosphorylation.

Oligomycin treatment significantly increased ($p = 0.042$) the level of phosphorylation at the N-terminus of GLUT4 isolated from insulin-stimulated cardiomyocytes. However, the increase in phosphorylation was not large enough to abolish the insulin-stimulated decrease in phosphorylation. At the C-terminus, the level of phosphorylation decreased to the same level after insulin and / or oligomycin treatment (~80% compared to the basal level of 100%). The data are from three to six independent experiments.

4.2.4.2.8 Relative Levels of Phosphorylation at the N- and C-terminus of GLUT4 Isolated From Cardiomyocytes

The relative levels of phosphorylation at both the N- and C-terminus of GLUT4 were calculated. The percentage phosphorylation was calculated from the total GLUT4 phosphorylation per condition which was set to 100%. In the basal state, 76.6% of GLUT4 phosphorylation occurred at the C-terminus and 23.4% was at the N-terminus (Figure 4.13). There was relatively less phosphorylation at the N-terminus in cardiomyocytes compared to adipocytes, as in adipocytes 56.0% of phosphorylation was at the C-terminus and 44.0% was at the N-terminus. There was a significant decrease ($p = 0.0391$) in the relative level of phosphorylation at the N-terminus of GLUT4 from insulin-stimulated cardiomyocytes, compared to cardiomyocytes in the basal state. Oligomycin treatment did not significantly change the relative level of phosphorylation in either basal or insulin-stimulated cardiomyocytes. The data are from three to six independent experiments.

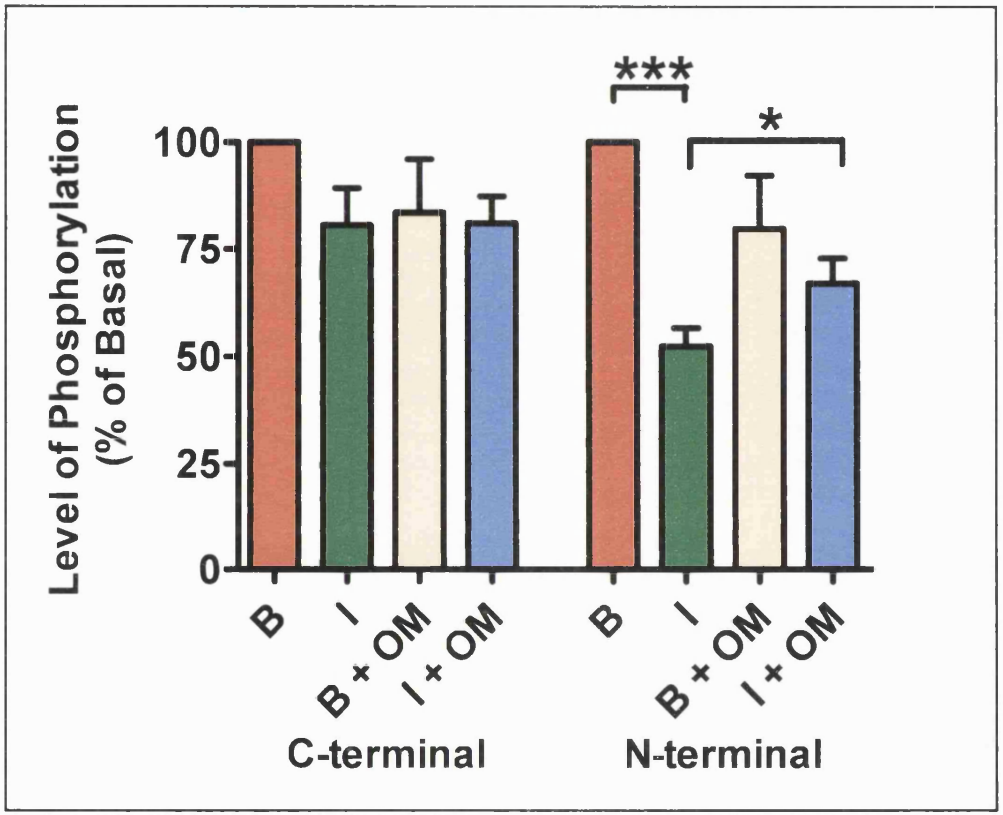

Figure 4.12 **The effect of insulin and / or oligomycin on the phosphorylation state at the N- and C-termini of GLUT4.** Cardiomyocytes were labelled with [$^{32}P_i$] and treated for 30 min with insulin and / or 90 min with oligomycin. The data are the combined mean ± S.E.M. from three to six independent experiments. *, $p<0.05$. ***, $p<0.001$ (paired t-test; insulin compared with basal and insulin + oligomycin compared with insulin).

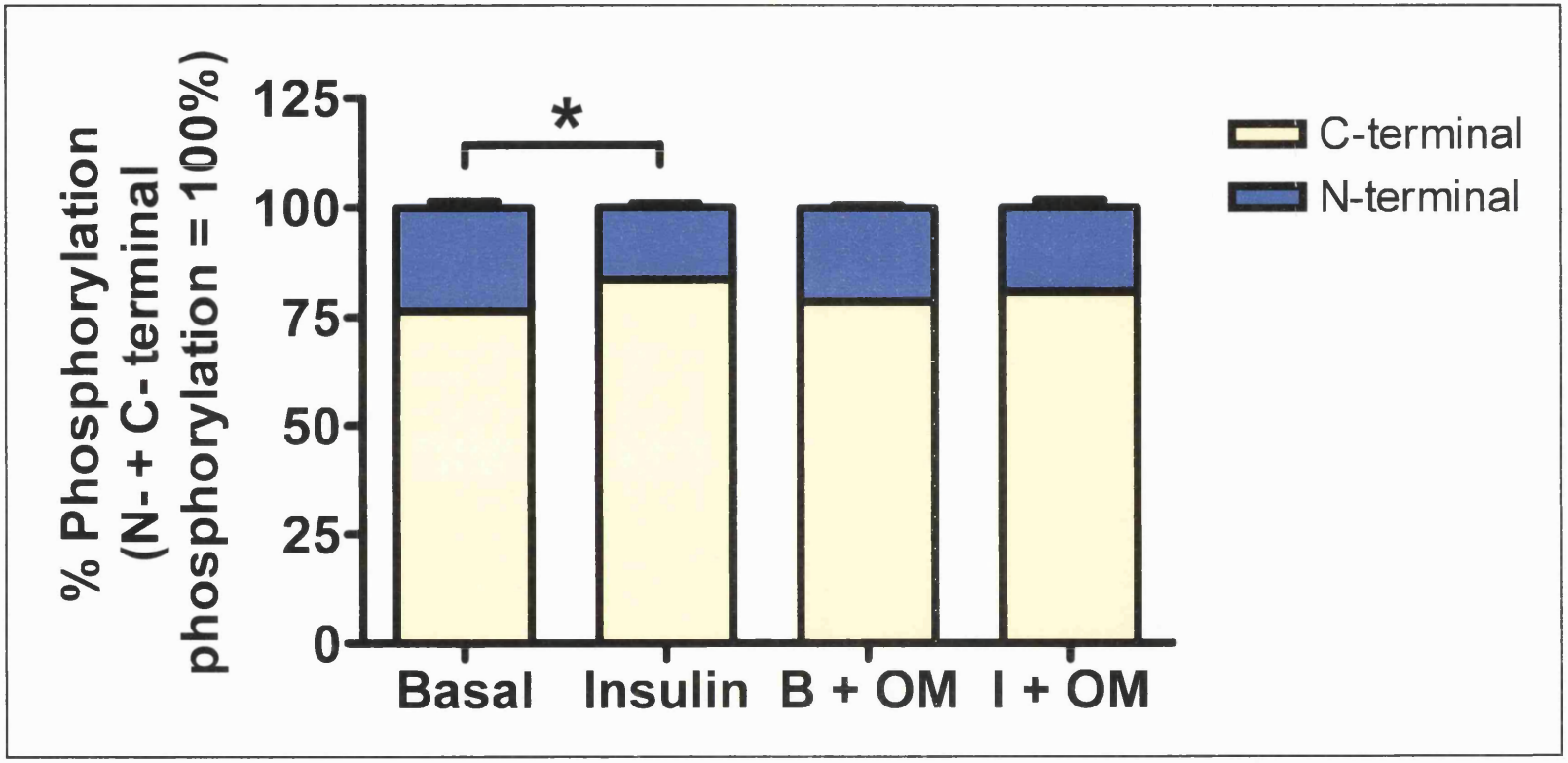

Figure 4.13 **Relative level of phosphorylation at the N- and C-terminus of GLUT4 in cardiomyocytes.** Total GLUT4 per lane was set to 100% and the percentage of this that was phosphorylation at the N- and C-termini was calculated. The data are the combined mean ± S.E.M. from three to six independent experiments. *, $p<0.05$ (paired t-test; compared with basal).

4.2.4.2.9 Level of Phosphorylation of GLUT4 in Cardiomyocytes

The level of phosphorylation (mole phosphate / mole GLUT4) was calculated for the uncleaved GLUT4 protein isolated from basal cardiomyocytes. The method used was similar to that used in adipocytes (Section 2.2.5) except that the composition of the PKA assay was changed.

To determine whether the PKA assay was giving accurate results (Section 4.2.4.2.6), the PKA assay was tested by the use of [γ-^{32}P] ATP [A]. The PKA assay was carried out using the [γ-^{32}P] ATP, and the phosphorylated kemptide was separated from [γ-^{32}P] ATP by the use of P81 phosphocellulose paper. The phosphorylated kemptide would bind to the P81 phosphocellulose but the [γ-^{32}P] ATP would not bind. The specific activity of the ATP (cpm / γ phosphate) was quantified from the scintillation counts of the P81 paper. The specific activity of the [γ-^{32}P] ATP was also calculated by direct counting of the ATP as the concentration of the stock [γ-^{32}P] ATP was known. Both methods (the PKA assay and the direct counting) gave the same specific activity result for the [γ-^{32}P] ATP. This indicated that the PKA assay and separation of the resulting phosphorylated peptide was accurate. This assay was therefore used for the calculation of the stoichiometry of phosphorylation in cardiomyocytes.

The specific activity of ATP was calculated (cpm / pmole γ phosphate) as well as the level of radioactivity incorporated into GLUT4 (cpm / pmole of GLUT4). The results were from three independent experiments and were reproducible. On average, there was 2.7 mole phosphate / mole GLUT4 (Table 4.7). This result was more sensible than the result obtained in adipocytes. However, the result may still be too high. If the value of 2.7 mole phosphate / mole GLUT4 was correct then there would need to be a third phosphorylation site present in GLUT4 in either the N- or the C-terminal peptides.

The concentration of ATP in the cardiomyocyte cell was calculated from the value of ATP, experimentally determined from the ATP determination assay. As with the adipocytes, the experimentally calculated value was compared to the published values of the concentration of ATP in cardiomyocytes. From the ATP determination assay, and using the protein assay following cell lysis, the concentration of ATP in the cell was calculated as 6.34, 0.34 and 0.44 nmole ATP / mg cell protein, for the three experiments respectively. These values differed from the published values of ATP in the cardiomyocyte. Values near to 20 nmole ATP / mg cell protein have been reported in cardiomyocytes (Geisbuhler et al., 1984, Smolenski, 2000) (19.5 and 22.1 nmole ATP / mg cell protein, respectively). The fact that the experimental and published values were not in agreement suggested that the ATP determination assay was not accurate in cardiomyocytes and, thus, the stoichiometry of GLUT4 phosphorylation may not be 2.7 mole phosphate / mole GLUT4.

Experiment	1	2	3
ATP (cpm)	9416.6	3508.7	10841.3
ATP (pmole)	353.4	35.5	63.7
ATP (cpm / pmole γ phosphate)	26.6	98.8	170.2
GLUT4 (cpm)	376	1255	1803
GLUT4 (pmole)	4.1	5.9	4.7
GLUT4 (cpm / pmole)	92.7	213.5	381.3
Phosphorylation Stoichiometry (mole phosphate / mole GLUT4)	**3.48**	**2.16**	**2.24**

Table 4.7 **Quantification of the level of phosphorylation in basal cardiomyocytes.** The level of phosphorylation was calculated from the GLUT4 cpm / pmole and the ATP cpm / pmole γ phosphate. The data are from three independent experiments.

4.3 Discussion

Previous studies have reported the phosphorylation of GLUT4 in both adipocytes and skeletal muscle, and this site has been localised to the C-terminus of the protein (James *et al.*, 1989a). However, no studies have investigated whether any of the other predicted phosphorylation sites were phosphorylated *in vivo* and, if they were, whether the phosphorylation had any significant effect on GLUT4 function. No studies had been carried out in cardiomyocytes.

The results presented in this chapter demonstrate that GLUT4 is phosphorylated in cardiomyocytes as well as in adipocytes. GLUT4 is therefore phosphorylated in all of the insulin responsive tissue in which it is expressed. In cardiomyocytes, glucose transport occurs in response to the stimulation of an additional pathway to the insulin signalling pathway that occurs in adipocytes. This additional pathway involves the activation of AMPK. The possibility therefore exists that the phosphorylation of GLUT4 may be involved in this additional pathway, as well as in the insulin signalling pathway.

The experiment carried out to determine the site of phosphorylation in primary adipocytes, by Lawrence *et al*, was repeated by Dr Françoise Koumanov (Lawrence, Jr. et al., 1990a). The same result was found, the major phosphorylation site identified was in the C-terminal peptide. A single strong band containing ^{32}P was identified at 10 kDa from the ^{32}P scan, compared to a band of 8 kDa by Lawrence (Lawrence, Jr. *et al.*, 1990a). The C- and N-terminal peptides did not run at their predicted molecular weight (7.4 and 9.4 kDa, respectively). This could be because both peptides have acidic regions which could affect how the peptides ran on an SDS-PAGE gel. The difference between the two studies was that Lawrence *et al* did not have the use of an anti-N-terminal GLUT4 antibody. The band detected by Lawrence *et al*, from

the use of an anti-C-terminal GLUT4 antibody, may have also contained the N-terminal peptide, which was not detected as there was no antibody available.

Cleaving GLUT4, isolated from 3T3-L1 adipocytes at day 5 of differentiation, resulted in the N- and C- terminal peptides resolving at a different molecular weight to the peptides that were derived from primary adipocyte cells. This could be because the GLUT4 was in the synthetic pathway and the 3T3-L1 adipocytes were not fully differentiated. A different level of glycosylation could have affected how the GLUT4 ran on the gel. The C-terminal peptide did not correspond to a ^{32}P-containing band but one of the bands identified by the anti-pSer^{10} antibody, raised in rabbit, did correspond to a ^{32}P-containing band. The remaining ^{32}P-containing band did not correspond to either the N- or C-terminal peptide. The fact that the C-terminal peptide appeared not to be phosphorylated could suggest that the N- but not the C-terminal peptide was phosphorylated during biosynthesis. This experiment was only carried out once and so it needs to be repeated to confirm this conclusion. However, the Western blot analysis did lead to the conclusion that the anti-pSer^{10} and the anti-C-terminal GLUT4 antibodies do not cross react with the opposing peptides.
Following CNBr cleavage of the GLUT4 isolated from primary adipocytes, both the N-and the C-terminal peptides were detected at the same molecular weight as the ^{32}P-containing band. Due to the fact that the antibodies do not cross react with the peptides, the N- and C- terminal peptides must be running at the same molecular weight, even though the predicted size of the two peptides differs. This provides an explanation as to why Lawrence *et al* did not identify the second phosphorylation site at the N-terminus of GLUT4.

To check that both the N- and the C-terminal peptides were phosphorylated in adipocytes, it would be useful to cleave GLUT4 with a different agent, other than CNBr, so that the N- and C-terminal peptides would be resolved at different molecular weights. This would also be essential for investigating the

differences in phosphorylation at each terminus, caused by different agents. As multiple bands were identified by the use of the anti-pSer^{10} antibody raised in rabbit, the use of a different anti-N-terminal antibody would help to identify the N-terminal peptide. Endo LysC was tested as an alternative to the use of CNBr. The monoclonal anti-C-terminal antibody and the anti-pSer^{10} antibody raised in sheep recognised the C- and N- terminal peptides respectively, at the predicted molecular weights. Endo LysC can, therefore, be used in the study of GLUT4 phosphorylation as the peptides from the N- and C- termini of GLUT4 resolve at different molecular weights on the gel and so phosphorylation at either site can be identified. The anti-pSer^{10} antibody raised in sheep, gave a stronger signal than that previously seen in the experiments with the anti-pSer^{10} antibody raised in rabbit. The sheep anti-pSer^{10} antibody was, therefore, used to identify the N-terminal peptide in future experiments.

Endo LysC proved to be a very a useful alternative to CNBr. The use of Endo LysC led to the identification of two distinct phosphorylation sites in GLUT4, both in adipocytes and cardiomyocytes. The phosphorylation sites occurred in peptide 1 – 50 and peptide 267 – 495. The potential phosphorylation sites in each of the peptides can be found by comparing the peptide sequence with the potential domains in which they are found in GLUT4 (Table 4.4). The red residues are found in the cytoplasmic region of the cell, the blue residues correspond to the transmembrane region and the green residues correspond to the extracellular domain. The potential phosphorylation sites will probably be intracellular (red) as they will be accessible to intracellular kinases. However, it cannot be ruled out that GLUT4 may be phosphorylated on extracellular residues (blue). In the recycling vesicles, the extracellular residues are intra-luminal and will be available for phosphorylation by kinases inside the vesicle. The first 24 amino acids in peptide 1 – 50 are predicted to be intracellular. This includes 2 serine, 2 threonine and 0 tyrosine residues (Ser^{3}, Ser^{10}, Thr^{21} and Thr$^{23)}$. Residues 46 – 50 are extracellular and do not contain any residues that could be phosphorylated. In peptide 267 – 495, there are 5 serine residues, 6

threonine residues and 0 tyrosine residues in the intracellular region of GLUT4 (Ser^{274}, Ser^{281}, Ser^{412}, Ser^{480}, Ser^{488}, Thr^{283}, Thr^{351}, Thr^{471}, Thr^{475}, Thr^{482} or Thr^{486}). The potential phosphorylation sites in the C-terminus can be narrowed down further by comparing the C-terminal peptide obtained from Endo LysC cleavage (residues 267 - 495) to the CNBr cleaved fragment (residues 446 – 509). There are no extracellular residues in the CNBr cleaved fragment and so phosphorylation must occur on the intracellular residues. There are 2 potential serine phosphorylation sites and 4 threonine sites between residues 446 – 495 (Ser^{480}, Ser^{488}, Thr^{471}, Thr^{475}, Thr^{482} or Thr^{486}). HPLC analysis showed that serine was the only phosphorylated residue present in GLUT4 (Lawrence, Jr. *et al.*, 1990a). Therefore the predicted phosphorylation sites would be serine 3 or serine 10 at the N-terminus and serine 480 or serine 488 at the C-terminus of GLUT4. The kinase must be located in the cytoplasm because the predicted phosphorylation sites occur on intracellular residues. When assessing these sites as potential phosphorylation sites, the phosphorylation 'score' (Table 4.1) needs to be taken into account. The score is a number between 0 – 1 and represents the likelihood that a site is phosphorylated. The higher the number, the more likely it is that the site is a phosphorylation site. In the N-terminal peptide, serine 3 and serine 10 have scores of 0.003 and 0.263 respectively. Although both numbers are below the usual threshold for phosphorylation of 0.5, serine 10 is the most likely candidate. A score of 0.003 is very low and so serine 3 is extremely unlikely to be phosphorylated. In the C-terminal peptide, serine 480 and serine 488 have scores of 0.204 and 0.993. As GLUT4 had previously been shown to be phosphorylated at serine 488 and because the score is high, it is fair to conclude that the phosphorylation site at the C-terminus is serine 488. A novel phosphorylation site at serine 10 has, therefore, been identified at the N-terminus of GLUT4, as well as confirming the presence of the phosphorylation site previously reported at serine 488 (Lawrence, Jr. *et al.*, 1990a). There was a possibility that other phosphorylation sites could have been missed i.e. if the phosphorylated peptides had been too small to be detected on the tris-tricine gel. The region where such peptides

could occur after Endo LysC cleavage is the large intracellular loop, residues 223 – 287. Four small peptides could be missed in this region (Table 4.4). However, an 18 kDa peptide, residues 196 – 360, would have been present on the ^{32}P scan after GLUT4 had been cleaved with CNBr. The 18 kDa peptide would have included the regions that could not have been detected after Endo LysC digestion. However, an 18 kDa ^{32}P-containing peptide was not present on the ^{32}P scan and so phosphorylation at in this region can be excluded. As cleavage had been carried out using two different methods, phosphorylation could have occurred in any of the intracellular sites and it would have been identified. This was also shown quantitatively. The sum of the intensities of the ^{32}P-containing N- and C- terminal peptides equals the intensity of the ^{32}P-containing, uncleaved GLUT4 band. This showed that all of the phosphorylation sites had been accounted for and are found in the N- and C-terminal peptides. The experimental data is only taken from one experiment so this needs to be repeated. However, the experimental data does corroborate the theoretical data.

Insulin and okadaic acid increased the level of phosphorylation of GLUT4 at both the N- and the C- termini. However, insulin had a greater increase at the N-terminus and okadaic acid had a greater increase at the C-terminus. It had previously been reported that insulin did not have any effect in the level of phosphorylation of GLUT4 (James *et al.*, 1989a). However, in the present study, insulin significantly increased the level of phosphorylation at both the N- and the C-terminus of GLUT4.

Okadaic acid (a protein phosphatase inhibitor) had been reported to increase the phosphorylation state of GLUT4 threefold at the plasma membrane relative to the intracellular pool. An increase of twofold was identified in this study. In the present study, the phosphorylation state was studied in total cellular GLUT4. The level of phosphorylation would therefore be lower than the three fold increase seen in plasma membrane. The experiment was only carried out once and needs to be repeated to get a more accurate result.

On average, 56% of the GLUT4 phosphorylation occurred at the C-terminus and 44% occurred at the N-terminus. This did not change significantly with insulin or okadaic acid treatment. Equal importance must therefore be given to each of the sites. The fact that both phosphorylation sites are phosphorylated to the same extent could lead to the conclusion that the phosphorylation sites are cooperative; one site has to be phosphorylated before the other site is phosphorylated.

CKII inhibitors were used to try and identify the kinase responsible for phosphorylating GLUT4 at serine 10. If the kinase could be identified, it might be useful when the function of the phosphorylation site has been clarified. The kinase (or phosphatase) could be a useful target if a defect in the GLUT4 phosphorylation was involved in the decreased effect of insulin signalling in Type 2 diabetes. Neither of the inhibitors tested had a definitive effect on the phosphorylation state of GLUT4. It is possible that GLUT4 is phosphorylated by an, as yet, unidentified kinase that is not inhibited by either of the inhibitors tested in this study. Neither CKII inhibitor affected the phosphorylation site in the C-terminus of GLUT4 but both CKII inhibitors did have an effect at the N-terminal peptide. DRB treatment only resulted in a small decrease in the level of phosphorylation at the N-terminus of GLUT4 from insulin-stimulated adipocytes. TBB treatment resulted in a greater decrease in the level of phosphorylation of GLUT4 from insulin-stimulated adipocytes rather than from basal adipocytes. The greatest decrease in phosphorylation was seen at the N-terminus of GLUT4 when insulin and isoproterenol treated adipocytes were subsequently treated with TBB. It would be expected that the CKII inhibitors would have a greater effect at the N-terminus of GLUT4 because there is not a CKII phosphorylation site in the C-terminal peptide. The fact that the results were variable between experiments or that only a single test experiment was carried out means that the experiments need to be repeated to confirm these results. However, both TBB and DRB did have an effect on N-terminal phosphorylation, even if it was small. The experiments that tested the kinase

inhibitors suggested that CKII was perhaps involved in phosphorylation at the N-terminus of GLUT4.

The calculation of the stoichiometry of phosphorylation in GLUT4 from basal adipocytes was neither sensible nor reproducible between the two experiments. The calculation of the specific activity of ATP (Table 4.6) did not correspond to the reported 500 cpm / pmole γ phosphate figure that had previously been reported (Nishimura *et al.*, 1991). If the specific activity of ATP was 500 cpm / pmole γ phosphate then the calculated stoichiometry was 0.1 mole phosphate / mole GLUT4 which corroborates the individual studies carried out by James and Nishimura (James et al., 1989a, Nishimura et al., 1991). If the level of phosphorylation was 0.1 mole phosphate / mole GLUT4, then 0.05 mol would be at the N-terminus and 0.05 mol would be at the C-terminus. Hence, only a small population of GLUT4 would be phosphorylated in adipocytes at any one time. The ATP determination assay appears to be accurate in determining the level of ATP. The PKA assay is therefore likely to be the part of the specific activity measurement in which the error has occurred. The specific activity measurements in adipocytes therefore need to be repeated but using the PKA assay carried out in cardiomyocytes. A control, using [γ-^{32}P] ATP as an ATP source, was carried out in cardiomyocytes which led to the conclusion that using the different method for the PKA assay was accurate (Section 4.2.4.2.9). This will confirm whether the stoichiometry of 0.1 mole phosphate / mole GLUT4 is correct.

When glucose transport was activated in cardiomyocytes, either by insulin and / or oligomycin, the level of phosphorylation decreased at both the N- and the C-termini of GLUT4, compared to the basal level of phosphorylation. Insulin significantly decreased the level of phosphorylation at the N-terminus of GLUT4 (Figure 4.12). This was the inverse to the effect insulin had on the adipocytes (Figure 4.8 A). In adipocytes it was thought that the phosphorylation of GLUT4 may promote internalisation (Section 1.6.3). However, this

hypothesis does not hold in cardiomyocytes. Oligomycin treatment significantly increased the level of phosphorylation at the N-terminus of insulin-stimulated cardiomyocytes.

Although the effect of insulin and oligomycin is to decrease the phosphorylation state of GLUT4, the function of the phosphorylation cannot be elucidated from this experimental data. There is a decrease in the level of GLUT4 phosphorylation in response to both signalling pathways in cardiomyocytes, both the insulin-stimulated and the AMPK-activated pathways. Phosphorylation of GLUT4 could therefore provide a point of convergence for the two pathways, for example, through the activation / deactivation of the kinase(s) and phosphatase(s) responsible for the phosphorylation state of GLUT4.

GLUT4 is phosphorylated to a greater extent at the C-terminus in cardiomyocytes. In the basal state, 76.6% of GLUT4 phosphorylation occurred at the C-terminus and 23.4% at the N-terminus. The stoichiometry of phosphorylation resulted in a level of 2.7 mole phosphate / mole GLUT4. This value is probably more accurate than that calculated from adipocytes. A test using [γ-^{32}P] ATP was carried out and the PKA assay and subsequent purification of peptide was accurate. No fat was present in the cardiomyocyte so no fat contamination could have affected the results. This ruled out the concerns from this experiment carried out in adipocytes. If cardiomyocytes had a total of 2.7 mole phosphate / mole GLUT4 then 2.07 mole of phosphate would be at the C-terminus and 0.63 mole of phosphate would be at the N-terminus. There would therefore be two phosphorylation sites at the C-terminus of GLUT4. It is likely that this would be at serine 480 as well as the already identified serine 488 and serine 10. No missed phosphorylation sites were identified in cardiomyocytes (Section 4.2.4.2.4). This confirmed that the phosphorylation sites were only present in the N- and C-terminal fragments. However, it did not confirm how many phosphorylation sites were on each peptide. Further investigation is needed to confirm this additional phosphorylation site. This could be done by using a different cleavage agent,

which would cleave GLUT4 between serine 480 and serine 488. Another alternative, discussed in chapter 5, involves the use of a GLUT4 construct with a haemagglutinin tag in the first exofacial loop, mutated at both serine 10 and serine 488. The serine residues are both mutated to alanine residues and cannot be phosphorylated. The mutated construct could be transfected into cells and the cells labelled with [$^{32}P_i$] as before. The mutated GLUT4 protein could be immunoprecipitated from the cell lysate by the use of an anti-HA antibody. Following Endo LysC cleavage, autoradiography would detect if there has been any ^{32}P incorporated into GLUT4 other than at serine 10 and serine 488.

The experimental and published values for the concentration of ATP in the cardiomyocyte were not in agreement. One conclusion would be that the ATP determination assay was not accurate in cardiomyocytes. However, it has been reported that in anaerobic conditions, the level of ATP in the cell is 0.4 nmole ATP / mg cell protein (Geisbuhler *et al.*, 1984). This value of 0.4 nmole ATP / mg cell protein is similar to two of the experimentally calculated values (0.34 and 0.44 nmole ATP / mg). Therefore, the ATP determination assay could be correct if the cells were hypoxic by the end of the two hour [$^{32}P_i$] incubation. If the cells were hypoxic then there could have been insufficient gassing of the buffer throughout the incubation or the amount of buffer in which the cells are suspended could have been too small. In which case, the stoichiometry calculated (~2 mole phosphate / mole GLUT4) is not representative of basal cardiomyocytes but rather that of hypoxic cardiomyocytes.
If the two hour [$^{32}P_i$] incubation does lead to the cells becoming hypoxic, then the results of the effect of insulin on the level of phosphorylation need to be taken with caution. Insulin caused an increase in the level of phosphorylation in adipocytes but a decrease in the level of phosphorylation in cardiomyocytes. It could therefore be that insulin, by itself, would also cause an increase in the level of phosphorylation in cardiomyocytes above the true basal level. If GLUT4 is phosphorylated at 2 mole phosphate / mole GLUT4 in hypoxic

conditions and insulin acts by decreasing the level of phosphorylation, insulin might be over-riding the affect of the hypoxia and decreasing the level of phosphorylation to a lower level (e.g. a level of 0.2 mole phosphate / mole GLUT4) but this may still be an increase in phosphorylation from true basal levels (0.1 mole phosphate / mole GLUT4). The fact that oligomycin did not have a significant effect on the level of phosphorylation would be explained by the fact that the cells are already hypoxic.

A lot of work needs to be carried out in the investigation of GLUT4 phosphorylation. One of the most important experiments that need to be carried out initially is the investigation into whether the ATP determination assay was accurate in cardiomyocytes. The ATP determination assay needs to be carried out on freshly isolated cardiomyocytes, cells that have been incubated for two hours under the experimental conditions previously used and cardiomyocytes incubated in anaerobic conditions (N_2 atmosphere and no glucose), the level of ATP in the cell can then be determined. The ATP determination assay also needs to be carried out to investigate different conditions for the two hour incubation, for example, incubating the cardiomyocytes in a larger volume of buffer, to help prevent the cells becoming hypoxic. This would then be used to determine the optimal conditions for the [$^{32}P_i$] incubation that will not lead to hypoxic cells.

Another important experiment that needs to be carried out is to find out whether the cardiomyocytes, after the two hour incubation, were in fact hypoxic. The release of lactate dehydrogenase (LDH) into the serum is a recognised marker for myocardial hypoxia. The cardiomyocytes can therefore be tested whether they are hypoxic by measuring the concentration of LDH in the extracellular medium. Commercial kits are available to measure the LDH concentration spectrophotometrically. If the cells are becoming hypoxic during the two hour incubation, then the effect of insulin and oligomycin on the level of GLUT4 phosphorylation of true basal cells needs to be tested again in cardiomyocytes.

The level of ATP / mg cell protein needs to be calculated for all the different conditions tested. If different conditions alter the level of ATP in the cell, then the stoichiometry of phosphorylation could not be calculated from the relative level of phosphorylation at each terminus from each condition (Figure 4.13). The specific activity of ATP would need to be calculated, separately, for each condition.

Once the labelling conditions have been optimised and the ATP determination assay results in a value similar to the published values for basal cardiomyocytes, then the ATP concentration, the ATP specific activity and the GLUT4 stoichiometry of phosphorylation need to be determined under basal, insulin and hypoxic conditions.

A further extension to this study would be to investigate whether GLUT4 is phosphorylated at both termini at the same time or if the phosphorylation sites have different effects and different locations within the cell. This could be investigated using confocal microscopy once highly phospho-specific antibodies have been raised to each phosphorylation site.

4.4 Conclusion

The research conducted and which is described in this chapter identified two phosphorylation sites in GLUT4. One of these is situated in the N-terminal peptide between residues 1 – 50 and the other in the C-terminal peptide between residues 267 – 495. From the use of a phosphorylation site prediction program, the sites of phosphorylation are predicted to be at serine 10 and serine 488. The site at the N-terminus of GLUT4 has not been identified prior to this study but a site at serine 10 was predicted to be phosphorylated due to its homology to the N-terminus of GAD65α and a known phosphorylation site at the corresponding serine residue. The phosphorylation site at the C-terminus of GLUT4 has previously been identified (Lawrence, Jr. *et al.*, 1990a). GLUT4

is phosphorylated in all of the insulin-responsive tissues in which the protein is expressed. Phosphorylation occurs in cardiomyocytes, which has not previously been investigated, in addition to the already identified adipocytes and skeletal muscle (James *et al.*, 1989a).

Insulin has opposing effects in the level of phosphorylation in adipocytes (increases) and cardiomyocytes (decreases). This difference could occur because adipocytes and cardiomyocytes are two distinct cell types. Insulin has a greater affect on the level of phosphorylation at the N-terminus compared to the C-terminus. Treatment with okadaic acid, the PPI and PPIIa inhibitor, leads to increases in glucose transport and the level of phosphorylation in adipocytes, in agreement with Lawrence *et al* (Lawrence, Jr. *et al.*, 1990b). This increase occurs at both termini, but okadaic acid treatment leads to a larger increase in the level of phosphorylation at the C- than at the N-terminus. 44% of the GLUT4 phosphorylation occurs at the N- terminus and 56% occurs at the C-terminus in basal adipocytes. The fact that each site is phosphorylated equally could suggest that phosphorylation at one site is required for phosphorylation at the second site. This ratio does not significantly change in response to stimulation by insulin or okadaic acid. The quantification of phosphorylation does not give a sensible result and error probably occurred during the estimation of the specific activity of ATP. However, if the value of the specific activity of ATP is taken from published data (Nishimura *et al.*, 1991), GLUT4 has 0.1 mole phosphate / mole GLUT4 which agrees with previous reports (James et al., 1989a, Nishimura et al., 1991). In which case, 0.05 mol phosphate occurs at the N-terminus and 0.05 mol phosphate at the C-terminus per pmole of GLUT4.

Due to inconsistencies in the experiments, the kinases responsible for phosphorylating GLUT4 in adipocytes were not definitively identified. However, the results suggest that CKII phosphorylates GLUT4 at serine 10. This agrees with the predicted kinase generated from a kinase prediction program.

In addition to insulin, oligomycin treatment leads to decreases in the phosphorylation state of GLUT4 in cardiomyocytes. There is a greater effect at the N-terminus than the C-terminus. GLUT4 phosphorylation decreases in response to stimulation of glucose transport. Glucose transport is stimulated by two different mechanisms in cardiomyocytes. One involves stimulation by insulin and the other by contraction and hypoxia which involves the activation of AMPK. Oligomycin activates AMPK and so stimulates the second mechanism. GLUT4 is phosphorylated to a higher extent in cardiomyocytes compared to adipocytes. In the basal state, there are 2.7 mole of phosphate / mole of GLUT4. 76% of this phosphorylation is at the C-terminus and 24% at the N-terminus. Thus, 2 moles of phosphate are at the C-terminus and 0.7 moles of phosphate at the N-terminus per mole of GLUT4. This would imply 2 phosphorylation sites at the C-terminus, the second site probably being at serine 480. The subcellular localisation of each site would be paramount in the understanding of the role of each phosphorylation site. Previous reports of subcellular localisation are misleading due the existence of additional phosphorylation sites. The study has provided an interesting point for future investigation; to elucidate the reason why insulin increases phosphorylation in adipocytes and decreases the phosphorylation in cardiomyocytes. Whilst this study quantified the level of phosphorylation at each terminus, it did not give any indication as to the function of each phosphorylation site. The effect each phosphorylation site has on the translocation of GLUT4 to the plasma membrane will be discussed in chapter 5.

5 The Effect of Each Phosphorylation Site on the Translocation of GLUT4 to the Plasma Membrane

5.1 Introduction

Phosphorylation is a transient phenomenon in living cells. It is, therefore, difficult to study the function of the phosphorylation site, especially if the kinase and phosphatase involved in the phosphorylation is unknown. Many studies designed to investigate the role of phosphorylation in various cellular proteins involve the use of site-directed mutagenesis to mutate the residues of interest. These mutant proteins were designed to mimic either a phosphorylated residue or a non-phosphorylated residue (Fushimi et al., 1997, Namchuk et al., 1997, Jarvis et al., 2004).

Transfection studies involving the mutant proteins are often carried out in cell lines that express very low levels of the protein of interest, so the effect of the mutation can be monitored without any interference from the wild type protein. When studying the effect of GLUT4 on insulin-stimulated glucose transport, NIH-3T3 fibroblasts and Chinese Hamster Ovary (CHO) cells are often the cell types of choice because the cells do not express GLUT4 (Hudson et al., 1992, Kanai et al., 1993b). However, caution must be taken in interpreting this data because NIH-3T3 fibroblasts and CHO cells cannot mimic the insulin sensitive tissues (adipose and muscle cells) in which GLUT4 is found. This is because they do not have the same cellular machinery. For example, the cells express very low levels of the insulin receptor (Kanai *et al.*, 1993a). This problem could partially be overcome by co-expressing the insulin receptor with GLUT4, but the cells are less insulin responsive than adipose cells and so are not an ideal model to use (Kanai *et al.*, 1993b). A tissue culture model of primary adipocytes is available in which 3T3-L1 fibroblasts are differentiated into adipose-like cells. Many groups in the GLUT4 field work exclusively with this

model and it is a frequently used model in GLUT4 transfection studies. The 3T3-L1 adipocyte cells have increased sensitivity to insulin (Reed et al., 1977, Rubin et al., 1978) and contain the correct insulin signalling machinery. However, there are problems in using 3T3-L1 adipocytes in studies involving the transfection of mutated GLUT4 proteins because the cells do not differentiate completely or uniformly. In addition, the cells have been immortalised and so have characteristics that are not found in normal cells, for example, aneuploidy (Quon *et al.*, 1993). These problems have been overcome by the development of a method for transfecting DNA into primary adipocyte cells by the use of electroporation. After one day in culture, there was a high level of expression of the transfected protein in the cells and the cells remained insulin responsive (Quon *et al.*, 1993). This was an advantage as it has been reported that primary adipocytes lose insulin responsiveness and GLUT4 expression after several days in culture (Hajduch et al., 1992, Gerrits et al., 1993). An epitope tag, haemagglutinin (HA), had been cloned between residues 67 and 68 in the first exofacial loop of GLUT4 (GLUT4-HA) (Quon *et al.*, 1994) and thus provides a method to discriminate between endogenous and transfected GLUT4. Following transfection of the GLUT4-HA construct into primary adipocytes, GLUT4 translocation could be studied by detection of the HA tag without any interference from wild type GLUT4 present in the cell. It has been reported that insulin stimulated a 4.3-fold recruitment of transfected GLUT4-HA to the cell surface (Quon *et al.*, 1994). This insulin response was not as large as that reported in freshly isolated cells (15- to 20-fold) (Holman *et al.*, 1990). This decrease in the fold insulin response, compared to freshly isolated cells, occurred because electroporation and culturing led to an elevated rate of basal glucose transport, i.e. more GLUT4 was present at the plasma membrane in basal adipocytes (Quon *et al.*, 1993). A double-antibody binding assay was carried out to detect the level of transfected GLUT4 at the plasma membrane in either basal or insulin-stimulated cells. The cells were incubated with an anti-HA antibody, followed by a secondary antibody. The anti-HA antibody would only bind to the GLUT4

at the plasma membrane in intact cells because the HA epitope was present in the first exofacial loop of GLUT4. The transfected GLUT4 was detected at the plasma membrane with no interference from the endogenous GLUT4 (Quon *et al.*, 1994).

The aim of the work described in this chapter was to mutate the two phosphorylated serine residues in GLUT4, serine 10 and serine 488. The effect of the mutations, and ultimately the effect of the phosphorylation sites, on the translocation of GLUT4 to the plasma membrane was investigated using an assay adapted from the translocation assay reported by Quon and colleagues (Quon *et al.*, 1994). The effects of single mutations (at one site only) and double mutations (at both phosphorylation sites) were both investigated.

5.2 Results

5.2.1 Site-Directed Mutagenesis of the Phosphorylation Sites at Serine 10 and Serine 488 in GLUT4

Site-directed mutagenesis is an invaluable technique in which specific mutations are carried out at specific sites in DNA. This allows an investigation into the contribution specific amino acids have on the function of the protein. More importantly, in the study described here, it was used to help to determine the effect each phosphorylation site had on GLUT4 translocation to the plasma membrane. The phosphorylated residue, serine in the case of GLUT4, was mutated to alanine to represent a constitutively unphosphorylated form of the residue. The serine was also mutated to aspartic acid to represent a constitutively phosphorylated form of the residue, by mimicking the negative charge of the phosphorylated serine (Figure 5.1).

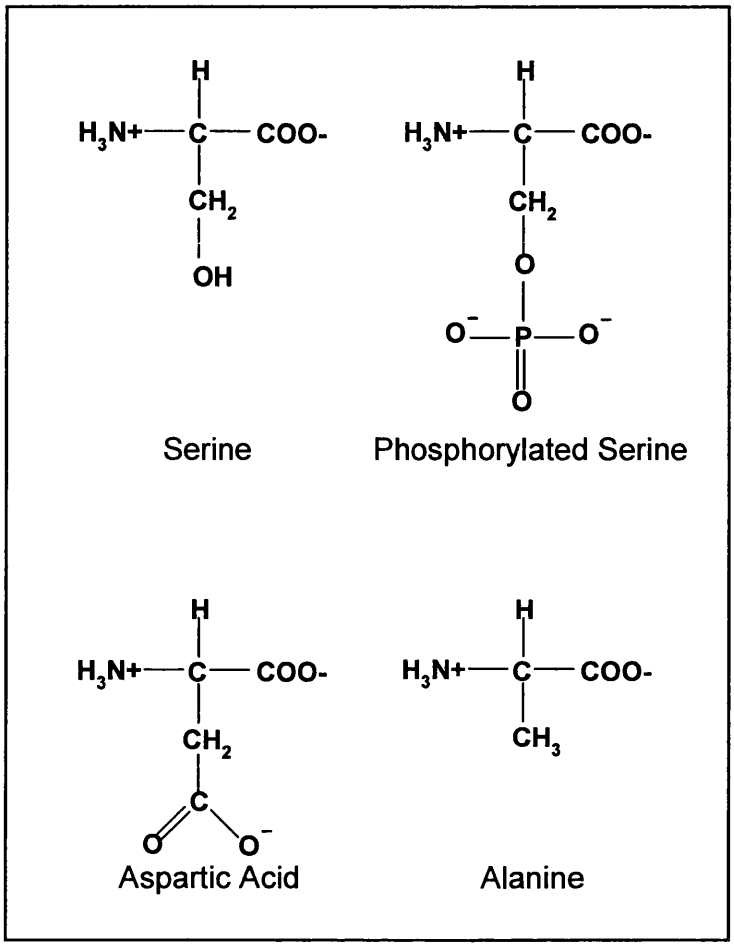

Figure 5.1 **The structure of the amino acids involved in the mutagenesis.**

The vector containing a haemagglutinin (HA) tagged human GLUT4 construct was a kind gift from Dr. S. W. Cushman. The GLUT4 DNA was originally cloned from human intestinal and muscle libraries (Fukumoto *et al.*, 1989). The site-directed mutagenesis was carried out on the double stranded GLUT4-HA DNA vector so single mutations were achieved, i.e. a mutated residue at one phosphorylation site and the wild type residue at the other phosphorylation site. Double mutants were also carried out so that each phosphorylated residue was mutated to the same residue i.e. alanine 10 and alanine 488 or aspartic acid 10

and aspartic acid 488. The nomenclature used to depict the mutations involves the use of the single letter abbreviation for the amino acids involved. The amino acid in wild type GLUT4 is given, followed by the position of the residue in the protein and finally the amino acid generated in the mutation. For example, mutating the serine residue at residue number 10 to alanine is written as S10A.

Oligonucleotide primers were designed to be complementary to the region of DNA surrounding the amino acids to be mutated. The serine at position 10 in GLUT4 was mutated from TCC to GCC (in the case of alanine) and to GAT (in the case of aspartic acid). The serine at position 488 was mutated from TCT to GCA (in the case of alanine) and to GAT (in the case of aspartic acid) (Section 2.2.11.1). An example of the S488A mutagenesis is given below. Essentially the same method was carried out for each mutation but the conditions used did differ and these will be outlined. A schematic of the method used is illustrated in Figure 5.2.

Polymerase chain reaction (PCR) was carried out using the wild type GLUT4-HA vector with the alanine 488 mutagenesis primers (Section 2.2.11.2). The primers were complementary to opposite strands of the vector and used to amplify and extend the vector. Incorporation of the primers would result in a mutated vector. Any vector that was produced during the PCR was selected by use of the endonuclease *Dpn* 1. *Dpn* 1 digests methylated and hemi-methylated DNA. Most of the DNA isolated from *E. coli* strains are methylated whereas the vector generated in the PCR is not methylated. *Dpn* 1 therefore digests the parental vector but leaves the PCR product intact. The *Dpn* 1 digested PCR product was run on an agarose gel to detect any vector present in the sample (Figure 5.3 A).

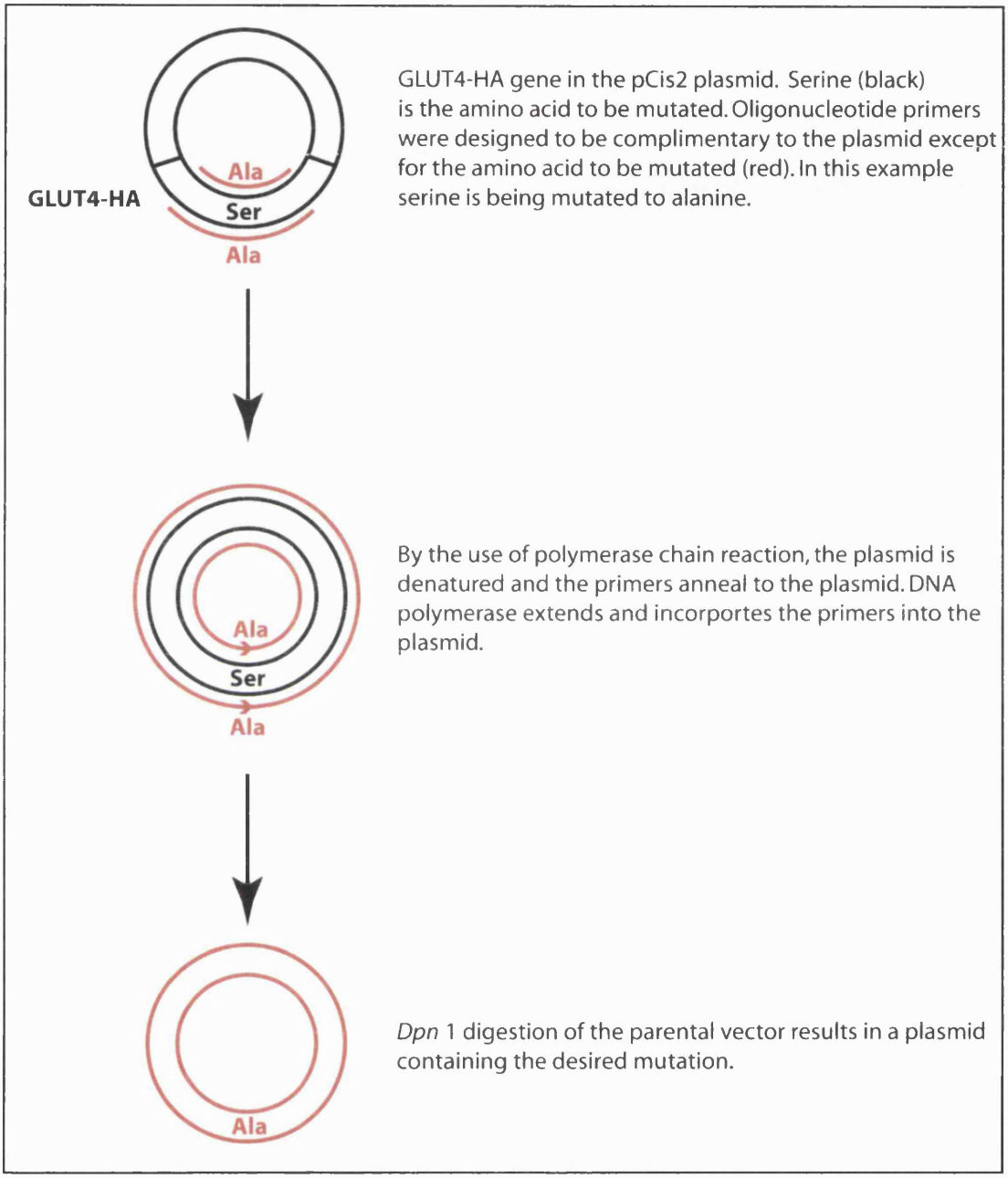

Figure 5.2 **A schematic of the method used to mutate the GLUT4-HA vector.**

A band was present in the PCR product at about 8 kb (Figure 5.3 A, lane 2), although there was a smear down the entire lane. The exact weight of the band was hard to determine as the markers (Figure 5.3 A, lane 1) were not well resolved in the 8 kb region. However, the band corresponded approximately to the molecular weight of the GLUT4-HA vector. The predicted molecular weight of the circularised GLUT4-HA vector was 7.4 kb; the pCis2 vector was 5.4 kb and GLUT4-HA was 2.0 kb. The vector was likely to contain GLUT4 that contained the S488A mutation because all of the parental vector should have been digested by *Dpn* 1. Lane 2 did contain a smear throughout the entire length of the lane. This was probably because the 7.4 kb vector was relatively large and so the DNA polymerase did not always amplify the entire vector in one continuous step. The smear was, therefore, probably due to different linear truncations of the GLUT4-HA vector generated during the amplification.

The mutations in the GLUT4-HA vector were all carried out using slightly different conditions to the one exemplified (Section 2.2.11.2). Initially, the DNA polymerase used in the mutagenesis PCR reaction was Platinum® *Pfx* DNA Polymerase [I]. The polymerase is in an inactive form, bound to the Platinum® antibody and, following the denaturation step in the PCR, the enzyme activity is restored. This imitates a 'hot start' and so the polymerase provides increased specificity, sensitivity and yield and is, therefore, an ideal candidate to be used in site-directed mutagenesis. Platinum® *Pfx* DNA Polymerase was successfully used in the generation of the S10A mutant. However, other mutations could not be generated in this way, so different DNA polymerases were also tested. *PfuTurbo* DNA polymerase [ST] and BIO-X-ACT Long DNA Polymerase [BL] were tested. Both of these polymerases are designed for use in the amplification of long, complex genomic targets with high-fidelity. BIO-X-ACT Long DNA polymerase was of no use in the mutagenesis because primer dimers formed and no other product was visible in the gel. A hot-start was carried out with the polymerase but the primer dimers still formed. The primer dimers did not form with either of the other two polymerases used. Therefore,

the BIO-X-ACT Long DNA polymerase was not used for generating any of the mutants. *PfuTurbo* DNA polymerase was used for the remaining mutagenesis reactions. *PfuTurbo* DNA polymerase produced a smear as identified by agarose gel electrophoresis (Figure 5.3). This could be due to mis-annealing of the primers so that the full-length product was not produced. However, the full length, circularised, mutated product could also be present. Increasing the annealing time in the PCR reaction did decrease the intensity of the smears on the gel. Different annealing temperatures (55 °C to 64 °C) were required for the generation of each mutant due to the different properties of the primers used in each case. Increasing the elongation time was the major factor which increased the efficiency of the mutagenesis. The elongation time was increased from 1 min / kb to 2.5 min / kb. This was because the vector was large and so the extra time would enable the additional elongation needed to generate the complete circularised vector.

Following the *Dpn* 1 digestion, the resulting vector was transformed into XL1 Blue *E. coli* competent cells. Single colonies were isolated and grown before the DNA was isolated and purified. A restriction digest was carried out on the resultant DNA using the enzyme *Xba* 1. This ensured that the vector contained GLUT4. There were two *Xba* 1 sites in the GLUT4-HA vector. One site was 35 residues before the initiation codon for GLUT4 and the second *Xba* 1 site was 1915 residues into the GLUT4 construct. Digestion using *Xba* 1 would generate a band of 1950 bp if the vector contained GLUT4-HA that had no insertions or deletions generated in the PCR. The restriction digest was also carried out using wild type GLUT4-HA DNA as a positive control. The products of the digestion were run on an agarose gel (Figure 5.3 B). The digest of the PCR product (Figure 5.3 B, Lane 2) and the positive control (Figure 5.3 B, Lane 3) each contained a fragment at the same molecular weight, about 2000 bp, which corresponded to the molecular weight of the product that would be generated if GLUT4-HA construct was present in the vector. As both digestions

contained a band at the same molecular weight, no insertions or deletions had occurred in the GLUT4-HA vector during the PCR.

To ensure that the vector contained the desired mutation in GLUT4, the DNA was sequenced (Figure 5.4). The red bases correspond to residues that were identical in both the wild type GLUT4-HA vector and the PCR product. The blue bases correspond to residues that were different in each sample i.e. a mutation had occurred. The desired mutation had occurred because serine 488 was mutated from TCT to GCA. This corresponded to alanine 488.

The first 35 residues sequenced did not have a strong correlation between the sequence of the PCR product and the wild type vector. This was because it took about 50 bases before the sequence started to become accurate after the sequencing primer bound to the vector. No other mutations had therefore occurred at the C-terminus of the vector apart from at alanine 488.

After all of the single mutants had been generated, the double mutation was made by mutating the GLUT4-HA vector (that contained a single mutation) at the second site. The mutagenesis was carried out successfully for all of the desired mutations. The mutations obtained at a single site in the vector were S10A, S10D, S488A, and S488D. Double mutations were obtained for S10A and S488A, or S10D and S488D.

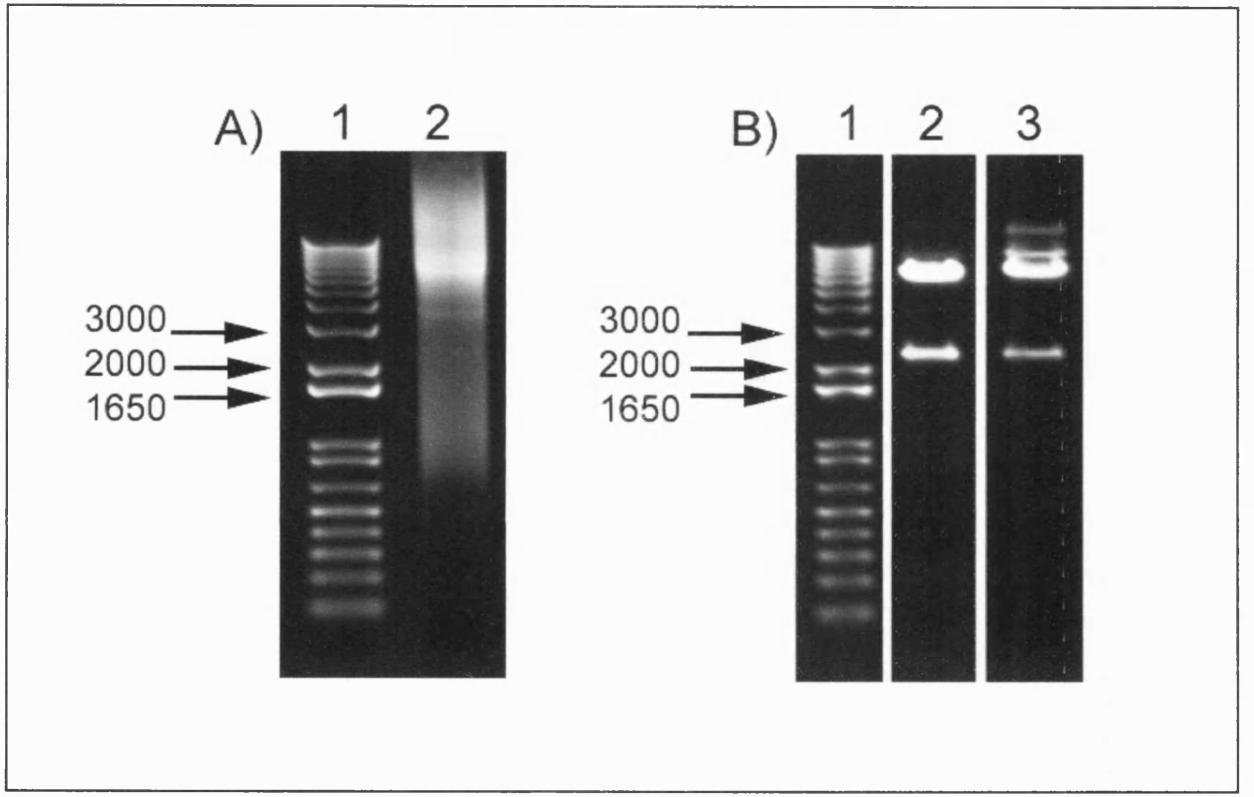

Figure 5.3 **Site-directed mutagenesis of serine 488 to alanine 488 at the C-terminus of GLUT4.** (A) PCR was carried out to specifically mutate serine 488 to alanine 488. Lane 1 = 1 kb plus DNA ladder [I], lane 2 = PCR product. (B) Restriction digestion of the mini-preped DNA. Lane 1 = 1 kb plus DNA ladder, lane 2 = DNA from PCR product, lane 3 = GLUT4-HA wild type positive control.

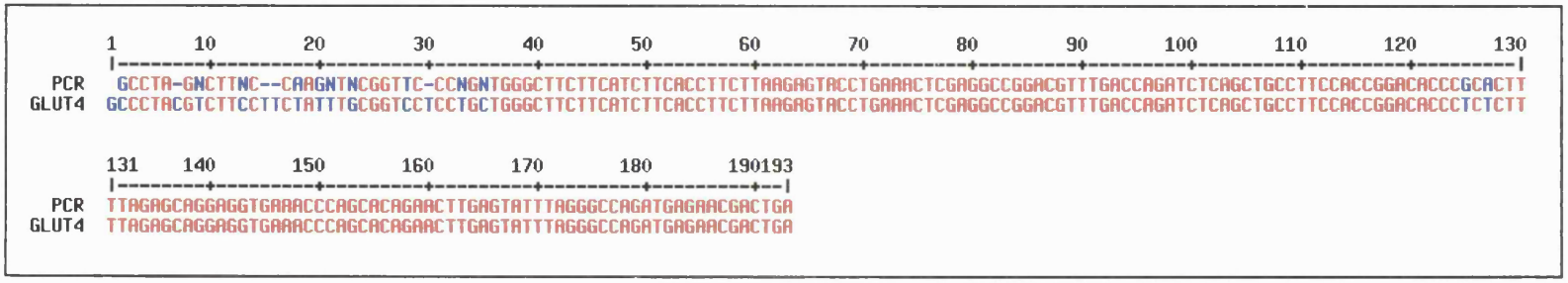

Figure 5.4 **Alignment of the DNA sequence following the site-directed mutagenesis PCR (PCR) with the sequence of wild type GLUT4 DNA (GLUT4).** The bases in red are identical in both wild type GLUT4 and the PCR sequence, whereas the bases in blue differ. – indicates where there are additional bases in one sequence. The alignment was carried out using Multalin (Corpet, 1988).

5.2.2 Transfection of the GLUT4-HA Constructs into Primary Adipocyte Cells

The method used to transfect primary adipocytes with the GLUT4-HA DNA was adapted by Dr. Scott Lawrence, for use in our laboratory, from the method carried out by Quon *et al* (Quon *et al.*, 1994). Electroporation conditions (the voltage, capacitance and the number of shocks) were investigated. It was concluded that the optimal electroporation conditions was one shock at 400 V and 500 μF. The length of time the cells were incubated in culture following transfection, to allow expression of the GLUT4-HA protein, was also investigated. Culture times of 5 h and 16 h were investigated. It was found that culturing for 16 h resulted in a higher level of overexpressed protein than at 5 h but the fold insulin response was lower. The decrease in the fold insulin response at 16 h was because the overexpressed GLUT4-HA protein was not targeted correctly to the plasma membrane following insulin stimulation, rather than the failure to keep the transfected GLUT4-HA protein in an intracellular location in basal adipocytes (Al Hasani *et al.*, 1999). This suggested that the cell had a limited capacity to recruit GLUT4 to the plasma membrane following insulin stimulation. As a result of the decreased response to insulin after 16 h in culture, the cells were incubated in culture for 5 h before the antibody-binding assay was carried out.

In a single experiment, wild type GLUT4-HA and one mutated construct was transfected into primary adipocytes. This was carried out, in triplicate, for each mutation.

5.2.3 Cell-Surface Expression of GLUT4-HA Constructs

The plasma membrane levels of GLUT4-HA, in response to insulin, were closely related to the level of GLUT-HA transfected into the cell. Therefore, it was essential to determine the expression levels of both the endogenous GLUT4 protein and the transfected GLUT4-HA protein, in each sample, before the effect of each mutation could be elucidated.

Following transfection of the wild type and mutated GLUT4-HA vectors (as well as a control containing no GLUT4-HA vector), the cells were allowed to recover for 5 hours. Each of the conditions were split into two and either left in the basal state or stimulated with insulin. Trafficking was then stopped by the addition of potassium cyanide. A sample of the cells was taken from each condition and run on an SDS-PAGE gel. Following transfer to nitrocellulose, Western blot analysis was carried out with a mouse monoclonal anti-HA antibody which was used to detect the transfected GLUT4-HA protein. An anti-C-terminal GLUT4 antibody raised in rabbit was also used to detect the total level of GLUT4 in the cell. For comparison between the different conditions, the level of transfected GLUT4-HA needed to be normalised to the level of heterologously expressed GLUT4. This is illustrated with an example of an experiment carried out using the GLUT4-HA S488A vector (Figure 5.5). GLUT4 was detected in each sample of the Western blot (Figure 5.5 a). There was an equal intensity of GLUT4 in each lane because the anti-C-terminal GLUT4 antibody was essentially only recognising the endogenous GLUT4 protein because the level of transfected GLUT4-HA in the cell was very low. The transfected GLUT4-HA protein, as identified with the anti-HA antibody, was detected in all of the samples that had had the GLUT4-HA vector transfected into the cell. No GLUT4-HA was detected in the control sample, lane 1 (Figure 5.5 b). As the anti-C-terminal GLUT4 antibody was essentially only recognising endogenous GLUT4, the intensity of the GLUT4-HA bands in each lane was normalised to an equal level of endogenous GLUT4. The percentage of GLUT4-HA in each lane was then calculated (Figure 5.5 c).

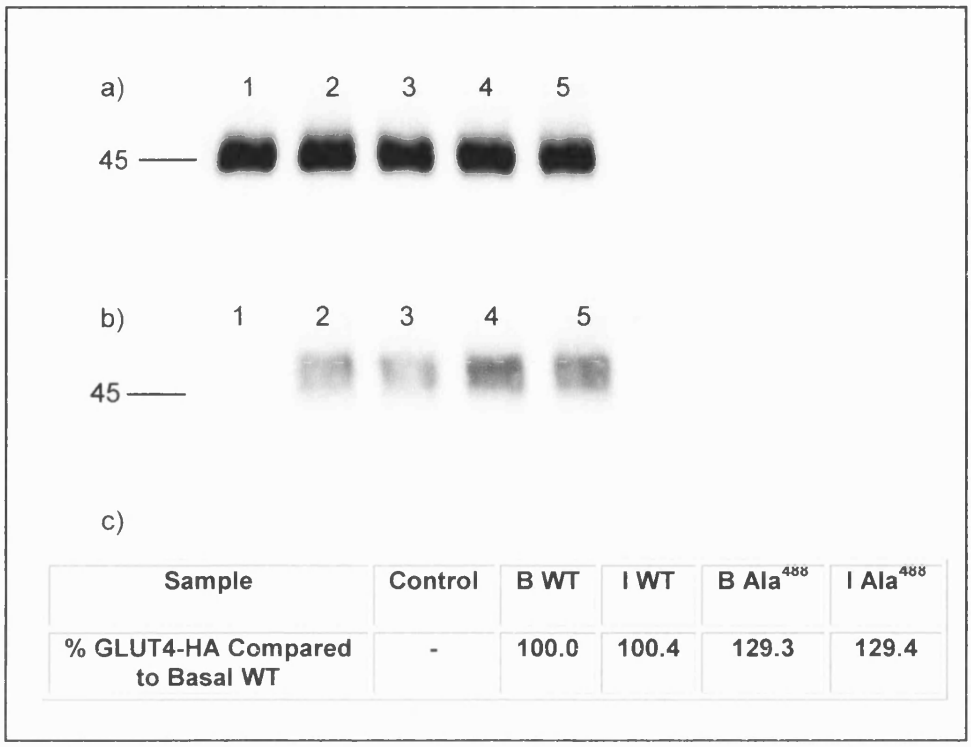

c)

Sample	Control	B WT	I WT	B Ala^{488}	I Ala^{488}
% GLUT4-HA Compared to Basal WT	-	100.0	100.4	129.3	129.4

Figure 5.5 **Relative protein expression levels of the GLUT4-HA wild type and GLUT4-HA S488A vectors.** Isolated rat adipocytes were transfected with 0.4 µg of plasmid DNA and 400 µg carrier DNA (sheared herring sperm DNA) per vector. Following recovery, an aliquot of basal and insulin stimulated cells was taken and run on an SDS-PAGE gel. Lane 1 = control (transfection only with the carrier DNA), lanes 2 and 3 = basal (2) and insulin (3) stimulated cells after transfection with the wild type GLUT4-HA vector, lanes 4 and 5 = basal (4) and insulin (5) stimulated cells after transfection with the GLUT4-HA S488A vector. Following transfer to nitrocellulose, Western blot analysis was carried out with the anti-C-terminal GLUT4 antibody (a) and the monoclonal anti-HA antibody (b). The antibodies detected heterologously expressed GLUT4 in the cell and transfected GLUT4-HA respectively. The amount of transfected plasmid in the cell was quantified (c). Results were normalised to an equal level of heterologously expressed GLUT4 in each of the samples.

There was an equal level of transfection in the basal and insulin-stimulated samples of the same vector. This was as expected because the cells transfected with the same vector were only split after transfection and so should have the same level of transfected vector. The mutated GLUT4-HA S488A vector had a 1.29-fold higher level of transfection than the wild type GLUT4-HA vector. This must be taken into account when comparing the level of GLUT4 at the plasma membrane between wild type and S488A transfected cells.

5.2.4 The Effect of the Mutations on the Level of GLUT4 at the Plasma Membrane

Dr. Scott Lawrence also optimised the antibody-binding assay for use in our laboratory. Different ways to detect the HA signal were investigated. Amplex® Red [MP] and fluorescein digalactosidase (FDG) [MP] were both tested for use as a substrate. Amplex Red, in the presence of peroxidase, reacts with H_2O_2 to produce resorufin, a red-fluorescent oxidation product. In contrast, FDG is a fluorogenic substrate for β-Galactosidase and is nonfluorescent. β-Galactosidase hydrolyses FDG, first to fluorescein monogalactosidase and finally to the highly fluorescent fluorescein. In each case, the secondary antibody was conjugated to horseradish peroxidase or β-Galactosidase, respectively. Both methods were successful in monitoring the level of GLUT4-HA at the plasma membrane. However, due to the presence of endogenous peroxides in the cell, the use of Amplex Red resulted in a higher level of background fluorescence. Conversely, FDG resulted in a low level of background fluorescence. The assay was originally carried out using a secondary antibody conjugated to [^{125}I] and the radioactivity was detected by use of a γ-counter (Quon et al., 1994, Al Hasani et al., 1999, Al Hasani et al., 2002). The choice of a fluorescent-based detection assay over a radioactivity-

based assay was due to the less hazardous working conditions of a fluorescent-based assay with no loss in detection sensitivity.

Following transfection of the various GLUT4-HA constructs, the cells were allowed to recover and express the transfected protein for 5 hours. An antibody-binding assay (Section 2.2.13) was then carried out. The principle of the assay was that incubation of the cells with an anti-HA antibody would result in the anti-HA antibody only binding to the transfected GLUT4-HA protein in the plasma membrane of the cells. A secondary antibody conjugated to β-Galactosidase was then incubated to bind to the primary antibody. The fluorogenic substrate FDG was added to an aliquot of cells and the fluorescence monitored was indicative of the level of GLUT4-HA at the plasma membrane. The fluorescence was measured on the FarCyte plate reader [A] over 100 cycles, to determine where the rate of reaction became linear. Each sample was analysed in quadruplicate. A protein assay was also carried out on a separate aliquot of cells. The change in fluorescence per second per mg protein was calculated over the range where the rate of reaction was first order. The average control sample was subtracted and the results were adjusted according to the level of transfection for each construct (Section 5.2.3). Finally, the results were normalised to that of the insulin wild type sample, which was set to 1. The effect of each mutant was tested in three independent experiments. The normalised data from each experiment was averaged before a comparison between the GLUT4-HA wild type vector and the mutant vectors was carried out (Figure 5.6). Any significant difference between the level of GLUT4-HA at the plasma membrane between the wild type and mutant proteins was analysed by use of an unpaired T-test.

To assess the full effects of the mutants, it was necessary to compare the level of GLUT4-HA at the plasma membrane in both basal and insulin-stimulated cells, and to calculate the fold change in the level of GLUT4-HA at the plasma membrane after the cells were stimulated with insulin. This will be referred to

as the fold insulin change in the remainder of the chapter. Use of the fold insulin change for comparisons ensures that any effect of the mutation was real and not due to an equal proportional increase of the level of GLUT4-HA at the plasma membrane in basal and insulin-stimulated cells. The fold insulin change was calculated, from Figure 5.6, as a difference in the mean values of the level of GLUT4-HA in the plasma membrane for basal and insulin-stimulated cells (Figure 5.7).

Insulin stimulated the translocation of all of the mutated GLUT4-HA proteins to the plasma membrane (Figure 5.6 (difference between the orange and blue bars) and Figure 5.7). There was an increase in the plasma membrane level of all of the mutated GLUT4-HA proteins in basal adipocytes, compared to the wild type GLUT4-HA protein. However, the differences between the plasma membrane levels of the wild type and mutated GLUT4-HA proteins were not significant in basal adipocytes (Figure 5.6, orange bars). The plasma membrane levels of the different mutated GLUT4-HA proteins varied in insulin-stimulated adipocytes. There was an extremely significant increase ($p = 0.0002$) in the plasma membrane level of the S488A GLUT4-HA protein compared to the wild type GLUT4-HA protein. There was also an extremely significant decrease ($p < 0.0001$) in the plasma membrane levels of the S10D GLUT4-HA protein compared to the wild type GLUT4-HA protein (Figure 5.6, blue bars). The function of the phosphorylation at each site appeared to be to retain GLUT4 in an intracellular compartment.

Insulin stimulation resulted in a fivefold increase in the plasma membrane levels of the wild type GLUT4-HA protein (Figure 5.7, red column). However, the fold insulin response observed by all the mutated GLUT4-HA proteins was less than that observed with the wild type transporter. There was a significant increase, as reported above, in the level of the S488A GLUT4-HA protein at the plasma membrane after insulin stimulation, in comparison with the wild type GLUT4-HA protein. However, the fold insulin response of the S488A

mutant was the same as the single S10A and the double S10A S488A mutants (fourfold insulin response). This was not hugely different to the wild type vector (fivefold insulin response). Therefore, there was a proportionally equal increase in the plasma membrane levels of S488A GLUT4-HA protein in both basal and insulin-stimulated adipocytes. Thus, the lack of a phosphorylation site at serine 488 does not result in an increased level of GLUT4-HA at the plasma membrane.

In comparison to the wild type GLUT4-HA protein, the S10D GLUT4-HA protein only had a 2.5-fold increase in the level of GLUT4-HA at the plasma membrane following insulin stimulation. The decrease in the plasma membrane level of the S10D GLUT4-HA protein, in insulin-stimulated adipocytes, was therefore real and not due to a corresponding decrease in the plasma membrane level of the S10D GLUT4-HA protein in basal adipocytes.

The only mutation that affected the plasma membrane levels of the GLUT4-HA protein was the S10D mutation. The S10D mutation resulted in a decrease in the level of GLUT4-HA at the plasma membrane and the fold insulin response was halved in comparison to the wild type GLUT4-HA protein. Thus, phosphorylation at serine 10 could result in GLUT4 being retained in an intracellular compartment.

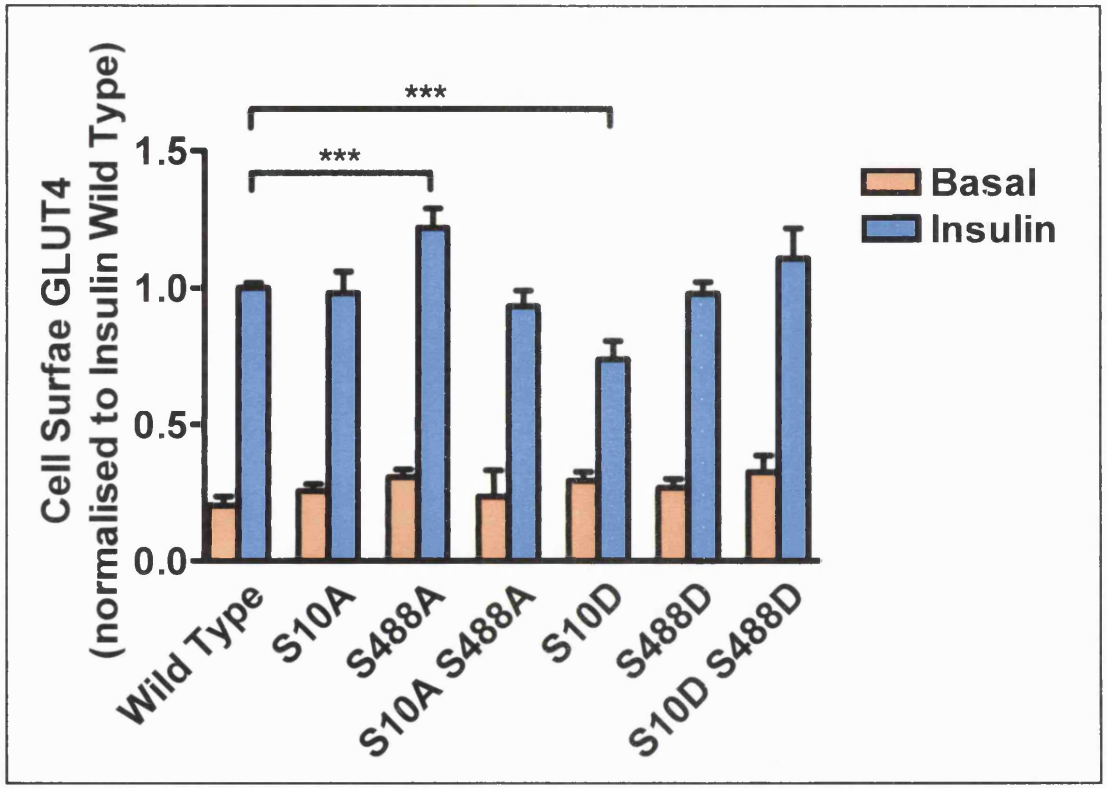

Figure 5.6 **Effect of the phosphorylation site at serine 10 and serine 488 on the translocation of GLUT4 to the cell surface in basal and insulin-stimulated adipocytes.** Isolated adipocyte cells were transfected with 0.4 µg plasmid DNA and cultured for 5 hours. After harvesting, the cells were incubated without (basal, orange bars) or with insulin (blue bars). The level of GLUT4 at the plasma membrane was determined using an antibody-binding assay (Section 2.2.13). The data for each mutant is the combined mean ± S.E.M. from 3 independent experiments performed in quadruplicate. The data for the wild type data is the combined mean ± S.E.M. from 18 independent experiments performed in quadruplicate. ***, $p<0.001$ (unpaired t-test; compared to wild type values).

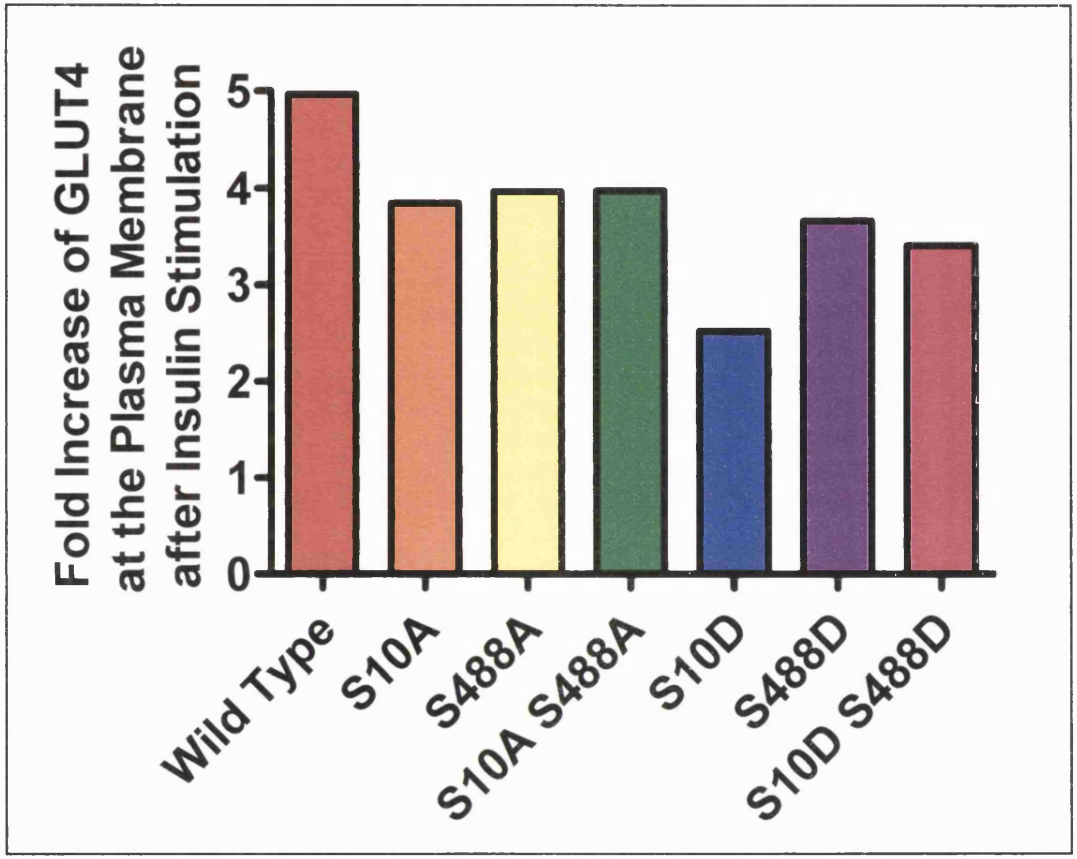

Figure 5.7 **Fold increase in the plasma membrane levels of GLUT4-HA after stimulation with insulin, for the wild type and mutated proteins.** The fold insulin change was calculated, from Figure 5.6, as a difference in the mean values of the level of GLUT4 in the plasma membrane between basal and insulin-stimulated cells.

5.3 Discussion

The targeting potential of the phosphorylation motifs was addressed by transfecting recombinant GLUT4-HA into a physiologically relevant cell type. The recombinant GLUT4-HA had either an aspartic acid or an alanine residue substitution at each of the phosphorylation sites, to mimic constitutively phosphorylated and non-phosphorylated forms of the protein respectively.

In the present study, there was a fivefold increase in the level of wild type GLUT4-HA at the cell surface in response to insulin. This was comparable to a previously reported value of 6.7-fold (Al Hasani *et al.*, 2002). The sensitivity of the assay was therefore similar to the original assay.

The only mutation to have a real effect on the translocation of GLUT4 was the S10D mutation. There was a significant decrease in the level of S10D GLUT4-HA at the plasma membrane of insulin-stimulated adipocytes. There was also a lower fold increase in the plasma membrane levels of the S10D GLUT4 protein following insulin stimulation, compared to the wild type GLUT4-HA protein.
There was a significantly higher level of the S488A GLUT4-HA protein in the plasma membrane of insulin-stimulated adipocytes, but there was also an increase in the level of S448A GLUT4-HA in basal adipocytes, although this was not significant. Therefore, following insulin stimulation, there was no fold change in the level of the S448A GLUT4-HA protein at the plasma membrane. This indicated the need for caution when analysing the effect of the mutations.

The result of the S10D mutation strongly argues that, following insulin stimulation, the function of the phosphorylation site at serine 10 is to retain GLUT4 in an intracellular compartment. This could occur in different ways. The phosphorylation could hold the GLUT4 in an intracellular compartment,

decrease the rate of exocytosis or increase the rate of endocytosis. Either way, the level of GLUT4 at the plasma membrane would decrease.

Even though the S10D mutation had an effect on the level of GLUT4 at the plasma membrane, the S10A mutation did not have an effect. The S10A mutation should not necessarily cause an increase in the level of GLUT4 at the plasma membrane (the opposite affect of S10D). The fact that the S10A mutant did not have an effect could be because it was the phosphorylation that retained GLUT4 in an intracellular localisation, and so no phosphorylation at serine 10 would result in the S10A GLUT4-HA protein acting like the wild type transporter. The double mutation was carried out to determine if the two phosphorylation sites were co-operative in function, i.e. if both sites were needed to be phosphorylated before an effect was observed. The double mutation, S10D and S488D, did not have any effect on the level of GLUT4 at the plasma membrane, even though the S10D mutation did have an effect. Therefore, phosphorylation at serine 488 is not required before the effect of the phosphorylation at serine 10 is observed. The effect of the mutation at serine 488 is unknown but appears to override the function of the phosphorylation at serine 10. It would be interesting to carry out double mutations, with alanine being mutated at one phosphorylation site and aspartic acid at the other site, and to determine the effect of this mutation on GLUT4 translocation.

Many other studies have used mutagenesis to investigate the role of particular amino acids in the function of GLUT4 (Marsh et al., 1995, Araki et al., 1996, Al Hasani et al., 2002). Most of the studies have not included the sites of phosphorylation but a few studies have mutated serine 10 and serine 488 (Garippa et al., 1996, Marsh et al., 1998, Khan et al., 2004).

Garippa *et al* investigated the effect of both the phosphorylation site at serine 488 and the dileucine motif in the trafficking of GLUT4 (Garippa *et al.*, 1996). Serine 488 was mutated to either alanine or aspartic acid and the dileucine motif (LL) was mutated to a dialanine motif (AA). The mutations at the LL and serine 488 resulted in a reduction in the rate of internalisation, with more

GLUT4 being present at the plasma membrane. The AA mutation reduced the rate of internalisation by tenfold but the serine 488 mutation only reduced it by threefold. As both mutations decreased the rate of internalisation, the study concluded that it was the Ser-Leu-Leu motif and not just the Leu-Leu motif that was an important signalling motif in GLUT4. The problem with the conclusion involving the serine 488 mutation was that both serine 488 mutated to alanine and to aspartic acid led to a threefold reduction in internalisation. Therefore, the presence of a phosphorylated residue did not change the rate of internalisation of the mutated protein. Thus, the experiment did not give a clear indication as to the effect of the phosphorylation at serine 488 (Garippa *et al.*, 1996). Garippa *et al* were studying the effect of the phosphorylation motif on the rate of internalisation in non-insulin-responsive cells. Therefore the results by Garippa *et al* should be compared to the plasma membrane levels of the GLUT4-HA protein in basal adipocytes from the present study. The results from the study by Garippa *et al* varied from the present study. In the present study, there was not a significant difference between the plasma membrane levels of the GLUT4-HA protein mutated at serine 488 and the wild type GLUT4-HA protein. The difference in the results between the two studies could be because different cell types were used. A physiologically relevant cell type (adipocytes) was used in this study and the whole GLUT4 protein was expressed. However, Garippa and colleagues only expressed their construct in CHO cells which do not contain the same cellular machinery as insulin-sensitive cells. The design of the construct used in CHO cells could also explain why different results were obtained. In CHO cells, only the C-terminus of GLUT4 was expressed as a chimera with the transferrin receptor (Garippa *et al.*, 1996). The transfected construct could also have been overexpressed to a higher level than in the present study, which could also account for the differences observed.

A study by Marsh *et al* investigated the role of the phosphorylation site at serine 488 in an insulin-responsive tissue (3T3-L1 adipocytes). Serine 488 was mutated into an alanine residue (S488A) and was transfected into 3T3-L1

fibroblasts. Phosphorylation of GLUT4 did not affect the subcellular localisation of GLUT4 in either basal or insulin-stimulated adipocytes (Marsh *et al.*, 1998). The present study is in agreement with the result by Marsh *et al* because the S488A mutation did not affect the level of GLUT4 at the plasma membrane.

The structural motifs involved in the initial sorting of GLUT4 from the biosynthetic pathway to the GLUT4 storage vesicle (GSV) have been investigated using GLUT4-GLUT1 chimeras (Khan *et al.*, 2004). The amino terminus and the large cytoplasmic loop between transmembrane domains 6 and 7 were found to be necessary for the efficient initial trafficking following biosynthesis of the GLUT4 protein. More importantly, residues Phe^{5} and Ile^{8} and to a lesser extent Asp^{12} and Gly^{13}, along with residues 229 – 271 in the large intracellular loop, were identified as the essential residues. The amino-terminus of GLUT4 is involved in the initial sorting step and in plasma membrane endocytosis (Al Hasani et al., 2002, Khan et al., 2004). The presence of a phosphorylated serine 10 residue could, therefore, differentiate between the two roles elicited by the FQQI motif. A S10A mutation was carried out by Khan and colleagues. The S10A mutation did not affect the entry of the mutated protein into the GSV (Khan *et al.*, 2004). The result from Khan *et al* is in agreement with the result from the present study in which S10A had no affect on the trafficking of GLUT4. However, it may not be the serine residue, *per se*, that is important but it may be the phosphate on the serine residue that primarily has an effect on the trafficking of GLUT4. It would have been interesting if Khan *et al* had mutated serine 10 to aspartic acid to identify if the phosphorylation at serine 10 had a role in the initial sorting step (from the biosynthetic pathway into the GSV) or if the phosphorylation was more likely to have a role in the endocytic pathway.

Each phosphorylation site in GLUT4 is in close proximity to a signalling motif (FQQI or LL) involved in the subcellular trafficking of GLUT4. The phosphorylation sites could modulate the effect of these signalling motifs.

Mutations have been carried out on the GLUT4-HA vector at the dileucine motif ($L^{489}L^{490}$) or at F^5 in the N-terminal FQQI motif (Al Hasani *et al.*, 2002). The specified residues were mutated to alanine residues. The LL motif is adjacent to the serine 488 phosphorylation site, and the F^5QQI motif is upstream of the serine 10 phosphorylation site. The level of the mutated GLUT4 protein at the plasma membrane was compared to that of the wild type. The $L^{498}L^{490} \rightarrow$ AA mutation did not have any effect on the cell surface expression of the GLUT4-HA protein. However, the F5A mutation resulted in an increase in the cell surface level of GLUT4 in both basal and insulin-stimulated adipocytes. The result documented in this chapter follows the result of the study investigating the effect of the trafficking motifs. Serine 488 or the LL motif did not have an effect in either study. It had been reported that the mutated LL motif only has an effect at high levels of overexpression (Marsh *et al.*, 1995). The study detailed in this chapter did not test high expression levels of the mutated DNA. However, high expression levels were tested by Al-Hasani *et al*, and there was no change in the plasma membrane expression levels in any of the constructs tested (Al Hasani *et al.*, 2002).

The F5A mutation decreases the rate of internalisation, i.e. there was more GLUT4 at the plasma membrane in both basal and insulin-stimulated cells (Al Hasani *et al.*, 2002). Perhaps, phenylalanine 5 and phosphorylation at serine 10 work together in the internalisation mechanism of GLUT4. It has been shown that F^5QQI is a binding site for the medium chain of the adaptor proteins μ1, μ2, and μ3A (Al Hasani *et al.*, 2002). The phosphorylation could be involved in modulating the binding site for the adaptor protein. The phosphorylation could also have an independent role. It would be interesting to investigate the subcellular trafficking kinetics of the S10D mutation and to calculate the rate of endocytosis (Araki et al., 1996, Al Hasani et al., 2002). This would give some indication of the role of the phosphorylation of serine 10 and any potential link to the trafficking of the FQQI motif. After transfection, the cells would be treated with insulin. Wortmannin treatment would then prevent

any further translocation. The rate of internalisation could be calculated using the antibody-binding assay at different times after the addition of wortmannin.

Due to the lack of time, further studies using the mutant GLUT4-HA vector generated in this chapter could not be carried out. Some of the follow up experiments are detailed below and would provide an interesting extension to the current study.

Phosphorylation at serine 10 decreases the level of GLUT4 at the plasma membrane of insulin-stimulated adipocytes but how the phosphorylation elicits the effect needs further investigation. Phosphorylation at serine 488 did not affect the level of GLUT4 at the plasma membrane in either basal or insulin-stimulated adipocytes. The antibody-binding assay cannot identify any changes in the intracellular compartment in which the GLUT4 resides. The serine 488 phosphorylation could therefore modulate the intracellular localisation of the GLUT4 protein. The subcellular localisation of the mutants could be investigated using confocal microscopy following the transfection of the GLUT4-HA mutants into primary adipocyte cells. Staining the transfected adipocytes with the anti-HA antibody would identify the localisation of the transfected construct. An anti-GLUT4 antibody could not be used to detect the endogenous protein as it would also stain the transfected GLUT4 protein. However, the insulin-responsive aminopeptidase (IRAP) protein has been identified as a major protein in GLUT4-containing vesicles (Keller *et al.*, 1995). There is evidence that GLUT4 and IRAP share the same trafficking routes in adipose cells (Ross et al., 1996, Garza and Birnbaum, 2000). Staining adipocytes using an anti-IRAP antibody would therefore identify the vesicles containing endogenous GLUT4.

The mutant constructs would be useful to corroborate the results from chapter 4 and to check if there are only two phosphorylated residues in GLUT4 or to identify if there is an additional phosphorylation site in the C-terminal peptide. Primary adipocyte cells would be transfected with the S10A S488A GLUT4-HA

vector. The S10A S488A mutant cannot be phosphorylated at either residue 10 or residue 488. The cells would then be labelled with [$^{32}P_i$] and the S10A S488A GLUT4-HA protein could be isolated from the endogenous protein by immunoprecipitation with the anti-HA antibody. Any incorporation of radioactivity into the mutant GLUT4 protein could be detected and therefore any phosphorylation sites, in addition to serine 10 and serine 488, would be identified.

Insulin had opposing effects on the phosphorylation state of GLUT4 in adipocytes and cardiomyocytes (chapter 4). To see if the phosphorylation has opposing functions between the two cell types, the antibody-binding assay needs to be carried out after cardiomyocytes have been transfected with the mutated GLUT4-HA constructs. However, cardiomyocytes cannot be transfected by electroporation. Transfection in cardiomyocytes is commonly carried out by the use of adenovirus. However, before this can be done, each of the mutated GLUT4-HA DNA constructs needs to be cloned into separate adenoviral plasmids and the transfection technique has to be optimised which can be a very lengthy process.

In addition to being involved in the translocation of GLUT4, the phosphorylation sites could also affect the transport activity of the transporter. Glucose uptake experiments, in which the mutated DNA is transfected into cells lacking endogenous GLUT4, would test whether the mutation influenced the transport activity of GLUT4.

5.4 Conclusion

The wild type GLUT4-HA vector has been mutated at the GLUT4 phosphorylation sites. The phosphorylated serines were successfully mutated to either aspartic acid, which mimics the negative charge of the phosphorylated

serine, or to alanine, which mimics the unphosphorylated form of the serine residue. These mutations were used to investigate the role of the phosphorylation in the translocation of GLUT4 to the plasma membrane in a physiologically relevant cell system. The phosphorylation at serine 10 appears to cause a decrease in the level of GLUT4 at the plasma membrane of insulin-stimulated adipocytes. Phosphorylation of serine 488 has a different role and this role could involve a change of localisation in the intracellular pool of GLUT4.

6 Overall Discussion

Phosphorylation sites have been identified in two regions in the GLUT4 protein. One site which has been identified previously is at the C-terminus of GLUT4 and is serine 488 (Lawrence, Jr. *et al.*, 1990a). The second site, at the N-terminus of GLUT4, is a novel site that was predicted from the homology of the N-terminus of GLUT4 with the α-subunit of GAD65. Comparison with a phosphorylation prediction program has led to the prediction that the sites of phosphorylation are at serine 10 and serine 488 in GLUT4. This study has focussed on the identification of the second phosphorylation site in GLUT4 and its function.

If the stoichiometry of the phosphorylation in basal adipocytes is 0.1 mole phosphate / mole GLUT4 (Section 4.2.4.2.6), then only a small population of GLUT4 is phosphorylated at one time (0.05 mole phosphate / mole GLUT4 at each terminus). There are two pieces of evidence that suggests that the GLUT4 phosphorylated at serine 10 has an intracellular location. Firstly, confocal microscopy studies using both of the anti-pSer^{10} antibodies raised in rabbit (purified from the second and final bleed serums) has identified a protein in the peri-nuclear region of the cell in both basal and insulin-stimulated conditions. No staining was present at the plasma membrane in either condition (Section 3.2.1.5). Secondly, mutation of the serine 10 residue to an aspartic acid residue (to mimic a constitutively phosphorylated residue), resulted in a decrease in the level of GLUT 4 at the plasma membrane, i.e. more GLUT4 had an intracellular location (Section 5.2.4). Therefore, the small pool of GLUT4 that is phosphorylated at the serine 10 has an intracellular localisation.

The small pool of GLUT4 that is phosphorylated at serine 10 could be GLUT4 that is in the synthetic pathway as previously discussed from the confocal microscopy study using brefeldin A in 3T3-L1 adipocytes (Section 3.2.1.5). A

study investigating the initial sorting of GLUT4, following biosynthesis, identified the N-terminus of GLUT4 as being an important region in the process (Khan *et al.*, 2004). However, a mutation of serine 10 to an alanine residue had no effect. It is possible that phosphorylation at serine 10 during biosynthesis is important in the initial intracellular sorting of GLUT4. When GLUT4 has reached the correct compartment, it could be dephosphorylated and then the GLUT4 would become available for insulin-responsive glucose transport. The FQQI motif is an important trafficking motif and is involved in the internalisation of GLUT4 from the plasma membrane. Phosphorylation of the serine 10 residue could work in combination with the FQQI and could therefore provide a distinction between the intracellular sorting of GLUT4 to the GSV and internalisation from the plasma membrane.

Alternatively, GLUT4 could be phosphorylated to retain the protein in an intracellular location. This could happen, for example, if the mechanism of GLUT4 cycling put forward by the James lab is correct (Govers et al., 2004, Coster et al., 2004). If there is a small latent pool of GLUT4 transporters, which do not translocate to the plasma membrane in either basal or insulin-stimulated cells, then phosphorylation at serine 10 could keep this pool tethered in an intracellular location (Section 1.5.2). Indeed the anti-pSer^{10} antibody staining remained intracellular in both basal and insulin-stimulated cells.

In adipocytes, insulin increases the level of phosphorylation of GLUT4 at serine 10 and the phosphorylated protein has an intracellular localisation. However, insulin also stimulates the translocation of GLUT4 to the plasma membrane. Therefore, insulin appears to have opposing functions regarding the subcellular localisation of the protein.

In adipocytes, only a small proportion of GLUT4 is phosphorylated at serine 10 and the translocation experiments identify the effect of the phosphorylation when the protein has been overexpressed. If serine 10 is phosphorylated 0.05 mole phosphate / mole GLUT4 in basal cells, then in insulin stimulated cells there would be 0.07 mole phosphate / mole GLUT4. The phosphorylated

GLUT4 could therefore be internalised after insulin stimulation, but due to the fact that there is a large movement of GLUT4 to the plasma membrane, this small effect is not identified.

The function of the phosphorylation at serine 488 has not been further elucidated in this study, although it is not involved in GLUT4 trafficking to the plasma membrane (Section 5.2.4). An antibody to the phosphorylated serine 488 has not been raised and production of such an antibody would aid the study of the function of this phosphorylation site both from use in Western blot analysis and confocal microscopy. The antibody would also be invaluable in the determination of the subcellular localisation of GLUT4 phosphorylated at serine 488.

7 Overall Conclusion

This thesis has included different approaches to investigating GLUT4 phosphorylation. Antibodies have been raised to the phosphorylated serine 10 residue in the N-terminus of GLUT4 and these antibodies have been purified and partially characterised. However, further characterisation is needed before the antibodies can be further used in the investigation of GLUT4 phosphorylation.

In the first study, the sites of phosphorylation were identified by the use of a technique in which adipocytes and cardiomyocytes were labelled with [$^{32}P_i$]. The effect insulin, okadaic acid, CKII inhibitors and oligomycin had on the phosphorylation state of GLUT4 was also investigated. Two phosphorylation sites have been identified, a novel phosphorylation site was identified at serine 10 at the N-terminus of GLUT4, and the second site was at serine 488 at the C-terminus of GLUT4 which had previously been identified (Lawrence, Jr. *et al.*, 1990a).

The second study involved the site-directed mutagenesis of the phosphorylated residues. The effect each phosphorylation site had on the level of GLUT4 at the plasma membrane was investigated. The only mutation to have an effect was the mutation of serine 10 to an aspartic acid residue. Introduction of this mutation caused a decrease in the level of GLUT4 at the plasma membrane. Thus the role for the phosphorylation of serine 10 in defining an intracellular localisation was implicated, e.g. during biosynthesis or as an intracellular retention factor.

The ultimate objectives of this investigation would be to identify the function of each of the phosphorylation sites, to identify the role the phosphorylation has in glucose transport and to investigate how phosphorylation changes, if it does, in Type 2 diabetes. The work presented in this thesis, along with the future work

outlined in the discussion sections, can be combined and together may provide a useful insight into the mechanism whereby insulin stimulates the entry of glucose into insulin-responsive tissues.

People suffering from Type 2 diabetes have impaired insulin-stimulated glucose transport. However, when comparing diabetic patients to non-diabetic patients it was found that the levels of GLUT4 and GLUT1 expressed in the muscles of these patients are not altered (Kahn, 1992). Understanding the mechanism by which insulin stimulates glucose transport in adipocyte and muscle cells is therefore essential before this disease can be controlled.

8 References

Ahn, M.Y., K.D.Katsanakis, F.Bheda, and T.S.Pillay. 2004. Primary and Essential Role of the Adaptor Protein APS for Recruitment of Both c-Cbl and Its Associated Protein CAP in Insulin Signaling. *J. Biol. Chem.* 279:21526-21532.

Al Hasani, H., R.K.Kunamneni, K.Dawson, C.S.Hinck, D.Muller-Wieland, and S.W.Cushman. 2002. Roles of the N- and C-termini of GLUT4 in endocytosis. *J. Cell Sci.* 115:131-140.

Al Hasani, H., C.S.Hinck, and S.W.Cushman. 1998. Endocytosis of the Glucose Transporter GLUT4 Is Mediated by the GTPase Dynamin. *J. Biol. Chem.* 273:17504-17510.

Al Hasani, H., D.R.Yver, and S.W.Cushman. 1999. Overexpression of the glucose transporter GLUT4 in adipose cells interferes with insulin-stimulated translocation. *FEBS Lett.* 460:338-342.

Alessi, D.R., S.R.James, C.P.Downes, A.B.Holmes, P.R.Gaffney, C.B.Reese, and P.Cohen. 1997. Characterization of a 3-phosphoinositide-dependent protein kinase which phosphorylates and activates protein kinase Balpha. *Curr. Biol.* 7:261-269.

Araki, S., J.Yang, M.Hashiramoto, Y.Tamori, M.Kasuga, and G.D.Holman. 1996. Subcellular trafficking kinetics of GLU4 mutated at the N- and C-terminal. *Biochem. J.* 315:153-159.

Avruch, J., M.C.Alexander, J.L.Palmer, M.W.Pierce, R.A.Nemenoff, P.J.Blackshear, J.P.Tipper, and L.A.Witters. 1982. Role of insulin-stimulated protein phosphorylation in insulin action. *Fed. Proc.* 41:2629-2633.

Backer, J.M., M.G.Myers, Jr., S.E.Shoelson, D.J.Chin, X.J.Sun, M.Miralpeix, P.Hu, B.Margolis, E.Y.Skolnik, and J.Schlessinger. 1992. Phosphatidylinositol 3'-kinase is activated by association with IRS-1 during insulin stimulation. *EMBO J.* 11:3469-3479.

Bae, S.S., H.Cho, J.Mu, and M.J.Birnbaum. 2003. Isoform-specific Regulation of Insulin-dependent Glucose Uptake by Akt/Protein Kinase B. *J. Biol. Chem.* 278:49530-49536.

Bandyopadhyay, G., Y.Kanoh, M.P.Sajan, M.L.Standaert, and R.V.Farese. 2000. Effects of Adenoviral Gene Transfer of Wild-Type, Constitutively Active, and Kinase-Defective Protein Kinase C-λ on Insulin-Stimulated Glucose Transport in L6 Myotubes. *Endocrinology* 141:4120-4127.

Bandyopadhyay, G., M.L.Standaert, L.Galloway, J.Moscat, and R.V.Farese. 1997. Evidence for Involvement of Protein Kinase C (PKC)-ζ and Noninvolvement of Diacylglycerol-Sensitive PKCs in Insulin-Stimulated Glucose Transport in L6 Myotubes. *Endocrinology* 138:4721-4731.

Bandyopadhyay, G., M.L.Standaert, M.P.Sajan, Y.Kanoh, A.Miura, U.Braun, F.Kruse, M.Leitges, and R.V.Farese. 2004. Protein Kinase C-λ Knockout in Embryonic Stem Cells and Adipocytes Impairs Insulin-Stimulated Glucose Transport. *Mol. Endocrinol.* 18:373-383.

Bao, S., R.M.Smith, L.Jarett, and W.T.Garvey. 1995. The effects of brefeldin A on the glucose transport system in rat adipocytes. Implications regarding the intracellular locus of insulin-sensitive Glut4. *J. Biol. Chem.* 270:30199-30204.

Batteiger, B., W.J.Newhall, and R.B.Jones. 1982. The use of Tween 20 as a blocking agent in the immunological detection of proteins transferred to nitrocellulose membranes. *J. Immunol. Methods* 55:297-307.

Baumann, C.A., V.Ribon, M.Kanzaki, D.C.Thurmond, S.Mora, S.Shigematsu, P.E.Bickel, J.E.Pessin, and A.R.Saltiel. 2000. CAP defines a second signalling pathway required for insulin-stimulated glucose transport. *Nature* 407:202-207.

Begum, N., W.Leitner, J.E.Reusch, K.E.Sussman, and B.Draznin. 1993. GLUT-4 phosphorylation and its intrinsic activity. Mechanism of Ca(2+)-induced inhibition of insulin-stimulated glucose transport. *J. Biol. Chem.* 268:3352-3356.

Belke, D.D., S.Betuing, M.J.Tuttle, C.Graveleau, M.E.Young, M.Pham, D.Zhang, R.C.Cooksey, D.A.McClain, S.E.Litwin, H.Taegtmeyer, D.Severson, C.R.Kahn, and E.D.Abel. 2002. Insulin signaling coordinately regulates cardiac size, metabolism, and contractile protein isoform expression. *J. Clin. Invest.* 109:629-639.

Belsham, G.J., R.M.Denton, and M.J.Tanner. 1980. Use of a novel rapid preparation of fat-cell plasma membranes employing Percoll to investigate the effects of insulin and adrenaline on membrane protein phosphorylation within intact fat-cells. *Biochem. J.* 192:457-467.

Berwick, D.C., G.C.Dell, G.I.Welsh, K.J.Heesom, I.Hers, L.M.Fletcher, F.T.Cooke, and J.M.Tavare. 2004. Protein kinase B phosphorylation of PIKfyve regulates the trafficking of GLUT4 vesicles. *J. Cell Sci.* 117:5985-5993.

Bialojan, C. and A.Takai. 1988. Inhibitory effect of a marine-sponge toxin, okadaic acid, on protein phosphatases. Specificity and kinetics. *Biochem. J.* 256:283-290.

Birnbaum, M.J. 1989. Identification of a novel gene encoding an insulin-responsive glucose transporter protein. *Cell* 57:305-315.

Bjornholm, M., A.R.He, A.Attersand, S.Lake, S.C.Liu, G.E.Lienhard, S.Taylor, P.Arner, and J.R.Zierath. 2002. Absence of functional insulin receptor substrate-3 (IRS-3) gene in humans. *Diabetologia* 45:1697-1702.

Blom, N., S.Gammeltoft, and S.Brunak. 1999. Sequence and structure-based prediction of eukaryotic protein phosphorylation sites. *J. Mol. Biol.* 294:1351-1362.

Blom, N., T.Sicheritz-Ponten, R.Gupta, S.Gammeltoft, and S.Brunak. 2004. Prediction of post-translational glycosylation and phosphorylation of proteins from the amino acid sequence. *Proteomics* 4:1633-1649.

Bose, A., A.Guilherme, S.I.Robida, S.M.Nicoloro, Q.L.Zhou, Z.Y.Jiang, D.P.Pomerleau, and M.P.Czech. 2002. Glucose transporter recycling in response to insulin is facilitated by myosin Myo1c. *Nature* 420:821-824.

Bravo, D.A., J.B.Gleason, R.I.Sanchez, R.A.Roth, and R.S.Fuller. 1994. Accurate and efficient cleavage of the human insulin proreceptor by the human proprotein-processing protease furin. Characterization and kinetic parameters using the purified, secreted soluble protease expressed by a recombinant baculovirus. *J. Biol. Chem.* 269:25830-25837.

Brazil, D.P. and B.A.Hemmings. 2001. Ten years of protein kinase B signalling: a hard Akt to follow. *Trends Biochem. Sci.* 26:657-664.

Brooks, C.C., P.E.Scherer, K.Cleveland, J.L.Whittemore, H.F.Lodish, and B.Cheatham. 2000. Pantophysin is a phosphoprotein component of adipocyte transport vesicles and associates with GLUT4-containing vesicles. *J. Biol. Chem.* 275:2029-2036.

Cai, D., S.Dhe-Paganon, P.A.Melendez, J.Lee, and S.E.Shoelson. 2003. Two New Substrates in Insulin Signaling, IRS5/DOK4 and IRS6/DOK5. *J. Biol. Chem.* 278:25323-25330.

Cain, C.C., W.S.Trimble, and G.E.Lienhard. 1992. Members of the VAMP family of synaptic vesicle proteins are components of glucose transporter-containing vesicles from rat adipocytes. *J. Biol. Chem.* 267:11681-11684.

Carpenter, C.L., B.C.Duckworth, K.R.Auger, B.Cohen, B.S.Schaffhausen, and L.C.Cantley. 1990. Purification and characterization of phosphoinositide 3-kinase from rat liver. *J. Biol. Chem.* 265:19704-19711.

Chang, L., S.H.Chang, and A.R.Saltiel. 2005. Insulin Signaling and the Regulation of Glucose Transport. *Mol. Med.* Epub ahead of print.

Chang, L., R.D.Adams, and A.R.Saltiel. 2002. The TC10-interacting protein CIP4/2 is required for insulin-stimulated Glut4 translocation in 3T3L1 adipocytes. *Proc. Natl. Acad. Sci. U. S. A* 99:12835-12840.

Charron, M.J., F.C.Brosius, III, S.L.Alper, and H.F.Lodish. 1989. A glucose transport protein expressed predominately in insulin-responsive tissues. *Proc. Natl. Acad. Sci. U. S. A* 86:2535-2539.

Chiang, S.H., C.A.Baumann, M.Kanzaki, D.C.Thurmond, R.T.Watson, C.L.Neudauer, I.G.Macara, J.E.Pessin, and A.R.Saltiel. 2001. Insulin-stimulated GLUT4 translocation requires the CAP-dependent activation of TC10. *Nature* 410:944-948.

Chiang, S.H., J.C.Hou, J.Hwang, J.E.Pessin, and A.R.Saltiel. 2002. Cloning and Functional Characterization of Related TC10 Isoforms, a Subfamily of Rho Proteins Involved in Insulin-stimulated Glucose Transport. *J. Biol. Chem.* 277:13067-13073.

Clarke, J.F., P.W.Young, K.Yonezawa, M.Kasuga, and G.D.Holman. 1994. Inhibition of the translocation of GLUT1 and GLUT4 in 3T3-L1 cells by the phosphatidylinositol 3-kinase inhibitor, wortmannin. *Biochem. J.* 300:631-635.

Clement, S., U.Krause, F.Desmedt, J.F.Tanti, J.Behrends, X.Pesesse, T.Sasaki, J.Penninger, M.Doherty, W.Malaisse, J.E.Dumont, Y.Marchand-Brustel, C.Erneux, L.Hue, and S.Schurmans. 2001. The lipid phosphatase SHIP2 controls insulin sensitivity. *Nature* 409:92-97.

Coba, M.P., D.Turyn, and C.Pena. 2003. Synthesis and immunogenic properties of phosphopeptides related to the human insulin receptor. *J. Pept. Res.* 61:17-23.

Coghlan, M.P., T.S.Pillay, J.M.Tavare, and K.Siddle. 1994. Site-specific anti-phosphopeptide antibodies: use in assessing insulin receptor serine/threonine phosphorylation state and identification of serine-1327 as a novel site of phorbol ester-induced phosphorylation. *Biochem. J.* 303:893-899.

Cohen, P., C.F.Holmes, and Y.Tsukitani. 1990. Okadaic acid: a new probe for the study of cellular regulation. *Trends Biochem. Sci.* 15:98-102.

Collawn, J.F., M.Stangel, L.A.Kuhn, V.Esekogwu, S.Q.Jing, I.S.Trowbridge, and J.A.Tainer. 1990. Transferrin receptor internalization sequence YXRF implicates a tight turn as the structural recognition motif for endocytosis. *Cell* 63:1061-1072.

Cope, D.L., S.Lee, D.R.Melvin, and G.W.Gould. 2000. Identification of further important residues within the Glut4 carboxy-terminal tail which regulate subcellular trafficking. *FEBS Lett.* 481:261-265.

Corpet, F. 1988. Multiple sequence alignment with hierarchical clustering. *Nucleic Acids Res.* 16:10881-10890.

Coster, A.C.F., R.Govers, and D.E.James. 2004. Insulin Stimulates the Entry of GLUT4 into the Endosomal Recycling Pathway by a Quantal Mechanism. *Traffic* 5:763-771.

Cushman, S.W. and L.J.Wardzala. 1980. Potential mechanism of insulin action on glucose transport in the isolated rat adipose cell. Apparent translocation of intracellular transport systems to the plasma membrane. *J. Biol. Chem.* 255:4758-4762.

Czech, M.P., A.Chawla, C.W.Woon, J.Buxton, M.Armoni, W.Tang, M.Joly, and S.Corvera. 1993. Exofacial epitope-tagged glucose transporter chimeras reveal COOH- terminal sequences governing cellular localization. *J. Cell Biol.* 123:127-135.

Ducluzeau, P.H., L.M.Fletcher, G.I.Welsh, and J.M.Tavare. 2002. Functional consequence of targeting protein kinase B/Akt to GLUT4 vesicles. *J. Cell Sci.* 115:2857-2866.

Egan, J.J., M.K.Chang, and C.Londos. 1988. A tandem chromatographic column method for assaying cAMP-dependent protein kinase and protein kinase C with synthetic peptide substrates. *Anal. Biochem.* 175:552-561.

Egert, S., N.Nguyen, F.C.Brosius, III, and M.Schwaiger. 1997. Effects of wortmannin on insulin- and ischemia-induced stimulation of GLUT4 translocation and FDG uptake in perfused rat hearts. *Cardiovasc. Res.* 35:283-293.

Eguez, L., A.Lee, J.A.Chavez, C.P.Miinea, S.Kane, G.E.Lienhard, and T.E.McGraw. 2005. Full intracellular retention of GLUT4 requires AS160 Rab GTPase activating protein. *Cell Metab.* 2:263-272.

Elchebly, M., P.Payette, E.Michaliszyn, W.Cromlish, S.Collins, A.L.Loy, D.Normandin, A.Cheng, J.Himms-Hagen, C.C.Chan, C.Ramachandran, M.J.Gresser, M.L.Tremblay, and B.P.Kennedy. 1999. Increased insulin sensitivity and obesity resistance in mice lacking the protein tyrosine phosphatase-1B gene. *Science* 283:1544-1548.

Farese, R.V. 2002. Function and dysfunction of aPKC isoforms for glucose transport in insulin-sensitive and insulin-resistant states. *Am. J. Physiol. Endocrinol. Metab.* 283:E1-11.

Fischer, Y., H.Rose, and H.Kammermeier. 1991. Highly insulin-responsive isolated rat heart muscle cells yielded by a modified isolation method. *Life Sci.* 49:1679-1688.

Flier, J.S., M.Mueckler, A.L.McCall, and H.F.Lodish. 1987. Distribution of glucose transporter messenger RNA transcripts in tissues of rat and man. *J. Clin. Invest.* 79:657-661.

Fritsche, J., B.F.Reber, B.Schindelholz, and C.E.Bandtlow. 1999. Differential cytoskeletal changes during growth cone collapse in response to hSema III and thrombin. *Mol. Cell. Neurosci.* 14:398-418.

Fujiwara, T., K.Oda, S.Yokota, A.Takatsuki, and Y.Ikehara. 1988. Brefeldin A causes disassembly of the Golgi complex and accumulation of secretory proteins in the endoplasmic reticulum. *J. Biol. Chem.* 263:18545-18552.

Fukumoto, H., T.Kayano, J.B.Buse, Y.Edwards, P.F.Pilch, G.I.Bell, and S.Seino. 1989. Cloning and characterization of the major insulin-responsive glucose transporter expressed in human skeletal muscle and other insulin-responsive tissues. *J. Biol. Chem.* 264:7776-7779.

Fuller, W., P.Eaton, R.A.Medina, J.Bell, and M.J.Shattock. 2001. Differential Centrifugation Separates Cardiac Sarcolemmal and Endosomal Membranes from Langendorff-Perfused Rat Hearts. *Anal. Biochem.* 293:216-223.

Fushimi, K., S.Sasaki, and F.Marumo. 1997. Phosphorylation of Serine 256 is Required for cAMP-dependent Regulatory Exocytosis of the Aquaporin-2 Water Channel. *J. Biol. Chem.* 272:14800-14804.

Garcia de Herreros, A. and M.J.Birnbaum. 1989. The acquisition of increased insulin-responsive hexose transport in 3T3- L1 adipocytes correlates with expression of a novel transporter gene. *J. Biol. Chem.* 264:19994-19999.

Garippa, R.J., T.W.Judge, D.E.James, and T.E.McGraw. 1994. The amino terminus of GLUT4 functions as an internalization motif but not an intracellular retention signal when substituted for the transferrin receptor cytoplasmic domain. *J. Cell Biol.* 124:705-715.

Garippa, R.J., A.Johnson, J.Park, R.L.Petrush, and T.E.McGraw. 1996. The Carboxyl Terminus of GLUT4 Contains a Serine-Leucine-Leucine Sequence That Functions as a Potent Internalization Motif in Chinese Hamster Ovary Cells. *J. Biol. Chem.* 271:20660-20668.

Garza, L.A. and M.J.Birnbaum. 2000. Insulin-responsive Aminopeptidase Trafficking in 3T3-L1 Adipocytes. *J. Biol. Chem.* 275:2560-2567.

Gasteiger, E., A.Gattiker, C.Hoogland, I.Ivanyi, R.D.Appel, and A.Bairoch. 2003. ExPASy: the proteomics server for in-depth protein knowledge and analysis. *Nucleic Acids Res.* 31:3784-3788.

Geisbuhler, T., R.A.Altschuld, R.W.Trewyn, A.Z.Ansel, K.Lamka, and G.P.Brierley. 1984. Adenine nucleotide metabolism and compartmentalization in isolated adult rat heart cells. *Circ. res.* 54:536-546.

Gerrits, P.M., A.L.Olson, and J.E.Pessin. 1993. Regulation of the GLUT4/muscle-fat glucose transporter mRNA in adipose tissue of insulin-deficient diabetic rats. *J. Biol. Chem.* 268:640-644.

Gibbs, E.M., W.J.Allard, and G.E.Lienhard. 1986. The glucose transporter in 3T3-L1 adipocytes is phosphorylated in response to phorbol ester but not in response to insulin. *J. Biol. Chem.* 261:16597-16603.

Gillingham, A.K., F.Koumanov, P.R.Pryor, B.J.Reaves, and G.D.Holman. 1999. Association of AP1 adaptor complexes with GLUT4 vesicles. *J. Cell Sci.* 112:4793-4800.

Govers, R., A.C.F.Coster, and D.E.James. 2004. Insulin Increases Cell Surface GLUT4 Levels by Dose Dependently Discharging GLUT4 into a Cell Surface Recycling Pathway. *Mol. Cell. Biol.* 24:6456-6466.

Grillo, S., T.Gremeaux, Y.Marchand-Brustel, and J.F.Tanti. 1999. Potential role of 3-phosphoinositide-dependent protein kinase 1 (PDK1) in insulin-stimulated glucose transporter 4 translocation in adipocytes. *FEBS Lett.* 461:277-279.

Guilherme, A. and M.P.Czech. 1998. Stimulation of IRS-1-associated Phosphatidylinositol 3-Kinase and Akt/Protein Kinase B but Not Glucose Transport by beta 1-Integrin Signaling in Rat Adipocytes. *J. Biol. Chem.* 273:33119-33122.

Guilherme, A., M.Emoto, J.M.Buxton, S.Bose, R.Sabini, W.E.Theurkauf, J.Leszyk, and M.P.Czech. 2000. Perinuclear Localization and Insulin Responsiveness of GLUT4 Requires Cytoskeletal Integrity in 3T3-L1 Adipocytes. *J. Biol. Chem.* 275:38151-38159.

Guilherme, A., J.K.Klarlund, G.Krystal, and M.P.Czech. 1996. Regulation of Phosphatidylinositol 3,4,5-Trisphosphate 5'-Phosphatase Activity by Insulin. *J. Biol. Chem.* 271:29533-29536.

Gustavsson, J., S.Parpal, M.Karlsson, C.Ramsing, H.Thorn, M.Borg, M.Lindroth, K.H.Peterson, K.E.Magnusson, and P.Stralfors. 1999. Localization of the insulin receptor in caveolae of adipocyte plasma membrane. *FASEB J.* 13:1961-1971.

Hajduch, E.J., M.C.Guerre-Millo, I.A.Hainault, C.M.Guichard, and M.M.Lavau. 1992. Expression of glucose transporters (GLUT 1 and GLUT 4) in primary cultured rat adipocytes: differential evolution with time and chronic insulin effect. *J Cell Biochem.* 49:251-258.

Haney, P.M., M.A.Levy, M.S.Strube, and M.Mueckler. 1995. Insulin-sensitive targeting of the GLUT4 glucose transporter in L6 myoblasts is conferred by its COOH-terminal cytoplasmic tail. *J. Cell Biol.* 129:641-658.

Hardie, D.G., D.Carling, and M.Carlson. 1998. The AMP-activated/SNF1 protein kinase subfamily: metabolic sensors of the eukaryotic cell? *Annu. Rev. Biochem.* 67:821-855.

Harper,D. Chartacterisation of a putative N-terminal GLUT4 kinase. 2002. University of Bath, UK.
Ref Type: Thesis/Dissertation

Haystead, T.A., A.T.Sim, D.Carling, R.C.Honnor, Y.Tsukitani, P.Cohen, and D.G.Hardie. 1989. Effects of the tumour promoter okadaic acid on intracellular protein phosphorylation and metabolism. *Nature* 337:78-81.

He, W., T.J.O'Neill, and T.A.Gustafson. 1995. Distinct Modes of Interaction of SHC and Insulin Receptor Substrate-1 with the Insulin Receptor NPEY Region via Non-SH2 Domains. *J. Biol. Chem.* 270:23258-23262.

Hediger, M.A., M.F.Romero, J.B.Peng, A.Rolfs, H.Takanaga, and E.A.Bruford. 2004. The ABCs of solute carriers: physiological, pathological and therapeutic implications of human membrane transport proteinsIntroduction. *Pflugers Arch.* 447:465-468.

Holman, G.D., I.J.Kozka, A.E.Clark, C.J.Flower, J.Saltis, A.D.Habberfield, I.A.Simpson, and S.W.Cushman. 1990. Cell surface labeling of glucose transporter isoform GLUT4 by bis- mannose photolabel. Correlation with stimulation of glucose transport in rat adipose cells by insulin and phorbol ester. *J. Biol. Chem.* 265:18172-18179.

Hosaka, T., C.C.Brooks, E.Presman, S.K.Kim, Z.Zhang, M.Breen, D.N.Gross, E.Sztul, and P.F.Pilch. 2005. p115 Interacts with the GLUT4 Vesicle Protein, IRAP, and Plays a Critical Role in Insulin-stimulated GLUT4 Translocation. *Mol. Biol. Cell* 16:2882-2890.

Hresko, R.C. and M.Mueckler. 2005. mTOR·RICTOR Is the Ser473 Kinase for Akt/Protein Kinase B in 3T3-L1 Adipocytes. *J. Biol. Chem.* 280:40406-40416.

Huang, C., A.C.P.Thirone, X.Huang, and A.Klip. 2005. Differential Contribution of Insulin Receptor Substrates 1 Versus 2 to Insulin Signaling and Glucose Uptake in L6 Myotubes. *J. Biol. Chem.* 280:19426-19435.

Huang, J., T.Imamura, and J.M.Olefsky. 2001. Insulin can regulate GLUT4 internalization by signaling to Rab5 and the motor protein dynein. *Proc. Natl. Acad. Sci. U. S. A* 98:13084-13089.

Hudson, A.W., M.Ruiz, and M.J.Birnbaum. 1992. Isoform-specific subcellular targeting of glucose transporters in mouse fibroblasts. *J. Cell Biol.* 116:785-797.

Ikonomov, O.C., D.Sbrissa, K.Mlak, and A.Shisheva. 2002. Requirement for PIKfyve Enzymatic Activity in Acute and Long-Term Insulin Cellular Effects. *Endocrinology* 143:4742-4754.

Inoue, M., L.Chang, J.Hwang, S.H.Chiang, and A.R.Saltiel. 2003. The exocyst complex is required for targeting of Glut4 to the plasma membrane by insulin. *Nature* 422:629-633.

Isakoff, S.J., C.Taha, E.Rose, J.Marcusohn, A.Klip, and E.Y.Skolnik. 1995. The Inability of Phosphatidylinositol 3-Kinase Activation to Stimulate GLUT4 Translocation Indicates Additional Signaling Pathways are Required for Insulin-Stimulated Glucose Uptake. *Proc. Natl. Acad. Sci. U. S. A* 92:10247-10251.

James, D.E., R.Brown, J.Navarro, and P.F.Pilch. 1988. Insulin-regulatable tissues express a unique insulin-sensitive glucose transport protein. *Nature* 333:183-185.

James, D.E., K.M.Burleigh, and E.W.Kraegen. 1986. In vivo glucose metabolism in individual tissues of the rat. Interaction between epinephrine and insulin. *J. Biol. Chem.* 261:6366-6374.

James, D.E., J.Hiken, and J.C.Lawrence, Jr. 1989a. Isoproterenol stimulates phosphorylation of the insulin-regulatable glucose transporter in rat adipocytes. *Proc. Natl. Acad. Sci. U. S. A* 86:8368-8372.

James, D.E., M.Strube, and M.Mueckler. 1989b. Molecular cloning and characterization of an insulin-regulatable glucose transporter. *Nature* 338:83-87.

James, D.E. 2005. MUNC-ing around with insulin action. *J. Clin. Invest.* 115:219-221.

Jarvis, M.A., T.R.Jones, D.D.Drummond, P.P.Smith, W.J.Britt, J.A.Nelson, and C.J.Baldick. 2004. Phosphorylation of human cytomegalovirus glycoprotein B (gB) at the acidic cluster casein kinase 2 site (Ser900) is required for localization of gB to the trans-Golgi network and efficient virus replication. *J. Virol.* 78:285-293.

JeBailey, L., A.Rudich, X.Huang, C.D.Ciano-Oliveira, A.Kapus, and A.Klip. 2004. Skeletal Muscle Cells and Adipocytes Differ in Their Reliance on TC10 and Rac for Insulin-Induced Actin Remodeling. *Mol. Endocrinol.* 18:359-372.

Jiang, T., G.Sweeney, M.T.Rudolf, A.Klip, A.Traynor-Kaplan, and R.Y.Tsien. 1998. Membrane-permeant Esters of Phosphatidylinositol 3,4,5-Trisphosphate. *J. Biol. Chem.* 273:11017-11024.

Jiang, Z.Y., Q.L.Zhou, K.A.Coleman, M.Chouinard, Q.Boese, and M.P.Czech. 2003. Insulin signaling through Akt/protein kinase B analyzed by small interfering RNA-mediated gene silencing. *Proc. Natl. Acad. Sci. U. S. A* 100:7569-7574.

Joost, H.G. and B.Thorens. 2001. The extended GLUT-family of sugar/polyol transport facilitators: nomenclature, sequence characteristics, and potential function of its novel members (review). *Mol. Membr. Biol.* 18:247-256.

Joost, H.G., T.M.Weber, S.W.Cushman, and I.A.Simpson. 1987. Activity and phosphorylation state of glucose transporters in plasma membranes from insulin-, isoproterenol-, and phorbol ester-treated rat adipose cells. *J. Biol. Chem.* 262:11261-11267.

Kaestner, K.H., R.J.Christy, J.C.McLenithan, L.T.Braiterman, P.Cornelius, P.H.Pekala, and M.D.Lane. 1989. Sequence, Tissue Distribution, and Differential Expression of mRNA for a Putative Insulin-Responsive Glucose Transporter in Mouse 3T3-L1 Adipocytes. *Proc. Natl. Acad. Sci. U. S. A* 86:3150-3154.

Kahn, B.B. 1992. Facilitative glucose transporters: regulatory mechanisms and dysregulation in diabetes. *J. Clin. Invest.* 89:1367-1374.

Kanai, F., K.Ito, M.Todaka, H.Hayashi, S.Kamohara, K.Ishii, T.Okada, O.Hazeki, M.Ui, and Y.Ebina. 1993a. Insulin-Stimulated GLUT4 Translocation Is Relevant to the Phosphorylation of IRS-1 and the Activity of PI3 Kinase. *Biochem. Biophys. Res. Commun.* 195:762-768.

Kanai, F., Y.Nishioka, H.Hayashi, S.Kamohara, M.Todaka, and Y.Ebina. 1993b. Direct demonstration of insulin-induced GLUT4 translocation to the surface of intact cells by insertion of a c-myc epitope into an exofacial GLUT4 domain. *J. Biol. Chem.* 268:14523-14526.

Kane, S., H.Sano, S.C.Liu, J.M.Asara, W.S.Lane, C.C.Garner, and G.E.Lienhard. 2002. A method to identify serine kinase substrates. Akt phosphorylates a novel adipocyte protein with a Rab GTPase-activating protein (GAP) domain. *J. Biol. Chem.* 277:22115-22118.

Kanzaki, M., S.Mora, J.B.Hwang, A.R.Saltiel, and J.E.Pessin. 2004. Atypical protein kinase C (PKCζ/λ) is a convergent downstream target of the insulin-stimulated phosphatidylinositol 3-kinase and TC10 signaling pathways. *J. Cell Biol.* 164:279-290.

Kao, A.W., B.P.Ceresa, S.R.Santeler, and J.E.Pessin. 1998. Expression of a Dominant Interfering Dynamin Mutant in 3T3L1 Adipocytes Inhibits GLUT4

Endocytosis without Affecting Insulin Signaling. *J. Biol. Chem.* 273:25450-25457.

Karylowski, O., A.Zeigerer, A.Cohen, and T.E.McGraw. 2004. GLUT4 Is Retained by an Intracellular Cycle of Vesicle Formation and Fusion with Endosomes. *Mol. Biol. Cell* 15:870-882.

Kashiwagi, A., T.P.Hueckstead, and J.E.Foley. 1983. The regulation of glucose transport by cAMP stimulators via three different mechanisms in rat and human adipocytes. *J. Biol. Chem.* 258:13685-13692.

Kasuga, M., F.A.Karlsson, and C.R.Kahn. 1982a. Insulin stimulates the phosphorylation of the 95,000-dalton subunit of its own receptor. *Science* 215:185-187.

Kasuga, M., Y.Zick, D.L.Blith, F.A.Karlsson, H.U.Haring, and C.R.Kahn. 1982b. Insulin stimulation of phosphorylation of the beta subunit of the insulin receptor. Formation of both phosphoserine and phosphotyrosine. *J. Biol. Chem.* 257:9891-9894.

Keller, S.R., H.M.Scott, C.C.Mastick, R.Aebersold, and G.E.Lienhard. 1995. Cloning and characterization of a novel insulin-regulated membrane aminopeptidase from Glut4 vesicles. *J. Biol. Chem.* 270:23612-23618.

Khan, A.H., E.Capilla, J.C.Hou, R.T.Watson, J.R.Smith, and J.E.Pessin. 2004. Entry of Newly Synthesized GLUT4 into the Insulin-responsive Storage Compartment Is Dependent upon Both the Amino Terminus and the Large Cytoplasmic Loop. *J. Biol. Chem.* 279:37505-37511.

Kimura, A., C.A.Baumann, S.H.Chiang, and A.R.Saltiel. 2001. The sorbin homology domain: A motif for the targeting of proteins to lipid rafts. *Proc. Natl. Acad. Sci. U. S. A* 98:9098-9103.

Kohn, A.D., S.A.Summers, M.J.Birnbaum, and R.A.Roth. 1996. Expression of a Constitutively Active Akt Ser/Thr Kinase in 3T3-L1 Adipocytes Stimulates Glucose Uptake and Glucose Transporter 4Translocation. *J. Biol. Chem.* 271:31372-31378.

Kolter, T., I.Uphues, A.Wichelhaus, H.Reinauer, and J.Eckel. 1992. Contraction-induced translocation of the glucose transporter Glut4 in isolated ventricular cardiomyocytes. *Biochem. Biophys. Res. Commun.* 189:1207-1214.

Koumanov, F., B.Jin, J.Yang, and G.D.Holman. 2005. Insulin signaling meets vesicle traffic of GLUT4 at a plasma-membrane-activated fusion step. *Cell Metab.* 2:179-189.

Kuri-Harcuch, W. and H.Green. 1977. Increasing activity of enzymes on pathway of triacylglycerol synthesis during adipose conversion of 3T3 cells. *J. Biol. Chem.* 252:2158-2160.

Kuroda, M., R.C.Honnor, S.W.Cushman, C.Londos, and I.A.Simpson. 1987. Regulation of insulin-stimulated glucose transport in the isolated rat adipocyte. cAMP-independent effects of lipolytic and antilipolytic agents. *J. Biol. Chem.* 262:245-253.

Laemmli, U.K. 1970. Cleavage of structural proteins during the assembly of the head of bacteriophage T4. *Nature* 227:680-685.

Larance, M., G.Ramm, J.Stockli, E.M.van Dam, S.Winata, V.Wasinger, F.Simpson, M.Graham, J.R.Junutula, M.Guilhaus, and D.E.James. 2005. Characterisation of the role of the RabGAP AS160 in insulin-regulated GLUT4 trafficking. *J. Biol. Chem.* 280:37803-37813.

Lasa-Benito, M., O.Marin, F.Meggio, and L.A.Pinna. 1996. Golgi apparatus mammary gland casein kinase: monitoring by a specific peptide substrate and definition of specificity determinants. *FEBS Lett.* 382:149-152.

Lavan, B.E., V.R.Fantin, E.T.Chang, W.S.Lane, S.R.Keller, and G.E.Lienhard. 1997a. A novel 160-kDa phosphotyrosine protein in insulin-treated embryonic kidney cells is a new member of the insulin receptor substrate family. *J. Biol. Chem.* 272:21403-21407.

Lavan, B.E., W.S.Lane, and G.E.Lienhard. 1997b. The 60-kDa phosphotyrosine protein in insulin-treated adipocytes is a new member of the insulin receptor substrate family. *J. Biol. Chem.* 272:11439-11443.

Lawrence, J.C., Jr., J.F.Hiken, and D.E.James. 1990a. Phosphorylation of the glucose transporter in rat adipocytes. Identification of the intracellular domain at the carboxyl terminus as a target for phosphorylation in intact-cells and in vitro. *J. Biol. Chem.* 265:2324-2332.

Lawrence, J.C., Jr., J.F.Hiken, and D.E.James. 1990b. Stimulation of glucose transport and glucose transporter phosphorylation by okadaic acid in rat adipocytes. *J. Biol. Chem.* 265:19768-19776.

Lee, J. and P.F.Pilch. 1994. The insulin receptor: structure, function, and signaling. *Am. J. Physiol. Cell Physiol.* 266:C319-C334.

Lemieux, M.J., J.Song, M.J.Kim, Y.Huang, A.Villa, M.Auer, X.D.Li, and D.N.Wang. 2003. Three-dimensional crystallization of the Escherichia coli glycerol-3-phosphate transporter: A member of the major facilitator superfamily. *Protein Sci.* 12:2748-2756.

Li, L.V. and K.V.Kandror. 2005. Golgi-localized, gamma-ear-containing, Arf-binding protein adaptors mediate insulin-responsive trafficking of glucose transporter 4 in 3T3-L1 adipocytes. *Mol. Endocrinol.* 19:2145-2153.

Lin, B.Z., P.F.Pilch, and K.V.Kandror. 1997. Sortilin Is a Major Protein Component of Glut4-containing Vesicles. *J. Biol. Chem.* 272:24145-24147.

Litchfield, D.W. 2003. Protein kinase CK2: structure, regulation and role in cellular decisions of life and death. *Biochem. J.* 369:1-15.

Liu, J., A.Kimura, C.A.Baumann, and A.R.Saltiel. 2002. APS Facilitates c-Cbl Tyrosine Phosphorylation and GLUT4 Translocation in Response to Insulin in 3T3-L1 Adipocytes. *Mol. Cell. Biol.* 22:3599-3609.

Luiken, J.J.F.P., S.L.M.Coort, J.Willems, W.A.Coumans, A.Bonen, G.J.van der Vusse, and J.F.C.Glatz. 2003. Contraction-Induced Fatty Acid Translocase/CD36 Translocation in Rat Cardiac Myocytes Is Mediated Through AMP-Activated Protein Kinase Signaling. *Diabetes* 52:1627-1634.

Lund, S., G.D.Holman, O.Schmitz, and O.Pedersen. 1995. Contraction Stimulates Translocation of Glucose Transporter GLUT4 in Skeletal Muscle Through a Mechanism Distinct from that of Insulin. *Proc. Natl. Acad. Sci. U. S. A* 92:5817-5821.

Lund, S., P.R.Pryor, S.Ostergaard, O.Schmitz, O.Pedersen, and G.D.Holman. 1998. Evidence against protein kinase B as a mediator of contraction-induced glucose transport and GLUT4 translocation in rat skeletal muscle. *FEBS Lett.* 425:472-474.

Luo, K.X., T.R.Hurley, and B.M.Sefton. 1991. Cyanogen bromide cleavage and proteolytic peptide mapping of proteins immobilized to membranes. *Methods Enzymol.* 201:149-152.

Mackall, J.C., A.K.Student, S.E.Polakis, and M.D.Lane. 1976. Induction of lipogenesis during differentiation in a "preadipocyte" cell line. *J. Biol. Chem.* 251:6462-6464.

Malide, D., G.Ramm, S.W.Cushman, and J.W.Slot. 2000. Immunoelectron microscopic evidence that GLUT4 translocation explains the stimulation of glucose transport in isolated rat white adipose cells. *J. Cell Sci.* 113:4203-4210.

Malide, D., N.K.Dwyer, E.J.Blanchette-Mackie, and S.W.Cushman. 1997. Immunocytochemical Evidence that GLUT4 Resides in a Specialized Translocation Post-endosomal VAMP2-positive Compartment in Rat Adipose Cells in the Absence of Insulin. *J. Histochem. Cytochem.* 45:1083-1096.

Marsh, B.J., R.A.Alm, S.R.McIntosh, and D.E.James. 1995. Molecular regulation of GLUT-4 targeting in 3T3-L1 adipocytes. *J. Cell Biol.* 130:1081-1091.

Marsh, B.J., S.Martin, D.R.Melvin, L.B.Martin, R.A.Alm, G.W.Gould, and D.E.James. 1998. Mutational analysis of the carboxy-terminal phosphorylation site of GLUT-4 in 3T3-L1 adipocytes. *Am. J. Physiol. Endocrinol. Metab.* 275:E412-E422.

Marshall, B.A., H.Murata, R.C.Hresko, and M.Mueckler. 1993. Domains that confer intracellular sequestration of the Glut4 glucose transporter in Xenopus oocytes. *J. Biol. Chem.* 268:26193-26199.

Martin, L.B., A.Shewan, C.A.Millar, G.W.Gould, and D.E.James. 1998. Vesicle-associated Membrane Protein 2 Plays a Specific Role in the Insulin-dependent Trafficking of the Facilitative Glucose Transporter GLUT4 in 3T3-L1 Adipocytes. *J. Biol. Chem.* 273:1444-1452.

Martin, S., J.Tellam, C.Livingstone, J.W.Slot, G.W.Gould, and D.E.James. 1996. The glucose transporter (GLUT-4) and vesicle-associated membrane protein-2 (VAMP-2) are segregated from recycling endosomes in insulin-sensitive cells. *J. Cell Biol.* 134:625-635.

Martinez-Arca, S., V.S.Lalioti, and I.V.Sandoval. 2000. Intracellular targeting and retention of the glucose transporter GLUT4 by the perinuclear storage compartment involves distinct carboxyl-tail motifs. *J. Cell Sci.* 113:1705-1715.

Melvin, D.R., B.J.Marsh, A.R.Walmsley, D.E.James, and G.W.Gould. 1999. Analysis of amino and carboxy terminal GLUT-4 targeting motifs in 3T3-L1 adipocytes using an endosomal ablation technique. *Biochemistry* 38:1456-1462.

Miinea, C.P., H.Sano, S.Kane, E.Sano, M.Fukuda, J.Peranen, W.S.Lane, and G.E.Lienhard. 2005. AS160, the Akt substrate regulating GLUT4 translocation, has a functional Rab GTPase-activating protein domain. *Biochem. J.* 391:87-93.

Millar, C.A., T.Meerloo, S.Martin, G.R.Hickson, N.J.Shimwell, M.J.Wakelam, D.E.James, and G.W.Gould. 2000. Adipsin and the glucose transporter GLUT4 traffic to the cell surface via independent pathways in adipocytes. *Traffic* 1:141-151.

Min, J., S.Okada, M.Kanzaki, J.S.Elmendorf, K.J.Coker, B.P.Ceresa, L.J.Syu, Y.Noda, A.R.Saltiel, and J.E.Pessin. 1999. Synip: A Novel Insulin-Regulated Syntaxin 4-Binding Protein Mediating GLUT4 Translocation in Adipocytes. *Mol. Cell* 3:751-760.

Mitra, P., X.Zheng, and M.P.Czech. 2004. RNAi-based Analysis of CAP, Cbl, and CrkII Function in the Regulation of GLUT4 by Insulin. *J. Biol. Chem.* 279:37431-37435.

Molero, J.C., J.P.Whitehead, T.Meerloo, and D.E.James. 2001. Nocodazole Inhibits Insulin-stimulated Glucose Transport in 3T3-L1 Adipocytes via a Microtubule-independent Mechanism. *J. Biol. Chem.* 276:43829-43835.

Montessuit, C., I.Papageorgiou, A.Remondino-Muller, I.Tardy, and R.Lerch. 1998. Post-ischemic Stimulation of 2-deoxyglucose Uptake in Rat Myocardium: Role of Translocation of Glut-4. *J. Mol. Cell. Cardiol.* 30:393-403.

Mora, A., K.Sakamoto, E.J.McManus, and D.R.Alessi. 2005. Role of the PDK1-PKB-GSK3 pathway in regulating glycogen synthase and glucose uptake in the heart. *FEBS Lett.* 579:3632-3638.

Morris, N.J., S.A.Ross, W.S.Lane, S.K.Moestrup, C.M.Petersen, S.R.Keller, and G.E.Lienhard. 1998. Sortilin Is the Major 110-kDa Protein in GLUT4 Vesicles from Adipocytes. *J. Biol. Chem.* 273:3582-3587.

Mu, J., J.T.Brozinick, Jr., O.Valladares, M.Bucan, and M.J.Birnbaum. 2001. A role for AMP-activated protein kinase in contraction- and hypoxia-regulated glucose transport in skeletal muscle. *Mol. Cell* 7:1085-1094.

Mueckler, M., C.Caruso, S.A.Baldwin, M.Panico, I.Blench, H.R.Morris, W.J.Allard, G.E.Lienhard, and H.F.Lodish. 1985. Sequence and structure of a human glucose transporter. *Science* 229:941-945.

Nakashima, N., P.M.Sharma, T.Imamura, R.Bookstein, and J.M.Olefsky. 2000. The Tumor Suppressor PTEN Negatively Regulates Insulin Signaling in 3T3-L1 Adipocytes. *J. Biol. Chem.* 275:12889-12895.

Namchuk, M., L.Lindsay, C.W.Turck, J.Kanaani, and S.Baekkeskov. 1997. Phosphorylation of serine residues 3, 6, 10, and 13 distinguishes membrane anchored from soluble glutamic acid decarboxylase 65 and is restricted to glutamic acid decarboxylase 65alpha. *J. Biol. Chem.* 272:1548-1557.

Nielsen, M.S., P.Madsen, E.I.Christensen, A.Nykjaer, J.Gliemann, D.Kasper, R.Pohlmann, and C.M.Petersen. 2001. The sortilin cytoplasmic tail conveys Golgi-endosome transport and binds the VHS domain of the GGA2 sorting protein. *EMBO J.* 20:2180-2190.

Nishimura, H., J.Saltis, A.D.Habberfield, N.B.Garty, A.S.Greenberg, S.W.Cushman, C.Londos, and I.A.Simpson. 1991. Phosphorylation State of the GLUT4 Isoform of the Glucose Transporter in Subfractions of the Rat Adipose Cell: Effects of Insulin, Adenosine, and Isoproterenol. *Proc. Natl. Acad. Sci. U. S. A* 88:11500-11504.

Nishimura, H., M.J.Zarnowski, and I.A.Simpson. 1993. Glucose transporter recycling in rat adipose cells. Effects of potassium depletion. *J. Biol. Chem.* 268:19246-19253.

Olson, A.L., J.B.Knight, and J.E.Pessin. 1997. Syntaxin 4, VAMP2, and/or VAMP3/cellubrevin are functional target membrane and vesicle SNAP receptors for insulin-stimulated GLUT4 translocation in adipocytes. *Mol. Cell. Biol.* 17:2425-2435.

Omata, W., H.Shibata, L.Li, K.Takata, and I.Kojima. 2000. Actin filaments play a critical role in insulin-induced exocytotic recruitment but not in endocytosis of GLUT4 in isolated rat adipocytes. *Biochem. J.* 346:321-328.

Orci, L., M.Tagaya, M.Amherdt, A.Perrelet, J.G.Donaldson, J.Lippincott-Schwartz, R.D.Klausner, and J.E.Rothman. 1991. Brefeldin A, a drug that blocks secretion, prevents the assembly of non-clathrin-coated buds on Golgi cisternae. *Cell* 64:1183-1195.

Palacios, S., V.Lalioti, S.Martinez-Arca, S.Chattopadhyay, and I.V.Sandoval. 2001. Recycling of the insulin-sensitive glucose transporter GLUT4. Access of

surface internalized GLUT4 molecules to the perinuclear storage compartment is mediated by the Phe5-Gln6-Gln7-Ile8 motif. *J. Biol. Chem.* 276:3371-3383.

Patki, V., J.Buxton, A.Chawla, L.Lifshitz, K.Fogarty, W.Carrington, R.Tuft, and S.Corvera. 2001. Insulin Action on GLUT4 Traffic Visualized in Single 3T3-L1 Adipocytes by Using Ultra-fast Microscopy. *Mol. Biol. Cell* 12:129-141.

Pessin, J.E. and G.I.Bell. 1992. Mammalian facilitative glucose transporter family: structure and molecular regulation. *Annu. Rev. Physiol.* 54:911-930.

Pinna, L.A. and M.Ruzzene. 1996. How do protein kinases recognize their substrates? *Biochim. Biophys. Acta.* 1314:191-225.

Piper, R.C., D.E.James, J.W.Slot, C.Puri, and J.C.Lawrence, Jr. 1993a. GLUT4 phosphorylation and inhibition of glucose transport by dibutyryl cAMP. *J. Biol. Chem.* 268:16557-16563.

Piper, R.C., C.Tai, P.Kulesza, S.Pang, D.Warnock, J.Baenziger, J.W.Slot, H.J.Geuze, C.Puri, and D.E.James. 1993b. GLUT-4 NH2 terminus contains a phenylalanine-based targeting motif that regulates intracellular sequestration. *J. Cell Biol.* 121:1221-1232.

Piper, R.C., C.Tai, J.W.Slot, C.S.Hahn, C.M.Rice, H.Huang, and D.E.James. 1992. The efficient intracellular sequestration of the insulin-regulatable glucose transporter (GLUT-4) is conferred by the NH2 terminus. *J. Cell Biol.* 117:729-743.

Poirier, M.A., W.Xiao, J.C.Macosko, C.Chan, Y.K.Shin, and M.K.Bennett. 1998. The synaptic SNARE complex is a parallel four-stranded helical bundle. *Nat. Struct. Biol.* 5:765-769.

Pryor, P.R., S.C.Liu, A.E.Clark, J.Yang, G.D.Holman, and D.Tosh. 2000. Chronic insulin effects on insulin signalling and GLUT4 endocytosis are reversed by metformin. *Biochem. J.* 348:83-91.

Puertollano, R., R.C.Aguilar, I.Gorshkova, R.J.Crouch, and J.S.Bonifacino. 2001. Sorting of Mannose 6-Phosphate Receptors Mediated by the GGAs. *Science* 292:1712-1716.

Quon, M.J., M.Guerre-Millo, M.J.Zarnowski, A.J.Butte, M.Em, S.W.Cushman, and S.I.Taylor. 1994. Tyrosine Kinase-Deficient Mutant Human Insulin Receptors (Met1153 → Ile) Overexpressed in Transfected Rat Adipose Cells Fail to Mediate Translocation of Epitope-Tagged GLUT4. *Proc. Natl. Acad. Sci. U. S. A* 91:5587-5591.

Quon, M.J., M.J.Zarnowski, M.Guerre-Millo, S.M.de la Luz, S.I.Taylor, and S.W.Cushman. 1993. Transfection of DNA into isolated rat adipose cells by electroporation: evaluation of promoter activity in transfected adipose cells which are highly responsive to insulin after one day in culture. *Biochem. Biophys. Res. Commun.* 194:338-346.

Ramm, G., J.W.Slot, D.E.James, and W.Stoorvogel. 2000. Insulin Recruits GLUT4 from Specialized VAMP2-carrying Vesicles as well as from the Dynamic Endosomal/Trans-Golgi Network in Rat Adipocytes. *Mol. Biol. Cell* 11:4079-4091.

Rapoport, I., Y.C.Chen, P.Cupers, S.E.Shoelson, and T.Kirchhausen. 1998. Dileucine-based sorting signals bind to the beta chain of AP-1 at a site distinct and regulated differently from the tyrosine-based motif-binding site. *EMBO J.* 17:2148-2155.

Rea, S., L.B.Martin, S.McIntosh, S.L.Macaulay, T.Ramsdale, G.Baldini, and D.E.James. 1998. Syndet, an Adipocyte Target SNARE Involved in the Insulin-

induced Translocation of GLUT4 to the Cell Surface. *J. Biol. Chem.* 273:18784-18792.

Reaven, G.M., C.Hollenbeck, C.Y.Jeng, M.S.Wu, and Y.D.Chen. 1988. Measurement of plasma glucose, free fatty acid, lactate, and insulin for 24 h in patients with NIDDM. *Diabetes* 37:1020-1024.

Reed, B.C., S.H.Kaufmann, J.C.Mackall, A.K.Student, and M.D.Lane. 1977. Alterations in insulin binding accompanying differentiation of 3T3-L1 preadipocytes. *Proc. Natl. Acad. Sci. U. S. A* 74:4876-4880.

Ren, M., G.Xu, J.Zeng, C.Lemos-Chiarandini, M.Adesnik, and D.D.Sabatini. 1998. Hydrolysis of GTP on rab11 is required for the direct delivery of transferrin from the pericentriolar recycling compartment to the cell surface but not from sorting endosomes. *Proc. Natl. Acad. Sci. U. S. A* 95:6187-6192.

Reusch, J.E., N.Begum, K.E.Sussman, and B.Draznin. 1991. Regulation of GLUT-4 phosphorylation by intracellular calcium in adipocytes. *Endocrinology* 129:3269-3273.

Reusch, J.E., K.E.Sussman, and B.Draznin. 1993. Inverse relationship between GLUT-4 phosphorylation and its intrinsic activity. *J. Biol. Chem.* 268:3348-3351.

Robinson, L.J., S.Pang, D.S.Harris, J.Heuser, and D.E.James. 1992. Translocation of the glucose transporter (GLUT4) to the cell surface in permeabilized 3T3-L1 adipocytes: effects of ATP insulin, and GTP gamma S and localization of GLUT4 to clathrin lattices. *J. Cell Biol.* 117:1181-1196.

Robinson, M. 2004. Adaptable adaptors for coated vesicles. *Trends Cell Biol.* 14:167-174.

Ross, S.A., H.M.Scott, N.J.Morris, W.Y.Leung, F.Mao, G.E.Lienhard, and S.R.Keller. 1996. Characterization of the Insulin-regulated Membrane Aminopeptidase in 3T3-L1 Adipocytes. *J. Biol. Chem.* 271:3328-3332.

Rubin, C.S., A.Hirsch, C.Fung, and O.M.Rosen. 1978. Development of hormone receptors and hormonal responsiveness in vitro. Insulin receptors and insulin sensitivity in the preadipocyte and adipocyte forms of 3T3-L1 cells. *J. Biol. Chem.* 253:7570-7578.

Russ, M. and J.Eckel. 1995. Insulin action on cardiac glucose transport: studies on the role of protein kinase C. *Biochim. Biophys. Acta* 1265:73-78.

Russell, R.R., III, R.Bergeron, G.I.Shulman, and L.H.Young. 1999. Translocation of myocardial GLUT-4 and increased glucose uptake through activation of AMPK by AICAR. *Am. J. Physiol. Heart Circ. Physiol.* 277:H643-H649.

Sadowski, H.B., T.T.Wheeler, and D.A.Young. 1992. Gene expression during 3T3-L1 adipocyte differentiation. Characterization of initial responses to the inducing agents and changes during commitment to differentiation. *J. Biol. Chem.* 267:4722-4731.

Sakamoto, K., W.G.Aschenbach, M.F.Hirshman, and L.J.Goodyear. 2003. Akt signaling in skeletal muscle: regulation by exercise and passive stretch. *Am. J. Physiol. Endocrinol. Metab.* 285:E1081-E1088.

Sakamoto, K., M.F.Hirshman, W.G.Aschenbach, and L.J.Goodyear. 2002. Contraction Regulation of Akt in Rat Skeletal Muscle. *J. Biol. Chem.* 277:11910-11917.

Saltiel, A.R. and C.R.Kahn. 2001. Insulin signalling and the regulation of glucose and lipid metabolism. *Nature* 414:799-806.

Sano, H., S.Kane, E.Sano, and G.E.Lienhard. 2005. Synip phosphorylation does not regulate insulin-stimulated GLUT4 translocation. *Biochem. Biophys. Res. Commun.* 332:880-884.

Sano, H., S.Kane, E.Sano, C.P.Miinea, J.M.Asara, W.S.Lane, C.W.Garner, and G.E.Lienhard. 2003. Insulin-stimulated Phosphorylation of a Rab GTPase-activating Protein Regulates GLUT4 Translocation. *J. Biol. Chem.* 278:14599-14602.

Sarbassov, D.D., D.A.Guertin, S.M.Ali, and D.M.Sabatini. 2005. Phosphorylation and regulation of Akt/PKB by the rictor-mTOR complex. *Science* 307:1098-1101.

Satoh, S., H.Nishimura, A.E.Clark, I.J.Kozka, S.J.Vannucci, I.A.Simpson, M.J.Quon, S.W.Cushman, and G.D.Holman. 1993. Use of bismannose photolabel to elucidate insulin-regulated GLUT4 subcellular trafficking kinetics in rat adipose cells. Evidence that exocytosis is a critical site of hormone action. *J. Biol. Chem.* 268:17820-17829.

Schagger, H. and G.von Jagow. 1987. Tricine-sodium dodecyl sulfate-polyacrylamide gel electrophoresis for the separation of proteins in the range from 1 to 100 kDa. *Anal. Biochem.* 166:368-379.

Scheepers, A., H.G.Joost, and A.Schurmann. 2004. The glucose transporter families SGLT and GLUT: molecular basis of normal and aberrant function. *JPEN J. Parenter. Enteral Nutr.* 28:364-371.

Schurmann, A., G.Mieskes, and H.G.Joost. 1992. Phosphorylation of the adipose/muscle-type glucose transporter (GLUT4) and its relationship to glucose transport activity. *Biochem. J.* 285:223-228.

Shepherd, P.R. 2005. Mechanisms regulating phosphoinositide 3-kinase signalling in insulin-sensitive tissues. *Acta Physiol. Scand.* 183:3-12.

Shepherd, P.R., D.J.Withers, and K.Siddle. 1998. Phosphoinositide 3-kinase: the key switch mechanism in insulin signalling. *Biochem. J.* 333:471-490.

Shewan, A.M., B.J.Marsh, D.R.Melvin, S.Martin, G.W.Gould, and D.E.James. 2000. The cytosolic C-terminus of the glucose transporter GLUT4 contains an acidic cluster endosomal targeting motif distal to the dileucine signal. *Biochem. J.* 350:99-107.

Shewan, A.M., E.M.van Dam, S.Martin, T.B.Luen, W.Hong, N.J.Bryant, and D.E.James. 2003. GLUT4 Recycles via a trans-Golgi Network (TGN) Subdomain Enriched in Syntaxins 6 and 16 But Not TGN38: Involvement of an Acidic Targeting Motif. *Mol. Biol. Cell* 14:973-986.

Shi, J. and K.V.Kandror. 2005. Sortilin is essential and sufficient for the formation of Glut4 storage vesicles in 3T3-L1 adipocytes. *Dev. Cell* 9:99-108.

Shigematsu, S., A.H.Khan, M.Kanzaki, and J.E.Pessin. 2002. Intracellular Insulin-Responsive Glucose Transporter (GLUT4) Distribution But Not Insulin-Stimulated GLUT4 Exocytosis and Recycling Are Microtubule Dependent. *Mol. Endocrinol.* 16:1060-1068.

Shoelson, S.E., S.Chatterjee, M.Chaudhuri, and M.F.White. 1992. YMXM Motifs of IRS-1 Define Substrate Specificity of the Insulin Receptor Kinase. *Proc. Natl. Acad. Sci. U. S. A* 89:2027-2031.

Slot, J.W., H.J.Geuze, S.Gigengack, G.E.Lienhard, and D.E.James. 1991. Immuno-localization of the insulin regulatable glucose transporter in brown adipose tissue of the rat. *J. Cell Biol.* 113:123-135.

Smith, U., M.Kuroda, and I.A.Simpson. 1984. Counter-regulation of insulin-stimulated glucose transport by catecholamines in the isolated rat adipose cell. *J. Biol. Chem.* 259:8758-8763.

Smolenski, R.T. 2000. Elevation of the adenylate pool in rat cardiomyocytes by S-adenosyl-L-methionine. *Acta Biochim. Pol.* 47:1171-1178.

Standaert, M.L., G.Bandyopadhyay, Y.Kanoh, M.P.Sajan, and R.V.Farese. 2001. Insulin and PIP3 activate PKC-zeta by mechanisms that are both dependent and independent of phosphorylation of activation loop (T410) and autophosphorylation (T560) sites. *Biochemistry* 40:249-255.

Sun, D., N.Nguyen, T.R.DeGrado, M.Schwaiger, and F.C.Brosius, III. 1994. Ischemia induces translocation of the insulin-responsive glucose transporter GLUT4 to the plasma membrane of cardiac myocytes. *Circulation* 89:793-798.

Sun, X.J., M.Miralpeix, M.G.Myers, Jr., E.M.Glasheen, J.M.Backer, C.R.Kahn, and M.F.White. 1992. Expression and function of IRS-1 in insulin signal transmission. *J. Biol. Chem.* 267:22662-22672.

Sun, X.J., P.Rothenberg, C.R.Kahn, J.M.Backer, E.Araki, P.A.Wilden, D.A.Cahill, B.J.Goldstein, and M.F.White. 1991. Structure of the insulin receptor substrate IRS-1 defines a unique signal transduction protein. *Nature* 352:73-77.

Sun, X.J., L.M.Wang, Y.Zhang, L.Yenush, M.G.Myers, Jr., E.Glasheen, W.S.Lane, J.H.Pierce, and M.F.White. 1995. Role of IRS-2 in insulin and cytokine signalling. *Nature* 377:173-177.

Suzuki, K. and T.Kono. 1980. Evidence that insulin causes translocation of glucose transport activity to the plasma membrane from an intracellular storage site. *Proc. Natl. Acad. Sci. U. S. A* 77:2542-2545.

Tachibana K, Scheuer PJ, Y.Tsukitani, Kikuchi H, Van Engen D, Clardy J, Gopichand Y, and Schmitz FJ. 2005. Okadiac acid, a cytotoxic polether from two marine sponges of the genus *Halichondria*. *J. Am. Chem. Soc.* 103:2469-2471.

Takei, K. and V.Haucke. 2001. Clathrin-mediated endocytosis: membrane factors pull the trigger. *Trends Cell Biol.* 11:385-391.

Taylor, W.M., M.L.Mak, and M.L.Halperin. 1976. Effect of 3':5'-cyclic AMP on glucose transport in rat adipocytes. *Proc. Natl. Acad. Sci. U. S. A* 73:4359-4363.

Tellam, J.T., S.L.Macaulay, S.McIntosh, D.R.Hewish, C.W.Ward, and D.E.James. 1997. Characterization of Munc-18c and syntaxin-4 in 3T3-L1 adipocytes. Putative role in insulin-dependent movement of GLUT-4. *J. Biol. Chem.* 272:6179-6186.

Thomas, G. 2002. Furin at the cutting edge: from protein traffic to embryogenesis and disease. *Nat. Rev. Mol. Cell Biol.* 3:753-766.

Thurmond, D.C., B.P.Ceresa, S.Okada, J.S.Elmendorf, K.Coker, and J.E.Pessin. 1998. Regulation of Insulin-stimulated GLUT4 Translocation by Munc18c in 3T3L1 Adipocytes. *J. Biol. Chem.* 273:33876-33883.

Till, M., T.Kolter, and J.Eckel. 1997. Molecular mechanisms of contraction-induced translocation of GLUT4 in isolated cardiomyocytes. *Am. J. Cardiol.* 80:85A-89A.

Till, M., D.M.Ouwens, A.Kessler, and J.Eckel. 2000. Molecular mechanisms of contraction-regulated cardiac glucose transport. *Biochem. J.* 346:841-847.

Timmers, K.I., A.E.Clark, M.Omatsu-Kanbe, S.W.Whiteheart, M.K.Bennett, G.D.Holman, and S.W.Cushman. 1996. Identification of SNAP receptors in rat adipose cell membrane fractions and in SNARE complexes co-immunoprecipitated with epitope-tagged N-ethylmaleimide-sensitive fusion protein. *Biochem. J.* 320:429-436.

Uchida, T., M.G.Myers, Jr., and M.F.White. 2000. IRS-4 Mediates Protein Kinase B Signaling during Insulin Stimulation without Promoting Antiapoptosis. *Mol. Cell. Biol.* 20:126-138.

van der Bliek, A.M., T.E.Redelmeier, H.Damke, E.J.Tisdale, E.M.Meyerowitz, and S.L.Schmid. 1993. Mutations in human dynamin block an intermediate stage in coated vesicle formation. *J. Cell Biol.* 122:553-563.

Vanhaesebroeck, B. and D.R.Alessi. 2000. The PI3K-PDK1 connection: more than just a road to PKB. *Biochem. J.* 346:561-576.

Vanhaesebroeck, B., S.J.Leevers, G.Panayotou, and M.D.Waterfield. 1997. Phosphoinositide 3-kinases: A conserved family of signal transducers. *Trends Biochem. Sci.* 22:267-272.

Verhey, K.J. and M.J.Birnbaum. 1994. A Leu-Leu sequence is essential for COOH-terminal targeting signal of GLUT4 glucose transporter in fibroblasts. *J. Biol. Chem.* 269:2353-2356.

Verhey, K.J., S.F.Hausdorff, and M.J.Birnbaum. 1993. Identification of the carboxy terminus as important for the isoform- specific subcellular targeting of glucose transporter proteins. *J. Cell Biol.* 123:137-147.

Voliovitch, H., D.G.Schindler, Y.R.Hadari, S.I.Taylor, D.Accili, and Y.Zick. 1995. Tyrosine Phosphorylation of Insulin Receptor Substrate-1 in Vivo

Depends upon the Presence of Its Pleckstrin Homology Region. *J. Biol. Chem.* 270:18083-18087.

Wang, Q., R.Somwar, P.J.Bilan, Z.Liu, J.Jin, J.R.Woodgett, and A.Klip. 1999. Protein Kinase B/Akt Participates in GLUT4 Translocation by Insulin in L6 Myoblasts. *Mol. Cell. Biol.* 19:4008-4018.

Watson, R.T., A.H.Khan, M.Furukawa, J.C.Hou, L.Li, M.Kanzaki, S.Okada, K.V.Kandror, and J.E.Pessin. 2004a. Entry of newly synthesized GLUT4 into the insulin-responsive storage compartment is GGA dependent. *EMBO J.* 23:2059-2070.

Watson, R.T., M.Kanzaki, and J.E.Pessin. 2004b. Regulated Membrane Trafficking of the Insulin-Responsive Glucose Transporter 4 in Adipocytes. *Endocr. Rev.* 25:177-204.

Welsh, G.I., I.Hers, D.C.Berwick, G.Dell, M.Wherlock, R.Birkin, S.Leney, and J.M.Tavare. 2005. Role of protein kinase B in insulin-regulated glucose uptake. *Biochem. Soc. Trans.* 33:346-349.

White, M.F. 1998. The IRS-signalling system: a network of docking proteins that mediate insulin action. *Mol. Cell. Biochem.* 182:3-11.

Widberg, C.H., N.J.Bryant, M.Girotti, S.Rea, and D.E.James. 2003. Tomosyn Interacts with the t-SNAREs Syntaxin4 and SNAP23 and Plays a Role in Insulin-stimulated GLUT4 Translocation. *J. Biol. Chem.* 278:35093-35101.

Wilcke, M., L.Johannes, T.Galli, V.Mayau, B.Goud, and J.Salamero. 2000. Rab11 Regulates the Compartmentalization of Early Endosomes Required for Efficient Transport from Early Endosomes to the trans-Golgi Network. *J. Cell Biol.* 151:1207-1220.

Wolf, G., T.Trub, E.Ottinger, L.Groninga, A.Lynch, M.F.White, M.Miyazaki, J.Lee, and S.E.Shoelson. 1995. PTB Domains of IRS-1 and Shc Have Distinct but Overlapping Binding Specificities. *J. Biol. Chem.* 270:27407-27410.

Yamada, E., S.Okada, T.Saito, K.Ohshima, M.Sato, T.Tsuchiya, Y.Uehara, H.Shimizu, and M.Mori. 2005. Akt2 phosphorylates Synip to regulate docking and fusion of GLUT4-containing vesicles. *J. Cell Biol.* 168:921-928.

Yang, J., J.F.Clarke, C.J.Ester, P.W.Young, M.Kasuga, and G.D.Holman. 1996. Phosphatidylinositol 3-kinase acts at an intracellular membrane site to enhance GLUT4 exocytosis in 3T3-L1 cells. *Biochem. J.* 313:125-131.

Yang, J. and G.D.Holman. 1993. Comparison of GLUT4 and GLUT1 subcellular trafficking in basal and insulin-stimulated 3T3-L1 cells. *J. Biol. Chem.* 268:4600-4603.

Yang, J. and G.D.Holman. 2005. Insulin and Contraction Stimulate Exocytosis, but Increased AMP-activated Protein Kinase Activity Resulting from Oxidative Metabolism Stress Slows Endocytosis of GLUT4 in Cardiomyocytes. *J. Biol. Chem.* 280:4070-4078.

Yenush, L., K.J.Makati, J.Smith-Hall, O.Ishibashi, M.G.Myers, Jr., and M.F.White. 1996. The Pleckstrin Homology Domain Is the Principle Link between the Insulin Receptor and IRS-1. *J. Biol. Chem.* 271:24300-24306.

Young, L.H., Y.Renfu, R.Russell, X.Hu, M.Caplan, J.Ren, G.I.Shulman, and A.J.Sinusas. 1997. Low-Flow Ischemia Leads to Translocation of Canine Heart GLUT-4 and GLUT-1 Glucose Transporters to the Sarcolemma In Vivo. *Circulation* 95:415-422.

Zeigerer, A., M.A.Lampson, O.Karylowski, D.D.Sabatini, M.Adesnik, M.Ren, and T.E.McGraw. 2002. GLUT4 Retention in Adipocytes Requires Two Intracellular Insulin-regulated Transport Steps. *Mol. Biol. Cell* 13:2421-2435.

Zeigerer, A., M.K.McBrayer, and T.E.McGraw. 2004. Insulin Stimulation of GLUT4 Exocytosis, but Not Its Inhibition of Endocytosis, Is Dependent on RabGAP AS160. *Mol. Biol. Cell* 15:4406-4415.

Zhou, Q.L., J.G.Park, Z.Y.Jiang, J.J.Holik, P.Mitra, S.Semiz, A.Guilherme, A.M.Powelka, X.Tang, J.Virbasius, and M.P.Czech. 2004. Analysis of insulin signalling by RNAi-based gene silencing. *Biochem. Soc. Trans.* 32:817-821.

Zimmet, P., K.G.Alberti, and J.Shaw. 2001. Global and societal implications of the diabetes epidemic. *Nature* 414:782-787.